# Mechanisms of Hematopoietic Progenitor Genome Sensing of Inflammation

By

Vu Le-Huy Tran

A dissertation submitted in partial fulfillment of

the requirements for the degree of

Doctor of Philosophy

(Cancer Biology)

at the

UNIVERSITY OF WISCONSIN-MADISON

2025

Date of final oral examination: 07/21/2025

The dissertation is approved by the following members of the Final Oral Committee:

Emery H. Bresnick, Professor, Cell and Regenerative Biology
Jenny E. Gumperz, Professor, Medical Microbiology & Immunology
Xuan Pan, Associate Professor, Medical Sciences
Igor Slukvin, Professor, Pathology & Laboratory Medicine
Owen Tamplin, Assistant Professor, Cell and Regenerative Biology
Jing Zhang, Professor, Oncology

# Contents

# List of Figures

# List of Tables

# Acknowledgments

I especially thank my advisor, Dr. Emery Bresnick, for his excellent mentorship, which has transformed my intellectual and professional development during my doctoral study. Dr. Bresnick sets an example of an effective mentor and a world-class scientist with an innovative research program. I am grateful for the collaborative scholarly environment at the Wisconsin Blood Cancer Research Institute (WBCRI) that Dr. Bresnick has established and been leading.

I thank the thesis committee, including Drs. Jenny Gumperz, Igor Slukvin, Owen Tamplin, Xuan Pan, and Jing Zhang, for their intellectual support and valuable advice on my thesis and career development. I thank the faculty and program coordinators of McArdle Laboratory for Cancer Research and the Department of Cell and Regenerative Biology for their great support.

I thank the current and past members of the Bresnick laboratory, including Kirby Johnson, Alexandra Soukup, Koichi Katsumura, JeongAh Kim, Ruiqi Liao, Charu Mehta, Isabela Fraga de Andrade, Mabel Jung, Christina Jurotich, and Tim Xiong, for their scientific discussion and technical support on my thesis project. I thank Dr. Peng Liu for his excellent collaboration in bioinformatic analyses. I thank Dr. Marjorie Brand and Audrey Kopp for their guidance on CUT&Tag experimentation. I am grateful for the collaborative work with my undergraduate students, including Erin Kim, Bjorn Schoff, Zamaans Ahmad, and Ashley Mattina.

I am grateful for the mental support of my wife Mong Ho and family (my father Hong

Tran, my mother Hoang Le, my brother Thanh Tran, and my sister My Tran). My friends at WBCRI, University of Wisconsin-Madison Graduate School, the Innovative BioScience Group, the International Society for Experimental Hematology, and Madison community are great sources of positive energy to fuel my scientific endeavor.

I thank the Carbone Cancer Center Flow Laboratory for flow cytometry and cell sorting services, the Research Animal Resources and Compliance for animal care, and Cancer Informatics Shared Resource for bioinformatic analysis support.

This work was supported by the National Institute of Health grants T32 HL07899 and F31 DK138794-01A1.

# Thesis Abstract

Genetic variation in hematopoietic stem cell genomes predisposes cells to hematologic malignancies, and aberrant inflammatory signaling acts as a secondary insult to drive pathogenesis. However, how the genome senses and adapts to the dynamically changing signaling milieu is not fully understood. GATA Binding Protein 2 (GATA2), a master transcription factor essential for embryonic and adult hematopoiesis, is an exemplary case. Mutations in the coding or non-coding regions of *GATA2* cause GATA2 Deficiency Syndrome with a wide variety of hematologic manifestations, including immunodeficiency, bone marrow failure, Myelodysplastic Syndrome, and Acute Myeloid Leukemia. Genetic ablation of *Gata2* $-77$ kb enhancer is embryonically lethal after embryonic day 15.5, downregulates *Gata2* expression in myeloerythroid progenitors, and upregulates the expression of genes encoding innate immune machinery, including Interferon Regulatory Factor 8 (IRF8) and Toll-Like Receptors (TLRs). These expression changes elevate Interferon-gamma (IFN$\gamma$) and TLR1/2 and TLR2/6 signaling. GATA2 reduction increases Monocyte Progenitors (MPs) and decreases Granulocyte Progenitors (GPs). Blocking IFN$\gamma$ signaling by *Irf8* ablation in $-77^{-/-}$ embryos increases GPs and decreases MPs to normalize the progenitor imbalance. In this thesis, I demonstrated that genetic ablation of gene encoding TLR adaptor Myeloid Differentiation 88 (MYD88) attenuated the elevated TLR signaling in $-77^{-/-}$ progenitors. MYD88 deletion reduced GP and MP numbers but did not reverse the imbalance. Mechanistically, the elevated signaling in GATA2-deficient progenitors required activity of the hematopoietic transcription factor PU.1. In one cohort of inflammation-activated genes, PU.1 preoccupied

the accessible loci in the steady state, and inflammatory signaling amplified the magnitude of transcriptional responses. In another cohort, inflammation induced PU.1 chromatin occupancy, and the transcriptional responses exhibited greater sensitivity to IKK$\beta$ inhibition. GATA2 co-occupies chromatin with heptad transcription factors, including RUNX1, and they may function collectively. Unexpectedly, GATA2 opposes the activity of RUNX1 to regulate qualitatively different inflammatory signaling pathways. In aggregate, the thesis research advances the understanding of how hematopoietic transcription factors allow the progenitor genome to sense and respond to inflammation.

# List of Publications

The following are publications that were produced during my PhD training with Dr. Emery Bresnick.

## Primary Research Articles

1. Vu L. Tran, Peng Liu, Koichi R. Katsumura, Alexandra A. Soukup, Audrey Kopp, Zamaan Ahmad, Ashley E. Mattina, Marjorie Brand, Kirby D. Johnson, and Emery H. Bresnick. Dual mechanism of inflammation sensing by the hematopoietic progenitor genome. *Science Advances* 2025.

2. Fatemeh Alikarami, Hongbo M. Xie, Simone S. Riedel, Haley Goodrow, Declan Raymond Barrett, Leila Mahdavi, Alexandra Lenard, Changya Chen, Taylor Yamauchi, Etienne Danis, Zhendong Cao, Vu L. Tran, Mabel Minji Jung, Yapeng Li, Hua Huang, Junwei Shi, Kai Tan, David Trent Teachey, Emery H. Bresnick, Tobias Neff, and Kathrin Maria Bernt. GATA2 links stemness to chemotherapy resistance in acute myeloid leukemia. *Blood* 2025.

3. Adhithi Rajagopalan, Yubin Feng, Meher B. Gayatri, Erik A. Ranheim, Taylor Klungness, Daniel R. Matson, Moon Hee Lee, Mabel Minji Jung, Yun Zhou, Xin Gao, Kalyan V.G. Nadiminti, David T. Yang, Vu L. Tran, Eric Padron, Shigeki Miyamoto, Emery H. Bresnick, and Jing Zhang. A gain-of-function p53 mutant synergizes with oncogenic NRAS to promote acute myeloid leukemia in mice. *Journal of Clinical Investigation* 2023.

4. Vu L. Tran, Peng Liu, Koichi R. Katsumura, Erin Kim, Bjorn M. Schoff, Kirby D. Johnson, and Emery H. Bresnick. Restricting genomic actions of innate immune mediators on fetal hematopoietic progenitor cells. *iScience* 2023.

## Submission/Under Review

1. Alexandra A. Soukup, Mona Mohammadhosseini, Ruiqi Liao, Vu L. Tran, Kirby D. Johnson, Anupriya Agarwal, and Emery H. Bresnick. Fungal infection unveils pathogenicity of conditionally pathogenic genetic variation predisposing to bone marrow failure. (under review)

2. Mabel M. Jung, Vu L. Tran, Yue Xiong, Kirby D. Johnson, Koichi R. Katsumura, Peng Liu, and Emery H. Bresnick. GATA2 decommissioning of enhancers: A mechanism to constrain inflammatory signaling. (under review).

## Review Articles

1. Vu L. Tran, Myriam L.R. Haltalli, Jingjing Li, Dawn S. Lin, Masayuki Yamashita, Shalin H. Naik, and Ellen V. Rothenberg. Ever-evolving insights into the cellular and molecular drivers of lymphoid cell development. *Experimental Hematology* 2024 (Contribution to ISEH New Investigator Committee).

2. Kirby D. Johnson, Mabel M. Jung, Vu L. Tran, and Emery H. Bresnick. Interferon Regulatory Factor-8-dependent innate immune alarm senses GATA2 deficiency to alter hematopoietic differentiation and function. *Current Opinion in Hematology* 2023.

# Chapter 1

# Hematopoietic Genome Sensing of Inflammation in Physiology and Pathogenesis

# Abstract

Genetic variation predisposes hematopoietic stem and progenitor cells to hematologic malignancies, and secondary insults promote pathogenesis. Besides acquiring collaborating mutations, an aberrant inflammatory signaling milieu drives leukemogenesis. However, many questions remain unanswered regarding how inflammatory signaling influences hematopoietic genome function and how the genome senses and responds to inflammation. This review focuses on the mechanisms underlying inflammation sensing and how germline and/or somatic variation influence genome function in inflammation contexts.

## 1.1 Introduction

Inflammation is a biological process initiated by the invasion of pathological agents or the intrinsic perturbations in the cells. The pathogen-associated molecular patterns, including structural components of bacterial cell walls and nucleic acid molecules of viral and bacterial agents, are detected by an array of pattern recognition receptors that are conserved across different species throughout evolution [1, 2]. These receptors form families based on their similarity in structure and function, including Toll-Like Receptors (TLRs) [3–7]. The receptor-ligand interactions initiate the activation and assembly of signal adaptors and transducers, which are components of inflammatory signaling pathways [2]. These constituents then activate signal-dependent transcription factors to regulate expression of genes encoding inflammatory mediators, such as cytokines and chemokines, which respond to and/or sustain inflammatory signaling. Inflammation can also occur independently of the receptor-ligand paradigm, where perturbations in the genome and/or epigenome lead to sterile inflammatory responses in diverse contexts, including aging and hematologic malignancies. The L265P mutation in the adaptor protein Myeloid Differentiation 88 (MYD88) assembles a Myddosome complex containing Interleukin 1 Receptor Associated Kinase 2 (IRAK2) and IRAK4, constitutively activating inflammatory signaling independently of TLR activity in a subtype of Diffuse Large B-cell Lymphoma [8, 9]. Janus Kinase 2 (JAK2) V617F mutation alters the three-dimensional structure of a pseudokinase domain JH2, leading to the phosphorylation of JH1 domain and promoting constitutive activation of JAK signaling in Myeloproliferative Neoplasm (MPN) [10–14]. A common thread between pathogen and non-pathogen inflammation mechanisms is that the inflammatory signaling cascades utilize similar signaling devices, including Nuclear Factor $\kappa$-Light Chain Enhancer of Activated B Cells (NF-$\kappa$B), Activator Protein 1 (AP1), Signal Transducers and Activators of Transcription (STATs), and Interferon (IFN) Regulatory Factors (IRFs) [15–21].

The inflammatory machinery plays a dual role in development and defense, and the quali-

tative and quantitative considerations of inflammatory signaling need to be tightly controlled to prevent disruptive consequences. The hematopoietic cluster cells expressing Ly6A-GFP with lymphoid potential in the Aorta-Gonad-Mesonephros (AGM), umbilical, and vitelline arteries at embryonic day (E) 10.5 exhibit an inflammatory gene expression program with elevated TLRs and IFN-related genes relative to Ly6A-GFP$^-$ hematopoietic cluster and endothelial cells in the same anatomical sites [22]. Genetic ablation of genes encoding IFN$\alpha$ Receptor 1 (*Ifnar1*), IFN$\gamma$ Receptor 1 (*Ifngr1*), or IFN$\gamma$ reduces the number of E10.5 lymphoid progenitors, and IFN$\gamma$ signaling regulates the functional AGM Hematopoietic Stem and Progenitor Cells (HSPCs) in a limiting-dilution transplantation assay [22]. Single-cell transcriptome (scRNA-seq) analysis revealed an impulse of type I IFN signaling at E18.5 during the gradual transition from fetal to adult hematopoiesis [23, 24]. IFNAR1 loss reduces the number of Hematopoietic Stem Cells (HSCs) in the postnatal day (P) 0 fetal liver, neonatal, and juvenile bone marrow [23]. Integrated single-cell transcriptome and surface marker analyses recapitulated the reduction in immunophenotypic HSCs in the absence of IFNAR1 [25]. Still, the transcriptionally defined Multipotent Progenitors (MPPs) are modestly reduced without affecting the differentiated cells in the peripheral blood postnatally [25]. During gestation, maternally derived inflammation induces cytokine production, including IFN$\gamma$, which can pass through the maternal-fetal barrier to influence fetal HSPC function, enhancing HSPC expansion, self-renewal, and differentiation potential [26–28].

Experimental evidence from many laboratories has established a stepwise model to understand the interaction between inflammation and genetic variation in human pathologies (Figure 1.1). HSPCs carry a germline genetic variant that predisposes them to hematologic malignancies, such as those associated with *GATA2* or *RUNX1*, or acquire a somatic mutation that causes Clonal Hematopoiesis of Indeterminate Potential (CHIP), which includes mutations in *DNMT3A*, *TET2*, and *ASXL1* [29–31]. Through the subsequent acquisition of additional mutations and/or the influence of aberrant inflammatory milieu, the pre-malignant HSPCs gain competitive advantages and transformation to promote leuke-

mogenesis [32, 33]. While many animal models have been developed to study the contribution of collaborating mutations in driving hematologic malignancy, how the hematopoietic cell genome senses and responds to inflammation is not well established. In this review, we described the mechanisms underlying the inflammation sensing by the hematopoietic stem/progenitor genome and the influence of genetic variations on inflammatory responses.

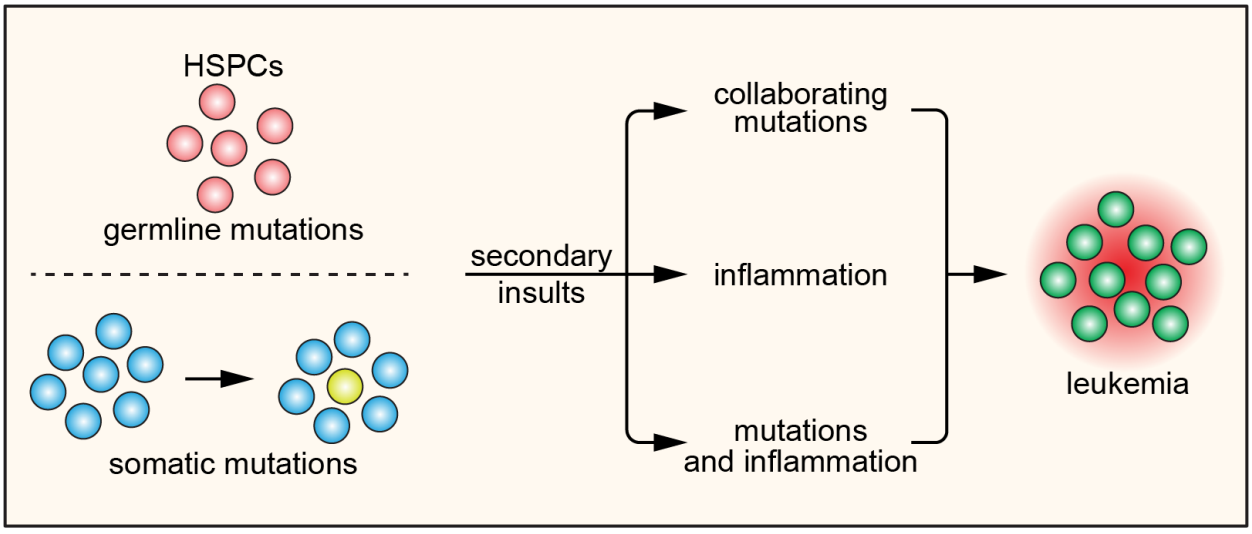


**Figure 1.1: Genetic variations and inflammation interact to promote leukemogenesis.** Hematopoietic Stem and Progenitor Cells (HSPCs) with germline genetic mutations (red), such as those in *GATA2* or *RUNX1*, or somatic mutations (yellow), including those in *DNMT3A*, *TET2*, and *ASXL1*, are predisposed to hematologic malignancies. A secondary insult, such as collaborating mutations, inflammation, or both, drives HSPC leukemogenesis (green).

## 1.2 Inflammation disrupts hematopoietic genome function

Since the cells sense the presence of inflammatory cues using an arsenal of cell surface- and intracellular receptors, in principle, the hematopoietic transcription factors might directly or indirectly regulate the expression of genes encoding receptors or downstream signaling components. Once activated, inflammatory signaling may regulate the activation and/or chromatin occupancy of transcription factors to drive cellular responses and differentiation. The

current paradigm establishes that inflammation activates a class of signal-dependent transcription factors, such as NF-$\kappa$B, AP1, STATs, and IRFs, to regulate the cytokine/chemokine expression whose proteins mediate inflammatory responses. This paradigm does not predict how inflammation influences the activity of lineage-determining (*e.g.*, hematopoietic) transcription factors to establish and/or maintain genetic networks to sense and respond to inflammation.

An exemplar is the GATA Binding Protein 2 (GATA2), a master regulator of hematopoiesis [34–38]. Coding or non-coding mutations in *GATA2* cause GATA2 Deficiency Syndrome with diverse clinical manifestations, including mycobacterial infection, lymphedema, bone marrow failure, and predisposition to Myelodysplastic Syndrome (MDS) and Acute Myeloid Leukemia (AML) [39–41]. GATA2 deficiency resulting from the *Gata2* $-77$ kb enhancer (human $-110$ kb enhancer) deletion reduces GATA2 level by $\sim$75% and disrupts normal hematopoiesis in the murine fetal liver, causing the loss of multi-fate system and the retention of monocytic fate potential [38, 42–44]. GATA2 reduction increases the number of Common Myeloid Progenitors (CMPs) but depletes Megakaryocyte-Erythroid Progenitors (MEPs), causing severe erythropoietic defects and anemia in embryos [38, 43–45]. Although the number of Granulocyte Monocyte Progenitors (GMPs) is maintained at a similar level relative to wild type, GATA2 reduction decreases Granulocyte Progenitors (GPs), increases Monocyte Progenitors (MPs), causing an imbalance in GP:MP ratio within the Ly6C$^+$ GMP population [44, 45]. Single-cell RNA-seq and proteomic analyses of CMP/GMP pool revealed that the aberrant hematopoiesis correlates with an inflammatory-responsive transcriptome resembling IFN$\gamma$ signaling, and re-expressing GATA2 in primary and ER-HOXB8-immortalized (hi) $-77^{-/-}$ progenitors in bulk RNA-seq analyses suppresses this inflammatory-responsive signature genome-wide [43, 46]. Lowering GATA2 elevates the expression of inflammatory machinery, including genes encoding IFN signaling component IRF8, pattern recognition receptors TLR1/2/6, and cytokine receptors IL6ST/IL6RA, rendering $-77^{-/-}$ myeloerythroid progenitors and their differentiating progeny hypersensitive

to the corresponding signaling [43, 45, 46]. As with $-77^{-/-}$ embryos, GATA2 reduction resulting from a compound $Nras^{G12D/+}$;$p53^{R172H/+}$ mutation in an AML mouse model correlates with elevated inflammatory machinery, including *Tlr1*, *Irf5*, *Irf8*, and *Il6ra* [47].

The dysregulated hematopoiesis and aberrant inflammatory-responsive transcriptome intrinsically instigated by GATA2 deficiency in fetal progenitors resembles the influence of extrinsic inflammatory cues on normal hematopoiesis. In a chronic inflammatory mouse model, IFN$\gamma$ signaling induces monocyte expansion and reduces neutrophil production in peripheral blood and bone marrow, causing the monocyte:neutrophil imbalance and the elevation of IRF8 and E26 Transformation-Specific (ETS) transcription factor PU.1 [48]. IFN$\gamma$ signaling induced by acute lymphochoriomeningitis viral infection promotes monopoiesis while not impacting lymphopoiesis in peripheral blood [49]. In *ex vivo* differentiation assays, IFN$\gamma$ increases the number of monocyte progeny and decreases the number of granulocyte progeny produced by GMPs, recapitulating the GP:MP imbalance in $-77^{-/-}$ fetal liver [43, 48]. Blocking IFN$\gamma$ signaling via genetic ablation of *Irf8* in $-77^{-/-}$ fetal liver increases GP, decreases MP, and reverses GP:MP imbalance [44]. Bacterial and viral mimetic-induced inflammation using synthetic ligands for TLR2, TLR4, and TLR9 exclusively induces monocyte and macrophage differentiation from HSPCs both *ex vivo* and *in vivo* independently of the bone marrow niche [50, 51]. These findings are aligned with the elevated TLR1/2 and TLR2/6 signaling of $-77^{-/-}$ progenitors and the retention of monocytic differentiation potential [43, 45, 52]. Attenuating TLR signaling via genetic ablation of *Myd88* in the context of *Gata2* $-77^{-/-}$ further reduces the number of GP and Colony-Forming-Unit Granulocytes [45]. In contrast to *Irf8* ablation, *Myd88* deletion does not reverse GP:MP imbalance in $-77^{-/-}$ fetal liver [44, 45].

Differing from *Gata2* $-77^{-/-}$ fetal myeloerythroid progenitors, GATA2 acts as an activator or repressor of inflammation in other contexts. In human umbilical vein endothelial cells, GATA2 co-occupies chromatin with AP1 components Jun Proto-oncogene (c-JUN) or FBJ Murine Osteosarcoma Viral Oncogene Homolog (c-FOS) to activate the expression of inflam-

matory genes, including *IL8*, *CXCL2*, and *CSF2* [53]. Mechanistically, GATA2 is required for the chromatin occupancy of phosphorylated c-JUN [53]. Reducing GATA2 lowers phosphorylated c-JUN occupancy but does not affect the total c-JUN and c-FOS occupancy [53]. By contrast, c-JUN reduction does not influence GATA2 pre-occupancy at inflammatory loci [53]. c-JUN is a coactivator of PU.1, and point mutations (Q202L, F203Y, or Y252N) in the PU.1 ETS domain abrogate PU.1−c-JUN *in vitro* interaction, terminate embryo viability after E16.5, and corrupt myeloid differentiation in fetal livers [54, 55]. In murine mast cells, GATA2 and PU.1 co-occupy the *Il6* −39 kb enhancer to upregulate *Il6* expression in response to TLR4 ligand Lipopolysaccharide (LPS) [56]. Forced expression of GATA2 in a murine kidney cell line elevates the transcriptional responses of inflammatory genes to acute Tumor Necrosis Factor $\alpha$ (TNF$\alpha$) signaling, including *Il6*, *Cxcl10*, and *Csf1* [57]. GATA2 occupies inflammation-regulated loci that harbor AP1 binding motifs, and pharmacological inhibition of AP1 attenuates *Cxcl10* and *Csf1* responsiveness to TNF$\alpha$ signaling in the presence of enforced GATA2 [57]. Acute inflammation induced by TLR4 signaling results in lower cytokine production in the peritoneal cavity lavage fluid and plasma in *Gata2*$^{+/-}$ compared to wild-type mice [58]. Since systemic inflammation activates both hematopoietic and non-hematopoietic cells and whether the inflammatory inducers present in the bone marrow at effective doses are not determined, the cytokine production might be compromised by the defective hematopoietic cells generated from the progenitor imbalance in GATA2 deficiency. To address the direct effects of GATA2 heterozygosity on inflammation, it will be instructive to determine whether a 50% reduction in GATA2 levels influences the expression of pattern recognition receptors and whether HSPC compartments isolated from *Gata2*$^{+/-}$ bone marrow are responsive to inflammatory signaling. By contrast, the long non-coding RNA (lncRNA) ROCKI suppresses GATA2 expression in human primary macrophages, and ROCKI deficiency or GATA2 overexpression downregulates pro-inflammatory proteins, including IL1$\beta$, IL8, CXCL8, and CCL20 [59]. In aggregate, the contribution of GATA2 in inflammation-regulated mechanisms is highly cell-type-specific and locus-dependent.

Analogous to *Gata2* $-77^{-/-}$ deficiency, genetic ablation of other hematopoietic transcription factors alters the expression of signaling devices responsible for inflammation sensing and generates progenitors and progeny hyperresponsive to inflammatory signaling. The zinc finger transcription factor Kruppel-Like Factor 4 (KLF4) regulates monocytic differentiation, and neonates lacking KLF4 die shortly after birth [60, 61]. In adult bone marrow, conditional deletion of *Klf4* upregulates multiple *Tlr* genes and elevates TLR4 protein levels in HSCs [62]. Runt-Related Transcription Factor 1 (RUNX1) is a master regulator of hematopoiesis, essential for AGM HSC emergence, megakaryopoiesis, and lymphopoiesis [63–66]. In human pathologies, several common clinical manifestations of GATA2 and RUNX1 deficiency are defective megakaryopoiesis, incomplete penetrance of thrombocytopenia, and MDS/AML predisposition [67]. Differing from GATA2 Deficiency Syndrome, human pathogenic variants in the coding sequence of RUNX1 cause Familial Platelet Disorder [68, 69]. *Runx1*$^{-/-}$ mouse models lack fetal liver hematopoiesis and are embryonically lethal at E12.5 [63, 64]. RUNX1 deletion in human CD34$^{+}$ HSPCs using the CRISPR/Cas9 gene editing tool reduces granulocytic and increases monocytic differentiation in colony-forming unit and liquid differentiation assays, mirroring GP:MP imbalance in the GATA2-deficient condition [70]. Single-cell RNA-seq analysis of the murine bone marrow Lineage$^{-}$Sca1$^{-}$cKit$^{+}$ (LSK) cells revealed that RUNX1 loss generates inflammatory signature transcriptomes in GMP populations [71]. RUNX1 loss remodels the chromatin landscape in the GMP genome, increasing accessibility at inflammation-activated loci [72]. RUNX1 occupies loci encoding components of TLR4 and IFN signaling pathways, including receptors (*Cd14* and *Ifnar1/2*) and transcription factors (*Stat* and *Irf* genes) in steady-state GMPs [72]. As with $-77^{-/-}$ myeloerythroid progenitors, RUNX1$^{null}$ GMPs produce neutrophils with elevated TLR4 and multiple TLR and IFN$\alpha$ pathway components, rendering cells hyperresponsive to corresponding signaling [71].

GATA2 and RUNX1 govern transcriptional networks to establish and/or maintain normal hematopoiesis, yet, how these factors interact to regulate inflammatory responses is

not well understood. GATA2 utilizes a DNA motif WGATAR (W = A/T and R = A/G) for chromatin occupancy [73–75], while RUNX1 dimerizes with Core Binding Factor $\beta$ to occupy chromatin at a YGYGGTY (Y = C/T) consensus DNA sequence [76–78]. GATA2 and RUNX1 are components of a heptad complex, consisting of TAL1, LYL1, LMO2, FLI1, and ERG, in mouse and human, indicating that they may function collectively [79–83]. The *Gata2* +9.5 kb enhancer (human intron 5) harbors an E-box-spacer-WGATAR composite element (CATCTG-8bp-AGATAA) for chromatin occupancy and assembly of a TAL1-GATA2 complex containing co-regulators LDB1 and LMO2 [80, 84]. Using this composite element as a reference and by varying the spacer length between E-box and WGATAR motifs, an HSPC cistrome was mapped out genome-wide [85]. Whether such a composite element for the GATA and RUNX motifs exists, how many base pairs these individual motifs are separated within the motif combination, and how frequently the composite motif is present at heptad-bound loci are not determined. Coimmunoprecipitation assay demonstrates GATA2-RUNX1 protein interaction and interactions with other heptad factors [83]. Although *Gata2*$^{+/-}$ and *Runx1*$^{+/-}$ mice exhibit modest alterations in hematopoiesis [38, 86–88], the compound *Gata2*$^{-/-}$;*Runx1*$^{-/-}$ heterozygosity is embryonically lethal [83]. Since $-77^{-/-}$ progenitors and RUNX1$^{null}$ neutrophils are hypersensitive to TLR1/2-IFN$\gamma$ and TLR4-IFN$\alpha$ signaling, respectively [43, 45, 52, 71, 72], the heptad complex paradigm may predict that GATA2 and RUNX1 function collectively to regulate transcriptional responses to inflammation. Unpredictably of the cooperativity paradigm, RUNX1 deletion in hi$-77^{-/-}$ progenitors attenuates the transcriptional responses of a cohort of genes to TLR1/2 and IFN$\gamma$ combinatorial signaling, suggesting that GATA2 and RUNX1 have opposing activities under inflammatory conditions [45]. In contrast to the elevated *Tlr1/2* expression in hi$-77^{-/-}$ progenitors, RUNX1 loss upregulates *Tlr4* expression, explaining the differential contributions of GATA2 and RUNX1 to qualitatively distinct inflammatory signaling pathways [45, 71, 72]. Together, these data support a model in which the hematopoietic transcription factors regulate an inflammation-related transcriptional circuitry to promote multi-fate potentials, and alter-

ations in dosage/activity of these factors dysregulate this inflammation circuit to promote select lineages while suppressing others.

As with GATA2 and RUNX1 antagonism, the opposing activities of GATA2 and other transcription factors regulate hematopoiesis. The heptad complex component ETS-Related Gene (ERG) is crucial for definitive hematopoiesis, and a loss-of-function homozygous mutation in the ERG DNA-binding domain renders murine fetal HSCs defective in self-renewal capacity and embryonic lethality at E12.5 [89, 90]. Expressing human ERG in a mouse transgenic model promotes AML and T-cell Acute Lymphoblastic Leukemia [91]. GATA2 opposes ERG activity, and a single *Gata2* allele deletion in ERG transgenic mice accelerates AML development, indicating *Gata2* as a tumor suppressor gene [92]. Ecotropic Viral Integration Site 1 (EVI1), encoded by *MECOM*, is another member of the ETS family. 3q chromosomal rearrangements [inv(3)(q21;q26) or t(3;3)(q21;q26)] relocate the *GATA2* −110 enhancer upstream, next to *MECOM*, inducing *MECOM* expression while downregulating *GATA2* expression as a mechanism of human leukemogenesis [41, 93, 94]. As with transgenic $ERG;Gata2^{+/-}$ mice, *Gata2* heterozygous deletion in 3q21q26 mice promotes early onset of leukemia, implying an antagonistic interaction between GATA2 and EVI1 [95]. GATA2 deficiency resulting from −77 enhancer deletion elevates the activity of another ETS factor PU.1, without affecting its expression, to regulate myeloid and B-lineage gene networks in hi$-77^{-/-}$ progenitors [46]. Differing from the $Erg^{-/-}$ mice, genetic interventions in different parts of the *Spi1* locus, encoding PU.1, dysregulate myelopoiesis and lymphopoiesis, affect vitality at different stages of development, but do not impact erythropoiesis and megakaryopoiesis [96, 97]. Disrupting a portion of exon 5 encoding amino acids (aa) 200-272 of PU.1 DNA binding domain is embryonically lethal at E18 [96]. Loss of the entire exon 5 generates neonates with severe septicemia due to the absence of B cells, T cells, macrophages, and neutrophils [97]. Antibiotic treatment prolongs survival for ∼2 weeks and promotes T cell development [97]. Unlike *Spi1* deletion homozygosity, genetic ablation of the *Spi1* −14 kb Upstream Regulatory Element (URE) permits animal survival up to eight months of age,

reduces PU.1 levels in bone marrow cells by 80%, and promotes AML development [98, 99]. Single-molecule RNA fluorescent in situ hybridization imaging demonstrated the co-expression of *Spi1*, *Gata1*, and *Gata2* mRNA in the same single CMPs, GMPs, and MEPs [100]. These lines of evidence support a model in which GATA factors antagonize ETS factors to regulate hematopoiesis.

Varying the levels of the antagonistic hematopoietic transcription factors reveals the mechanisms by which the genome senses inflammation. The elevated IFN$\gamma$ and TLR1/2 signaling are synergistic in $-77^{-/-}$ progenitors [45, 52]. Lowering PU.1 levels by ablation of *Spi1* URE impairs the transcriptional responses of hi$-77^{-/-}$ progenitors to inflammatory signaling, demonstrating the requirement of PU.1 in GATA2-dependent genome sensing of inflammation [45]. In a cohort of inflammation-activated genes that are accessible in the steady state, GATA2 and PU.1 pre-occupy chromatin, and inflammatory signaling amplifies transcription (Figure 1.2) [45]. In another cohort, GATA2 and PU.1 do not bind chromatin, and inflammatory signaling induces the occupancy of these factors to regulate transcription [45]. The responsiveness of these GATA2- and PU.1-recruited genes are uniquely sensitive to the pharmacological inhibition of IKK$\beta$ upstream of the NF-$\kappa$B signaling pathway [45]. Oncogenic RAS G12V mutant elevates p38 Mitogen-Activated Protein Kinase (MAPK) signaling, inducing multi-site phosphorylation of GATA2 to activate the expression of inflammatory genes [101, 102]. Whether inflammation-induced GATA2 and PU.1 chromatin occupancy requires post-translational modifications by IKK$\beta$ or MAPK activity in myelo-erythoid progenitors is not yet determined. Inflammation-activated transcription factors NF-$\kappa$B and IRF1 bind chromatin to induce chromatin accessibility, and the loss of NF-$\kappa$B components, RELA and REL, or IRF1 makes chromatin less accessible in response to inflammation in bone marrow-derived macrophages [103, 104]. It is instructive to determine whether chromatin occupancy of these canonical signal-dependent transcription factors enables GATA2 and PU.1 occupancy upon inflammation, or inflammation activates GATA2 and PU.1 to bind and remodel chromatin for signal-dependent transcription factor assembly.

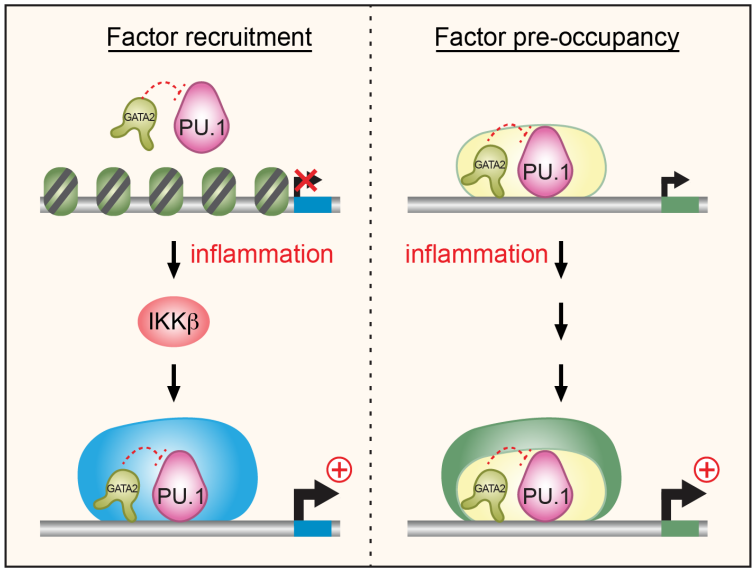


**Figure 1.2: Dual mechanism of inflammation sensing by the hematopoietic progenitor genome.** Left, A class of inflammation-activated genes is less accessible in the steady state, and inflammatory signaling induces hematopoietic transcription factor occupancy to regulate transcriptional responses, which uniquely require IKK$\beta$ activity. Right, Chromatin in another class of inflammation-activated genes is accessible in the steady state, hematopoietic transcription factors pre-occupy chromatin to induce basal transcription, and inflammatory signaling further elevates transcription.

## 1.3 Impact of germline genetic variation on genome sensing of inflammation

Since the context dependence of human pathogenic variants goes beyond the simplistic binary models of gain-of-function versus loss-of-function consequences, genetic variations of genes encoding hematopoietic transcription factors exert different influences on how the genome senses and responds to inflammation. Besides the acquisition of somatic mutations, inflammation triggers a transition from a silent phenotype associated with an initial predisposing mutation to pathogenic manifestations. This predisposing mutation might induce molecular alterations with or without functional consequences in the steady state, and such alterations become pathogenic following aberrant inflammatory signaling. Alternatively, the predisposing mutation is strictly silent without molecular abnormality, and inflammatory signaling

induces alterations at a measurable level.

The GATA2 mutations provide case studies for how mutations in different anatomical sites of a gene qualitatively and quantitatively contribute to hematologic malignancy predisposition, and the differential impact of these mutations on inflammation is beginning to be tested. GATA2 amino-terminal (N-finger) and carboxy-terminal (C-finger) zinc fingers are connected by an inter-zinc finger spacer, and each finger utilizes four cysteines for $Zn^{2+}$ bonding to stabilize finger structure (Figure 1.3A). C-finger mediates GATA2 binding to DNA at the WGATAR motif, and germline variants in C-fingers affect GATA2 chromatin occupancy, constituting GATA2 Deficiency Syndrome [105]. Differing from the T355Δ mutation, which is largely inactive, the T354M mutant still retains GATA2 activities at varying levels, including hematopoietic differentiation and transcriptional regulation [106, 107]. As with GATA2, T354M suppresses monocytic but promotes granulocytic and eosinophilic differentiation in fetal progenitors [106, 107]. GATA2 regulates mast-cell-specific genes and primes mast cell differentiation in progenitors [107]. Although T354M still retains the ability to regulate a subset of mast-cell-specific genes, T354M fails to induce immunophenotypic mast cell differentiation in a liquid culture assay [107]. Interestingly, another C-finger mutation, R362Q, not only regulates T354M-related genes but also induces mast cell differentiation to a similar level as GATA2 [107]. By contrast, the transcriptional regulation capacity and differentiation-regulatory activity of R362P are much weaker than those of T354M, and R362P did not induce mast cell differentiation [107]. A frameshift mutation at R330 in the GATA3 C-finger (equivalent to GATA2 R362) reduces GATA3 chromatin occupancy and increases chromatin accessibility at inflammation-activated genes in breast cancer cells [108]. Expressing GATA3 R330 mutant in $GATA3^{-/-}$ cells elevates phosphorylation levels of Serine/Threonine-Protein Kinase TBK1 and IRF3 and generates a transcriptome with upregulated Interferon-inducible genes [108]. Given the highly conserved structure of GATA factors, it is interesting to ask if GATA2 R362 mutants might also elevate IFN signaling. The aa 396-399 fragment RNRK, located in the vicinity of the C-finger, is highly conserved

among GATA factors and is required for the *in vitro* DNA binding activity of GATA1 [109]. Differing from $Gata2^{-/-}$ embryos [34], homozygous R398W is embryonically lethal after E14.5 [110]. Compound $Gata2^{R396Q/-}$ embryos surpass E10.5, still survive at E12.5, but are not present after birth, indicating that the defective C-finger mutants contribute to development [111]. R396Q murine heterozygosity exhibits elevated long-term (LT-) HSCs and myeloid-biased MPP1 and MPP2 while reducing short-term (ST-) HSCs in E14.5 fetal liver and persists to adulthood [111, 112]. Transcriptome analysis reveals that the $Gata2^{R396Q/-}$ LSK population exhibits gene signatures related to elevated inflammatory responses and attenuation of IFN signaling [111]. LPS-induced TLR4 signaling further increases the elevated $Gata2^{R396Q/-}$ MPP2 relative to wild type [111]. In wild type, LPS suppresses LT- and ST-HSC frequencies, but the $Gata2^{R396Q/-}$ $CD150^{high}$ LT-HSC and ST-HSC populations are not responsive or further reduced [111, 112].

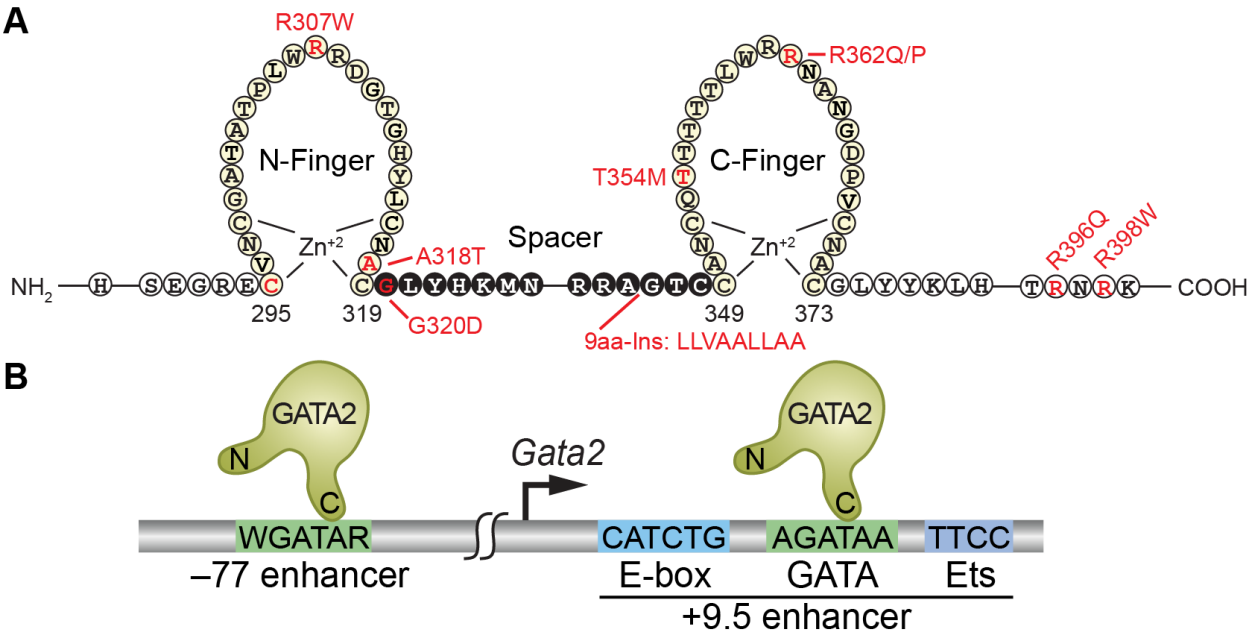


**Figure 1.3: Coding and non-coding GATA2 mutations differentially influence inflammatory responses.** (**A**) GATA2 protein sequence depicting amino- and carboxy-terminal zinc fingers, inter-zinc finger spacer, and their select mutations. (**B**) *Gata2* −77 kb enhancer and +9.5 kb enhancer.

Although the *in vivo* function of GATA2 N-finger is not fully understood, the consequences of genetic mutations in the N-finger provide mechanistic insights into how the N-

finger operates individually or in coordination with the C-finger to mount GATA2 activities. R307W mutant occupies chromatin to a lesser extent compared to GATA2 at GATA2 target loci, demonstrating that the N-finger stabilizes DNA binding activity of the C-finger [106]. R307W and A318T mutants regulate monopoiesis, granulopoiesis, and eosinophilopoiesis at similar levels with GATA2, but these N-finger mutants lack mast cell differentiation activity [107, 113]. Although the chromatin occupancy is impaired, T354M and R307W mutants retain the ability to regulate a subset of GATA2 target genes while acquiring ectopic transcriptional activities at loci not normally regulated by GATA2 [107]. While the integrity of the C-finger structure is essential for GATA2 chromatin occupancy and transcriptional regulation, the C295A mutant disrupting N-finger integrity still regulates certain but not all GATA2- and T354M-regulated genes [107]. GATA2 represses the transcription of *Irf8*, rendering $-77^{-/-}$ progenitors hyperresponsive to IFN$\gamma$ signaling [43, 45, 52]. C295A or T354M mutant retains the transcriptional repression of *Irf8*, but the dual mutant does not repress *Irf8* [107]. This raises the question whether T354M with a corrupted N-finger will be hypersensitive to IFN$\gamma$ signaling, as with $-77^{-/-}$ progenitors. Mutations in the N-terminal (Lp30 loss) and C-terminal (K313KK) sequences of *Cebpa*, encoding the myeloid transcription factor CCAAT Enhancer Binding Protein $\alpha$, cause human and mouse AML [114, 115]. GATA2 N-finger mutation G320D synergizes with compound heterozygous *Cebpa* mutation to promote both myeloid and erythroid lineage transformation into Acute Erythroid Leukemia at an early onset compared to the compound heterozygous *Cebpa* alone [116]. In human biallelic *CEBPA* AML patients, additional *TET2* mutations downregulate *GATA2* and upregulate multiple inflammatory signaling components, including *TLR1*, *TLR5*, *IFNGR1*, *IFNGR2*, and *IL6ST*, resembling the $-77^{-/-}$ model [117]. It is attractive to ascertain how *GATA2* mutations in $CEBPA^{Lp30/K313KK}$ leukemic stem and progenitor cells confer sensitivity to inflammation and how inflammatory signaling influences the dual mutant *CEBPA*;*GATA2* leukemogenesis.

A newly defined germline genetic variant altering the inter-zinc finger spacer presents a

unique opportunity to investigate how spatial constraints between GATA2 N- and C-fingers influence GATA2 activity. This variant involves the insertion of 27 nucleotides into the GATA2 exon 5 to prolong the distance between two fingers by nine aa (A345delinsALLVAALLAA or 9aa-Ins) [118]. The 9aa-Ins mutant is largely attenuated in chromatin remodeling and occupancy yet retains its regulatory role on a minority of GATA2-regulated genes [46]. 9aa-Ins is incapable of suppressing the elevated *Irf8*, *Il6st*, and *Il6ra* in a genetic rescue assay [46], suggesting that 9aa-Ins hematopoietic progenitors may be hyperresponsive to the corresponding signaling. Varying the insertion length with engineered constructs (2-, 4-, 6-, and 8aa-Ins) reveals that the spacer constraint is more sensitive to activation than repression, in which insertions $\geq$ 2aa corrupt GATA2-regulated activation and $\leq$ 6aa retain GATA2-regulated repression [46]. Since GATA2 deficiency elevates the activity of PU.1 in myeloerythroid progenitors [46], it is informative to test whether GATA2-PU.1 antagonistic interaction tolerates 2, 4, or 6 aa insertion and whether the insertion mutants influence PU.1 chromatin occupancy in response to inflammatory signaling.

The complexity of GATA2 non-coding mutations further expands the predisposition mechanisms, and enhancer motif-structure−function analyses using a series of mouse models reveal how a human disease-instigated enhancer influences inflammatory responses. +9.5 enhancer harbors the E-box-spacer-WGATAR composite element and an Ets motif 19 nucleotides away from WGATAR for heptad transcription factors to occupy chromatin and recruit coregulators (Figure 1.3B) [84, 119]. Known factors include T-cell Acute Lymphocytic Leukemia 1 (TAL1) at E-box (CANNTG), GATA2 at WGATAR, and ETS family members Friend Leukemia Integration 1 (FLI1) and ERG at Ets motif (GGAW) [79, 80, 120, 121]. Genetic ablation of individual or combinatorial motifs reveals their differential and synergistic contributions to hematopoiesis and pathogenesis. The loss of composite element [+9.5(E-box-spacer-WGATAR)$^{-/-}$ or +9.5$^{-/-}$ for short] or E-box and Ets while retaining WGATAR [+9.5(E-box;Ets)$^{-/-}$] disrupts AGM HSC emergence and generates embryos with defective fetal liver hematopoiesis and lethality at E14.5 [36, 37, 122]. By contrast, a

mouse strain defective in one nucleotide of the E-box (CATCTG to GATCTG) and lacking 27 upstream nucleotides survives to adulthood with a minimal phenotype [123]. Since the DNA-binding affinity to transcription factors may become impaired or unchanged following a single nucleotide alteration in the binding motif [124], and it is not known if such alteration influences heptad complex assembly at the +9.5 enhancer, genetic ablation of the entire E-box while retaining the integrity of WGATAR and Ets may be required to give a definitive phenotype compared to the described +9.5(E-box)$^{-/-}$ strain. Genetic ablation of the Ets motif [+9.5(Ets)$^{-/-}$] reduces *Gata2* expression but does not impact the transcriptome nor hematopoiesis in steady-state embryos and adults [122]. In contrast to the +9.5(E-box)$^{-/-}$ model, the deleterious impact of Ets deletion is only revealed under the influence of additional insults, demonstrating the silent nature of the predisposing mutation. The absence of +9.5 Ets suppresses *Gata2* induction in response to the myeloablation-activated stress using the chemotherapy drug 5-Fluorouracil (5-FU), rendering bone marrow HSPCs defective in regeneration capacity with a hyporesponsive transcriptome and prolonging marrow hypocellularity [122]. Systemic 5-FU induces inflammation and cytokine production in multiple organs [125, 126]. TLR3-mediated chronic inflammation promotes mortality and hypocellular bone marrow, indicating a bone marrow failure predisposition in the +9.5(Ets)$^{-/-}$ model relative to wild type [123]. +9.5 Ets deletion therefore establishes a conditionally pathogenic paradigm in which the variant displays a benign phenotype in the steady state, and its pathogenicity is only present following a secondary insult, such as inflammation.

An innovative mouse strain, modeling the epigenetic silencing mechanism on one *Gata2* allele (E-box-spacer-WGATAR) and Ets motif ablation on the other allele, further reveals how non-coding *GATA2* variants influence inflammatory responses. The compound heterozygous (CH) mice have a minimal phenotype with modest alterations in steady-state bone marrow hematopoiesis [123]. Although *Gata2* expression is not affected by the compound variants, 5-FU−induced myeloablation stress abrogates HSPC regeneration and reduces CH mouse survival to a greater extent relative to +9.5$^{-/-}$ and +9.5(Ets)$^{-/-}$ models [123]. The

compound variants render HSPCs non-responsive to acute TLR4 signaling [123]. Despite normal levels of the Granulocyte Colony-Stimulating Factor (G-CSF) Receptor, CH HSPCs do not respond to the stem cell mobilizing agents G-CSF, IL8, or Very Late Antigen 4 antagonist, save Plerixafor [123, 127]. These selective defects demonstrate the complexity of enhancer variations in regulating inflammatory and cytokine signaling.

Following GATA2 germline variants, other predisposing mutations might directly induce transcriptome alteration with an inflammatory signature or synergize with pre-existing inflammatory aberrations to develop hematologic malignancies. An example is the ETS Variant 6 (ETV6), whose hereditary mutations predispose patients to thrombocytopenia and lymphoblastic leukemia [128–130]. In a murine $Etv6^{R355X/+}$ strain to model human R359X heterozygosity in Thrombocytopenia 5 disorder, the HSPC composition in steady-state bone marrow exhibits minimal deviation, but R355X heterozygosity reduces B-cell/myeloid engraftment and abrogates tertiary reconstitution capacity in serial transplantation assays [131]. ETV6 preoccupies chromatin of inflammation-activated loci, including *Tnf*, *Ccl3*, *Il1b*, *Tlr4*, and *Myd88*, and R355X heterozygosity reduces ETV6 occupancy at ∼800 loci [131]. Under regeneration-induced stress, such as transplantation, R355X heterozygosity elevates inflammatory gene expression transcriptome-wide and TNF production relative to wild-type HSPCs [131]. However, whether this aberrant TNF signaling drives leukemogenesis is not yet determined. Another example is the RUNX1 frameshift mutant S291fsX300. As microRNA miR-146a is a negative regulator of TRAF6 and RIPK2 signaling, genetic ablation of *miR-146a* models a persistent inflammatory condition [132, 133]. RUNX1 S291fsX300 mutant alters the transcriptome of $miR\text{-}146a^{-/-}$ HSPCs and upregulates innate immune machinery genes, including *Tlr1*, *Tlr7*, and *Tlr13* [134]. This cooperative activity exaggerates the aberrant inflammatory phenotype to promote HSPC expansion, MDS, and bone marrow failure, which progress to AML in subsequent transplanted murine recipients.

## 1.4 Impact of somatic variation on genome sensing of inflammation

Aging-associated spontaneous mutations in epigenetic regulator genes, most frequently *DNMT3A*, *TET2*, and *AXSL1*, drive progressive clonal hematopoiesis and are associated with increased risk of hematologic malignancies and cardiovascular diseases [29–31]. DNA Methyltransferase 3A (DNMT3A) is a member of the DNA Methyltransferase family, which catalyzes the addition of a methyl group to the 5' position of the Cytosine in the CpG dinucleotide [135, 136]. By contrast, Ten-Eleven Translocation 2 (TET2) is responsible for the conversion of 5'-Methylcytosine to 5'-Hydroxymethylcytosine that can be further oxidized and excised to become unmethylated Cytosine [137, 138]. TET2-mediated enhancer demethylation facilitates chromatin accessibility and promotes gene expression [139, 140]. DNMT3A mutations cause DNA hypomethylation genome-wide, while the active euchromatic compartment of the TET2-deficient genome is DNA hypermethylated [141–143]. Although these two DNA methylation machineries have opposing activities, murine models reveal similar biological consequences of their deficiency, including clonal expansion and predisposition to myeloid/lymphoid malignancies [144–150]. Interestingly, $Tet2^{-/-}$ HSPCs expressing $Dnmt3a^{R882H}$ mutant or dual ablation of *Tet2* and *Dnmt3a* in a mouse model reveal cooperative activities of these two molecules to amplify HSPC expansion, drive leukemia/lymphoma, and reduce survival [151, 152]. TET2 is required for DNMT3A localization in the heterochromatin compartment [143]. Therefore, a combinatorial deficiency promotes heterochromatic DNA hypomethylation but euchromatic DNA hypermethylation [143]. Additional Sex Comb-Like 1 (ASXL1) is a member of the Enhancers of Trithorax and Polycomb, and it interacts with BRCA1 Associated Protein 1 to form Polycomb Repressive Deubiquitinase Complex, which removes monoubiquitin from H2AK119Ub [153]. In the $Asxl1^{tm/+}$ mouse strain, G646fs heterozygosity reduces heterochromatic H3K9me2 and H3K9me3 and euchromatic H2AK119Ub deposition to modulate gene expression [154].

These data support a model in which DNMT3A, TET2, and ASXL1 promote chromatin integrity, and their clonal hematopoiesis-associated mutations derepress the expression of heterochromatic genes, including transposable elements and genes related to inflammation [154].

Since these chromatin regulators are important for transcription, their mutations might rewire the HSPC transcriptome, deviating the expression of genes encoding receptors and inflammatory mediators as a mechanism to sense and respond to inflammation. Alpha Kinase 1 (ALPK1) is a cytosolic pattern recognition receptor that recognizes the presence of ADP-D-glycero-$\beta$-D-manno-heptose (ADP-heptose), a soluble LPS intermediate released by Gram-negative bacteria and circulated in the blood system of older individuals [155, 156]. DNMT3A deficiency or heterozygous R878H mutant upregulates *ALPK1* expression, rendering mutant HSCs hypersensitive to APD-heptose signaling to promote pre-leukemic stem/progenitor cell expansion as a mechanism for clonal hematopoiesis [156]. In NOD SCID Gamma mice with fatty bone marrow to model age-related accumulation of adipocytes, human HSPCs carrying DNMT3A R882H mutant exhibit an inflammatory transcriptome and elevated IL6 production [157]. Neutralizing IL6 with antibodies reduces clonal expansion to levels similar to normal bone marrow [157]. Similarly, a high-fat diet induces macrophage infiltration in the adipose tissue and plasma IL6 elevation after long-term *Dnmt3a*$^{+/-}$ HSPC transplantation [158]. Genetic ablation of *Tet2* upregulates multiple components of inflammatory signaling in HSPCs, including *Tlr4*, *Nfkbiz*, *Stat3*, and *Il6*, rendering *Tet2*$^{-/-}$ mice hyperresponsive to LPS stimulation with elevated serum cytokine/chemokine production, including IL6 [159]. TLR4 signaling activates phospho-STAT3 and upregulates lncRNA *Morrbid* to promote a pro-survival gene expression program and confer *Tet2*$^{-/-}$ HSPCs competitive advantages in clonal expansion and reconstitution capacity [159]. Under a different secondary insult, such as genetically induced hyperglycemia stress by an Insulin point mutation (*Ins2*$^{Akita/+}$), the proinflammatory transcriptome established by *Tet2* heterozygosity is amplified to promote myelopoiesis and MPN/AML-like phenotypes [160]. Genetic

deletion of one *Morrbid* allele alleviates inflammatory responses and attenuates the proliferation advantage of *Tet2*$^{+/-}$ HSPCs to physiological levels [159, 160]. The elevated inflammatory transcriptome and aberrant myelopoiesis in compound *Tet2*$^{+/-}$;*Ins2*$^{Akita/+}$ model are associated with *Spi1* upregulation and *Gata2* downregulation [160]. In bone marrow dendritic cells and macrophages, the transcription factor I$\kappa$B$\zeta$, encoded by *Nfkbiz*, mediates TET2 interaction with the *Il6* promoter, and TET2 recruits Histone Deacetylase 2 to repress *Il6* transcription in response to TLR4 signaling [161]. These data might provide a mechanistic explanation for the elevated IL6 production in clonal hematopoiesis models of TET2 deficiency.

## 1.5 Conclusions and general principles

Mounting of experimental evidence establishes models for understanding inflammation sensing in the genome. The hematopoietic genome controls the expression of signaling devices and inflammatory mediators essential for sensing and responding to inflammation (Figure 1.4A). Imbalance in transcription factor levels/activities by genetic variations disrupts the stem and progenitor genetic network, elevating or reducing the expression of the signaling machinery and altering the cellular sensitivity and fate potential in response to inflammatory signaling (Figure 1.4B). Beyond the paradigm of canonical signal-dependent transcription factors, emerging data demonstrate that inflammation influences the activity of hematopoietic transcription factors, *e.g.*, GATA2 and PU.1, at chromatin or post-chromatin processes [45]. GATA2 and PU.1 chromatin occupancy parses inflammation-activated genes into two classes with different signaling requirements. In one class, genes are preoccupied by GATA2 and PU.1 and transcribed in the basal state, and inflammation elevates transcription. In another class, GATA2 and PU.1 only occupy chromatin upon signaling, and transcription is uniquely sensitive to IKK$\beta$ inhibition. Since the promoters and introns of inflammation-activated genes harbor motifs for many transcription factors not known to be linked to signaling, this dual mechanism raises the question of whether other lineage-determining

transcription factors important for development are also responsive to inflammation in a similar fashion. A CRISPR screening strategy coupled with an inflammation-sensitive assay will be instructive to evaluate which developmental regulators are inflammation activators or repressors.

Besides germline variants, somatic mutations that arise during aging in genes encoding chromatin regulators provide a mechanistic depth for genome function to sense and respond to inflammation. While mutations in transcription factors might expel factors from a subset of their target loci, induce ectopic activity to regulate genes not normally regulated, or be largely inactive, chromatin-regulator mutations influence the epigenetic layer by methylating or demethylating enhancers and promoters or derepressing heterochromatin to modulate the transcriptional activity of genes related to inflammation. Together, dysregulated inflammatory signaling and/or additional mutations trigger leukemia-predisposed HSPCs to hematologic malignancies.

New generation sequencing technologies and large-scale population surveys enable the identification of new genetic variants in human diseases, but laborious efforts are required to understand the functional consequences of the expanding variant repertoire. Innovative animal models and rigorous biochemical and genetic assays provide an essential toolbox to dissect the mechanisms underlying predisposition and/or pathogenicity of genetic variants. The integration of inflammation and collaborating mutations as secondary triggers to drive pathogenesis nominates inflammation as an important activity metric to quantify the severity of genetic variants to inform clinical assessments.

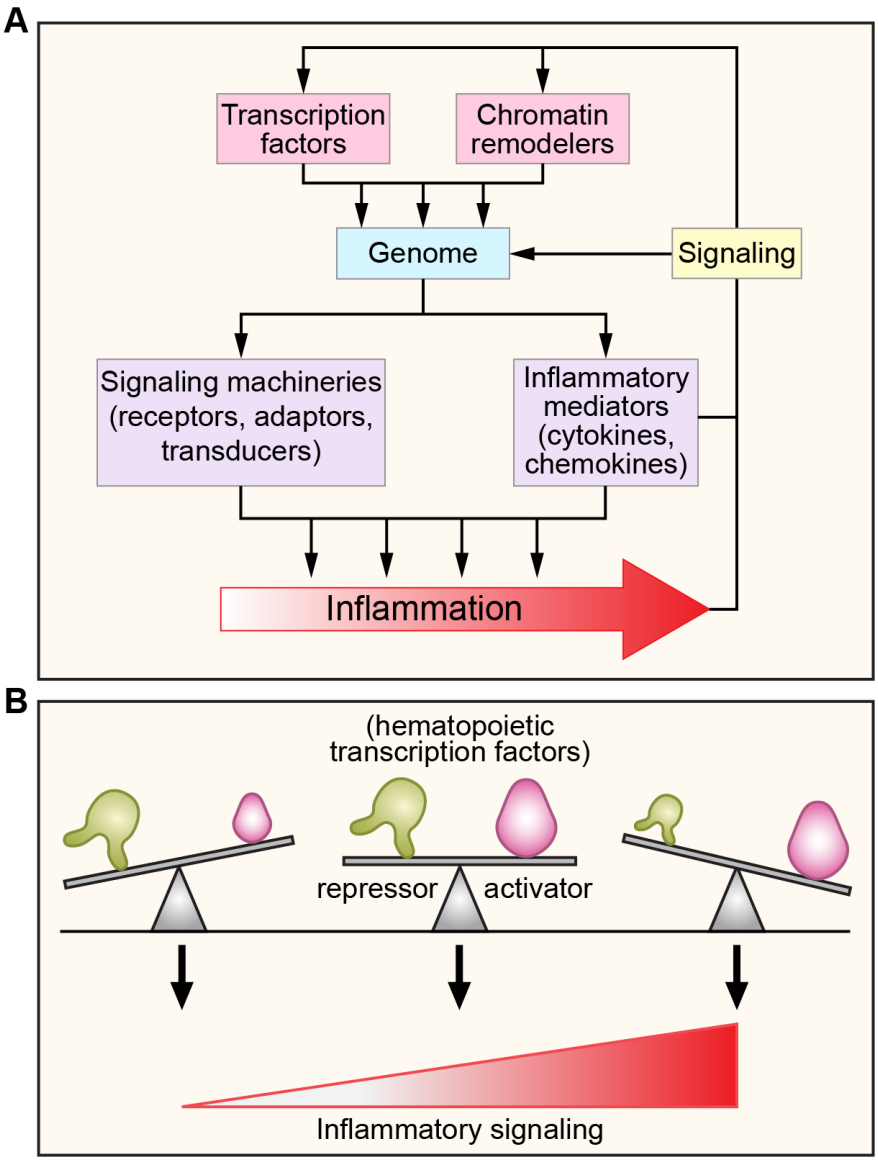


**Figure 1.4: Genetic and epigenetic mechanisms governing inflammation sensing.** (**A**) Transcription factors and chromatin remodelers regulate the expression of signaling machineries (receptors, adapters, and transducers) and inflammatory mediators (cytokines and chemokines) to sense and respond to inflammation. The inflammatory signaling feeds back to transcription factors and chromatin remodelers to regulate their genome function. (**B**) The balanced activities of hematopoietic activators and repressors establish and maintain physiological homeostasis, and genetic perturbations affecting factor concentration/activity disrupt transcriptional responses to inflammatory signaling.

# Chapter 2

# Materials and Methods

## 2.1 Experimental models and subject details

### 2.1.1 Mouse models and husbandry

The generation of *Gata2* $-77^{-/-}$ mice was previously described [38]. *Myd88*$^{-/-}$ mice were purchased from Jackson Laboratory (009088). These mice were crossed to generate *Gata2* $-77^{+/-}$; *Myd88*$^{-/-}$ mice for timed matings. The animal protocol was approved by the Institutional Animal Care and Use Committee at the University of Wisconsin-Madison with the approval number M005602, following regulations from the Association for Assessment and Accreditation of Laboratory Animal Care International. Timed matings were performed using 8-18 week-old female mice. Embryos were genotyped as described in the Genotype Analysis section.

### 2.1.2 Cultured cells

hi$-77^{+/+}$ (wild-type), hi$-77^{-/-}$ (GATA2$^{low}$), and hi$-77^{-/-}$;*Spi1* URE$^{-/-}$ (GATA2$^{low}$PU.1$^{low}$) progenitor lines were previously generated and described [43, 46]. hi$-77^{-/-}$;*Runx1*$^{-/-}$ (GATA2$^{low}$RUNX1$^{null}$) and hi-*Runx1*$^{-/-}$ (RUNX1$^{null}$) progenitor lines were generated in this study by Dr. Koichi R. Katsumura using CRISP/Cas9 gene editing tool. hi-cells were cultured in OPTI-MEM (31985-070; Fisher Scientific) supplemented with 10% Fetal Bovine Serum [(FBS) 100-106; GeminiBio], 1% Penicillin-Streptomycin (SV30079.01; Cytiva), 1% Stem Cell Factor (SCF)-conditioned medium, 30 $\mu$M 2-Mercaptoethanol (M3148; Sigma-Aldrich), 1 $\mu$M $\beta$-Estradiol, and 500 $\mu$g/mL G418 (400-111P-001; Gemini Bio).

## 2.2 Method details

### 2.2.1 Primary fetal progenitor cell isolation

The protocol was described previously [162]. *Gata2* $-77^{+/-}$ and *Gata2* $-77^{+/-}$;*Myd88*$^{-/-}$ male and female mice were subjected to timed-matings, and the day in which the vaginal

plug was detected was day 0.5. Pregnant females were euthanized with $CO_2$ on day 14.5, and the embryos were placed into Iscove's Modified Dulbecco's Medium (IMDM, Life Technologies) containing 10% FBS. Fetal tail clips were used for genotyping. The fetal livers were harvested, and lineage depletion was conducted with Biotinylated antibodies (CD3e, CD11b, CD19, CD45R, GR-1, CD71, and Ter119) and MojoSort Streptavidin Nanobeads (BioLegend). The lineage-negative ($Lin^-$) progenitors were maintained in IMDM containing 20% FBS, 4% SCF-conditioned medium, 4% IL3-conditioned medium, and 1% Penicillin-Streptomycin. For cellular response analysis, 100,000 primary E14.5 $Lin^-$ progenitor cells were treated with Phosphate-Buffered Saline (PBS) containing 0.1% Bovine Serum Albumin [(vehicle) A30075; Research Products International], 100 ng/mL TLR1/2 agonist $Pam_3CSK_4$ (tlrl-pms; InvivoGen), 10 ng/mL TLR2/6 agonist $Pam_2CSK_4$ (tlrl-pm2s-1; InvivoGen), 100 ng/mL TLR4 agonist Lipopolysaccharide LPS (L2630; Sigma-Aldrich), or 1 ng/mL mouse Interferon-gamma (IFN$\gamma$) (315-05-100UG; PeproTech) for 4 h. Cells were harvested for mRNA isolation.

### 2.2.2 Genotype analysis

Harvest a small piece of the tail tip ($\sim$5$-$10 mm) at weaning, half of a fetal tail during embryo harvest, or a million cells into an Eppendorf tube. Added 600 $\mu$L Lysis Solution [containing 4 mL of 1 M Tris-HCl (pH 8.0), 6 mL of 5 M NaCl, 40 mL of 0.5 M Ethylenediaminetetraacetic Acid (EDTA), and 20 mL of 10% Sodium Dodecyl Sulfate (SDS) in a final volume of 200 mL] and 3 $\mu$L of 20 mg/mL Proteinase K (8107S; New England Biolabs) and incubated overnight or until dissolved at $55^0$C. Let the tube cool to room temperature, then added 200 $\mu$L Protein Precipitation Solution (A7953; Promega). Vortexed for $\sim$20 s then centrifuged at 15,000 rpm for 3 min. Transfered $\sim$600 $\mu$L of the supernatant to a clean tube. Added of 100% Isopropanol, and gently inverted the tube $\sim$50 times to precipitate the DNA. Centrifuged at 15,000 rpm for 3 min, then poured off the supernatant. Washed the pellet with 200 $\mu$L of 70% Ethanol and inverted 5 times. Centrifuged at 15,000 rpm for 3 min, then discarded

the supernatant with a 200 $\mu$L pipette tip. Air dried the DNA pellet for 5-10 min, then dissolved the pellet in 100 $\mu$L water or TE Buffer. Incubated for 10 min at 55$^0$C to ensure the DNA pellet was solubilized. For PCR reaction, prepared a master mix as in Table 2.1. The primers were provided in Table 2.2. Transfered 49 $\mu$L of master mix into a PCR tube and added 1 $\mu$L of genomic DNA. Conducted the PCR reaction with a thermocycler. Load 10 $\mu$L of the PCR product on a 1% Agarose gel containing 5% of Ethidium Bromide (10 mg/mL) and ran the gel at ~105 V and 75-88 mA for 30-45 min. *Gata2* −77 primer set would give a 350 bp wild-type band and a 195 bp mutant band. *Myd88* primer set would give a 266 bp wild-type band and ~520 bp mutant band.

| **Reagent** | **n = 1 (*Gata2* −77 enhancer or *Runx1*)** | **n = 1 (*Myd88*)** |
|---|---|---|
| 5X GoTaq Buffer | 10 $\mu$L | 10 $\mu$L |
| 10 mM dNTPs | 1 $\mu$L | 1 $\mu$L |
| Primers | 2 $\mu$L | 3 $\mu$L |
| Water | 35.75 $\mu$L | 34.75 $\mu$L |
| Taq DNA Polymerase | 0.25 $\mu$L | 0.25 $\mu$L |

**Table 2.1: PCR reaction for mouse genotype analysis**

| **Primer** | **Forward (5'>3')** | **Reverse (5'>3')** |
|---|---|---|
| *Gata2* −77 | GGTATGTCGTGGGAGGCTGTTGA | GTTCTGCCCACCGCACAGCA |
| *Myd88* | wild-type: GTTGTGTGTGTCCGACCGT mutant: CCACCCTTGATGACCCCCTA | GTCAGAAACAACCACCACCATGC |
| *Runx1* | CTTCCTCTGCTCCGTGCTAC | GTTTTCATCGTTGCCTGCCA |

**Table 2.2: Primers for genotype analysis**

### 2.2.3 CRISPR/Cas9 gene editing

Guide sequences were designed by Integrated DNA Technologies (IDT) tools (idtdna.com). 100 pmol of CRISPR RNAs [(crRNAs), IDT] were mixed with 200 pmol of trans-activating CRISPR RNA [(tracrRNA), IDT] and incubated at 37$^0$C for 30 min. Eight $\mu$g of Cas9

(Aldevron) was added to the mixture and incubated at $37^0$C for 15 min. $2 \times 10^5$ hi−77 cells were resuspended in 20 $\mu$L of P3 Buffer with 22% Supplement (Lonza) and added to the RNP Complex. Electroporation was performed using the EO-100 program on a Nucleofector 4D (Lonza). After 72 h, cells were seeded into 96-well plates (0.5 cell/well), cultured, and transferred to 24-well plates. Clones were genotyped using a PCR assay. For homozygous mutant clones, the genomic DNA fragment including the deleted sequence was amplified by GoTaq DNA polymerase, cloned into the pBluescript vector, and sequenced. hi$-77^{-/-}$;*Runx1*$^{-/-}$ and hi-*Runx1*$^{-/-}$ progenitor lines were genotyped using the primer set provided in Table 2.2.

### 2.2.4 Cellular response analysis

For gene expression kinetics, 50,000 hi$-77^{+/+}$ and hi$-77^{-/-}$ cells were cultured in complete media containing $\beta$-Estradiol and G418, and cells were split every 2 days. Cells were harvested at days 2, 4, 6, 12, and 18 for mRNA isolation and protein analysis. To induce differentiation, cells were cultured in media without $\beta$-Estradiol and G418 for 2 days. The undifferentiated and differentiated cells were treated with vehicle, IFN$\gamma$, $Pam_3CSK_4$, $Pam_2CSK_4$, or their combinations for 4 h. For antagonizing NF-$\kappa$B signaling, cells were pretreated with increasing concentrations of IKK$\beta$ inhibitors before being stimulated with both IFN$\gamma$ and $Pam_3CSK_4$ for 4 h. IKK$\beta$ inhibitors are from Selleck Chemicals: BMS-345541 (S8044) or a gift from Dr. Shigeki Miyamoto (UW-Madison): IKK16 (S2882). For antagonizing JAK1/2 signaling, cells were pretreated with increasing concentrations of JAK1/2 inhibitor Ruxolitinib before being stimulated with both IFN$\gamma$ and $Pam_3CSK_4$ for 4 h.

### 2.2.5 Gene expression analysis

The protocol was previously described [43]. Cells were harvested and centrifuged at 2,500 rpm for 5 min at $4^0$C to remove the supernatant. Cell pellets were dissociated in 50 $\mu$L residual supernatant before adding 1 mL TRIzol (15596026; Invitrogen). For a low number of cells (*e.g.*, 20,000), cells were kept overnight in the cold room to facilitate TRIzol

digestion. Otherwise, cells were incubated in TRIzol for 10-15 min at room temperature. Added 250 $\mu$L Chloroform and shook the tube vigorously for about 15 s. Let the tube sit at room temperature for 5 min. Centrifuged at 14,500 rpm for 15 min. During centrifugation, prepared new 1.5 $\mu$L Eppendorf tubes and added 500 $\mu$L Isopropanol. After centrifugation, the mixture would form three layers: Top: clear, aqueous; Middle/interphase: white precipitated DNA; Bottom: pink organic phase. Carefully transfered the top aqueous phase using a p200 pipette into the labeled Eppendorf tube. Added 1.5 $\mu$L Linear Acrylamide, inverted tubes to mix, and let tubes sit at room temperature for 5-10 min. Centrifuged at 14,500 rpm for 10 min. Poured off Isopropanol and added 1 $\mu$L 75% Ethanol. Mixed gently and centrifuged at 10,00 rpm for 5 min. Pulled off the wash with p1000 pipette. Performed a quick spin to bring residual wash to the bottom of the tube and removed with p10 pipette. Air dried the RNA pellet for 5 min. Added approximately 15–25 $\mu$L (depending on the size of the pellet) of either sterilized TE Buffer or autoclaved water to dissolve the RNA pellet. RNA concentration was measured using a Nanodrop. The 260/280 ratio should be greater than 1.8 for high quality RNA samples.

To prepare complementary DNA (cDNA), transfered 500 - 1,000 ng of RNA (final volume of 6 $\mu$L) into a PCR tube and digested contaminated genomic DNA with 1 $\mu$L DNase I (18068015; Invitrogen) and 1 $\mu$L DNAase Buffer for 15 min at room temperature. DNase I was deactivated with 1 $\mu$L EDTA at $65^0$C for 10 min. Added 1.5 $\mu$L of the primer cocktail [prepared with 10 $\mu$L Random Hexamer (C1181; Promega) and 40 $\mu$L Oligo dT primer in a final volume of 100 $\mu$L] into the 9 $\mu$L of DNA-digested RNA above and heated at $68^0$C for 10 min using a thermocycler. Added 9.5 $\mu$L of a master mix [containing 4 $\mu$L 5X First Strand Buffer, 2 $\mu$L 0.1 M Dithiothreitol DTT, 1 $\mu$L Deoxynucleoside Triphosphates dNTP, 0.5 $\mu$L RNasin Ribonuclease Inhibitor (N2611; Promega), and 0.25 $\mu$L MMLV Reverse Transcriptase (18080093; Invitrogen) per reaction] to the RNA/primer coctail mixture. Included a no-Reverse Transcriptase control using a random sample. Incubated at $42^0$C for 1 h. Heated at $95^0$C for 5 min. Increased the final volume to 100 $\mu$L with autoclaved water.

| Primer | Forward (5'>3') | Reverse (5'>3') |
|---|---|---|
| *Gata2* mRNA | GCAGAGAAGCAAGGCTCGC | CAGTTGACACACTCCCGGC |
| *Irf8* mRNA | TGCCACTGGTGACCGGATAT | GCCCCCGTAGTAGAAGCTGA |
| *Spi1* mRNA | AGCTCAGCTGGATGTTACAG | TCGTAAGTAACCAAGTCATCCG |
| *Runx1* mRNA | TCACTGGCGCTGCAACAA | TCTGCCGAGTAGTTTTCATCGTT |
| *Tlr1* mRNA | AGCATTGCCACATGGGTATAG | GTTTGTGAATGCAGTTGGTGAA |
| *Tlr2* mRNA | TCGTAGCATCCTCTGAGATTTG | TCTCTGGAGCATCCGAATTG |
| *Tlr4* mRNA | CTCCTGGCTAGGACTCTGAT | CTGATCCATGCATTGGTAGGT |
| *Tlr6* mRNA | TCTTGGCTCATGTTGCAGAG | GTACCGTCAGTGCTGGAAATAG |
| *Tnf* mRNA | CAGCTGCTCCTCCACTTG | CAAATGGCCTCCCTCTCATC |
| *Cxcl10* mRNA | TCAGACATCTCTGCTCATCATTC | TCATCCCTGCGAGCCTAT |
| *Cd40* mRNA | GGGCTGCTTGTTGACAG | TGGCCATCGTGGAGGTA |
| *Gbp2* mRNA | GCAGCACCTTCATCTACAACA | GTCAGGTGATGACTTTGACTTGATA |
| *Gbp5* mRNA | CGTTCAAGGATGAGGGTGAAT | AGCATCCGCGTTCTTCTTAC |
| *Gbp6* mRNA | TTCCACAAGGCAAATGGGA | GCTGAGAACTGCACTTGGA |
| *Gbp7* mRNA | GCAGCAGCAAGCCTAAAG | CTCCATGTTGGGACCAGAT |
| *Ifi204* mRNA | CCACCACTTCTATGCTTCCTG | CTTCTGGAGCAGTGTTCTATGG |
| *Iigp1* mRNA | TATTCCTCTCAGGAGCAGTGAG | GAACAGCTGACCCATGACTT |
| *Ccl3* mRNA | GTGGAATCTTCCGGCTGTAG | CTTCTCTGTACCATGACACTCTG |
| *Ccl4* mRNA | TTCTGTGCTCCAGGGTTCTC | GCTGCCGGGAGGTGTAA |
| *Ccl5* mRNA | CACACTTGGCGGTTCCTT | CGTCAAGGAGTATTTCTACACCAG |
| *Cd69* mRNA | TTGTGGTTCACGGACACG | GACATGGAAATGGGCAAATGG |
| *Cmpk2* mRNA | TGCCATTGAAGGACTGGATG | GGCGACTGTAGGAGGACA |
| *Stat1* mRNA | GGCCCAGTGGCTGGAAA | CTGTGAGAGGAGGTCATGGAAG |
| 18S rRNA | CGCCGCTAGAGGTGAAATTCT | CGAACCTCCGACTTTCGTTCT |

**Table 2.3: Primers for mouse RT-qPCR analysis**

The cDNA was analyzed for genes of interest by Quantitative Real Time Polymerase Chain Reaction (RT-qPCR) using a ViiA 7 Real-Time PCR cycler. For a 20 $\mu$L reaction, used 1.5 $\mu$L cDNA with 7.7 $\mu$L *Power* SYBR Green PCR Master Mix (4367659; Applied Biosystems) and 0.8 $\mu$L primer solution (prepared by 10 $\mu$L of 100 $\mu$M Forward and 100 $\mu$M Reverse in 180 $\mu$L water). Quantities were determined using a standard curve and normalized to 18S rRNA control. Primer sequences were provided in Table 2.3.

### 2.2.6 Western blot analysis

Cells ($1 \times 10^6$/condition) were harvested by centrifuging at 2,500 rpm for 5 min at $4^0$C and washing with 1 mL of ice-cold PBS. Cell pellets were resuspended in 50 $\mu$L of ice-cold PBS

and 50 $\mu$L of 2X SDS Sample Buffer (0.378 g Tris, 1 g SDS, 10 mg Bromophenol Blue, 5 mL Glycerol, and 2.5 mL $\beta$-Mercaptoethanol in 20 mL autoclaved water; adjusted pH to 6.8 with HCl and added water to a final volume of 25 mL) and boiled for 10 min at $95^0$C. Prepared 2 mini gels using 15 mL 8% Resolving gel [6 mL water, 3 mL 40% Acrylamide and Bis-Acrylamide solution (1610144; Bio-Rad), 5.7 mL 1 M Tris pH 8.8, 150 $\mu$L 10% SDS, 150 $\mu$L 10% Ammonium Persulfate (APS), and 15 $\mu$L TEMED (1610800; Bio-Rad)] and 5 mL 4% Stacking gel (3.7 mL water, 500 $\mu$L 40% Acrylamide and Bis-Acrylamide solution, 630 $\mu$L 1 M Tris pH 6.8, 50 $\mu$L 10% SDS, 50 $\mu$L 10% APS, and 7.5 $\mu$L TEMED). Used 1 mL Isopropanol to straighten the top border when making Resolving gel, and washed away Isopropanol with water before pouring Stacking gel. Allowed $\sim$30 min to polymerize each gel.

Cells (100,000 per condition) were analyzed on 8% Resolving gels by SDS Polyacrylamide Gel Electrophoresis with 1X SDS Running Buffer (prepared 10X solution with 30.3 g Tris, 144.2 g Glycine, and 10 g SDS in a final volume of 1 L, pH 8.1-8.8). Ran the gel for 30 min at 20 mA through the Stacking gel and for $\sim 2-2.5$ h at 25 mA through the Resolving gel. Proteins were transferred to Polyvinylidene Difluoride PVDF membranes with 1X Transfer Buffer (prepared 10X solution with 30.3 g Tris and 144.2 g Glycine in a final volume of 1 L, pH 8.1-8.8) containing 20% Methanol at 200 V for 1 h. Used ice to cool the heat during the transfer. The membranes were blocked with 5% milk in Tris-Buffered Saline with Polysorbate (Tween) 20 and incubated with primary antibodies overnight with agitation in the cold room. GATA2 antibody was described previously [163]. The following antibodies were from Cell Signaling: p-STAT1 (9167), STAT1 (14995), p-STAT3 (9145), STAT3 (12640), p-ERK1/2 (9101), ERK1/2 (9102), p-p38 (9216), p38 (8690), p-JNK (9255), JNK (9252), PU.1 (2258), $\alpha$-Tubulin (3873), and $\beta$-Actin (3700). RUNX1 (sc-365644) antibody was from Santa Cruz Biotechnology. Secondary antibodies were from Jackson Laboratory. Proteins were detected and quantified with Chemiluminescence (West Femto, 34094; Thermo Fisher) using LI-COR imaging instrument, and densitometry analysis was performed with Image Studio.

### 2.2.7 Cytokine/chemokine protein quantification

200,000 undifferentiated or 2-day differentiated hi$-77^{+/+}$ or hi$-77^{-/-}$ cells were treated with IFN$\gamma$, $Pam_3CSK_4$, $Pam_2CSK_4$, or combinations with IFN$\gamma$ for 4 h. Supernatants were collected for TNF$\alpha$, CCL3, CCL4, and CCL5 protein analysis using mouse 4 plex (Millipore, MCYTOMAG-70K-04) for Millipore Luminex 2000.

### 2.2.8 GATA2 rescue and signaling analyses

GATA2 deficiency in hi$-77^{-/-}$ progenitors was rescued by infection with GATA2-expressing retrovirus as described. Murine *Gata2* cDNA and Murine Stem Cell Virus plasmid pMSCV were packaged in HEK293T cells. 24 h and 48 h post-transfection, the retrovirus-containing supernatant was harvested and stored at -80$^0$C. GATA2 retrovirus was spinoculated with hi$-77^{-/-}$ progenitors for 90 min at 2,800 rpm at 30$^0$C. Cells were expanded in OPTI-MEM containing 10% FBS, 1% Penicillin-Streptomycin, 1% SCF-conditioned medium, 30 $\mu$M 2-Mercaptoethanol, and 1 $\mu$M $\beta$-Estradiol for 24 h. Infected cells were selected with Puromycin at a final concentration of 2 $\mu$g/mL for 48 h. Cells were counted, and 50,000-100,000 cells were treated with different concentrations of $Pam_3CSK_4$ for 4 h. Cells were harvested for RNA isolation and RT-qPCR analysis. For signaling rescue analysis, 200,000-500,000 cells were treated with IFN$\gamma$ and $Pam_3CSK_4$ for 1 h. Cells were harvested for Western blot analysis.

### 2.2.9 Flow cytometry and cell sorting

The cellular composition of E14.5 fetal liver was quantified using Attune (Thermo Fisher Scientific) flow cytometers, and Common Myeloid Progenitors and Granulocyte Monocyte Progenitors were sorted using FACSAria (BD Biosciences) as previously described. Unless specified, most antibodies were from BioLegend. Fluorescein Isothiocyanate-conjugated B220 (103206), TER-119 (116206), CD3 (100306), CD5 (11-0193-85; Thermo Fisher Scientific), CD11b (101206), CD11c (117306), CD49b (108906), Ly6G (127606), and Sca1

(108106) antibodies were used for lineage exclusion. Other antibodies were Blue Violet (BV) 605-conjugated CD16/CD32 (563006; BD Biosciences), BV711-conjugated Ly6C (128017), Phycoerythrin-conjugated CD115 (135506), eFluor 660-conjugated CD34 (50-0341; Thermo Fisher Scientific), Peridinin Chlorophyll-efluor710-conjugated CD135 (461351; Thermo Fisher Scientific), and Phycoerythrin-Cy7-conjugated cKit (105814). Cells were washed with ice-cold PBS containing 10% FBS and resuspended in 49,6-diamidino-2-phenylindole (DAPI, 100 ng/mL) buffer for live-dead detection.

### 2.2.10 RNA-sequencing

Two RNA-seq experiments were conducted in this study. In the first experiment (GSE218445), hi$-77^{+/+}$ and hi$-77^{-/-}$ cells were treated with vehicle, IFN$\gamma$, $Pam_3CSK_4$, or both agonists for 4 h. In the second experiment (GSE279155), hi$-77^{-/-}$ and hi$-77^{-/-}$;*Spi1* $URE^{-/-}$ cells were treated with vehicle, IFN$\gamma$, $Pam_3CSK_4$, or both agonists for 4 h; hi$-77^{+/+}$ cells were treated with vehicle or both agents (n = 4 independent treatments). RNA was isolated using TRIzol and purified using RNeasy MinElute Cleanup Kit (74204; Qiagen). The RNA library was prepared with Illumina TruSeq Stranded Total RNA (rRNA reduction) and sequenced using Illumina NovaSeq 6000 by the UW-Madison Gene Expression Center. Read alignment was performed by STAR (version 2.5.2b) [164] to the mouse genome (version mm10). Gene expression levels were quantified by RSEM (version 1.3.0) [165] and differential expression was determined with edgeR (version 3.36.0) [166]. A Differentially Expressed Gene (DEG) was defined as having $|log_2(fold\ change)| \geq 1$, adjusted $P < 0.05$, and Transcripts per Million (TPM) $\geq 1$ in all the replicates in at least one of the two conditions. DEGs were divided into activated, which had higher expression in the numerator condition than in the denominator condition, and repressed, which had lower expression in the numerator condition than in the denominator condition. Kyoto Encyclopedia of Genes and Genomes (KEGG) terms were determined with kegga function from limma (version 3.50.1) [167]. Motif analysis was conducted with AME from MEME (version 5.3.3) [168] on proximal promoters and introns

of DEGs. The proximal promoters were defined as from 1 kb upstream of the Transcription Start Site (TSS) to 100 bp downstream of the TSS. The proximal promoters and introns of protein-coding or lincRNA-expressing genes on chromosomes 1-19, X, or Y, were analyzed. Chromosome M was excluded.

### 2.2.11 Cleavage under target and tagmentation (CUT&Tag)

CUT&Tag was conducted as previously described [169–171].

Day 1: Concanavalin A magnetic beads (BP531; Bangs Laboratories) were activated by washing twice in Binding Buffer (20 mM HEPES pH 7.9, 10 mM KCl, 1 mM $CaCl_2$, 1 mM $MnCl_2$, and 0.1% BSA). Before CUT&Tag, hi$-77^{+/+}$, hi$-77^{-/-}$, and hi$-77^{-/-}$;*Spi1* URE$^{-/-}$ were treated with vehicle or IFN$\gamma$-Pam$_3$CSK$_4$ combination for 4 h. hi-cells were gently crosslinked with 0.1% Formaldehyde for 2 min and quenched with 75 mM Glycine. Cells were washed twice in 1.5 mL of Wash Buffer (20 mM HEPES pH 7.5, 150 mM NaCl, 0.83 mM Spermidine, 0.1% BSA, and one Roche Complete Protease Inhibitor EDTA-free tablet) and resuspended in 1 mL Wash Buffer. For 4 antibodies, 600,000 cells in 1 mL final volume of Wash Buffer were mixed with 40 $\mu$L activated bead suspension and rotated for 30 min at room temperature. On a magnetic rack, wash buffer was replaced with 600 $\mu$L of Antibody Buffer (Wash Buffer plus 0.1 $\mu$g/mL Digitonin and 2 mM EDTA), and aliquoted into 4 tubes (150 $\mu$L each). 1.2 $\mu$g affinity-purified rabbit polyclonal anti-GATA2 antibody [81, 163], 1.2 $\mu$g anti-PU.1 mouse antibody (sc-390405; Santa Cruz), 1 $\mu$g H3K4me3 rabbit antibody (ab213224; Abcam), or 1 $\mu$g rabbit IgG isotype-matched control (10500C; Invitrogen) was added to each tube. Tubes were rotated overnight at $4^0$C on a nutator.

Day 2: After a quick spin, tubes were replaced on a magnetic stand, and Antibody Buffer was replaced with 150 $\mu$L Dig-Wash Buffer (Wash Buffer plus 0.1 $\mu$g/mL Digitonin) containing secondary antibody (1:100 dilution) for either rabbit or mouse antibody. After an hour on the nutator at room temperature, cells were washed three times with Dig-Wash Buffer. Resuspended cells in 150 $\mu$L Dig-300 Buffer (20 mM HEPES pH 7.5, 300 mM

NaCl, 0.83 mM Spermidine, 0.1 $\mu$g/mL Digitonin, 0.1% BSA, and one Roche Complete Protease Inhibitor EDTA-free tablet) containing pA-Tn5 pre-loaded with MEDS adapters (1:250 dilution). After nutating at room temperature for 1 h, cells were washed three times with Dig-300 Buffer. 300 $\mu$L Tagmentation Buffer (Dig-300 Wash plus 10 mM $MgCl_2$) was added, and cells were nutated at $37^0$C for 1 h. Cells were isolated by centrifugation, and 10 $\mu$L 0.5 M EDTA was added to stop tagmentation, followed by the addition of 3 $\mu$L 10% SDS and 3 $\mu$L Proteinase K [(20 mg/mL) P8107S; New England Biolabs]. Cells were incubated at $37^0$C overnight on a thermomixer at 600 rpm.

Day 3: DNA was purified by either Phenol-Chloroform extraction followed by Ethanol precipitation or spin columns. The following will describe spin column method using DNA Purification Buffers and Spin Columns (ChIP, CUT&RUN, CUT&Tag) kit (14209; Cell Signaling) according to the manufacturer's protocol with modifications. After overnigh incubation, centrifuged tubes at room temperature for 2 min at 15,000 g and placed tubes on the magnetic rack for 30 s to 2 min. Transfered the supernatant (containing CUT&Tag DNA fragments) to new 2 mL tubes. The volume of the supernatant was 316 $\mu$L (= 300 $\mu$L Tagmentation Buffer + 10 $\mu$L EDTA + 3 $\mu$L SDS + 3 $\mu$L Proteinase K). At this point, samples could be stored at $-20^0$C for up to a week. If doing so, samples need to be warmed to room temperature before DNA purification. Added DNA Binding Buffer with a volume five times the volume of the sample (in this case, 1580 $\mu$L). Inverted a few times to mix. Transfered 600 $\mu$L of each sample to a DNA spin column in a collection tube. Centrifuged at 15,000 g in a microcentrifuge for 30 s. Detached the spin column from the collection tube and discarded the liquid. Put the spin column back into the empty collection tube. Transfered the same amount of each sample and spin again until the entire sample had been spun through the spin column. Added 750 $\mu$L of DNA Wash Buffer to the spin column in the collection tube. Centrifuged at 15,000 g for 30 s. Discarded the liquid. Centrifuged at 15,000 g for 30 s to dry the column. Discarded the collection tube and liquid. Placed the spin column in a 1.5 mL clean Eppendorf tube. Added 30 $\mu$L of DNA Elution Buffer to the

center of the column. Centrifuged at 15,000 g for 30 s to elute DNA. Discarded the spin column. Samples could be stored at $-20^0$C for up to 6 months.

Library preparation: To determine the number of cycles needed for library preparation, 1.31 $\mu$L DNA was analyzed by RT-qPCR in a 25 $\mu$L reaction containing 0.5 $\mu$L of 10 $\mu$M i5 primer, 0.5 $\mu$L of 10 $\mu$M i7 primer, 12.5 $\mu$L PowerUp SYBR Green Master Mix (A25742; Applied BioSystems), and 10.19 $\mu$L water. A standard curve was not needed for this RT-qPCR assay. The PCR was set up as in Figure 2.1.

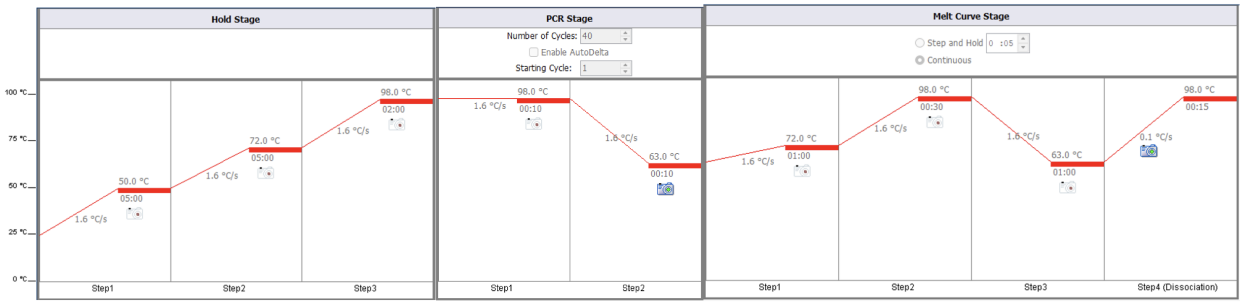


**Figure 2.1: Program for RT-qPCR assay with CUT&Tag DNA.**

Libraries were prepared with 21 $\mu$L of CUT&Tag DNA, 25 $\mu$L NEB Next HiFi 2X PCR Master Mix (M0514S; New England Biolabs), 0.5 $\mu$L of 10 $\mu$M i5 primer, and 0.5 $\mu$L of 10 $\mu$M i7 primer. The number of PCR cycles was determined based on the 1.31 $\mu$L DNA-test RT-qPCR above (Figure 2.2). The thermocycler was set up as in Table 2.4. Sample concentration was determined using Qubit 1X dsDNA HS Assay (Q33231; Thermo Fisher). The quality of the library was assessed using Bioanalyzer High Sensitivity DNA Analysis (Agilent). Samples were pooled and sequenced on NovaSeq 6000 using 50 bp paired-end sequencing at about 10 million reads per sample.

Before sending libraries for sequencing, 2 $\mu$L of a library was used for a diagonistic RT-qPCR assay at predicted occupancy sites. Added 2 $\mu$L of the library on to the column membrane (*e.g.*, QIAprep Spin Miniprep Kit) to clean up the DNA. Added 750 $\mu$L Wash Buffer. Spun down at 15,000 rpm for 1 min. Discarded the flow-through. Spun down again to remove residual liquid. Added 50 $\mu$L Elution Buffer. Spun down at 15,000 rpm for 1 min. Samples could be stored in $-20^0$C. Used 1.5 $\mu$L of the clean-up DNA library with 2.5 $\mu$L

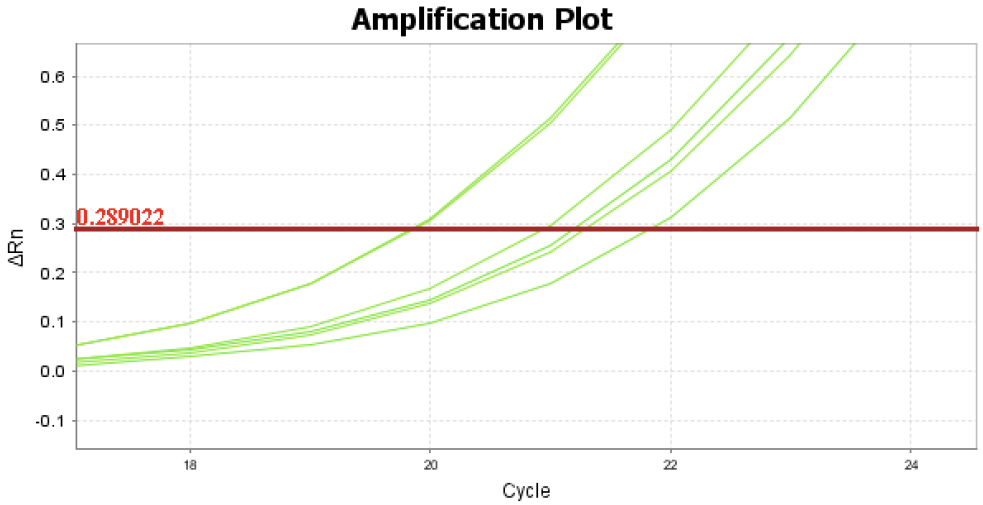


**Figure 2.2: Amplification plot for determining PCR cycle number for CUT&Tag library preparation.** This example showed six samples (different conditions with the same antibody) that would be compared in the final analysis. 21 cycles would be selected so that all six samples would be amplified to the optimal range of $\Delta R_n$ of 0.15 - 0.5. In the real library preparation PCR reaction, 21 $\mu$L of CUT&Tag DNA was used in a 50 $\mu$L reaction; in this test PCR reaction, 1.31 $\mu$L of CUT&Tag DNA was used in a 25 $\mu$L reaction. The real PCR reaction would be $log_2[(21/50)/(1.31/25)] = 3$ cycles earlier. Therefore, the number of PCR cycles needed for library preparation of these six samples $= 21 - 3 = 18$.

| **Step** | **Program** |
|---|---|
| Step 1 | $72^0$C for 5 min |
| Step 2 | $98^0$C for 45 s |
| Step 3 | $98^0$C for 10 s |
| Step 4 | $63^0$C for 10 s |
| Repeat step 3-4 | (N − 1) times |
| Step 5 | $72^0$C for 1 min |
| Step 6 | hold at $4^0$C |

**Table 2.4: Thermocycler set up for CUT&Tag library preparation.** N was determined as in Figure 2.2 from the test RT-qPCR reaction using 1.31 $\mu$L of CUT&Tag DNA.

*Power* SYBR Green PCR Master Mix (4367659; Applied Biosystem), 0.2 $\mu$L primers for a specific occupancy site, and 5.8 $\mu$L water.

The CUT&Tag analyses were conducted in collaboration with Dr. Peng Liu. CUT&Tag FASTQ files were processed by removing the adapter `'CTGTCTCTTATACACATCT'` using the Cutadapt software (version 4.5) [172] and aligned to the mouse genome (version mm10) with Bowtie2 (version 2.5.1) [173]. Duplicated fragments were marked and removed with Picard (version 3.1.1). The CUT&Tag raw data were deposited in Gene Expression Omnibus with the accession number GSE279156.

## 2.3 Quantification and statistical analysis

Quantitative data were presented as mean ± SEM (Standard Error of the Mean) or as box-and-whisker plots in which the box represents $25^{th}$ and $75^{th}$ percentile, the line is the median, and the whisker ranges from minimum to maximum. The two-tailed unpaired Student's t test was used for statistical comparisons with Prism (GraphPad Software), and a $P$ value $< 0.05$ was considered significant. Outliers were identified using the Grubbs or Robust Regression and Outlier Updated Test (ROUT) test. The interaction between IFN$\gamma$ and TLR agonists was assessed using combination index analysis with CompuSyn software in which an index $< 1$ reflects synergism and $> 1$ indicates antagonism [174]. Sample sizes are indicated in each figure, and all experiments were performed in at least three independent replicates. All statistical details for individual experiments can be found in the figure legends.

# Chapter 3

# Restricting Genomic Actions of Inflammatory Mediators on Fetal Hematopoietic Progenitor Cells

This chapter is an adaptation of the following published work by the author.

Vu L. Tran, Peng Liu, Koichi R. Katsumura, Erin Kim, Bjorn M. Schoff, Kirby D. Johnson, and Emery H. Bresnick. Restricting genomic actions of innate immune mediators on fetal hematopoietic progenitor cells. *iScience* 26, no. 4 (2023).

# Abstract

Innate immune signaling protects against pathogens, controls hematopoietic development and functions in oncogenesis, yet the relationship between these mechanisms is undefined. Downregulating the GATA2 transcription factor in fetal hematopoietic progenitor cells upregulates genes encoding innate immune regulators, increases Interferon-$\gamma$ (IFN$\gamma$) signaling and disrupts differentiation. We demonstrate that deletion of an enhancer that confers GATA2 expression in fetal progenitors elevated Toll-Like Receptor (TLR) 1/2 and 2/6 expression and signaling. Rescue by expressing GATA2 downregulated elevated TLR signaling. IFN$\gamma$ amplified TLR1/2 and TLR2/6 signaling in GATA2-deficient progenitors, synergistically activating cytokine/chemokine genes and elevating cytokine/chemokine production in myeloid cell progeny. Genomic analysis of how innate immune signaling remodels the GATA2-deficient progenitor transcriptome revealed hypersensitive responses at innate immune genes harboring motifs for signal-dependent transcription factors and factors not linked to these mechanisms. As GATA2 establishes a transcriptome that constrains innate immune signaling, insufficient GATA2 renders fetal progenitor cells hypersensitive to innate immune signaling.

## 3.1 Introduction

Innate immunity protects organisms by creating a first line of defense against pathogens [1]. The mechanisms involve pattern recognition receptors, including Toll-Like Receptors (TLRs), that bind structural components and genetic material of bacteria, viruses, fungi, and parasites termed pathogen-associated molecular patterns [175, 176]. In addition to expression in differentiated immune cells, these receptors are expressed in Hematopoietic Stem and Progenitor Cells (HSPCs) [177, 178]. While innate immune signaling in HSPCs impacts proliferation, differentiation, and cytokine generation [50, 177, 179–187], many questions remain regarding the relationship between pattern recognition receptor-dependent HSPC mechanisms and anti-pathogen mechanisms in immune cells.

The Gram-negative bacterial cell wall component and TLR4 agonist Lipopolysaccharide (LPS) [5] acts on HSPCs and non-hematopoietic cells in the hematopoietic microenvironment to promote the transition from a dormant to a proliferative state and increase inflammatory mediator generation [188–190]. Chronic inflammation induced by repetitive treatment of TLR4 [190] or TLR2 [185] agonists suppresses HSC self-renewal. In a NUP98-HOXD13 Myelodysplastic Syndrome mouse model, TLR2 loss [191] or chronic TLR2/6 agonist treatment expands HSPCs and promotes leukemogenesis [192]. TLR mechanisms in HSPCs may also impact differentiated cell progeny. TLR2-activated HSPCs generate macrophages with reduced cytokine and reactive oxygen species [179]. RUNX1 loss in neutrophil precursors upregulates TLR expression and increases cytokine production by bone marrow neutrophils upon infection [71, 72].

While elucidating genetic networks controlled by GATA2, a vital transcriptional regulator of HSPC development and function [34], we discovered that GATA2 reduction in fetal progenitors downregulates genes mediating erythroid, megakaryocytic, and granulocytic differentiation and upregulates innate immune genes [43]. Germline GATA2 mutations cause bone marrow failure and leukemia predisposition [36, 105, 193–197], and the mechanisms

are being dissected in adults [116, 122, 123, 198, 199]. GATA2 expression in HSPCs is conferred by two enhancers, 77 and 9.5 kb upstream and downstream, respectively, of the mouse *Gata2* start site [36, 38, 42, 122, 123, 200]. Whereas the +9.5 enhancer triggers the emergence of Hematopoietic Stem Cells (HSCs) in the Aorta-Gonad-Mesonephros region [37], the −77 enhancer is dispensable for HSC genesis [38]. However, ablation of the murine −77 enhancer is embryonic lethal, and the mutant progenitors lose the capacity to differentiate into diverse hematopoietic progeny and generate predominantly macrophage-like cells [38, 43]. Loss of the −77 enhancer downregulates *Gata2* mRNA ∼5-fold in fetal liver Common Myeloid Progenitor (CMP) and Granulocyte Monocyte Progenitor (GMP) populations but does not significantly affect expression in Lineage$^-$Sca1$^+$cKit$^+$ (LSK) cells [38]. $-77^{-/-}$ embryos exhibit increased numbers of CMP in the fetal liver with reduced Megakaryocyte Erythroid Progenitors (MEP) [44]. In adult bone marrow, *Gata2* expression was similarly reduced in *Gata2*$^{+/-}$ and $-77^{+/-}$ LSK, CMP, GMP, and MEP compared to wild-type controls [201]. A similar number of genes are up- and down-regulated upon loss of the −77 in fetal liver progenitors [43]. Upregulated genes include a cohort of innate immune genes, including Interferon-$\gamma$ (IFN$\gamma$) pathway components, *e.g.*, the transcription factor Interferon Regulatory Factor 8 (IRF8), and multiple TLRs [43]. GATA2-deficient progenitors exhibit supra-physiological IFN$\gamma$ signaling that is attenuated by JAK1/2 kinase inhibition and contributes to diminished granulocytic differentiation [43]. *Irf8* ablation, combined with the $-77^{-/-}$ allele, partially rescues granulopoiesis [44]. Thus, IRF8 upregulation contributes to the differentiation defect [44]. As inflammation suppresses hematopoiesis and promotes clonal hematopoiesis [202–207], it is instructive to ask if GATA2-deficient progenitors acquire ectopic signaling involving diverse innate immune systems.

In response to pathogen-associated molecular patterns, TLR signaling initiates an innate immune response to confer anti-pathogen defense [175, 176]. Although GATA2 suppresses IFN$\gamma$ signaling [43], whether GATA2 regulates TLR signaling was unknown. *In vivo* analyses indicate that GATA2 is required, directly or indirectly, for TLR responses [123]. The

*Gata2* +9.5 enhancer that elevates *Gata2* expression in HSPCs and harbors an E-box-spacer-WGATAR composite element [84] confers resistance to stresses, including myeloablation, transplantation, and inflammation, both acute and chronic [122, 123, 208]. Mice harboring a human GATA2 genetic variant, a single-nucleotide change in an Ets motif, within the murine *Gata2* locus are hypersensitive to the deleterious impact of chronic inflammation induced by the viral mimetic and TLR3 agonist Polyinosinic:Polycytidylic Acid [123]. A compound heterozygous *Gata2* +9.5 enhancer-mutant mouse, containing the Ets motif variant on one allele and a disrupted E-box-spacer-WGATAR motif on the other allele, which epigenetically silences the locus, attenuates HSPC expansion in response to LPS-mediated TLR4 activation [123].

Herein, we tested whether GATA2 deficiency resulting from −77 loss upregulates TLR signaling, or if upregulated TLR mRNAs reflect locus priming to prepare for high-level transcription and signaling in progeny, with no progenitor cell-intrinsic consequences. Using a genetic rescue system, we demonstrate that TLR1/2 and TLR2/6 signaling is elevated in GATA2-deficient progenitors, GATA2 expression restricts TLR expression and activity, and IFN$\gamma$-TLR signaling crosstalk elevates expression of a gene cohort including those encoding cytokines and chemokines. As many questions remain unanswered regarding mechanisms underlying GATA2 function in fetal HSPCs, our demonstration that GATA2 loss in fetal progenitors engages innate immune signaling systems provides mechanistic insights with biological and pathological implications.

## 3.2 Stably elevated Toll-Like Receptor gene expression in GATA2-deficient fetal progenitor cells

GATA2 deficiency resulting from genetic ablation of the *Gata2* −77 enhancer in mice results in E14.5 fetal liver myeloerythroid progenitors with elevated levels of pattern recognition receptors TLR2 and TLR9 (Figure 3.1A) [43]. To determine if GATA2 broadly impacts the expression of TLR gene family, we mined our RNA-seq data that compares wild-type and

$-77^{-/-}$ E14.5 primary fetal liver hematopoietic progenitor transcriptomes (Figure 3.1B). $-77$ enhancer deletion reduced *Gata2* mRNA and protein by 7.0- and 4.7-fold, respectively [43], which increased the expression of TLR1, 2, 3, 4, 6, 7, 8, and 9 genes (Figure 3.1C). Retroviral-mediated expression of GATA2 at near-physiological levels in $-77^{-/-}$ progenitors reduced *Tlr* expression to resemble that of wild-type progenitors (Figure 3.1C). The genetic rescue analysis established that GATA2 loss in $-77^{-/-}$ progenitors elevated *Tlr* expression.

Since inflammatory stimuli activate TLR genes, their elevated expression in GATA2-deficient progenitors might reflect an inflammatory microenvironment *in vivo* that establishes an ectopic expression pattern. The progenitors isolated by flow cytometry might retain elevated TLR transcripts that were induced *in vivo*. Alternatively, the elevated expression might reflect the low GATA2 level in progenitors, independent of the microenvironment. To test these possibilities, we utilized a system in which primary fetal liver progenitors ($-77^{+/+}$ or $-77^{-/-}$) were immortalized via stable expression of an Estrogen Receptor hormone binding domain fusion to HOXB8 [(hi) $-77^{-/-}$ progenitors]. hi$-77^{-/-}$ progenitors resemble primary $-77^{-/-}$ progenitors in expressing elevated TLR transcripts [43]. To determine if elevated TLR expression is stable to prolonged culture, hi$-77^{+/+}$ (wild-type) and hi$-77^{-/-}$ (GATA2$^{low}$) progenitors were cultured for 20 days, and gene expression was quantified by Quantitative Real-Time Polymerase Chain Reaction (RT-qPCR). *Gata2* mRNA (Figure 3.1D) and protein (Figure 3.1E) were stably reduced in GATA2$^{low}$ progenitor cells. *Tlr1*, *Tlr2*, *Tlr4*, and *Tlr6* mRNA were elevated during the extended culture (Figure 3.1F). *Irf8* expression in GATA2$^{low}$ progenitors did not significantly change during the 18-day culture. As the elevated innate immune gene expression in GATA2$^{low}$ progenitors was stable to multiple rounds of cellular division, an inflammatory microenvironment is not required to maintain the aberrant gene expression signature.

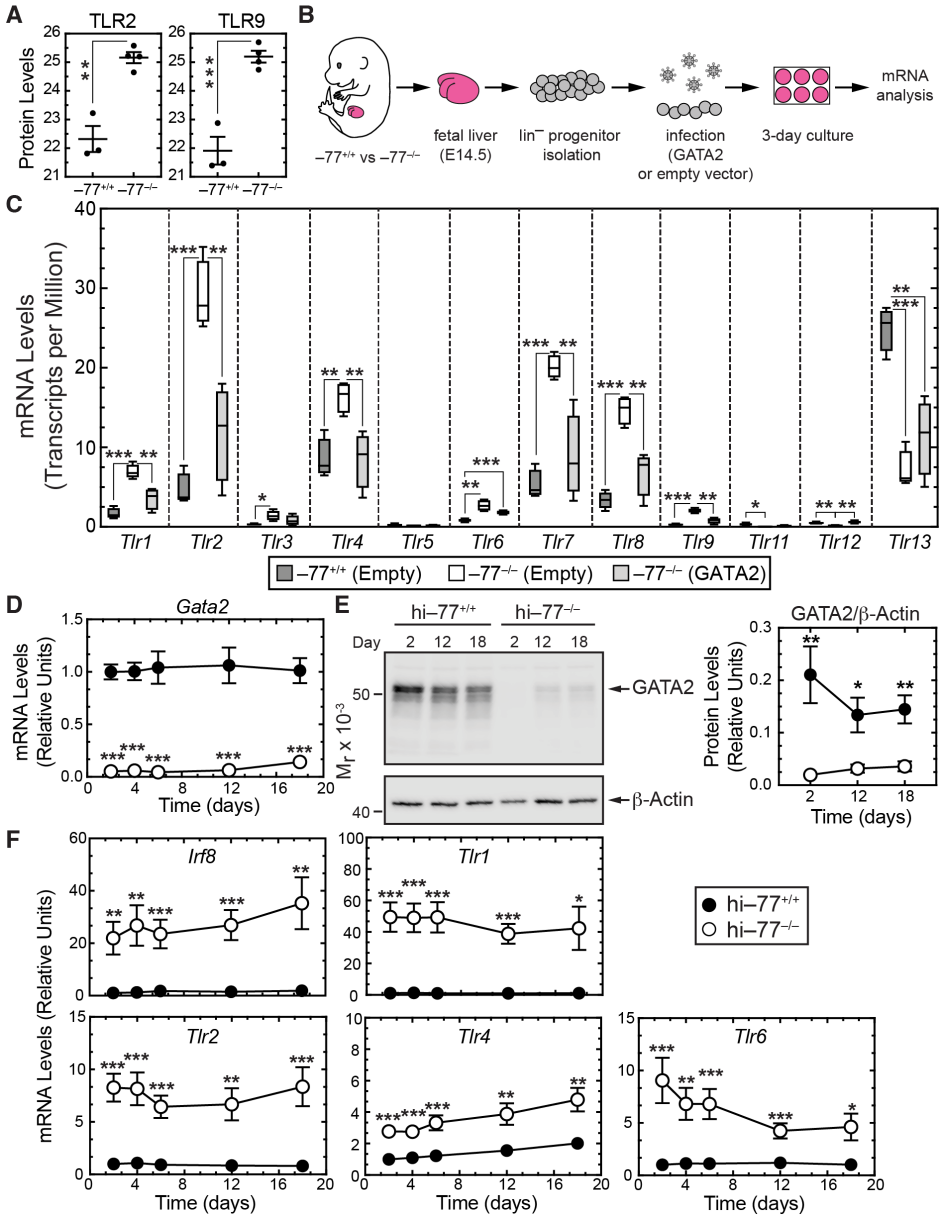


**Figure 3.1: Elevated Toll-Like Receptor expression in GATA2-deficient hematopoietic progenitor cells.** (**A**) TLR2 and TLR9 protein levels in $-77^{+/+}$ and $-77^{-/-}$ progenitors from proteomic data (PXD013855). (**B**) GATA2 genetic rescue assay in primary E14.5 fetal liver progenitors. (**C**) Expression profile of genes encoding Toll-Like Receptors in $-77^{+/+}$, $-77^{-/-}$, and GATA2-rescued $-77^{-/-}$ progenitors from RNA-seq data (GSE133606). (**D**) *Gata2* expression kinetics in ER-HOXB8-immortalized (hi)$-77^{+/+}$ and hi$-77^{-/-}$ progenitors. 50,000 cells were cultured in complete media containing $\beta$-Estradiol and G418, and cells were split every 2 days. Cells were harvested at indicated days for mRNA isolation (in D and F) and protein analysis (in E). (**E**) Left, Representative Western blot analysis of GATA2 expression at days 2, 12, and 18 of culture with $\beta$-Actin as a control. Right, Densitometric analysis of band intensities for GATA2 (n = 6). (**F**) *Irf8* and *Tlr* gene expression kinetics normalized to 18S rRNA. In (D) and (F), data pooled from five independent experiments (n = 3 per experiment) were presented as mean ± SEM. * $P < 0.05$, ** $P < 0.01$, *** $P < 0.001$ (unpaired two-tailed Student's t test).

## 3.3 GATA2 deficiency in fetal progenitor cells elevates TLR signaling capacity

Since −77 enhancer deletion increased TLR gene expression in progenitors, we asked if primary $-77^{-/-}$ fetal liver progenitors respond to TLR agonists. Lineage-negative progenitors were isolated from $-77^{+/+}$, $-77^{+/-}$, and $-77^{-/-}$ E14.5 fetal liver and treated with TLR1/2 ($Pam_3CSK_4$) [209, 210], TLR2/6 ($Pam_2CSK_4$) [211] and TLR4 (LPS) [5, 7] agonists for 4 h. As TLR signaling metrics, we quantified the expression of TLR-activated genes (*Tnf*, *Ccl3*, and *Ccl4*) [212]. The agonists increased TLR target gene expression in $-77^{-/-}$ vs. $-77^{+/+}$ progenitors (Figure 3.2A). *Tnf* expression was induced similarly in $-77^{+/-}$ vs. $-77^{+/+}$ progenitors (Figure 3.2A). By contrast, *Ccl3* and *Ccl4* induction was significantly higher in $-77^{+/-}$ vs. $-77^{+/+}$ progenitors (Figure 3.2A). The $-77^{+/-}$ progenitors expressed reduced levels of *Gata2* mRNA, which was decreased further in $-77^{-/-}$ progenitors (Figure 3.2B). The $-77^{+/-}$ progenitors exhibited higher *Tlr6* expression vs. $-77^{+/+}$ (Figure 3.2B).

To ascertain the molecular and cellular implications of the GATA2-dependent TLR response, we considered the following models. The pre-induced TLR genes in $GATA2^{low}$ progenitors might generate a quantitatively greater response (increased efficacy) to TLR stimulation in comparison to wild-type cells, confer hypersensitivity to low TLR agonist concentrations (increased potency) without altering the maximal response, or a hypersensitive response and increased efficacy might occur concomitantly (Figure 3.2C). To test these models, we asked if elevated TLR expression in $GATA2^{low}$ progenitors increases TLR agonist efficacy and/or potency. Wild-type and $GATA2^{low}$ progenitors were treated with increasing concentrations of the TLR1/2 agonist $Pam_3CSK_4$ for 4 h and *Tnf*, *Ccl3*, and *Ccl4* mRNA levels were quantified. Although *Tnf*, *Ccl3*, and *Ccl4* were expressed similarly in vehicle-treated wild-type and $GATA2^{low}$ progenitors, $Pam_3CSK_4$ induced their expression to a greater extent in the mutant cells (Figure 3.2D). *Ccl3* and *Ccl4* were non-responsive in wild-type progenitors (Figure 3.2D). The indistinguishable dose-response curves for induc-

tion of *Tnf* and *Ccl4* expression in wild-type and GATA2$^{low}$ progenitors indicate that −77 enhancer deletion increased agonist efficacy without impacting potency (Figure 3.3).

Beyond agonist-induced dimerization of TLR1 with TLR2 [213, 214], TLR2 also heterodimerizes with TLR6 [211, 215]. As *Tlr6* mRNA was upregulated in $-77^{-/-}$ primary progenitors, we asked if −77 enhancer deletion affected TLR2/6 functions. Treatment of hi$-77^{+/+}$ and hi$-77^{-/-}$ progenitors with the TLR2/6 agonist $Pam_2CSK_4$ or $Pam_3CSK_4$ for four hours induced a greater response in mutant versus wild-type cells (Figure 3.2E).

The −77 enhancer deletion dysregulates many genes important for cellular physiology. To establish rigorously whether the elevated TLR-dependent gene expression responses of GATA2$^{low}$ fetal progenitors are caused by insufficient GATA2, we asked whether restoring GATA2 at a near-physiological level reduces the responses. The GATA2$^{low}$ progenitors were infected with GATA2-expressing or empty retroviruses, cells were selected with Puromycin, cultured for 48 h, and treated with two TLR1/2 agonist concentrations (Figure 3.4A). Exogenous GATA2 expression (Figure 3.4B) reduced the high innate immune gene expression to a level resembling that of wild-type progenitors infected with empty retrovirus (Figure 3.4C). The induction of *Tnf* and *Ccl3* expression in GATA2$^{low}$ progenitors was attenuated to a level resembling wild-type progenitors (Figure 3.4D). Thus, GATA2-mediated suppression of TLR expression in GATA2$^{low}$ progenitors limits TLR-induced gene expression responses.

Previously, we demonstrated that GATA2$^{low}$ progenitors upregulate IFN$\gamma$ signaling pathway components and establish hypersensitivity to IFN$\gamma$ [43]. As IFN$\gamma$ and TLR signaling pathways activate the Mitogen-Activated Protein Kinases (MAPK) ERK1/2, p38, and JNK [216–220], we asked if the elevated response of GATA2$^{low}$ progenitors to IFN$\gamma$ and TLR alters the magnitude or dynamics of MAPK and JAK/STAT signaling. Wild-type and GATA2$^{low}$ progenitors were treated with IFN$\gamma$ and $Pam_3CSK_4$ for 4 h, and p38, JNK1/2, ERK1/2, STAT1, and STAT3 phosphorylation levels were quantified. Phospho-p38 and -JNK increased maximally after 1 h (Figures 3.5A and 3.5B). p38 phosphorylation was sustained, while JNK phosphorylation was detected at 60 min, but not thereafter, in GATA2$^{low}$

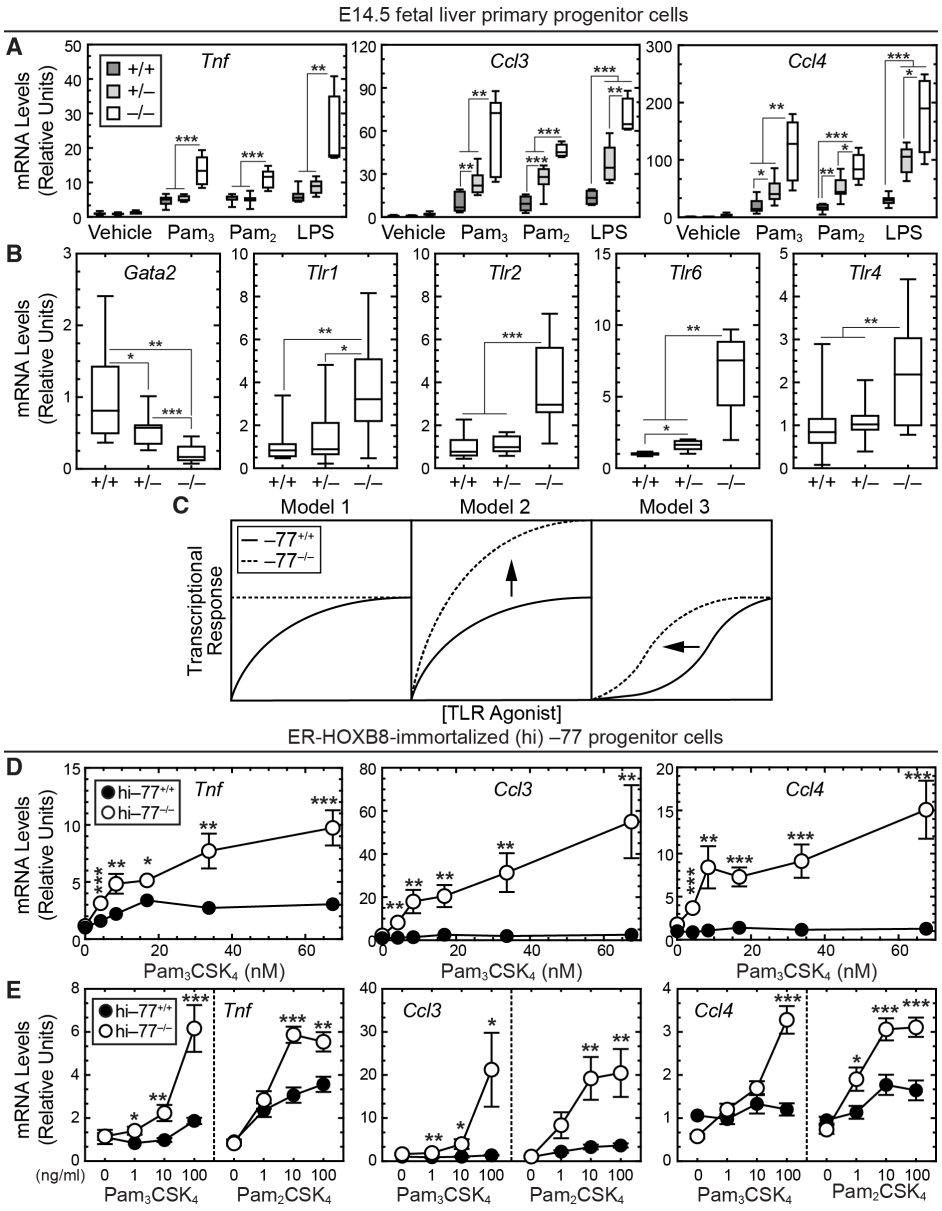


**Figure 3.2: Hyperresponsive TLR signaling in E14.5 GATA2-deficient progenitor cells.** (**A**) TLR agonist responsiveness of *Tnf*, *Ccl3*, and *Ccl4* in E14.5 $-77^{+/+}$, $-77^{+/-}$, and $-77^{-/-}$ Lin$^-$ progenitors. Primary E14.5 Lin$^-$ progenitor cells were treated with TLR1/2 agonist $Pam_3CSK_4$ (100 ng/ml), TLR2/6 agonist $Pam_2CSK_4$ (10 ng/ml), or TLR4 agonist LPS (100 ng/ml) for 4 h (n = 4-8 fetal livers). (**B**) *Gata2* and *Tlr* expression in E14.5 $-77^{+/+}$, $-77^{+/-}$, and $-77^{-/-}$ Lin$^-$ progenitors (n = 4-8 fetal livers). (**C**) Models depicting potential relationships between GATA2 deficiency and cellular responsiveness of $-77^{-/-}$ versus $-77^{+/+}$ progenitors to TLR activation. (**D**) Dose-dependent responsiveness of *Tnf*, *Ccl3*, and *Ccl4* expression to $Pam_3CSK_4$. hi$-77^{+/+}$ and hi$-77^{-/-}$ progenitors were treated with increasing concentrations of $Pam_3CSK_4$ for 4 h (4 independent experiments). (**E**) Responsiveness of *Tnf*, *Ccl3*, and *Ccl4* expression in hi$-77^{+/+}$ and hi$-77^{-/-}$ progenitors to $Pam_3CSK_4$ or $Pam_2CSK_4$ for 4 h (4 independent experiments). In (D) and (E), data were presented as mean ± SEM. mRNA was quantified using RT-qPCR and normalized to 18S rRNA. * $P < 0.05$, ** $P < 0.01$, *** $P < 0.001$ (unpaired two-tailed Student's t test).

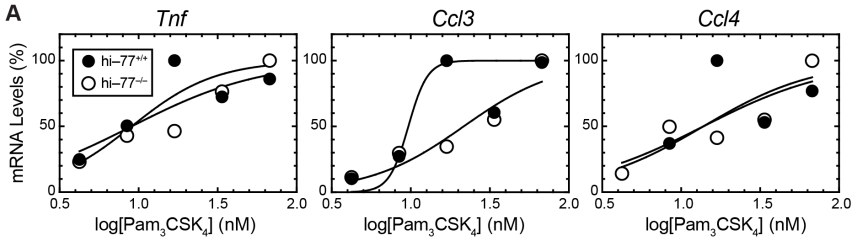


$EC_{50}$ (nM)

| | hi–$77^{+/+}$ | hi–$77^{-/-}$ | *P* value |
|---|---|---|---|
| *Tnf* | 7.513 | 12.83 | 0.0877 |
| *Ccl3* | 9.656 | 21.62 | 0.0336 |
| *Ccl4* | 11.77 | 16.36 | 0.6047 |

**Figure 3.3: TLR1/2 agonist-mediated stimulation of TLR target genes in GATA2$^{low}$ progenitors.** (**A**) Dose-response curves of $Pam_3CSK_4$ to regulate gene expression. *Tnf*, *Ccl3*, and *Ccl4* expression were quantified by RT-qPCR. (**B**) $EC_{50}$ values of $Pam_3CSK_4$ in hi$-77^{+/+}$ and hi$-77^{-/-}$ progenitor cells were calculated based on the transformed curves of (A).

progenitors (Figures 3.5A and 3.5B). Phospho-ERK1/2 was weakly activated in both cell types after 15 min of stimulation (Figures 3.6A and 3.6B). The kinetics of STAT1/3 phosphorylation in GATA2$^{low}$ and wild-type were similar with phospho-STAT3 being 30% higher ($P = 0.0027$) in GATA2$^{low}$ after 2 h of stimulation (Figures 3.6A and 3.6B). In wild-type and GATA2$^{low}$ progenitors, IFN$\gamma$, with or without the TLR1/2 agonist, comparably induced phospho-STAT1 (Figures 3.6C and 3.6D) without affecting phospho-ERK1/2 (Figures 3.6C and 3.6D). By contrast, a one-hour treatment with $Pam_3CSK_4$ increased phospho-p38, and IFN$\gamma$ further increased phospho-p38 ($P = 0.0014$) in GATA2$^{low}$ cells (Figures 3.5C and 3.5D). Only in GATA2$^{low}$ progenitors, the TLR1/2 agonist, with or without IFN$\gamma$, strongly increased phospho-JNK by 5.9-fold ($P = 0.009$) and 5.5-fold ($P = 0.018$), respectively (Figures 3.5C and 3.5D).

Genetic ablation of both JNK1 and JNK2 in the mouse is embryonically lethal at E12.5, and conditional ablation of JNK1 and JNK2 in macrophages abrogates IFN$\gamma$ and TLR signaling, rendering inflammatory genes, *e.g.*, *Tnf*, *Ccl2*, *Ccl5*, *Il1b*, and *Il6*, insensitive to LPS [221, 222]. Conditional ablation of p38 in macrophages impairs the TLR4 response and attenuates TNF$\alpha$, but not IL6, production [223]. Given the critical role of JNK in innate immunity, we asked if GATA2 restores JNK phosphorylation to wild-type levels in response

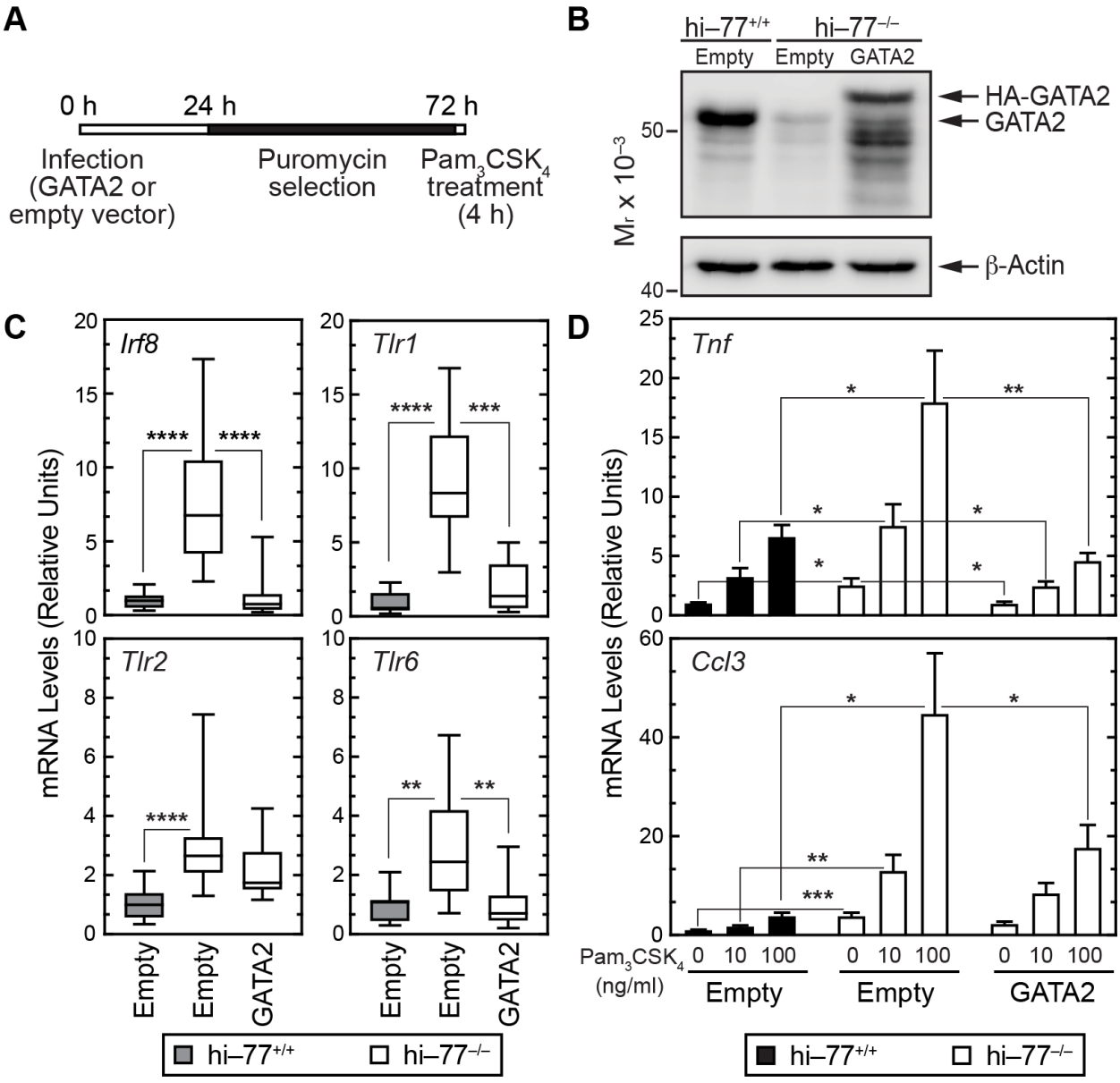


**Figure 3.4: GATA2 rescues ectopically elevated TLR signaling in GATA2$^{low}$ progenitor cells.** (**A**) Schematic presentation of GATA2 rescue and TLR1/2 agonist treatment. (**B**) Representative Western blot analysis of GATA2 expression in hi$-77^{+/+}$, hi$-77^{-/-}$, and GATA2-rescued hi$-77^{-/-}$ progenitor cells. Retrovirally-expressed GATA2 is distinguishable from endogenous by decreased mobility resulting from the N-terminal Hemagglutinin (HA) tag. $\beta$-Actin served as a loading control. (**C**) Quantitation of *Irf8*, *Tlr1*, *Tlr2*, and *Tlr6* in hi$-77^{+/+}$, hi$-77^{-/-}$, and GATA2-rescued hi$-77^{-/-}$ progenitor cells (5 independent experiments). (**D**) *Tnf* and *Ccl3* expression in hi$-77^{+/+}$, hi$-77^{-/-}$, and GATA2-rescued hi$-77^{-/-}$ treated with $Pam_3CSK_4$ (10 and 100 ng/ml) for 4 h (5 independent experiments, mean $\pm$ SEM). * $P < 0.05$, ** $P < 0.01$, *** $P < 0.001$ (unpaired two-tailed Student's t test).

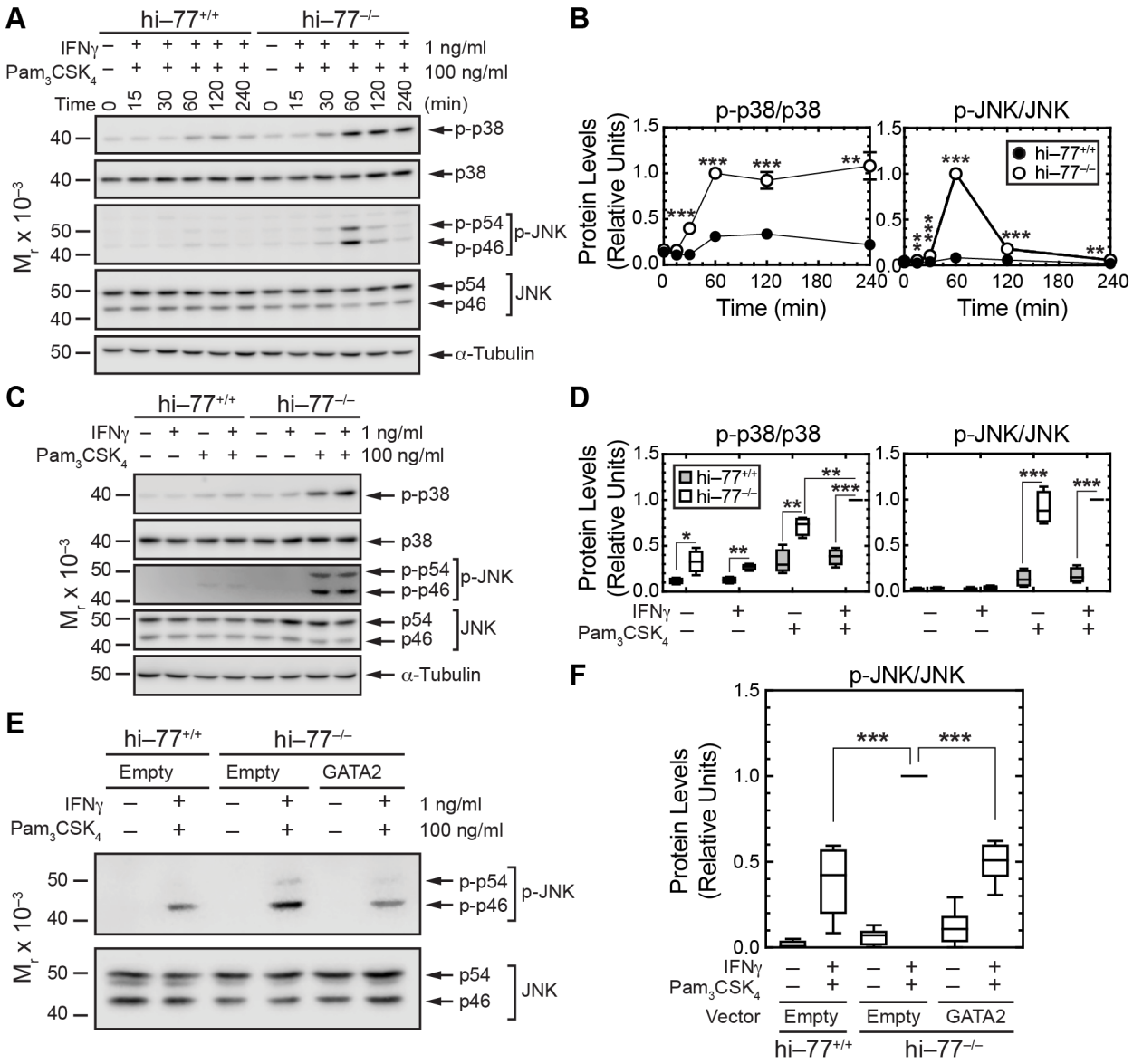


**Figure 3.5: Elevated inflammatory signaling efficacy in GATA2$^{low}$ progenitor cells.** (**A**) Representative Western blot analysis of phospho-p38 (p-p38) and -JNK (p-JNK) signaling in $-77^{+/+}$ and hi$-77^{-/-}$ progenitors. Cells were treated with IFN$\gamma$ (1 ng/ml) and $Pam_3CSK_4$ (100 ng/ml) for 4 h in complete media. (**B**) Densitometric analysis of band intensities for p-p38 and p-JNK (n = 4, mean ± SEM). (**C**) Representative Western blot analysis of p-p38 and p-JNK in response to IFN$\gamma$ and TLR1/2 stimulation. $-77^{+/+}$ and hi$-77^{-/-}$ cells were treated with agonists in complete media for 1 h. (**D**) Densitometric analysis of band intensities for phospho-p38 and -JNK in (C) (n = 4). (**E**) Representative Western blot analysis of p-JNK in combination-stimulated $-77^{+/+}$ vs hi$-77^{-/-}$ cells. hi$-77^{-/-}$ cells were infected with GATA2-expressing retrovirus, selected with 2 $\mu$g/ml Puromycin for 48 h, and were treated with IFN$\gamma$ (1 ng/ml) and $Pam_3CSK_4$ (100 ng/ml) for 1 h. $-77^{+/+}$ and hi$-77^{-/-}$ cells infected with empty retrovirus served as controls. (**F**) Densitometric analysis of relative band intensities for p-JNK in (E) (n = 6). In (B), (D), and (F), data were normalized to the combination-treated hi$-77^{-/-}$ cells at 1 h. * $P < 0.05$, ** $P < 0.01$, *** $P < 0.001$ (unpaired two-tailed Student's t test).

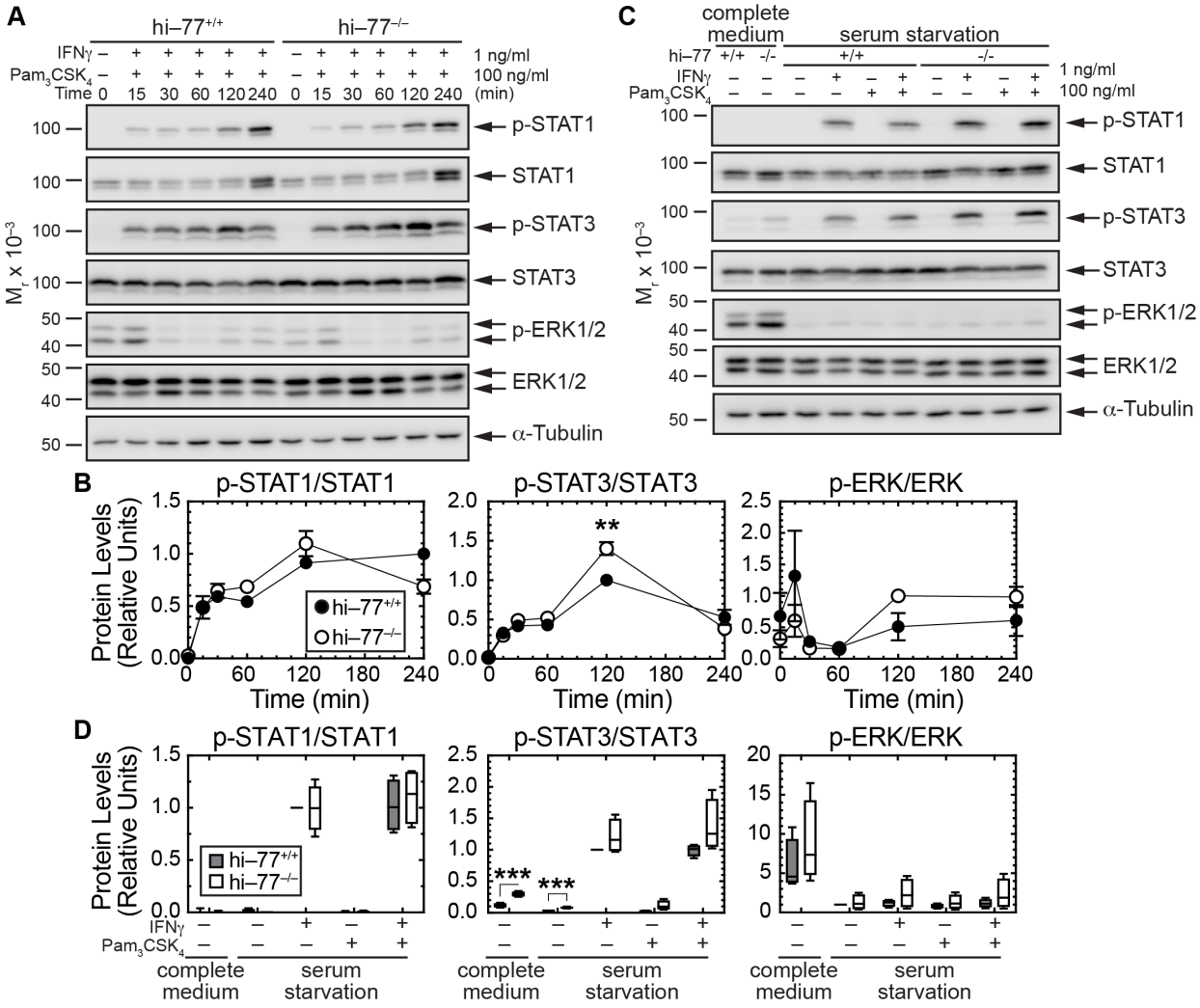


**Figure 3.6: The magnitude and dynamics of STAT1/3 and ERK1/2 phosphorylation in GATA2$^{low}$ progenitors in response to inflammatory signaling.** (**A**) Representative Western blot analysis of phospho-STAT1 (p-STAT1), -STAT3 (p-STAT3), and -ERK1/2 (p-ERK1/2) in hi$-77^{+/+}$ and hi$-77^{-/-}$ progenitors. Cells were serum-starved for 2-4 h and stimulated with IFN$\gamma$ (1 ng/ml) and $Pam_3CSK_4$ (100 ng/ml) for 4 h. (**B**) Densitometric analysis of band intensities for p-STAT1, p-STAT3, and p-ERK1/2 (n = 4-5, mean ± SEM). (**C**) Representative Western blot analysis of p-STAT1/3 and p-ERK1/2 in response to IFN$\gamma$ and TLR1/2 stimulation. hi$-77^{+/+}$ and hi$-77^{-/-}$ cells were serum-starved for 4h and treated with agonists for 15 min. (**D**) Densitometric analysis of band intensities for p-STAT1/3 and p-ERK1/2 in (C) (n = 4). * $P < 0.05$, ** $P < 0.01$, *** $P < 0.001$ (unpaired two-tailed Student's t test).

to IFN$\gamma$ and TLR signaling. hi$-77^{-/-}$ cells infected with GATA2-expressing retrovirus were selected with Puromycin and treated with vehicle or IFN$\gamma$ and $Pam_3CSK_4$ for 1 h. JNK phosphorylation in GATA2-expressing $GATA2^{low}$ cells was attenuated by 50.2% ($P < 0.0001$) to resemble wild-type cells infected with empty retrovirus (Figures 3.5E and 3.5F).

As *Gata2* $-77$ enhancer deletion upregulates IFN$\gamma$, TLR1/2, and TLR2/6 signaling, we evaluated the mechanistic ramifications of combined IFN$\gamma$ and TLR signaling. To test whether IFN$\gamma$ and TLR signaling are additive, synergistic, antagonistic, or independent, $GATA2^{low}$ progenitors were treated with IFN$\gamma$, $Pam_3CSK_4$, or both agonists, and combination index analysis was used to assess potential functional interactions [174]. Although IFN$\gamma$ alone did not alter *Tnf* or *Ccl3* expression, IFN$\gamma$ and $Pam_3CSK_4$ synergistically increased their expression (Figure 3.7A). To determine if the synergism is restricted to TLR1/2 or is applicable to a distinct TLR heterodimer, we treated $GATA2^{low}$ progenitors with IFN$\gamma$, $Pam_2CSK_4$, or both agonists and quantified gene expression. IFN$\gamma$ and TLR2/6 signaling synergistically induced *Tnf* and *Ccl3* expression (Figure 3.7B). IFN$\gamma$, but not the TLR1/2 or TLR2/6 agonists, increased *Irf8* expression, while the combination of IFN$\gamma$ and TLR agonists at higher concentrations further increased *Irf8* expression (Figures 3.7C and 3.7D). The TLR2/6, but not TLR1/2, agonist synergistically increased expression of the IFN$\gamma$ target gene *Stat1* (Figures 3.7C and 3.7D). At a maximal $Pam_3CSK_4$ concentration, *Stat1* expression in $GATA2^{low}$ progenitors treated with IFN$\gamma$ and $Pam_3CSK_4$ was higher ($P = 0.03$) than cells treated with IFN$\gamma$ alone (Figures 3.7C). Whereas the wild-type progenitors treated with IFN$\gamma$, $Pam_3CSK_4$, $Pam_2CSK_4$, or combinations of IFN$\gamma$ with TLR agonists did not secrete detectable levels of TNF$\alpha$ and CCL3 proteins, CCL3 was detected in supernatants of $GATA2^{low}$ progenitors 4h post-stimulation (Figure 3.7E). Thus, GATA2 loss in fetal progenitors elevates innate immune gene expression, creating an aberrant cell state with hyperresponsivity to IFN$\gamma$ and TLR signaling pathways.

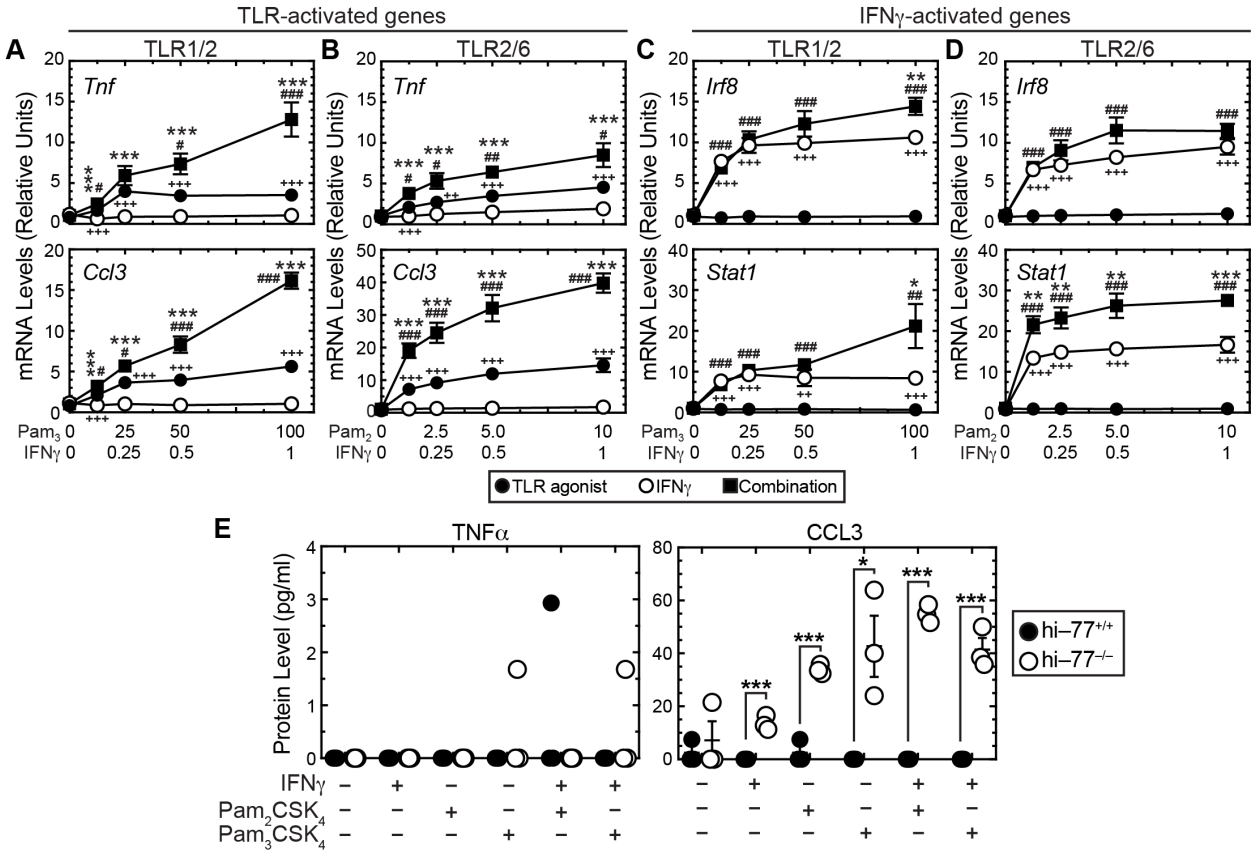


**Figure 3.7: Hyperresponsiveness of GATA2$^{low}$ progenitor cells to inflammatory signaling.** (**A-D**) hi$-77^{-/-}$ progenitors were treated with increasing concentrations of IFN$\gamma$, TLR1/2 agonist (A and C), TLR2/6 agonist (B and D), or combination of IFN$\gamma$ and TLR agonists for 4 h. The responsiveness of TLR-activated (*Tnf* and *Ccl3*) and IFN$\gamma$-activated (*Irf8* and *Stat1*) genes was quantified using RT-qPCR and normalized to 18s rRNA (n = 6-9, mean ± SEM). (**E**) hi$-77^{+/+}$ and hi$-77^{-/-}$ progenitors were treated with 1 ng/ml IFN$\gamma$, 100 ng/ml TLR1/2 agonist, 10 ng/ml TLR2/6 agonist, or combination of IFN$\gamma$ and TLR agonists for 4 h, and the supernatants were collected for quantification of TNF$\alpha$ and CCL3 proteins using a Luminex assay (n = 3). In (A-D), *, combination vs IFN$\gamma$; #, combination vs TLR agonist; +, TLR agonist vs IFN$\gamma$. * $P < 0.05$; ** $P < 0.01$; *** $P < 0.001$; similarly for # and + (unpaired two-tailed Student's t test).

## 3.4 Genomic consequences of GATA2-deficient progenitor cell hypersensitivity to innate immune mediators

To determine the genomic consequences of innate immune signaling in GATA2$^{low}$ progenitors, we used RNA-seq analysis to identify differentially expressed genes (DEGs) in hi$-77^{+/+}$ or hi$-77^{-/-}$ cells treated with vehicle, IFN$\gamma$, Pam$_3$CSK$_4$, or both agents for 4 h. Principal component analysis demonstrated strong reproducibility among the four biological replicates (Figure S3A).

We tested whether IFN$\gamma$- and TLR-regulated genes are sensitive or insensitive to GATA2 loss in the GATA2$^{low}$ cells. The DEGs revealed that a subset of IFN$\gamma$- and TLR-activated genes in GATA2$^{low}$ cells were not regulated in wild-type cells (Figure 3.9A). We asked if GATA2 deficiency alters the magnitude of gene expression responses at all or a subset of the IFN$\gamma$- and TLR-regulated genes. While a subset of the genes was regulated comparably in wild-type and GATA2$^{low}$ cells, the majority of genes were activated to a greater extent in GATA2$^{low}$ cells (Figure 3.9B). This analysis indicated that the GATA2$^{low}$ cell genome was hyperresponsive to innate immune mediators, both with individual agonists and the combination.

Inflammatory signaling activates a battery of transcription factors that function through their binding motifs within promoters, introns, and distal sites to activate or repress downstream target genes. The enrichment or absence of motifs at a regulated locus in response to inflammatory signaling can provide important mechanistic clues. To gain insights into mechanisms underlying the hypersensitive genomic response, we conducted motif enrichment analysis with promoter and intronic sequences of genes activated by IFN$\gamma$ and TLR1/2 agonist in wild-type and GATA2$^{low}$ cells. Consistent with established IFN$\gamma$ activity to induce STAT- and IRF-dependent transcriptional regulation, STAT1-5, IRF1-4, and IRF7-9 mo-

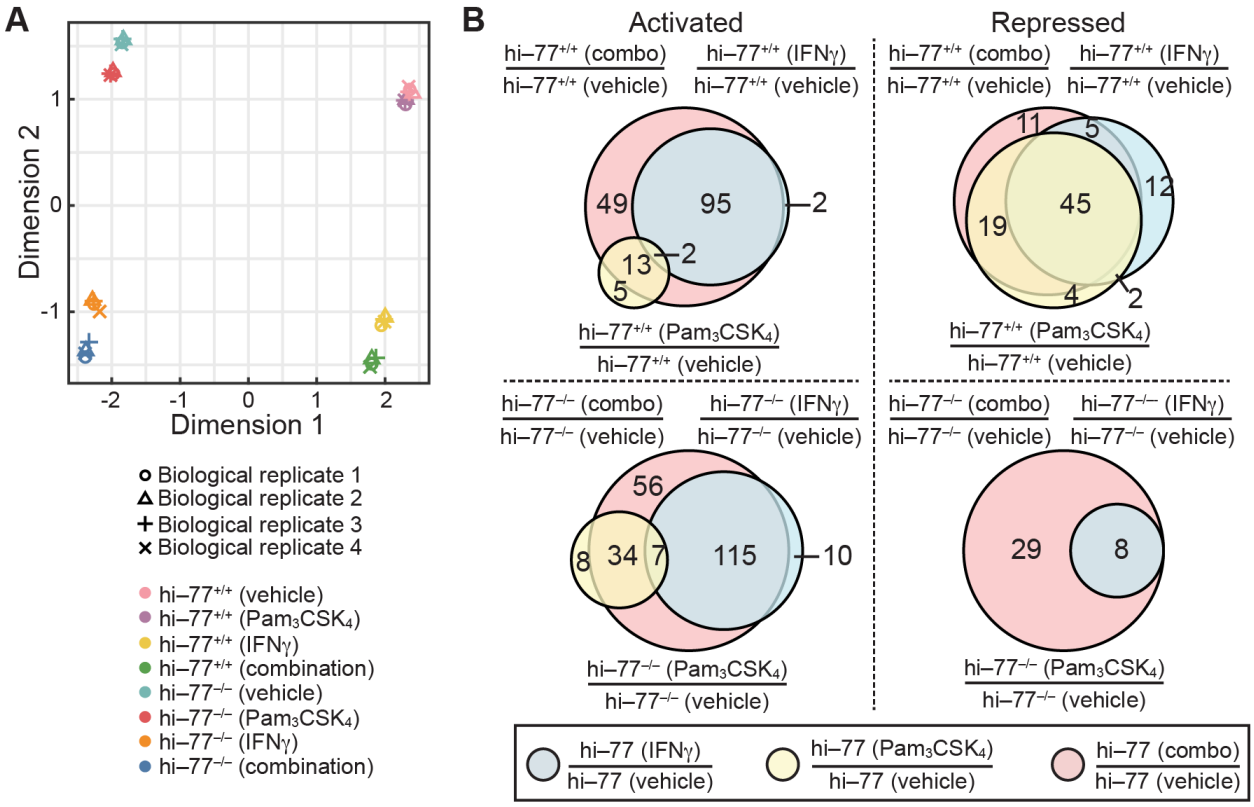


**Figure 3.8: Transcriptome responses of wild-type and GATA2$^{low}$ progenitors to inflammatory signaling.** (**A**) Principle component analysis showing the segregation of transcriptomes from the biological replicates (n = 4) for hi$-77^{+/+}$ vs hi$-77^{-/-}$ treated with vehicle, IFN$\gamma$, Pam$_3$CSK$_4$, or a combination of agonists. (**B**) Overlap of differentially expressed genes (DEGs) in hi$-77^{+/+}$ (top) or hi$-77^{-/-}$ (bottom) cells treated with IFN$\gamma$, Pam$_3$CSK$_4$, or both agonists were parsed into activated (left) or repressed (right). A DEG had $|log_2(fold\ change)| \geq 1$, adjusted $P$ value $< 0.05$, and Transcripts per Million (TPM) $\geq 1$ in all of the replicates in at least one of the two conditions compared. Activated DEGs had higher expression in the numerator condition than in the denominator condition, and repressed DEGs had lower expression in the numerator condition than in the denominator condition.

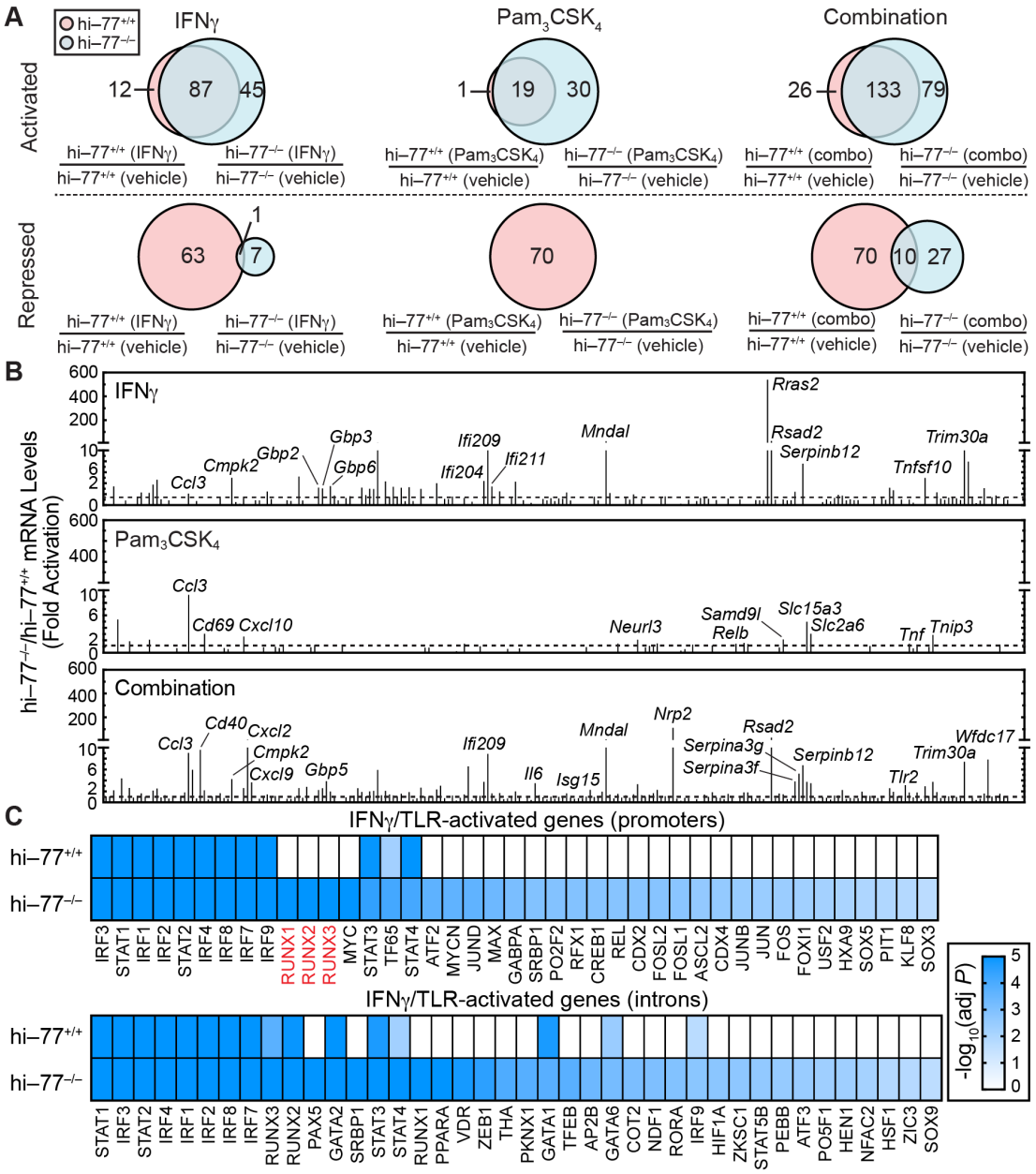


**Figure 3.9: GATA2 restricts genomic actions of inflammatory stimuli.** (**A**) Differentially expressed genes (DEG) overlap in hi$-77^{+/+}$ and hi$-77^{-/-}$ treated with IFN$\gamma$ (left), $Pam_3CSK_4$ (middle), or both agonists (right) were parsed into activated (top) or repressed (bottom). Activated DEGs had higher expression in the numerator condition than in the denominator condition, and repressed DEGs had lower expression in the numerator condition than in the denominator condition. (**B**) mRNA levels of activated gene sets in hi$-77^{-/-}$ treated with IFN$\gamma$ (top), $Pam_3CSK_4$ (middle), or a combination of agonists (bottom) normalized to hi$-77^{+/+}$ treated with the same agonists. (**C**) Heatmap showing motif enrichment, by MEME analysis, at promoters (top) and introns (bottom) of IFN$\gamma$– and TLR-activated genes in hi$-77^{+/+}$ and hi$-77^{-/-}$. Motifs binding canonical inflammation-activated transcription factors (STAT, IRF, and NF-$\kappa$B) are presented as positive controls. Motifs enriched in hi$-77^{-/-}$ but not hi$-77^{+/+}$ progenitors were ranked on the basis of $-\log_{10}$(adjusted $P$). Motifs with adjusted $P > 0.05$ were set to 1.

tifs were enriched significantly within IFN$\gamma$-activated promoters in wild-type cells (Figure 3.10A). KLF [KLF1 ($P = 1.6 \times 10^{-19}$), KLF3 ($P = 6.1 \times 10^{-28}$), KLF4 ($P = 5.0 \times 10^{-24}$), KLF5 ($P = 1.3 \times 10^{-23}$), KLF6 ($P = 3.6 \times 10^{-30}$), KLF15 ($P = 3.5 \times 10^{-29}$)], FOXA [FOXA1 ($P = 3.0 \times 10^{-6}$), FOXA2 ($P = 2.0 \times 10^{-5}$), and FOXA3 ($P = 2.0 \times 10^{-5}$)] , FOXO [FOXO1 ($P = 9.8 \times 10^{-8}$), FOXO3 ($P = 0.004$), and FOXO4 ($P = 6.0 \times 10^{-5}$)], and SP [SP1 ($P = 1.1 \times 10^{-33}$), SP2 ($P = 1.0 \times 10^{-28}$), SP3 ($P = 1.0 \times 10^{-29}$), SP4 ($P = 4.0 \times 10^{-31}$), and SP5 ($P = 5.7 \times 10^{-32}$) motifs were also associated with IFN$\gamma$ signaling in wild-type cells (Figure 3.10A). In response to TLR1/2 signaling, NFKB1 ($P = 0.009$), NFKB2 ($P = 0.02$), REL ($P = 2.0 \times 10^{-5}$), and RELB ($P = 9.0 \times 10^{-5}$) motifs were enriched in wild-type cells (Figure 3.10A), consistent with TLR-dependent NF-$\kappa$B activation [4]. The dual signaling in wild-type cells shared a subset of the enriched motifs *e.g.*, SP and KLF, and motifs not characteristic of the individual signaling conditions *e.g.*, NFYA ($P = 5.0 \times 10^{-4}$), NFYB ($P = 1.0 \times 10^{-4}$), and NFYC ($P = 4.0 \times 10^{-4}$) (Figure 3.10A). Both shared and unique motifs were enriched at IFN$\gamma$- and TLR-activated gene promoters in wild-type and GATA2$^{low}$ cells. The combinatorial signaling was associated with enriched MYC ($P = 3.5 \times 10^{-6}$), RUNX1 ($P = 8.9 \times 10^{-7}$), RUNX2 ($P = 1.3 \times 10^{-6}$), and RUNX3 ($P = 2.4 \times 10^{-6}$) motifs in promoter regions of GATA2$^{low}$, but not, wild-type progenitors (Figure 3.9C and 3.10A). In both cell types, these motifs were enriched in introns (Figure 3.10B). GATA1, GATA2, and GATA6 motifs were enriched in introns but not in the promoters of IFN$\gamma$- and TLR-regulated genes in both cell types (Figure 3.9C and 3.10B). GATA2 chromatin occupancy commonly occurs distal to promoters or within introns, although in certain cases, GATA2 occupies promoters [81, 119, 163]. In both cell types, select motifs were enriched significantly in activated and repressed genes *e.g.*, SP1-5, KLF3/4/5/6/8/15. Other motifs were enriched in activated, but not repressed, genes in both cell types *e.g.*, FOXA, FOXO, and IRF. NFYA/B/C motifs were enriched in promoters of repressed genes in wild-type but not GATA2$^{low}$ cells. E2F, ETS, ETV, FOXO, and IRF motifs were enriched in introns of activated, but not repressed, genes in wild-type cells (Figure 3.10B).

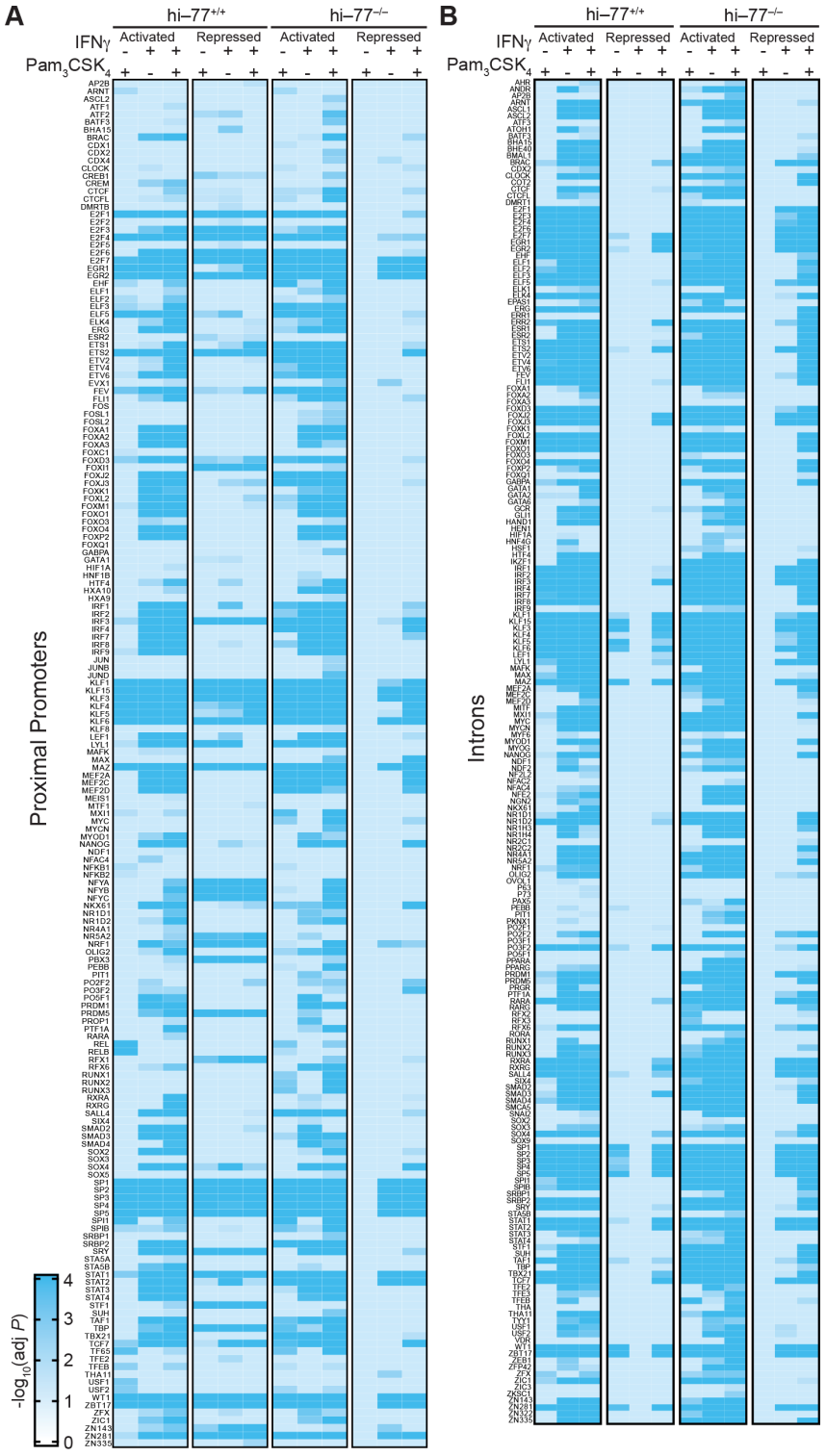


**Figure 3.10: Motif analysis of IFN$\gamma$ and TLR1/2-regulated genes in wild-type and GATA2$^{low}$ progenitor cells.** The DEGs from IFN$\gamma$, TLR1/2 agonist, or combination-treated hi$-77^{+/+}$ or hi$-77^{-/-}$ progenitors were used to conduct motif enrichment analysis in proximal promoters (**A**) and introns (**B**). Motifs with adjusted $P > 0.05$ were set to 0.05.

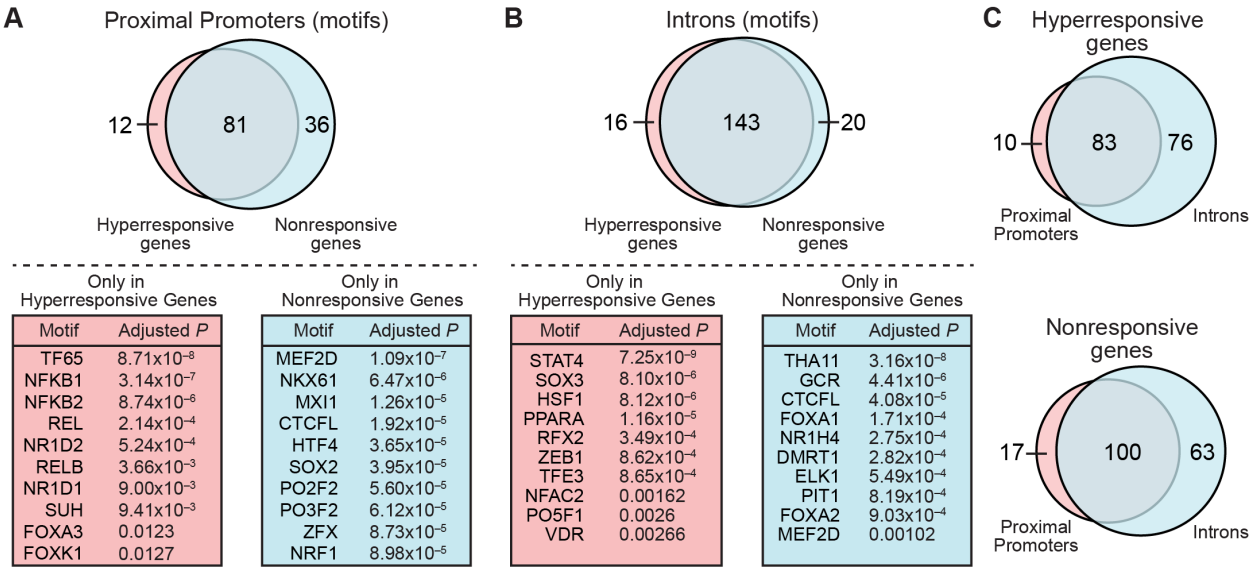


**Figure 3.11: Motif distributions for signal-dependent transcription factors in hyperresponsive genes.** (**A** and **B**) Top, Motifs in proximal promoters (A) or introns (B) of hyperresponsive genes versus nonresponsive genes. Bottom, Top ten motifs enriched only in the promoter (A) or introns (B) of the hyperresponsive or nonresponsive genes. (**C**) Motif overlap in proximal promoters and introns at hyperresponsive genes (top) or nonresponsive genes (bottom).

We tested whether motifs mediating binding of signal-dependent transcription factors reside more commonly at hyperresponsive genes in GATA2$^{low}$ vs. wild-type cells treated with IFN$\gamma$ and TLR agonist and/or are deficient at the hyperresponsive genes. The motif analysis revealed 12 motifs in promoters that were enriched at hyperresponsive, but not nonresponsive, genes (Figure 3.11A). These motifs included NF-$\kappa$B [NFKB1 ($P = 3.14 \times 10^{-7}$), NFKB2 ($P = 8.74 \times 10^{-6}$), REL ($P = 2.14 \times 10^{-4}$), and RELB ($P = 0.037$)] and the AP1 subunit FOSL2 ($P = 0.024$) (Figure 3.11A). In introns, 16 motifs were enriched at hyperresponsive, but not nonresponsive, genes, including STAT4 ($P = 7.25 \times 10^{-9}$), SOX3 ($P = 8.1 \times 10^{-6}$), HSF1 ($P = 8.12 \times 10^{-6}$), and PPARA ($P = 1.16 \times 10^{-5}$) (Figure 3.11B). Certain motifs (36 in promoters and 20 in introns) were enriched in nonresponsive, but not hyperresponsive, genes. CTCFL, MEF2D, and PIT1 motifs were enriched in promoters and introns of nonresponsive, but not hyperresponsive, genes (Figure 3.11A and 3.11B). The majority of genes encoding transcription factors binding these motifs were expressed in wild-type and GATA2$^{low}$ progenitors. The dearth of these motifs at hyperresponsive genes might

reflect their role in suppressing signal-dependent transcription. While most of the motifs were enriched in promoters and introns of hyperresponsive and nonresponsive genes, 76 and 63 motifs were enriched selectively in introns of hyperresponsive and nonresponsive genes, respectively (Figure 3.11C). The innate immune genes harbor motifs for signal-dependent transcription factors that can be shared by wild-type and GATA2$^{low}$ progenitors or unique to one genotype, and select motifs demarcate genes with hyperresponsive signal-dependent transcriptional responses.

## 3.5 Biological insights derived from GATA2-dependent inflammatory genomics

KEGG and STRING (https://string-db.org/) were utilized to predict biological insights into the genomic hypersensitivity to innate immune signaling in GATA2$^{low}$ cells. The DEGs highlighted JAK-STAT signaling and pattern-triggered immune signaling (Figure 3.12A). IFN$\gamma$-activated or TLR-activated genes in wild-type cells, and TLR-activated genes in GATA2$^{low}$ cells did not reveal significantly over-represented KEGG terms. The IFN$\gamma$-regulated genes included genes encoding Guanylate-Binding Proteins (GBPs) that functions in innate immune signaling [224]. GBP genes are clustered on chromosomes 3 (*Gbp1*, *2*, *3*, *5*, *7*, and pseudo *Gbp1*) and 5 (*Gbp4*, *6*, *8*, *9*, *10*, *11*, and pseudo *Gbp2*) [225]. Loss-of-function analyses revealed that GBP1 and GBP7 protect against listerial and mycobacterial infection [226]. Genetic ablation of *Gbp* loci sensitized animals to *Toxoplasma gondii*-infected lethality, and GBP1, GBP5, and GBP7 partially restored the capacity to inhibit bacterial burden in *Gbp*$^{chr3}$-deficient mice [227]. *Gbp5*$^{-/-}$ mice exhibited defects on NLRP3 inflammasome assembly and IL1$\beta$/IL18 production [228]. In wild-type cells, IFN$\gamma$ signaling induced expression of GBP family members, and IFN$\gamma$- and TLR-regulated combinatorial signaling further increased their expression (Figures 3.12B and 3.12C). GATA2 deficiency amplified this signal-dependent response (Figures 3.12B and 3.12C).

IFN$\gamma$ signaling controls the IFI200 gene cluster on murine chromosome 1 [229]. This

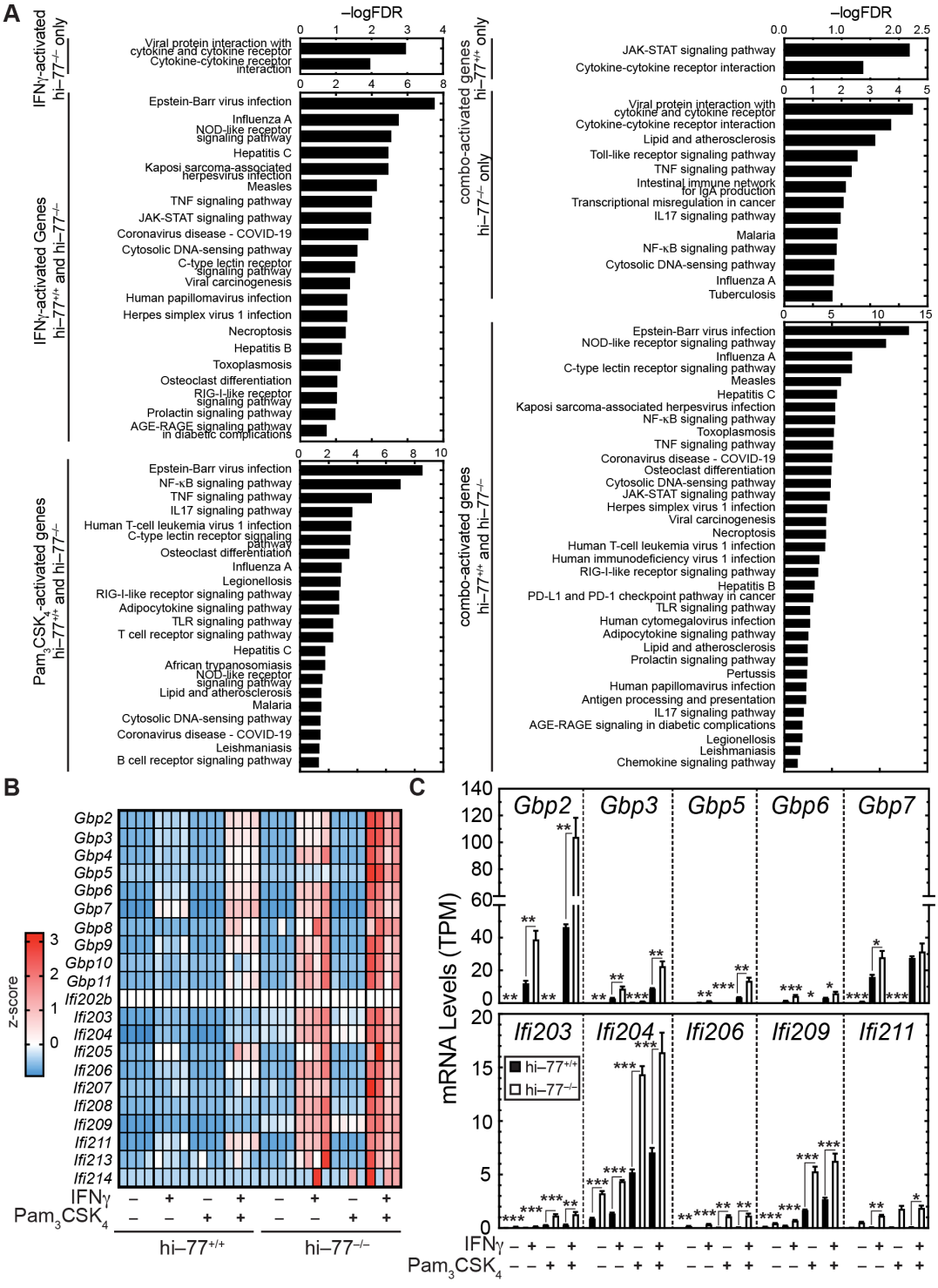


**Figure 3.12: Biological insights derived from IFN$\gamma$ and TLR-induced transcriptomic alterations.** (**A**) KEGG terms were generated from activated genes by IFN$\gamma$, TLR1/2-, or a combination of agonists in hi$-77^{+/+}$ and hi$-77^{-/-}$ progenitor cells. (**B**) Heatmap showing expression of *Gbp* and *Ifi200* gene families mined from RNA-seq dataset and presented as Z-score. (**C**) mRNA levels of select *Gbp* and *Ifi200* genes with TPM $> 1$. Data were presented as mean $\pm$ SEM. * $P < 0.05$, ** $P < 0.01$, *** $P < 0.001$ (unpaired two-tailed Student's t test).

cluster contains *Ifi203* encoding a cytoplasmic nucleic acid sensor, and IFI203 knockdown in macrophage cell lines reduces IFN production in response to murine leukemia virus and HIV [230]. IFI204 senses cytosolic dsDNA and bacterial infection to mount type I IFN responses [231]. Multiple members of the IFI200 cluster were expressed at higher levels in GATA2$^{low}$ vs. wild-type cells (Figures 3.12B and 3.12C). IFN$\gamma$ and TLR1/2 combinatorial signaling further enhanced their expression (Figures 3.12B and 3.12C).

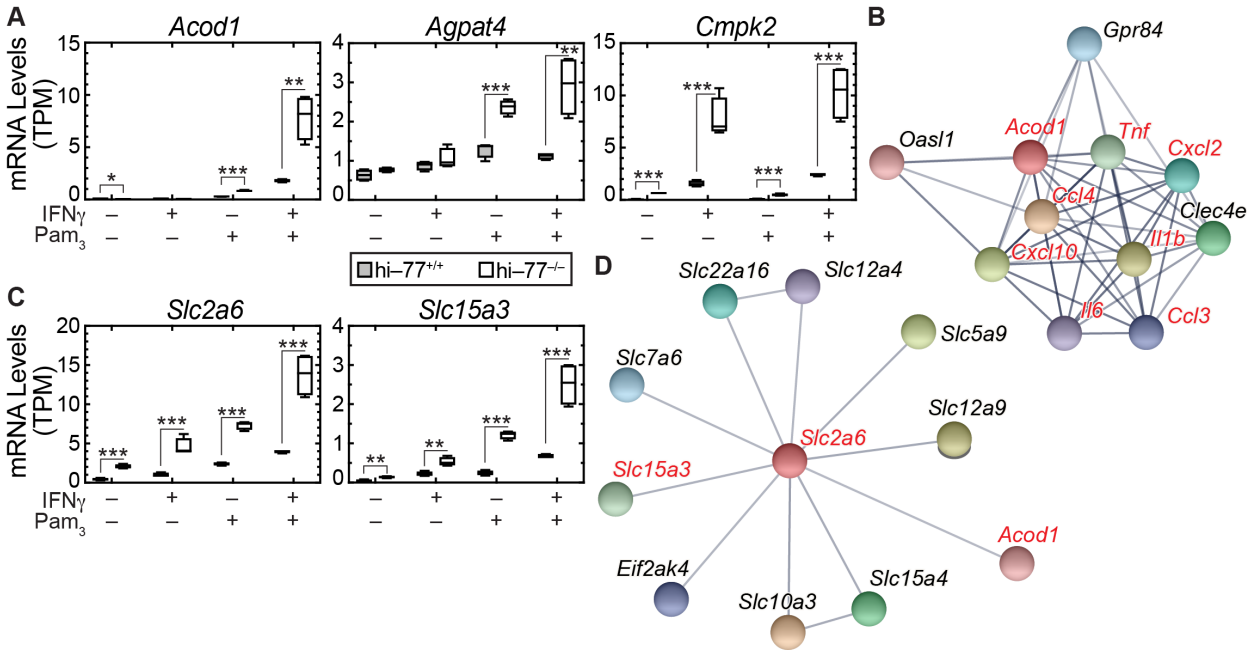


**Figure 3.13: GATA2 deficiency in fetal progenitor cells elevates expression of genes encoding metabolic enzymes and solute carrier transporters in response to inflammatory signaling.** (**A**) mRNA levels (TPM) of *Acod1*, *Agpat4*, and *Cmpk2*. (**B**) STRING analysis (https://string-db.org/) of genes linked to *Acod1*. (**C**) mRNA levels (TPM) of *Slc2a6* and *Slc15a3*. (**D**) STRING analysis of genes linked to *Slc2a6*. In (B) and (D), genes that were highly activated by IFN$\gamma$, Pam$_3$CSK$_4$ or both agonists in hi$-77^{-/-}$ progenitors were highlighted in red. * $P < 0.05$, ** $P < 0.01$, *** $P < 0.001$ (unpaired two-tailed Student's t test).

In GATA2$^{low}$ cells, combinatorial innate immune signaling activated genes encoding metabolic enzymes *e.g.*, *Acod1* (*Irg1*), *Agpat4*, and *Cmpk2* (Figure 3.13A). AGPAT4 functions in Triacylglycerol biosynthesis [232]. CMPK2 regulates UTP/CTP production for Nucleic Acid biosynthesis [233]. ACOD1 is a cis-Aconitate Decarboxylase that catalyzes the conversion of cis-Aconitate, a Krebs cycle intermediate, into Itaconate [234]. Itaconate regulates macrophage function by inhibiting metabolic enzymes and regulates transcription

factors mediating inflammatory responses [235, 236]. *Acod1* expression was low in wild-type cells (Figure 3.13A). Whereas it was not induced by IFN$\gamma$ and was slightly activated by $Pam_3CSK_4$ in GATA2$^{low}$ cells, the agonists synergistically induced its expression 4.4-fold ($P$ = 0.0013) higher vs. wild-type cells (Figure 3.13A). STRING revealed ACOD1 links to cytokines/chemokines whose expression was also upregulated by IFN$\gamma$ and TLR1/2 signaling in GATA2$^{low}$ cells (Figure 3.13B).

Combinatorial innate immune signaling activated solute carrier transporter genes including *Slc2a6*, encoding the glycolytic regulator Glucose Transporter 6 (GLUT6) [237] and *Slc15a3* encoding Peptide/Histidine Transporter 2, an endosomal and lysosomal transporter of Dipeptides, Peptidomimetics, and Histidine (Figure 3.13C) [238]. The STRING network identified links between *Slc2a6*, *Slc15a3* and *Acod1* (Figure 3.13D).

Based on the impact of GATA2 loss on responsiveness of the progenitor cell genome to innate immune signaling, we considered how this altered cellular state might influence myeloid cell progeny function. To induce myeloid differentiation, $\beta$-Estradiol was withdrawn from the culture media for 2 days, and cells were treated with IFN$\gamma$ and TLR1/2 or TLR2/6 agonists individually or together for 4 h. In vehicle-treated, differentiated GATA2$^{low}$ cells, *Tnf*, *Ccl3*, *Ccl4*, and *Ccl5* expression increased relative to undifferentiated cells. TLR agonists, with or without IFN$\gamma$, further increased expression (Figure 3.14A). Although IFN$\gamma$ did not induce cytokine/chemokine expression in undifferentiated cells, differentiation rendered GATA2$^{low}$ cells responsive to IFN$\gamma$. In differentiated GATA2$^{low}$ cells, the individual and combination treatments increased TNF$\alpha$, CCL3, CCL4, and CCL5 protein levels, with the combinatorial signaling inducing the highest levels of TNF, CCL4, and CCL5 (Figure 3.14B). The increased cytokine/chemokine production in differentiating GATA2$^{low}$ cells was commensurate with increased *Tlr1*, *Tlr2*, and *Tlr6* mRNA levels (Figure 3.14C). Thus, myeloid cell progeny from GATA2-deficient fetal progenitor cells liberated excessive levels of inflammatory mediators.

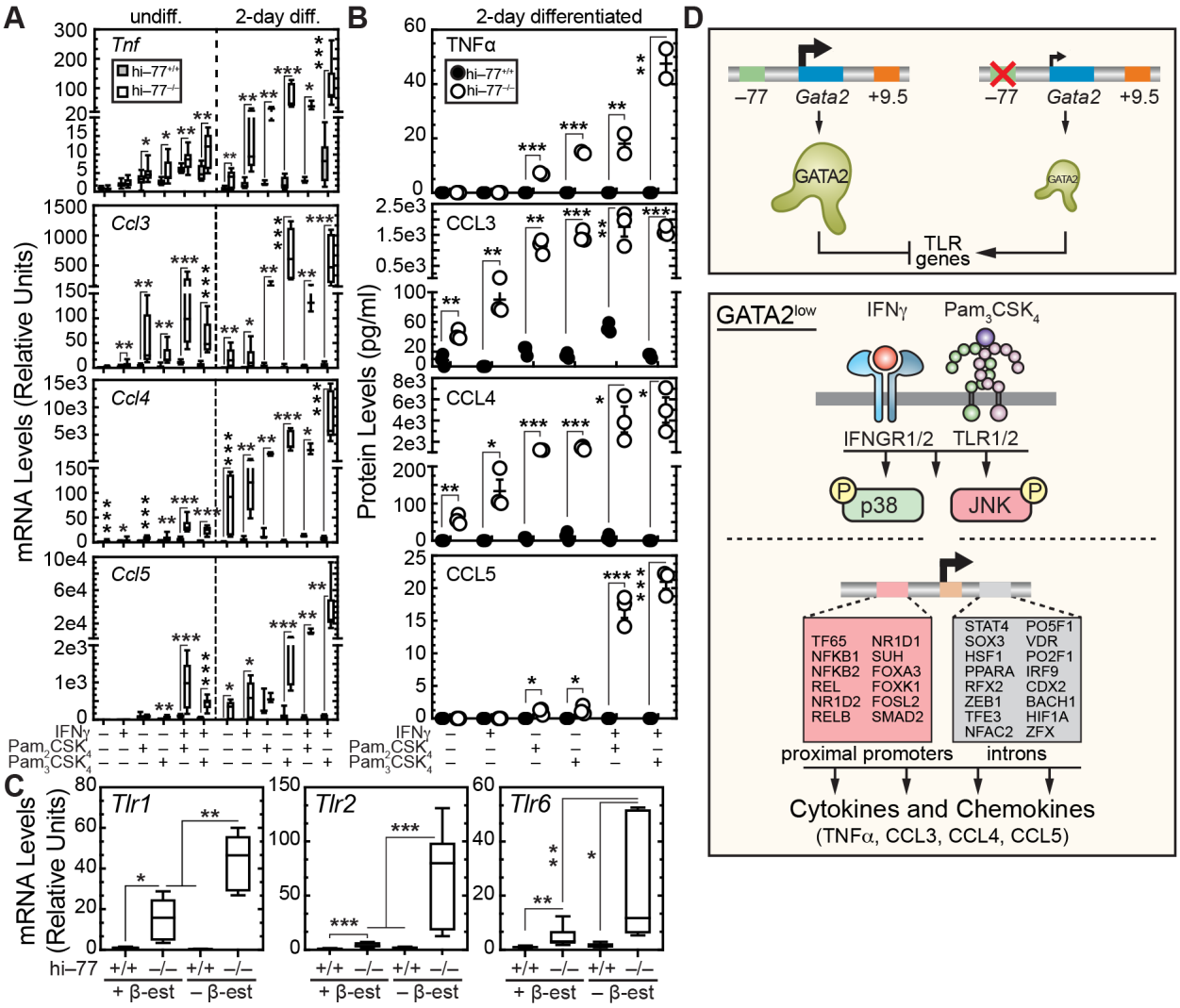


**Figure 3.14: GATA2-deficient fetal progenitors generate elevated levels of cytokines and chemokines upon myeloid differentiation.** (**A**) Extrinsic signal responsiveness of *Tnf*, *Ccl3*, *Ccl4*, and *Ccl5* in response to 4 h stimulation in undifferentiated hi−77 progenitors and cells induced to differentiate for two days (n = 3-12). (**B**) The differentiated hi−77 cells were treated as in (A), and the supernatants were collected 4 h post-agonist treatment for quantification of TNF$\alpha$, CCL3, CCL4, and CCL5 proteins using a Luminex assay (n = 3). (**C**) *Tlr1*, *Tlr2*, and *Tlr6* expression in undifferentiated and 2 d differentiated hi−$77^{+/+}$ vs hi−$77^{-/-}$ progenitors (n = 3-12). * $P < 0.05$, ** $P < 0.01$, *** $P < 0.001$ (unpaired two-tailed Student's t test). (**D**) The model depicts GATA2 regulation of a network of genes and proteins to establish progenitor functions in response to inflammatory stimuli. When the -77 enhancer is deleted, GATA2 expression decreases, causing the upregulation of TLR genes. GATA2 deficiency in fetal progenitors increases capacity of the cells to respond to inflammatory stimuli. IFN$\gamma$ and TLR signaling amplify the expression of innate immune genes harboring motifs (ordered based on adjusted $P$) for signal-dependent transcription factors and regulators of diverse pathways at proximal promoter and intronic regions in GATA2$^{low}$ progenitors. IFN$\gamma$ and TLR crosstalk elevate the expression of cytokines and chemokines, which mediate cell-intrinsic and -extrinsic functions.

## 3.6 Discussion

GATA2 deficiency in −77 enhancer mutant fetal progenitors disrupts a multi-fate differentiation program and upregulates innate immune genes, including those encoding IFN$\gamma$ signaling components [43]. Here, we demonstrated that GATA2 loss upregulated TLR genes and TLR signaling in primary and immortalized fetal progenitor cells and increased TLR signal transduction efficacy. In this context, TLR1/2 and IFN$\gamma$ signaling crosstalk elevated cytokine and chemokine generation, and the impact of GATA2 loss on inflammatory machinery was amplified upon myeloid differentiation (Figure 3.14D).

To address whether elevated inflammatory signaling in GATA2$^{low}$ progenitors involves intrinsic or extrinsic mechanisms, we asked if GATA2$^{low}$ progenitors require an *in vivo* microenvironment to maintain elevated TLR gene expression. Previously, primary and secondary transplants revealed that $-77^{-/-}$ donor fetal liver cells conferred multi-lineage long-term repopulating activity, but generated more monocytes and reduced lymphocytes, consistent with HSPC-intrinsic defects [38]. Herein, elevated innate immune gene expression was stable to extended culture without inflammatory stimuli. Genetic rescue to restore GATA2 to a physiological level reduced expression of multiple TLR genes in primary fetal $-77^{-/-}$ progenitor cells (Figure 3.1C) and hi$-77^{-/-}$ progenitors (Figure 3.4C). GATA2 rescued the gene expression response to TLR1/2 stimulation (Figure 3.4D) and rescued JNK phosphorylation in response to TLR1/2 and IFN$\gamma$ stimulation (Figure 3.5E-F) in GATA2$^{low}$ progenitors. Thus, multiple lines of evidence support a cell-intrinsic mechanism in which GATA2 deficiency in $-77^{-/-}$ fetal progenitors upregulates TLR gene expression and signaling.

In a model of GATA2 deficiency involving compound heterozygous +9.5 enhancer mutant mice, reduced *Gata2* expression in adult HSPCs is associated with attenuated HSPC expansion upon LPS-dependent acute inflammation, which involves TLR4 activation [123]. In LPS-treated *Gata2* heterozygous mice, cytokine production was reduced in peritoneal lavage fluids and plasma [58]. LPS activates TLR4, which was not upregulated in the fetal pro-

genitors. Although we have focused on hematopoietic cell-intrinsic actions of inflammatory signaling, the hematopoietic microenvironment can be a determinant of the inflammatory response. A reciprocal transplantation analysis revealed that hematopoietic cells require a normal bone marrow microenvironment to respond to TLR4 signaling [207, 239]. Cytokines released by TLR4-activated, non-hematopoietic cells impact HSPC expansion and activity. Reciprocal transplant analysis of *Gata2* +9.5 Ets motif mutant bone marrow revealed no impact of a mutant microenvironment on HSC long-term repopulating activity [123]. GATA2 deficiency consequences might differ in fetal vs. adult contexts due to intrinsic differences in the regulatory circuitry of fetal versus adult HSPCs or distinct microenvironments.

GATA2 regulates diverse signaling molecules, including c-Kit [240, 241], the facilitator of c-Kit signaling SamD14 [85, 242], IFN$\gamma$-inducible transcription factor IRF8 [43], and, as demonstrated in this study, TLRs. Elevated TLR signaling increased p38 and JNK, which regulate the AP1 transcription factor. Our prior genomic analysis of GATA2 function in endothelial cells revealed GATA2, c-JUN, and c-FOS co-occupancy at genes harboring WGATAR and AP1 motifs [53]. GATA2 and AP1 cooperatively regulate inflammatory gene expression [53]. Studies in mouse aortic endothelial and Kasumi-1 AML cell lines provided evidence for a signal-dependent GATA2 mechanism. HRAS G12V mutant utilizes p38 to induce GATA2 phosphorylation at Serine 192, which promotes multi-site phosphorylation [101]. IL1$\beta$ and CXCL2 also increased GATA2 phosphorylation [102]. GATA2 phosphorylation amplifies GATA2 activity to regulate cytokine/chemokine gene expression [101, 102, 243]. Our analysis in fetal progenitors revealed that GATA2 loss elevated p38 and JNK signaling in response to IFN$\gamma$ and TLR1/2 agonists.

In humans, GATA2 heterozygous mutations cause a highly variably penetrant syndrome involving Myelodysplastic Syndrome (MDS) with progression to AML [105, 193–195]. Although TLR2 expression is upregulated in MDS patient CD34$^+$ cells [244], TLR2 loss or sustained stimulation of TLR2/6 promotes leukemogenesis in a murine model [191]. TLR2 dimerizes with TLR1 or TLR6 to generate functional dimers, and alterations in one TLR

subunit may therefore impact the function of multiple TLR complexes [214, 245, 246]. In low/intermediate risk MDS patients, multiple bone marrow cell types exhibit elevated TLR1, TLR2, and TLR6 gene expression, and TLR1/2 and TLR2/6 agonists increase cytokine production [247]. We demonstrated that GATA2 loss elevated TLR1/2 and TLR2/6 signaling and fetal progenitor responses.

In summary, our study revealed that GATA2 loss increased the TLR signaling capacity of fetal progenitors. Elevated TLR signaling synergized with IFN$\gamma$ signaling to regulate genes that were not regulated by the individual pathways and amplified the expression of genes that were regulated by the individual pathways. These gene cohorts included numerous inflammatory genes. As HSPC development can be disrupted by acute or chronic inflammatory stimuli, our discovery of a mechanism that constrains inflammatory signaling by restricting genome responsiveness has important pathological implications. It will be instructive to determine if hypersensitivity to extrinsic inflammatory signaling in GATA2$^{low}$ fetal progenitors is exclusive to fetal development or if it similarly characterizes progenitors in a newborn context and thereafter. Given the embryonic lethality of the $-77^{-/-}$ mouse model, new systems will be required to address this issue.

# Chapter 4

# Dual Mechanism of Inflammation Sensing by the Hematopoietic Progenitor Genome

This chapter is an adaptation of the following published work by the author.

Vu L. Tran, Peng Liu, Koichi R. Katsumura, Alexandra A. Soukup, Audrey Kopp, Zamaan S. Ahmad, Ashley E. Mattina, Marjorie Brand, Kirby D. Johnson, and Emery H. Bresnick. Dual mechanism of inflammation sensing by the hematopoietic progenitor genome. *Science Advances* 11, no. 22 (2025): eadv3169.

# Abstract

Genomes adapt dynamically to alterations in the signaling milieu, including inflammation that transiently or permanently disrupts genome function. Here, we elucidate how a progenitor cell genome senses and responds to inflammation when the developmental and transcriptional regulator GATA2 is limiting, which causes bone marrow failure in humans and mice and predisposes to leukemia in humans. GATA2$^{low}$ murine progenitors are hypersensitive to inflammatory mediators. We discovered that the hematopoietic transcription factor PU.1 conferred transcriptional activation in GATA2$^{low}$ progenitors in response to Interferon-$\gamma$ and Toll-Like Receptor 1/2 agonists. In a locus-specific manner, inflammation reconfigured genome activity by promoting PU.1 recruitment to chromatin or tuning activity of PU.1-preoccupied chromatin. The recruitment mechanism disproportionately required IKK$\beta$ activity. Inflammation-activated genes were enriched in motifs for RUNX factors that cooperate with GATA factors. Contrasting with the GATA2 - RUNX1 cooperativity paradigm, GATA2 suppressed and RUNX1 promoted PU.1 mechanisms to endow the progenitor genome with inflammation-sensing capacity.

## 4.1 Introduction

Inflammation is vital for healing, yet dysregulated and/or excessive inflammation is deleterious to cells [2]. Inflammatory cytokines and chemokines activate cell-surface receptors, instigating genomic and non-genomic mechanisms that control cellular biology and physiology [2]. Given the numerous inflammatory mediators and effectors that impact chromatin and transcription, and inflammation promoting bone marrow failure and leukemia [248–251], it is instructive to consider how genomes sense and respond to inflammation. Although inflammation activates common transcription factors, *e.g.*, NF-$\kappa$B and AP1, there are many unanswered questions regarding how inflammation impacts genome function.

We discovered that reducing the levels of GATA2, a hematopoietic transcription factor essential for hematopoietic stem and progenitor cell (HSPC) development, activates genes encoding diverse inflammatory components [43, 46, 52]. Although GATA2 is not recognized as an inflammation-regulated transcription factor, oncogenic RAS/Mitogen-Activated Protein Kinase induces GATA2 phosphorylation, increasing its transcriptional regulatory activity [101, 102]. In GATA2-deficient murine fetal progenitors (GATA2$^{low}$), expression of genes encoding Interferon-$\gamma$ (IFN$\gamma$) receptor and Toll-Like Receptor (TLR) 1/2 and 2/6 is upregulated, and their agonists induce transcriptional responses considerably greater than in wild-type progenitors [43, 52]. Re-expressing GATA2 in GATA2$^{low}$ progenitors reduces the elevated expression of inflammatory components [43, 46, 52]. Pathogenic variants are defective in lowering the elevated inflammation-dependent transcriptional response [46, 106, 107]. Human GATA2 heterozygous genetic variation causes an immunodeficiency disorder termed GATA2 Deficiency Syndrome involving a bone marrow failure and acute myeloid leukemia (AML) predisposition [39, 40]. *Gata2* heterozygous mice and compound heterozygous mice with a human disease variant and enhancer-deleted allele, modeling epigenetic silencing of the normal allele, are relatively normal in the steady-state, yet chemotherapy or inflammation induces bone marrow failure [122, 123, 127]. As inflammation promotes

bone marrow failure and leukemia [32, 33], a leukemia predisposition variant combined with genome hypersensitivity to inflammation may have critical pathogenic implications.

Analogous to GATA2 deficiency, bone marrow Granulocyte Macrophage Progenitors (GMP) lacking the hematopoietic factor RUNX1 generate neutrophils with elevated IFN$\gamma$ and TLR4 signaling [71, 72]. Germline RUNX1 deficiency creates Familial Platelet Disorder with a predisposition to myeloid malignancy [67, 68]. RUNX1 occupies loci encoding multiple components of these pathways, and RUNX1 loss increases accessibility of these loci [72]. The ETS-domain factor ETS Variant 6 (ETV6) functions as a repressor to control HSPC function during stress hematopoiesis [131]. Germline ETV6 variants create a predisposition for acute lymphoblastic leukemia and thrombocytopenia [130]. An inhibitory ETV6 germline variant (R355X) elevates inflammatory gene expression in bone marrow of a mouse model [131]. HSPC functional defects can be associated with upregulated inflammatory components and may render cells hypersensitive to inflammatory mediators.

In GATA2$^{low}$ primary and ER-HOXB8-immortalized (hi-) murine fetal progenitors, GATA2 deficiency elevates activity of the ETS transcription factor PU.1 to induce a myeloid and B lineage gene expression program, including inflammatory genes [46]. GATA2 and PU.1 can be antagonistic, and balancing their activities ensures normal hematopoiesis [100, 252]. Genetic ablation of a *Gata2* allele promotes AML instigated by another ETS factor ERG in a transgenic mouse model, and GATA2 opposes ERG [92]. Although multiple lines of evidence support GATA2-ETS antagonism, the importance of this mechanism for HSPC genome sensing of inflammation is unknown.

To understand how transcription factor levels establish genome sensing and responsiveness to inflammation, we leveraged a system in which deletion of a *Gata2* enhancer 77 kb upstream of the promoter downregulates GATA2 by  75% in progenitors, including Common Myeloid Progenitors (CMP) and GMP [38, 43, 46, 52]. Herein, we elucidated the mechanism underlying hypersensitivity of GATA2$^{low}$ progenitors to inflammation by utilizing GATA2$^{low}$ progenitors that express  50% less PU.1 and analyzing how these factors

and IFN$\gamma$-TLR1/2 signaling target the genome. The genome-sensing mechanism involved inflammation-induced GATA2 and PU.1 recruitment to chromatin at a gene cohort and constitutive GATA2 and PU.1 occupancy at another cohort. Contrasting with a GATA2-RUNX1 cooperativity paradigm, their opposing activities dictated PU.1-dependent genome responses to inflammation, and they differentially conferred responses to qualitatively distinct inflammatory signals.

## 4.2 Toll-Like Receptor signaling contribution to GATA2-deficient hematopoietic progenitor levels and activities

GATA2 deficiency in primary and immortalized fetal myeloerythroid progenitors upregulates genes encoding IFN$\gamma$ and TLR signaling pathway components, conferring hypersensitivity to inflammation [43, 52]. Hypersensitivity is associated with reduced Granulocytic Progenitors (GP) and increased Monocytic Progenitors (MP) with retention of monocytic differentiation *ex vivo* [38, 43, 44]. The transcription factor Interferon Regulatory Factor 8 (IRF8) functions downstream of IFN$\gamma$ signaling to promote monocytic differentiation [253, 254]. Genetic ablation of *Irf8* in *Gata2* $-77^{-/-}$ embryos counteracted the disproportionately high monocytic differentiation [44]. Since GATA2 deficiency elevates IFN$\gamma$- and TLR-induced transcription [43, 52], we asked if attenuating the elevated TLR signaling of GATA2$^{low}$ progenitors mimics *Irf8* ablation to normalize lineage output. As Myeloid Differentiation Primary Response 88 (MYD88) is an adaptor crucial for canonical permutations of TLR1/2 and TLR2/6 signaling [255, 256], we ablated *Myd88* to attenuate TLR signaling *in vivo*. We generated $-77^{+/-}$;*Myd88*$^{-/-}$ mice and with two mating schemes generated $-77^{+/+}$, $-77^{-/-}$, *Myd88*$^{-/-}$, and $-77^{-/-}$;*Myd88*$^{-/-}$ E14.5 embryos to analyze signaling and progenitors (Fig. 4.1A).

$-77^{-/-}$;*Myd88*$^{-/-}$ embryos were anemic with reduced liver size and cell numbers, re-

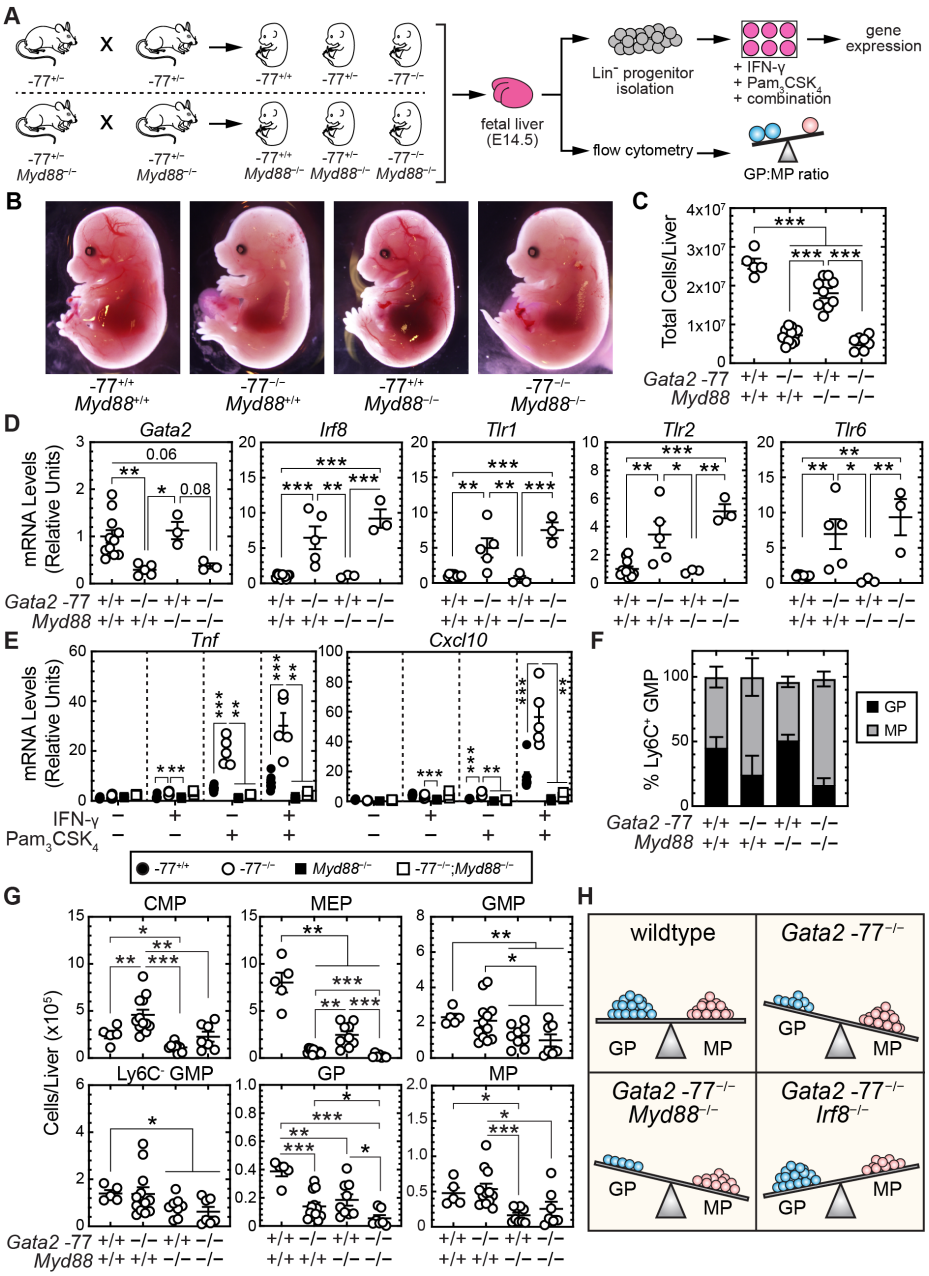


**Figure 4.1: *Myd88* ablation does not normalize the disproportionately high monocytic to granulocytic progenitor ratio of GATA2$^{low}$ mouse embryos.** (**A**) Strategy for attenuating TLR signaling. (**B**) Representative E14.5 embryos obtained from the mating schemes in panel A. (**C**) Total cellularity of E14.5 fetal livers. (**D**) The expression of select genes was quantitated using RT-qPCR. (**E**) The responsiveness of *Tnf* and *Cxcl10* to IFN$\gamma$ and $Pam_3CSK_4$ were quantitated using RT-qPCR. Statistics in (C) and (D) were one-way ANOVA with Tukey's multiple comparisons test and in (E) were multiple unpaired t-tests. (**F**) Quantitation of MP and GP frequency within the Ly6C$^+$ GMP population in E13.5-14.5 fetal liver obtained from 8 litters. (**G**) Quantitation of progenitor populations in E14.5 fetal livers obtained from 7 litters. Error bars for all plots represent mean $\pm$ standard deviation (SD). * $P < 0.05$, ** $P < 0.01$, *** $P < 0.001$; Welch's unequal variance t tests. (**H**) Model depicting *Irf8*, but not *Myd88*, ablation reverses the GP:MP imbalance resulting from *Gata2* $-77$ enhancer deletion. Though levels of GPs and MPs were reduced by *Myd88* ablation, the ratio was not altered.

sembling $-77^{-/-}$ embryos (Fig. 4.1, B and C). In $-77^{-/-}$ fetal livers, *Irf8*, *Tlr1*, *Tlr2*, and *Tlr6* expression were elevated as described (Fig. 4.1D). MYD88 loss in $-77^{-/-}$ embryos did not affect *Gata2* expression or upregulated *Irf8*, *Tlr1*, *Tlr2*, and *Tlr6* expression. *Myd88* ablation abrogated elevated TLR1/2 agonist ($Pam_3CSK_4$)-induced activation (without or with IFN$\gamma$) of TLR and IFN$\gamma$ target genes Tumor Necrosis Factor (*Tnf*) and C-X-C Motif Chemokine Ligand 10 (*Cxcl10*) in GATA2$^{low}$ Lin$^-$ progenitors (Fig. 4.1E). Since *Myd88* ablation blocked TLR1/2-activated transcription in $-77^{-/-}$ progenitors, we asked if this reversed the GP:MP imbalance. Using CD115 expression, Ly6C$^+$ GMP were parsed into GP and MP populations (Fig. 4.2, A and B). Unlike IRF8 loss, MYD88 loss did not reverse the GP:MP imbalance (Fig. 4.1F).

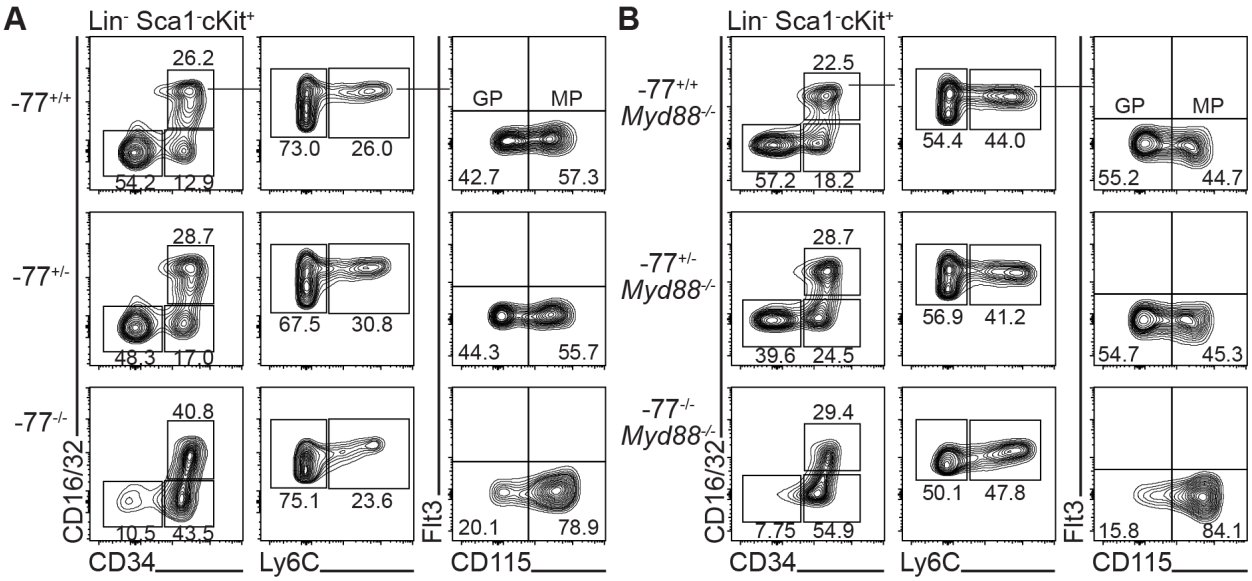


**Figure 4.2: *Myd88* ablation does not affect the cellular composition of *Gata2* $-77^{-/-}$ fetal liver.** (**A**) Representative flow cytometry analysis of progenitor populations in E14.5 fetal livers from $-77^{+/-}$ timed mating. (**B**) Representative flow cytometry analysis of progenitor populations in E14.5 fetal livers from $-77^{+/-}$;*Myd88*$^{-/-}$ timed mating. Granulocyte Progenitors (GP) and Monocyte Progenitors (MP) were distinguished from Granulocyte Monocyte Progenitors (GMP) (Lin$^-$Sca1$^+$cKit$^+$CD34$^+$CD16/32$^{high}$) by expression of Ly6C and from each other by M-CSFR (CD115).

Since $-77^{-/-}$ and *Myd88*$^{-/-}$ embryos had smaller livers, we tested if MYD88 loss reduced total progenitor numbers. GATA2 deficiency increased CMP in fetal liver 1.8-fold ($P = 0.0081$). MYD88 loss decreased CMP 2.2-fold ($P = 0.024$) (Fig. 4.1G). CMP lev-

els were comparable in $-77^{-/-}$;*Myd88*$^{-/-}$ and wild-type littermates. Relative to wild-type embryos, Megakaryocyte Erythroid Progenitors (MEPs) in $-77^{-/-}$ livers were 12-fold lower ($P < 0.0001$). MYD88 loss reduced MEPs 3.3-fold ($P < 0.0001$). MEPs were 37-fold ($P < 0.0001$) lower in $-77^{-/-}$;*Myd88*$^{-/-}$ vs. wild-type. Thus, MYD88 contributes to establishment and/or maintenance of MEPs in GATA2$^{low}$ fetal liver. MYD88 loss, with or without $-77$ ablation, reduced the GMP population relative to wild-type (2.3-fold, $P = 0.0087$ and 1.8-fold, $P = 0.0031$, respectively). Ly6C$^-$ GMPs were unaffected by $-77$ deletion but decreased upon MYD88 loss (2.3-fold, $P = 0.012$). Among the Ly6C$^+$ GMPs, GP numbers decreased 2.8- ($P = 0.0002$) and 2.1-fold ($P = 0.0028$) upon GATA2 deficiency and MYD88 loss, respectively. GP levels decreased an additional 7.1-fold ($P < 0.0001$) in $-77^{-/-}$;*Myd88*$^{-/-}$ vs. wild-type. Though MYD88 loss reduced MPs 2.9-fold ($P = 0.0121$), $-77^{-/-}$;*Myd88*$^{-/-}$ MPs were comparable to wild-type and slightly less than $-77^{-/-}$. These studies indicated that compromising TLR signaling reduced GPs and MPs without normalizing the imbalanced GP to MP ratio of GATA2$^{low}$ fetal livers (Fig. 4.1H), differing from the ramifications of disrupting IFN$\gamma$ function via IRF8 loss.

To determine if compromised TLR signaling impacts $-77^{-/-}$ progenitor function, progenitor activity was quantified with sorted E14.5 fetal liver CMPs and GMPs in a Colony-Forming Unit (CFU) assay. By comparison to $-77^{+/+}$ CMPs, $-77^{-/-}$ and *Myd88*$^{-/-}$ CMPs produced fewer (1.9-fold, $P = 0.0097$ and 2.0-fold, $P = 0.007$, respectively) CFU-Granulocyte (CFU-G) colonies (Fig. 2A). CFU-G generation from $-77^{-/-}$;*Myd88*$^{-/-}$ CMPs was even lower (5.2-fold, $P < 0.0001$) (Fig. 4.3A). These results were concordant with reduced GPs detected by flow cytometry (Fig. 4.1G). Thus, GATA2 and MYD88 collectively increased CMP-derived CFU-G. $-77$ deletion abrogated GMP-derived CFU-G, and MYD88 loss did not further affect CFU-G or elevated CFU-Monocytes (Fig. 4.3B). GATA2 deficiency abrogated CMP-derived CFU-Granulocyte, Erythrocyte, Monocyte, Megakaryocyte (CFU-GEMM), and MYD88 loss did not affect CFU-GEMM (Fig. 4.3A). Individual or dual ablation of *Gata2* $-77$ and MYD88 did not affect CMP- or GMP-derived CFU-Granulocyte

Monocyte (CFU-GM) (Fig. 4.3). Analyses with the $-77^{-/-}$;$Myd88^{-/-}$ model, combined with our prior $Irf8^{-/-}$ analysis, revealed differential importance of distinct inflammatory mechanisms (IFN$\gamma$ vs. TLR pathways) for the lineage output of GATA2$^{low}$ fetal livers.

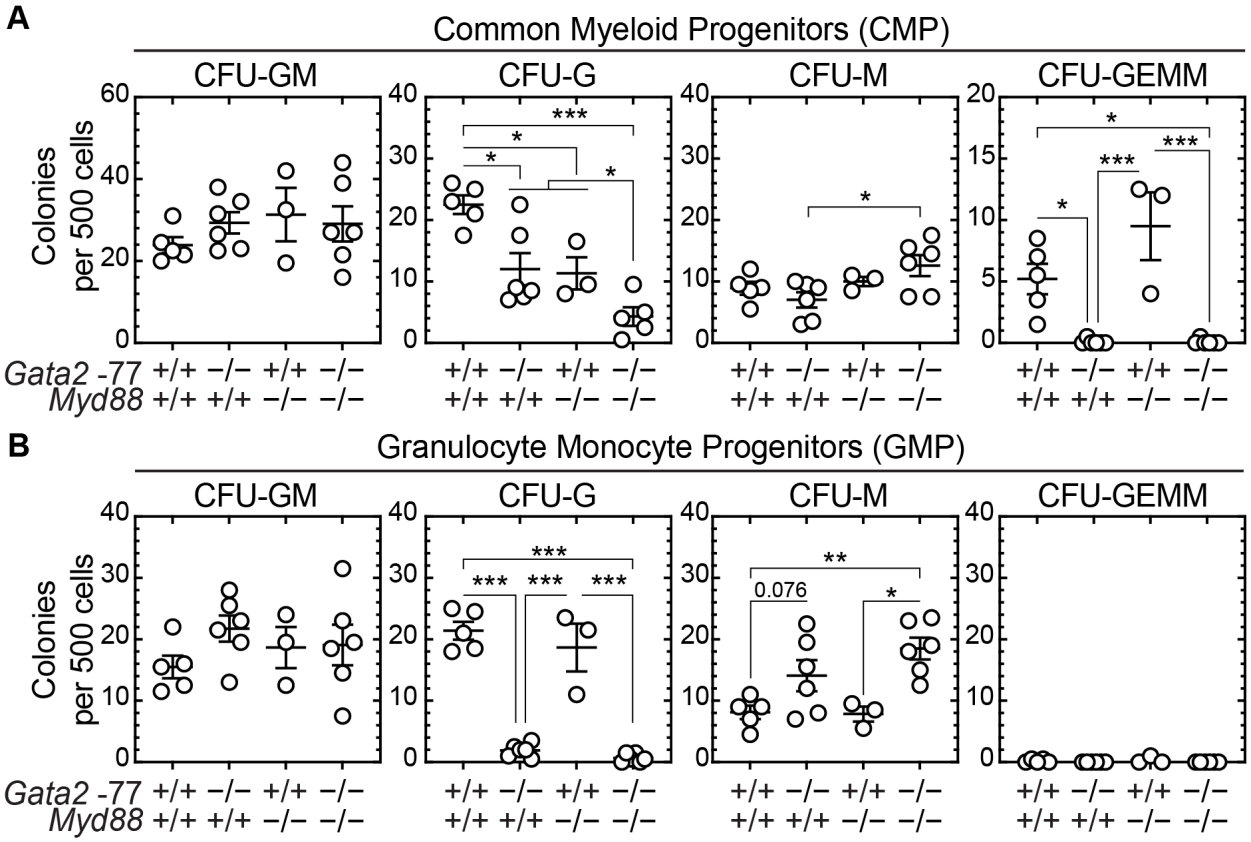


**Figure 4.3: Toll-Like Receptor signaling promotes hematopoietic progenitor granulopoietic activity in GATA2$^{low}$ mouse embryos.** Quantitation of colonies from sorted CMP (**A**) and GMP (**B**) (5 liters) plated in M3434 Methylcellulose media at 500 cells/plate. Colonies were enumerated for eythroid, granulocyte, and monocyte content as CFU-GM, CFU-G, CFU-M, or CFU-GEMM. Error bars for all plots represent mean ± standard deviation. Statistics: Welch's unequal variance t-tests. * $P < 0.05$, ** $P < 0.01$, *** $P < 0.001$.

## 4.3 Distinct GATA2 and PU.1 activities confer inflammation-induced transcriptional responses

Though GATA2, IRF8, and MYD88 control critical aspects of myeloid progenitor development and/or function, our analyses described above revealed functional differences between IRF8 and MYD88, and mechanistic relationships are unresolved. GATA2 deficiency elevates

activity of the hematopoietic transcription factor PU.1 to promote myeloid and B-lineage expression programs without affecting PU.1 levels [46]. IRF8 and transcription factors activated by IFN$\gamma$ and TLR signaling, such as NF-$\kappa$B, and AP1, can co-occupy chromatin with PU.1 [257–259]. Analysis of GATA2$^{low}$ progenitor transcriptomes revealed that genes activated by MYD88-dependent inflammatory signaling harbor motifs for signal-dependent factors and lineage-determining factors, including ETS motifs bound by PU.1 [52]. We hypothesized that PU.1 functions in inflammatory mechanisms involving GATA2, IRF8, and MYD88.

To establish if PU.1 is essential, contributory, or not required for IFN$\gamma$- and TLR1/2-mediated genomic responses, we utilized GATA2- and PU.1-deficient (hi$-77^{-/-}$;*Spi1*URE$^{-/-}$) fetal progenitors (Fig. 4.4A). Expression of *Spi1*, encoding PU.1, is controlled by a -14 kb enhancer (Upstream Regulatory Element = URE) [98, 260]. *Spi1* URE deletion reduced *Spi1* expression (Fig. 4.4B) 3.8-fold ($P < 0.001$) and PU.1 (Fig. 4.4C) 2.1-fold ($P < 0.0001$). Although *Gata2* mRNA was unaffected, GATA2 protein increased 1.8-fold ($P = 0.0084$) in hi$-77^{-/-}$;*Spi1*URE$^{-/-}$ vs. hi$-77^{-/-}$ cells. hi$-77^{-/-}$ (GATA2$^{low}$) and hi$-77^{-/-}$;*Spi1*URE$^{-/-}$ (GATA2$^{low}$PU.1$^{low}$) progenitors were treated with vehicle, IFN$\gamma$, TLR1/2 agonist $Pam_3CSK_4$, or both agents for 4 h, and RNA-seq analysis was conducted (Fig. 4.4A). As an additional control, hi$-77^{+/+}$ (wild-type) progenitors were treated with or without both agents. Principal component analysis revealed reproducible RNA-seq data from four biological replicates (Fig. 4.5A).

To determine the PU.1 contribution to TLR1/2-regulated transcription, we compared $Pam_3CSK_4$-induced differentially expressed genes (DEGs) between GATA2$^{low}$ and GATA2$^{low}$ PU.1$^{low}$ progenitors. $Pam_3CSK_4$ activated 33 genes in GATA2$^{low}$ cells, and lowering PU.1 ablated responses of 27 of these genes (Fig. 4.4D). Gene Ontology (GO) revealed that these PU.1-activated genes are linked to inflammatory response, cellular response to Lipopolysaccharide (LPS), and negative regulation of I$\kappa$B kinase/NF-$\kappa$B signaling (Fig. 4.5B). Though six TLR-regulated genes retained regulation in GATA2$^{low}$PU.1$^{low}$ progenitors, the magni-

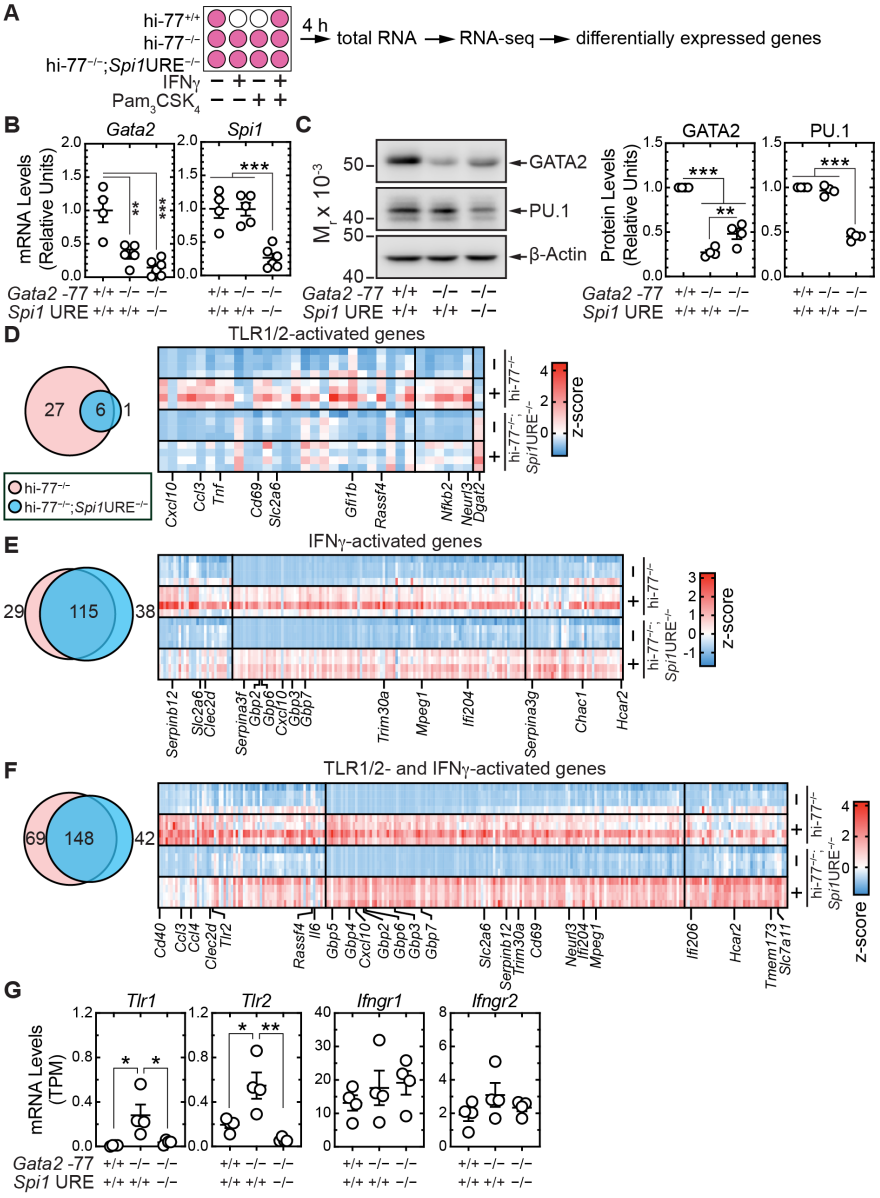


**Figure 4.4: Genome sensing of inflammatory stimuli in GATA2$^{low}$ progenitors.** (**A**) Strategy for gene expression analysis. hi$-77^{+/+}$ (wild-type), hi$-77^{-/-}$ (GATA2$^{low}$) and hi$-77^{-/-}$;*Spi1*URE$^{-/-}$ (GATA2$^{low}$PU.1$^{low}$) progenitors were treated with vehicle, IFN$\gamma$ (1 ng/ml), Pam$_3$CSK$_4$ (100 ng/ml), or both for 4 h (n = 4). Total RNA was isolated for RNA-seq. (**B**) RT-qPCR analysis of *Gata2* and *Spi1* expression (n = 4-6). (**C**) Left, representative Western blot of GATA2 and PU.1. Right, densitometric analysis of band intensities normalized to the loading control $\beta$-Actin (n = 4). Statistics in (B) and (C): One-way ANOVA with Tukey's multiple comparisons test. * $P < 0.05$, ** $P < 0.01$, *** $P < 0.001$. (**D** to **F**) Left, overlap of activated differentially expressed genes (DEGs) in GATA2$^{low}$ and GATA2$^{low}$PU.1$^{low}$ cells in response to Pam$_3$CSK$_4$ (D), IFN$\gamma$ (E), and both agents (F). Right, heat map depicting expression of activated DEGs in response to Pam$_3$CSK$_4$ (D), IFN$\gamma$ (E), and both agents (F) and presented as Z-scores of Transcripts per Million (TPM). Each section of the heatmaps in (D-F) corresponds to each section of Venn diagrams in the same order. (**G**) TLR gene (*Tlr1*, *Tlr2*) and IFN$\gamma$ receptor subunit (*Ifngr1*, *Ifngr2*) expression in GATA2$^{low}$ and GATA2$^{low}$PU.1$^{low}$ progenitors.

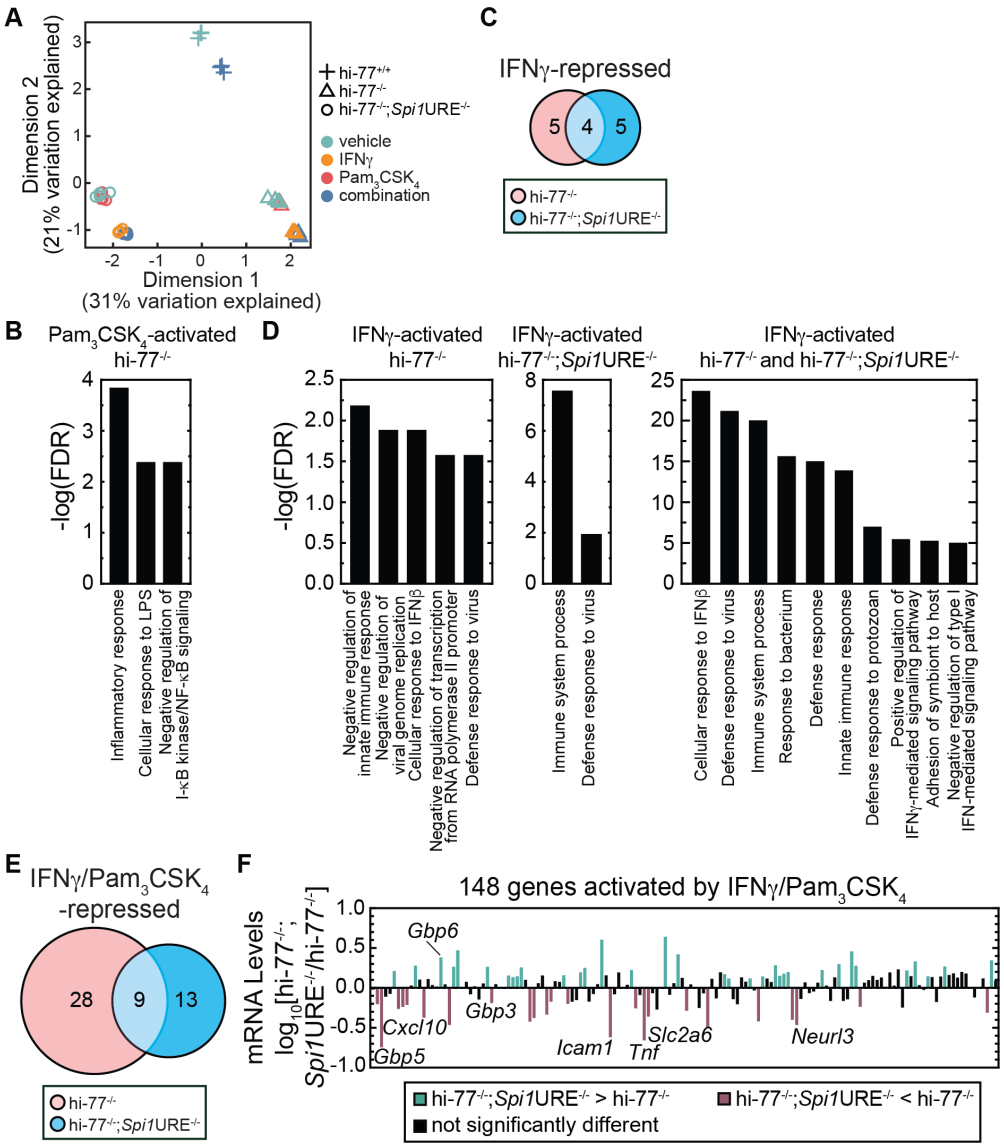


**Figure 4.5: Biological processes regulated by inflammation in GATA2/PU.1-deficient progenitors.** (**A**) Principle component analysis showing the segregation of transcriptomes for wild-type, GATA2$^{low}$, and GATA2$^{low}$PU.1$^{low}$ in response to inflammatory mediators. (**B**) Top categories with statistical significance from Gene Ontology (GO) analysis of TLR1/2-activated genes in GATA2$^{low}$ progenitors using DAVID Bioinformatics Resources (https://david.ncifcrf.gov). (**C**) Repressed DEGs overlapping between GATA2$^{low}$ and GATA2$^{low}$PU.1$^{low}$ progenitors in response to IFNγ. (**D**) Top categories with statistical significance from GO analysis of IFNγ-activated genes only in wild-type, only in GATA2$^{low}$, or in both progenitors. (**E**) Repressed DEGs overlapping between GATA2$^{low}$ and GATA2$^{low}$PU.1$^{low}$ progenitors in response to inflammation. (**F**) Transcript levels of 148 genes activated by inflammation in GATA2$^{low}$PU.1$^{low}$ versus GATA2$^{low}$ progenitors. Data were presented as $\log_{10}$[(GATA2$^{low}$PU.1$^{low}$ (combo) vs GATA2$^{low}$ (combo)]. Colored bars indicate the differential magnitude of responses with $P < 0.05$ by unpaired two-tail Student's t-tests.

tude of $Pam_3CSK_4$-induced expression was lower in GATA2$^{low}$PU.1$^{low}$ vs. GATA2$^{low}$ cells (Fig. 4.4D). PU.1 is therefore essential for TLR1/2-induced transcription in GATA2$^{low}$ progenitors.

Contrasting with TLR responses, reducing PU.1 in GATA2$^{low}$ progenitors did not alter responses of 115 IFN$\gamma$-activated genes, 87% of which were induced to a similar magnitude in GATA2$^{low}$ and GATA2$^{low}$PU.1$^{low}$ cells (Fig. 4.4E). Twenty-nine genes lost responsiveness to IFN$\gamma$ in GATA2$^{low}$PU.1$^{low}$ vs. GATA2$^{low}$ cells, reflecting their dependence upon PU.1 concentration (Fig. 4.4E). IFN$\gamma$ repressed a small number of genes in GATA2$^{low}$ and GATA2$^{low}$PU.1$^{low}$ cells (Fig. 4.5C). GO analysis revealed that the PU.1-activated genes are linked to negative regulation of biological processes, innate immune response, viral genome replication, and RNA Polymerase II transcription (Fig. 4.5D). IFN$\gamma$ signaling activated 38 genes in GATA2$^{low}$PU.1$^{low}$ cells that were not activated in GATA2$^{low}$ cells (Fig. 4.4E). Lowering PU.1 impaired transcriptional responses of certain, but not all, IFN$\gamma$-activated genes in GATA2$^{low}$ progenitors.

Since lowering PU.1 in GATA2$^{low}$ cells decreased TLR1/2- and attenuated IFN$\gamma$-mediated transcription, we hypothesized that GATA2$^{low}$PU.1$^{low}$ progenitors might respond to IFN$\gamma$ and TLR1/2 agonist similarly to IFN$\gamma$ alone. Reducing PU.1 decreased responses of 69 genes and conferred responsiveness of 42 genes that were not activated in GATA2$^{low}$ cells (Fig. 4.4F). Though TLR signaling did not repress genes, the combined signaling repressed twofold (in GATA2$^{low}$PU.1$^{low}$) to fourfold (in GATA2$^{low}$) more genes vs. IFN$\gamma$ signaling alone (Fig. 4.5E). Reducing PU.1 did not alter the responsiveness of 148 genes to inflammation (Fig. 4.4F). Among these genes, 33 (22%) were induced to a greater extent, and 24 (16%) induced less in GATA2$^{low}$PU.1$^{low}$ vs. GATA2$^{low}$ progenitors (Fig. 4.5F). To test if altered TLR1/2 and IFN$\gamma$ responses reflect dysregulation of the respective receptors, we quantified receptor mRNA levels. Lowering PU.1 abrogated upregulated *Tlr1* and *Tlr2* expression without affecting *Ifngr1* and *Ifngr2* (Fig. 4.4G). Thus, inflammation-activated genes in GATA2$^{low}$ progenitors can be sensitive or insensitive to PU.1. Furthermore, the defective responses are

associated with reduced *Tlr1* and *Tlr2* expression.

Our prior study revealed synergistic IFN$\gamma$ and TLR responses to induce cytokine/chemokine expression and production in GATA2$^{low}$ progenitors [52], but the mechanisms were not elucidated. To determine if PU.1 mediates synergistic responses in GATA2$^{low}$ progenitors, we asked if reducing PU.1 disrupts synergism. Among 217 IFN$\gamma$- and $Pam_3CSK_4$-activated genes, 178 genes were regulated synergistically (Fig. 4.6A). GATA2 repressed the response of 79 of these genes. Parsing the genes based on PU.1-mediated activation, -repression, or -insensitivity revealed cohorts with unique behaviors (Fig. 4.6B).

Tumor Necrosis Factor Receptor Superfamily Member 5 (*Cd40* or *Tnfrsf5*), which was highly activated by inflammation in GATA2$^{low}$ vs wild-type cells, exemplifies a GATA2-repressed, PU.1-activated gene that responds synergistically to the two factors. In a proteomic study, the ligand of CD40 receptor (CD40L) was detected in serum of GATA2 Deficiency Syndrome patients [40]. Reducing PU.1 by ~50% attenuated Cd40 expression to levels resembling wild-type cells (Fig. 4.6B). By contrast, the Interferon-activated, GATA2-repressed gene *Ifi204* was elevated further in GATA2$^{low}$PU.1$^{low}$ vs GATA2$^{low}$ cells, indicating a PU.1-dependent repression mechanism (Fig. 4.6B). Members of the Guanylate Binding Protein (GBP) family are Interferon-inducible genes encoding proteins that protect cells from pathogens [226, 228]. GATA2 represses, and IFN$\gamma$ and TLR synergistically induce *Gbp* genes. *Gbp5* encodes an activator of NLRP3 inflammasome assembly [228], and resembling *Cd40*, PU.1 promotes the transcriptional response (Fig. 4.6B). PU.1 repressed *Gbp6*, which was expressed in GATA2$^{low}$PU.1$^{low}$ cells greater than GATA2$^{low}$ cells (Fig. 4.6B). Reducing PU.1 did not affect inflammation-induced *Gbp2* and *Gbp7* expression (Fig. 4.6B). Inflammation responsiveness of these genes was also detected in primary Lin$^-$ progenitors from $-77^{+/+}$ and $-77^{-/-}$ E14.5 fetal livers (Fig. 4.6C). These studies demonstrated that PU.1 mediates a subset of inflammation-induced transcriptional responses in GATA2$^{low}$ progenitors.

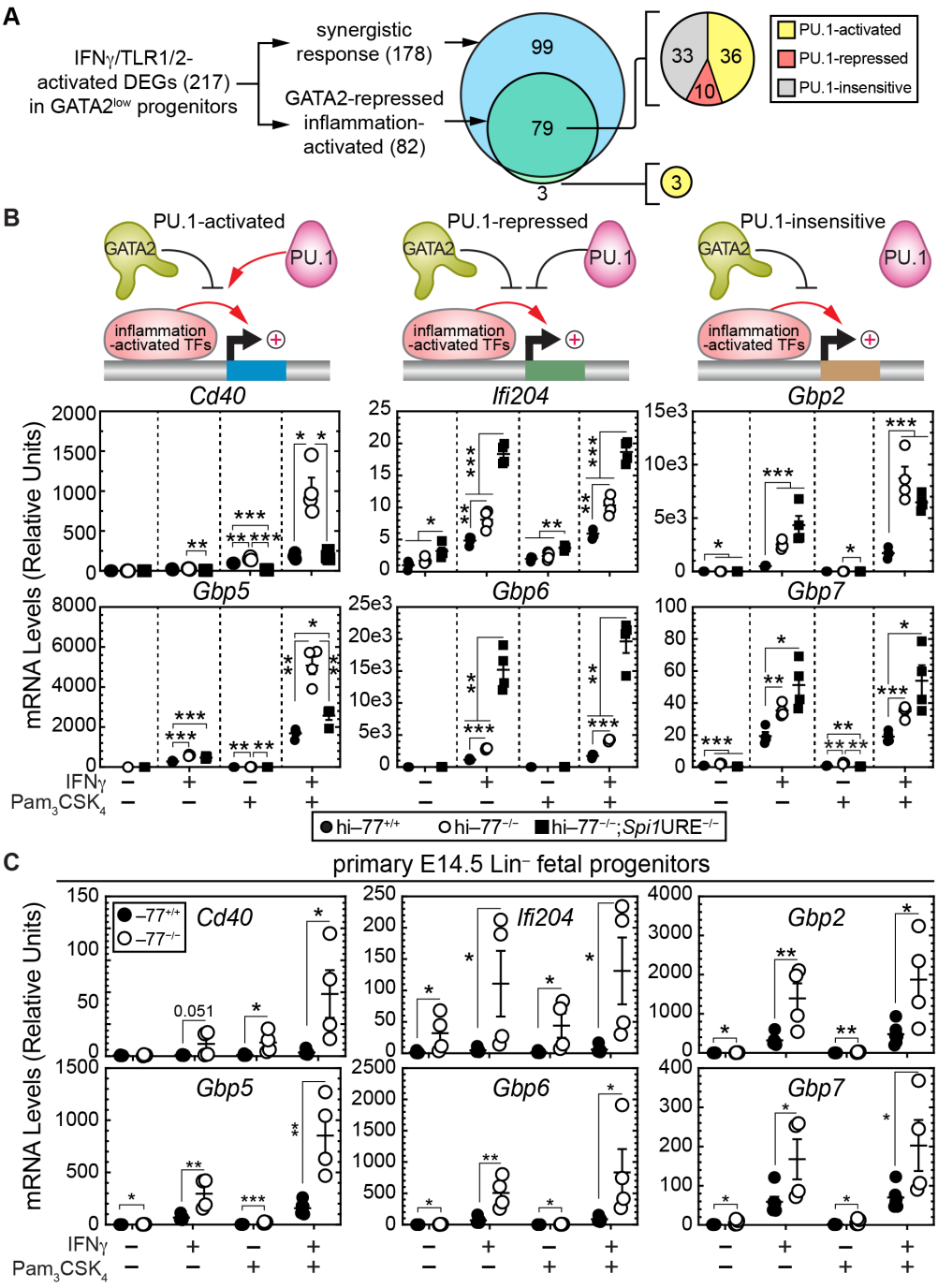


**Figure 4.6: Molecular determinants of inflammation-activated transcriptional responses.** (**A**) GATA2-repressed genes that were activated synergistically in GATA2$^{low}$ cells by IFNγ and $Pam_3CSK_4$ were parsed into PU.1-activated, PU.1-repressed, and PU.1-insensitive cohorts. The synergistic genes were defined as inflammation-activated DEGs with a larger $|log_2(fold\ change)|$ in combination vs. vehicle than that of IFNγ vs. vehicle and $Pam_3CSK_4$ vs. vehicle. (**B**) Top, models depicting different modes of regulation of signal-dependent genes by GATA2 and PU.1. Bottom, RT-qPCR analysis of representative synergistic genes were quantitated with RT-qPCR (n = 4). (**C**) The responsiveness of prioritized synergistic genes in primary lineage-depleted progenitors isolated from E14.5 fetal livers of $-77^{+/+}$ (n = 6) and $-77^{-/-}$ (n = 4) embryos (pooled from three liters). Statistics in (B) and (C): multiple unpaired t-tests. * $P < 0.05$, ** $P < 0.01$, *** $P < 0.001$.

## 4.4 Mechanisms underlying genome sensing of inflammation

How does PU.1 mediate IFN$\gamma$- and TLR-regulated genomic responses in GATA2$^{low}$ progenitors? PU.1 might occupy inflammation-regulated loci independent of inflammation, with signal-dependent steps occurring post-chromatin occupancy. Alternatively, PU.1 might be excluded from loci in the steady-state, and inflammation might promote PU.1 chromatin occupancy. We tested these models using Cleavage Under Target and Tagmentation (CUT&Tag) [169, 170] to establish GATA2 and PU.1 chromatin occupancy in hi$-77^{+/+}$, hi$-77^{-/-}$, and hi$-77^{-/-}$;*Spi1*URE$^{-/-}$ cells without or with inflammation (Fig. 4.7A). H3K4me3 was used to detect active promoters [261, 262], with Immunoglobulin G (IgG) as a negative control. To establish if GATA2 deficiency impacts GATA2 and PU.1 chromatin occupancy, we compared the average of normalized CUT&Tag signals from -2 kb upstream of the Transcription Start Site (TSS) to 1 kb downstream of the 3'-end of the gene at 217 inflammation-induced DEGs with wild-type, GATA2$^{low}$, and GATA2$^{low}$PU.1$^{low}$ cells. GATA2 occupancy was detected in wild-type cells and reduced in GATA2$^{low}$ cells (Fig. 4.8A). Lowering PU.1 in hi$-77^{-/-}$ restored GATA2 occupancy to levels resembling wild type. Thus, PU.1 restricts GATA2 occupancy. PU.1 occupancy was indistinguishable in all cell types (Fig. 4.8A).

To determine if inflammation influences PU.1 chromatin occupancy in GATA2$^{low}$ progenitors, we compared PU.1 CUT&Tag median signals at 217 inflammation-activated loci in GATA2$^{low}$ progenitors without or with inflammation (Fig. 4.7B). Since the PU.1 CUT&Tag signals were highest near the TSS (Fig. 4.8A), we analyzed PU.1 occupancy from 1 kb upstream to 1 kb downstream of the TSS. This analysis revealed that inflammation increased PU.1 occupancy at 53 loci (Fig. 4.7, B and C). By averaging PU.1 signals from four biological replicates, the range of signals at these loci in inflammation-treated GATA2$^{low}$ progenitors was higher than the unstimulated control (Fig. 4.7D). Among 217 inflammation-activated

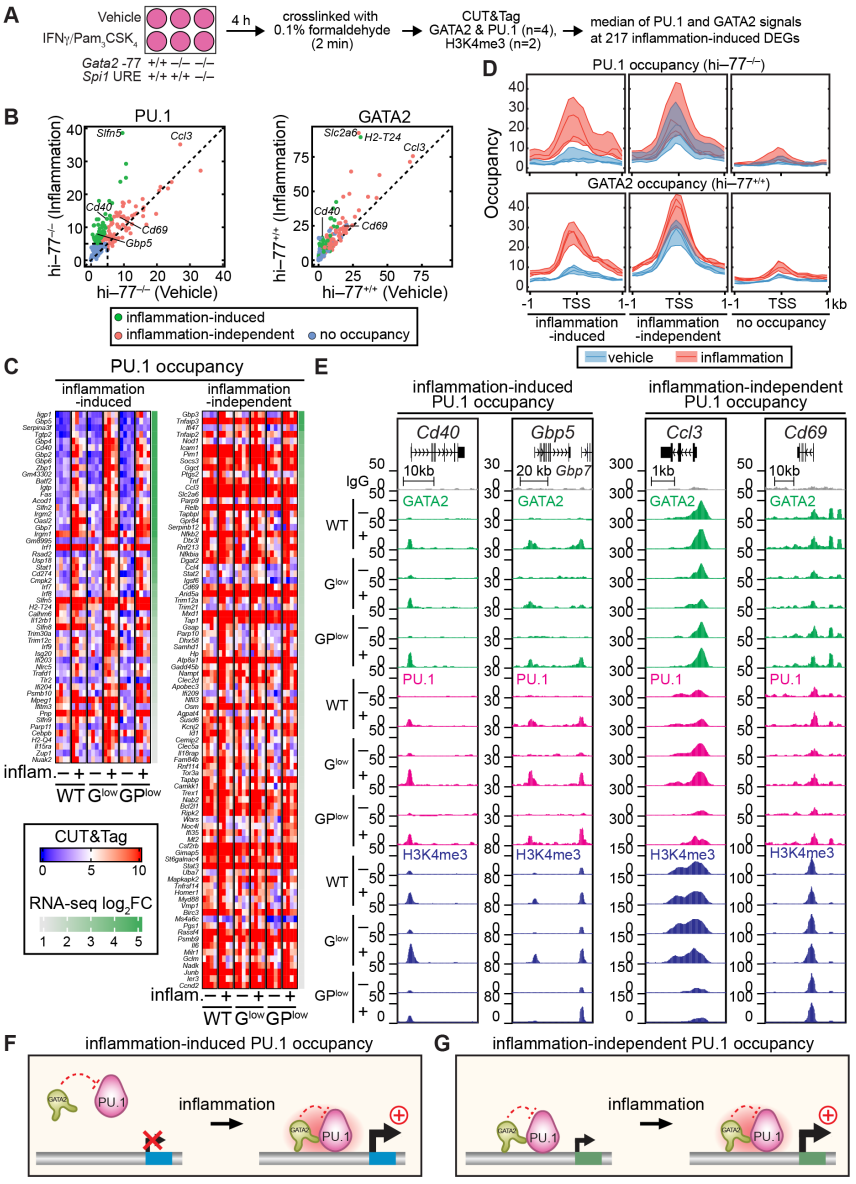


**Figure 4.7: Locus-specific mechanisms of inflammation-sensing in GATA2$^{low}$ progenitors.** (**A**) Schematic depicting the chromatin occupancy analysis. (**B**) Comparison of median PU.1 (left) and GATA2 (right) CUT&Tag signals at 217 differentially expressed genes (DEGs) in untreated vs inflammation-activated GATA2$^{low}$ and wild-type cells, respectively. DEGs were colored by their cluster identities. The median signal is the median of signals from 1 kb upstream to 1 kb downstream of the Transcription Start Site (TSS) of each DEG (n = 4). (**C**) Heatmaps depicting PU.1 CUT&Tag signals in untreated vs inflammation-treated wild-type (WT), GATA2$^{low}$ (G$^{low}$), and GATA2$^{low}$PU.1$^{low}$ (GP$^{low}$) progenitors. DEGs were ranked by their log$_2$(fold change) based on RNA-seq data of GATA2$^{low}$ (inflammation vs vehicle). (**D**) Range of signals for three categories of DEGs. The range is defined by the average signals of the four replicates from the same condition and presented as lines in the figure. Average signals are calculated over [TSS − 1 kb, TSS + 1 kb] with a bin width of 100 bp. (**E**) Representative CUT&Tag profiles (replicate 2) at select loci. (**F**) Model of signal-dependent GATA2 and PU.1 occupancy at inflammation-activated genes in GATA2$^{low}$ progenitors. (**G**) Model depicting GATA2 and PU.1 pre-occupancy at inflammation-activated genes.

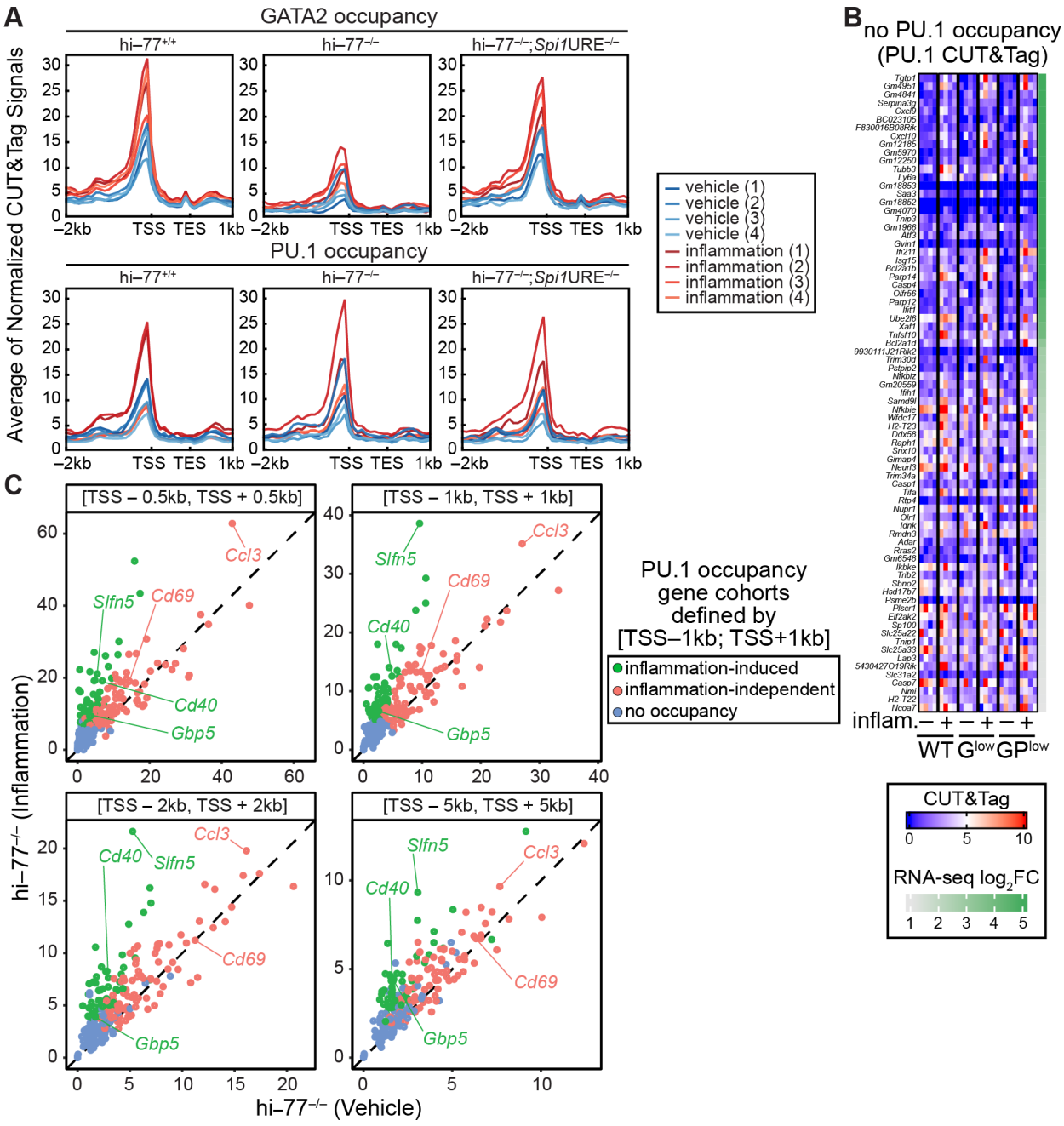


**Figure 4.8: GATA2 and PU.1 occupancy at 217 inflammation-induced genes.** (**A**) GATA2 (top) and PU.1 (bottom) occupancy at 217 differentially expressed genes (DEGs) in wild-type, GATA2$^{low}$, and GATA2$^{low}$PU.1$^{low}$ with or without inflammation are depicted as line plots from 2 kb upstream of the Transcription Start Site (TSS) to 1 kb downstream of the 3'-end of the gene (TES: Transcription End Site). Each line represents a biological replicate. (**B**) Heatmap depicting PU.1 CUT&Tag signals in untreated vs inflammation-activated GATA2$^{low}$ cells in inflammation-activated genes with no PU.1 occupancy. (**C**) Comparison of median PU.1 CUT&Tag signals at 217 DEGs in untreated vs inflammation-activated GATA2$^{low}$ cells using different intervals, including 0.5 kb, 1 kb, 2 kb, and 5 kb around the TSS (n = 4). DEGs were colored by their cluster identities as in [TSS − 1, TSS + 1] interval. Representative genes are indicated.

loci, PU.1 occupied 87 genes, and inflammation did not affect occupancy (Fig. 4.7, B to D). PU.1 occupancy was undetectable at 77 loci regardless of inflammation, suggesting that PU.1 regulates transcription at these loci indirectly, or occupancy cannot be detected (Fig. 4.7, B and D, and Fig. 4.8B). We also conducted the analysis using ranges from 0.5 kb, 1 kb, 2 kb, and 5 kb surrounding the TSS. The 0.5 kb and 2 kb interval analyses revealed results resembling the 1 kb interval (Fig. 4.8C). The 5 kb interval analysis revealed smaller PU.1 CUT&Tag signals with a reduced signal to noise. However, this analysis also identified genes with inflammation-induced vs inflammation-independent PU.1 occupancy. Using these gene cohorts, we asked if inflammation influences GATA2 occupancy. By comparing the median of GATA2 CUT&Tag signals between unstimulated vs. inflammation-treated wild-type cells, inflammation increased GATA2 occupancy at most genes with inflammation-increased PU.1 occupancy (Fig. 4.7, B and D, and Fig. 4.9A). Similarly, GATA2 pre-occupied most genes with PU.1, and inflammation increased GATA2 occupancy.

As *Cd40* and *Gbp5* exemplify inflammation-activated genes activated synergistically by IFN$\gamma$ and TLR1/2 (Fig. 4.6, B and C), we tested how inflammation affected GATA2 and PU.1 occupancy at these loci. In the steady state, GATA2 and PU.1 did not occupy *Cd40* and *Gbp5* (Fig. 4.7E). Inflammation induced GATA2 and PU.1 occupancy at the promoters in wild-type and GATA2$^{low}$ progenitors (Figs. 4.7, C and E). The ~75% reduction in GATA2 resulting from −77 enhancer deletion (GATA2$^{low}$, Fig. 4.4C) increased PU.1 occupancy relative to wild-type, and the ~50% PU.1 reduction in GATA2$^{low}$PU.1$^{low}$ (Fig. 4.4C) reduced PU.1 occupancy to resemble wild type (Fig. 4.7E). H3K4me3 was enriched at active promoters, complementing the *Cd40* and *Gbp5* expression data. Inflammation increased H3K4me3 in wild-type and GATA2$^{low}$ cells, and lowering PU.1 reduced H3K4me3 in response to inflammation (Fig. 4.7E). Inflammation is therefore required for GATA2 and PU.1 to occupy an inflammation-activated gene cohort (Fig. 4.7F).

*Ccl3* and *Cd69* exemplify inflammation-activated genes pre-bound by PU.1 (Fig. 4.7C). *Ccl3* encodes Macrophage Inflammatory Protein 1 Alpha, which is elevated in patients with

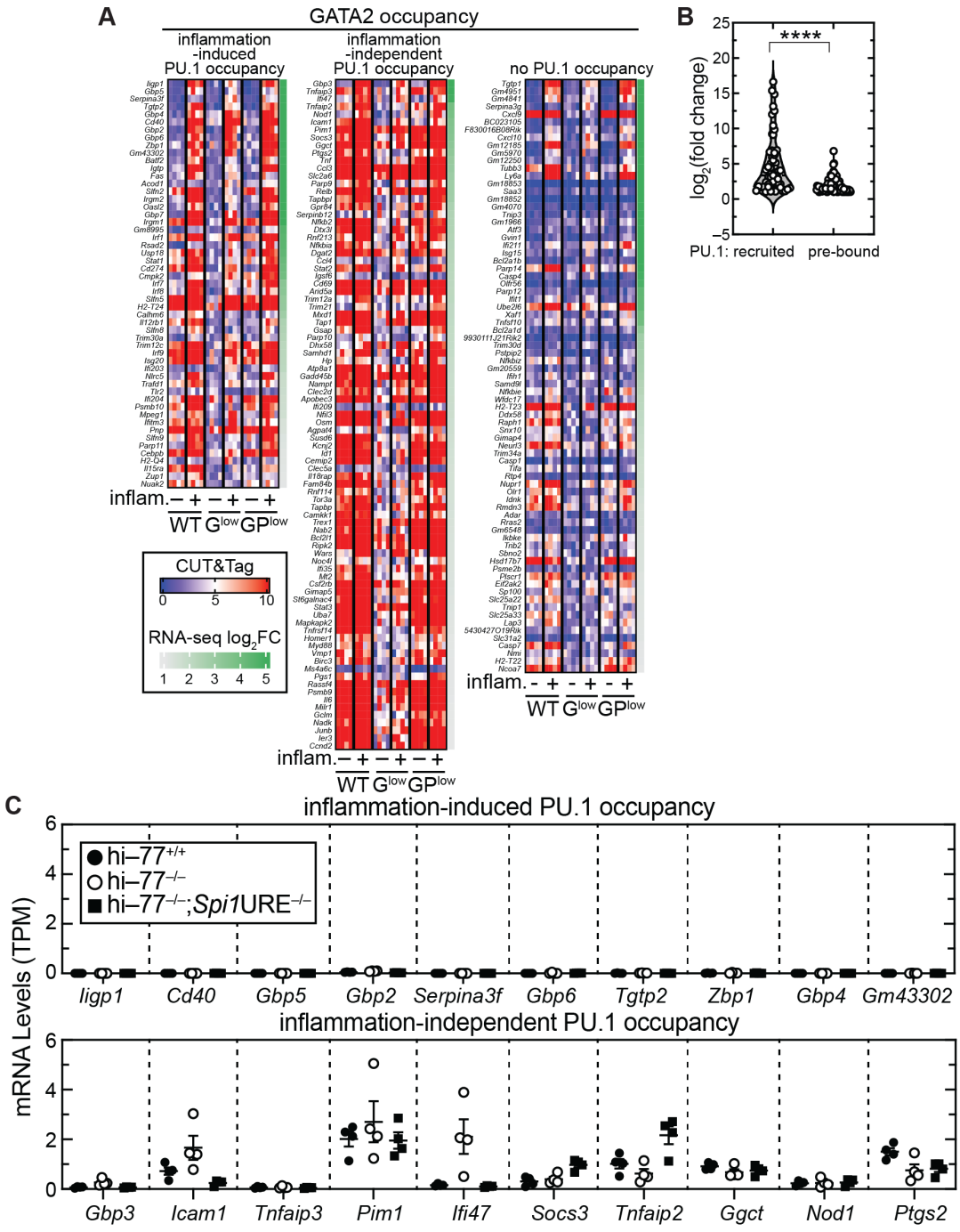


**Figure 4.9: Selective basal expression of inflammation-activated loci with pre-bound PU.1.** (**A**) Heatmaps depicting GATA2 CUT&Tag signals in untreated vs inflammation-activated wild-type (WT), GATA2$^{low}$ (G$^{low}$), and GATA2$^{low}$PU.1$^{low}$ (GP$^{low}$) progenitors. 217 DEGs were clustered as inflammation-induced, inflammation-independent, and no PU.1 occupancy, and ranked by their log$_2$(fold change) based on the RNA-seq data of GATA2$^{low}$ (inflammation) vs GATA2$^{low}$ (vehicle). (**B**) Violin plot depicting the RNA-seq log$_2$(fold change) (inflammation vs vehicle) between genes with inflammation-induced PU.1 occupancy and genes pre-bound by PU.1. Student's unpaired t-test. **** $P < 0.0001$. (**C**) Expression profiles of top-ten genes with inflammation-induced PU.1 occupancy (top) or genes with inflammation-independent PU.1 occupancy (bottom) from RNA-seq data (n = 4). TPM, Transcripts per Million.

Myeloproliferative Neoplasm [263, 264], and *Cd69* encodes a membrane protein important in lymphocytes [265, 266]. In the steady state, GATA2 and PU.1 occupied *Ccl3* and *Cd69* promoters, and inflammation did not affect GATA2 and PU.1 occupancy in wild-type progenitors (Fig. 4.7E). GATA2 deficiency reduced GATA2 and elevated PU.1 occupancy at these loci, and lowering PU.1 restored GATA2 and PU.1 occupancy to wild-type levels (Fig. 4.7E). GATA2 deficiency elevated PU.1 occupancy at the *Ccl3* promoter, and lowering PU.1 decreased PU.1 occupancy to levels resembling wild-type. Thus, GATA2 and PU.1 occupy select inflammation-activated loci independent of inflammation, and inflammation-activated transcription occurs post-chromatin occupancy at these loci (Fig. 4.7G).

What attributes distinguish the two modes of GATA2 and PU.1 function *vis-a-vis* inflammation-induced transcription? Comparing the magnitude of inflammation-induced transcription at genes exhibiting inflammation-induced PU.1 occupancy with PU.1-pre-bound genes revealed that genes regulated to the greatest extent exhibited inflammation-induced PU.1 occupancy (Fig. 4.7C and Fig. 4.9B). By contrast, most PU.1-pre-bound genes were less responsive to inflammation (Fig. 4.7C and Fig. 4.9B). We hypothesized that chromatin at pre-bound loci is accessible, and these loci are active in the basal state without inflammation, even though inflammation increased transcription. Chromatin at loci in which inflammation increases PU.1 occupancy would be inaccessible in the basal state, and these loci would require inflammation for transcription. To test this hypothesis, we analyzed chromatin accessibility in GATA2$^{low}$ progenitors using our previously described Assay for Transposase-Accessible Chromatin using Sequencing (ATAC-seq) data (GSE201968). Comparing accessibility of the top 10 genes [based on RNA-seq $\log_2$(fold change)] with inflammation-induced PU.1 occupancy to the top 10 PU1-pre-bound genes revealed 9/10 genes in the former group had closed chromatin in GATA2$^{low}$ progenitors (ATAC-seq signals $< 0.5$ in four replicates); the sole exception was *Cd40* (Fig. 4.10A). By contrast, 9/10 PU.1-pre-bound genes (except *Ifi47*) exhibited open chromatin in the basal state in GATA2$^{low}$ progenitors (Fig. 4.10A). The average ATAC-seq signal from the top 10 genes

exhibiting inflammation-induced PU.1 occupancy was significantly ($P = 0.0002$) lower than the top 10 genes with inflammation-independent PU.1 occupancy (Fig. 4.10B). The top 10 genes with inflammation-induced PU.1 occupancy were not expressed in the steady state (Fig. 4.9C) and had increased H3K4me3 upon inflammation (Fig. 4.11). By contrast, the top 10 PU.1-pre-bound genes were expressed at varying levels in the basal state (Fig. 4.9C). Among them, 9/10 had H3K4me3 in the uninduced state, and inflammatory signaling did not further increase H3K4me3 (Fig. 4.11). *Ccl3* and *Cd69* promoters were active in the basal state, and inflammation did not affect H3K4me3 at these loci (Fig. 4.7E). Inflammation increased H3K4me3 at *Cd40* and *Gbp5* promoters, correlating with increased GATA2 and PU.1 occupancy upon inflammation (Fig. 4.7E and Fig. 4.11). Thus, genes with inflammation-induced GATA2 and PU.1 occupancy are inaccessible in the steady state, and inflammation increases occupancy to activate transcription. At other loci, GATA2 and PU.1 pre-occupied active genes, and inflammation further increased transcription. Many PU.1-pre-bound genes are located distally on chromosomes, and some reside in clusters *e.g.*, *Ccl* loci on chromosome 11 (Fig. 4.12). Several GBP family members exhibit inflammation-induced PU.1 occupancy and cluster on chromosome 3. The sex chromosomes are devoid of inflammation-activated genes, save *5430427O19Rik*, encoding TLR Adaptor Interacting with Endolysosomal SLC15A4 protein [267].

Since chromatin at PU.1-pre-bound genes without inflammation was more accessible than at genes with inflammation-induced PU.1 occupancy, presumably, other transcription factors and chromatin regulators are also prebound before inflammation. Genes with inflammation-induced PU.1 occupancy might require inflammation-activated transcription factors *e.g.*, NF-$\kappa$B, for inflammation-dependent factor loading, while PU.1-pre-bound genes might not require inflammation-activated transcription factors for PU.1 occupancy, chromatin transitions, and/or activation. We asked if antagonizing inflammation-induced NF-$\kappa$B activation compromises the regulation of one or both gene cohorts. BMS-345541 binds IKK$\beta$ with a dissociation constant ($K_d$) of 130 nM, while having a very low affinity for other kinases ($K_d$

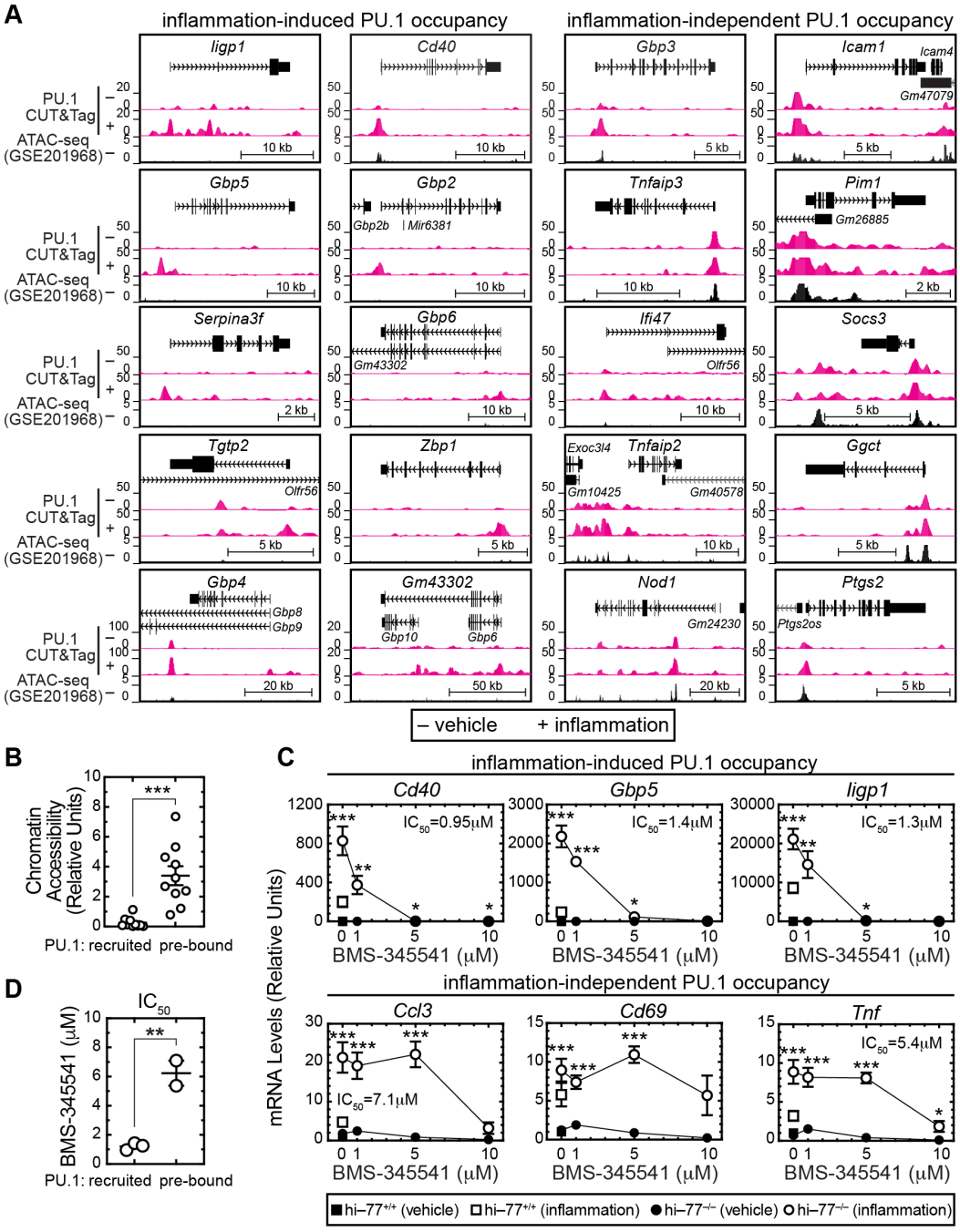


**Figure 4.10: Distinct molecular hallmarks of inflammation-activated genes with inflammation-induced or -independent PU.1 occupancy.** (**A**) ATAC-seq (GSE201968) profiles depicting chromatin accessibility of the top 10 genes with inflammation-induced (left) and inflammation-independent PU.1 occupancy (right) (CUT&Tag replicate 2) in vehicle-treated (−) and inflammation-treated (+) GATA2$^{low}$ cells. (**B**) Comparison of average ATAC-seq signals from n = 4 in (A). (**C**) Dose-response curve of three representative genes with inflammation-induced vs. inflammation-independent PU.1 occupancy to IKK$\beta$ inhibitor BMS-345541 (n = 6, mean ± SEM). $IC_{50}$ for each gene was calculated using Nonlinear Regression. *Cd69* $IC_{50}$ was uncalculated. (**D**) The $IC_{50}$ of genes with inflammation-induced PU.1 occupancy was compared to those of genes with inflammation-independent occupancy. Unpaired t-test in (B) and (D) and multiple unpaired t-test in (C). * $P < 0.05$, ** $P < 0.01$, *** $P < 0.001$.

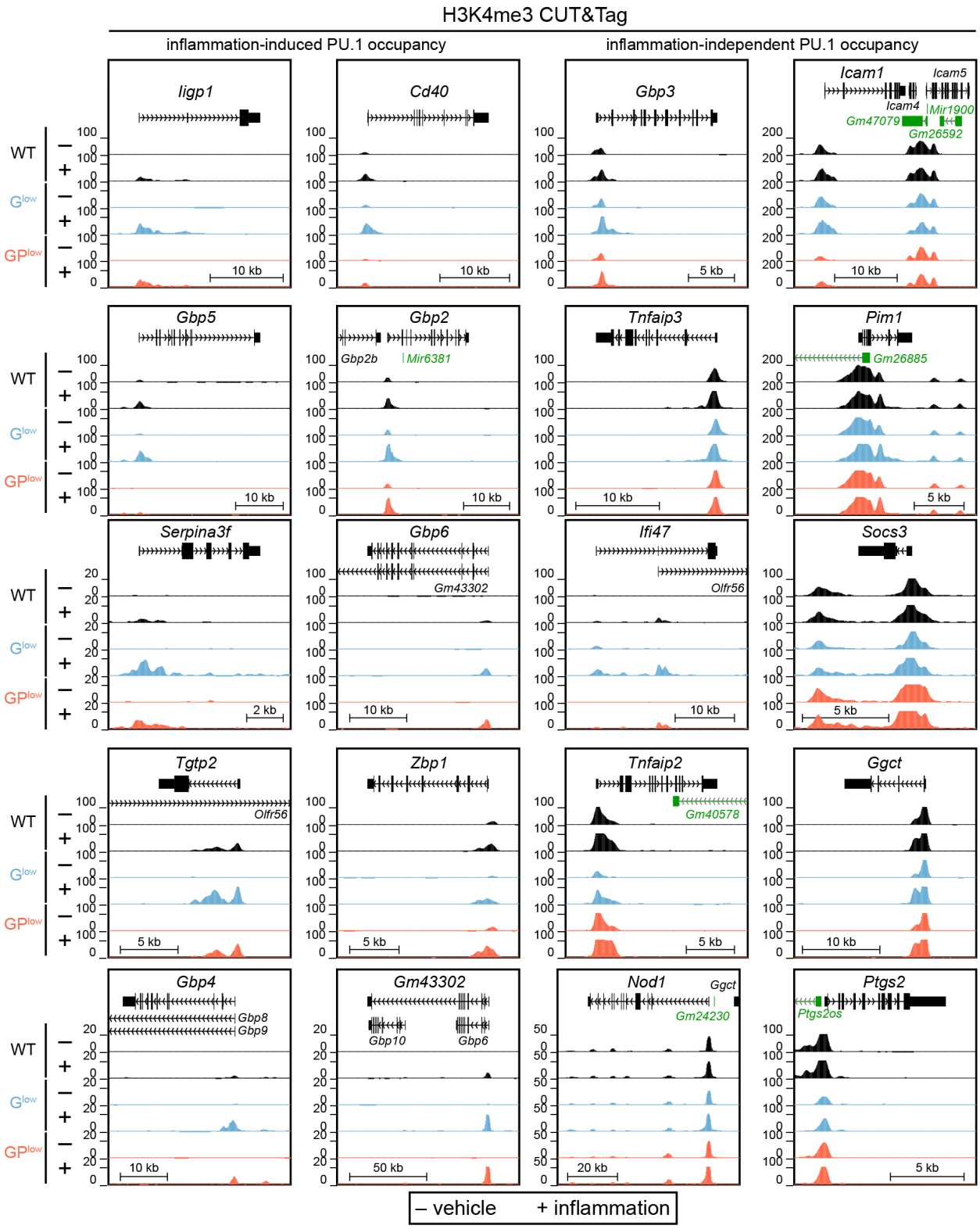


**Figure 4.11: Selective enrichment of H3K4me3 at inflammation-activated loci with pre-bound PU.1.** Representative H3K4me3 CUT&Tag profiles (replicate 1) at the top ten genes in wild-type (WT), GATA2$^{low}$ (G$^{low}$), and GATA2$^{low}$PU.1$^{low}$ (GP$^{low}$) progenitors without (−) or with (+) inflammation.

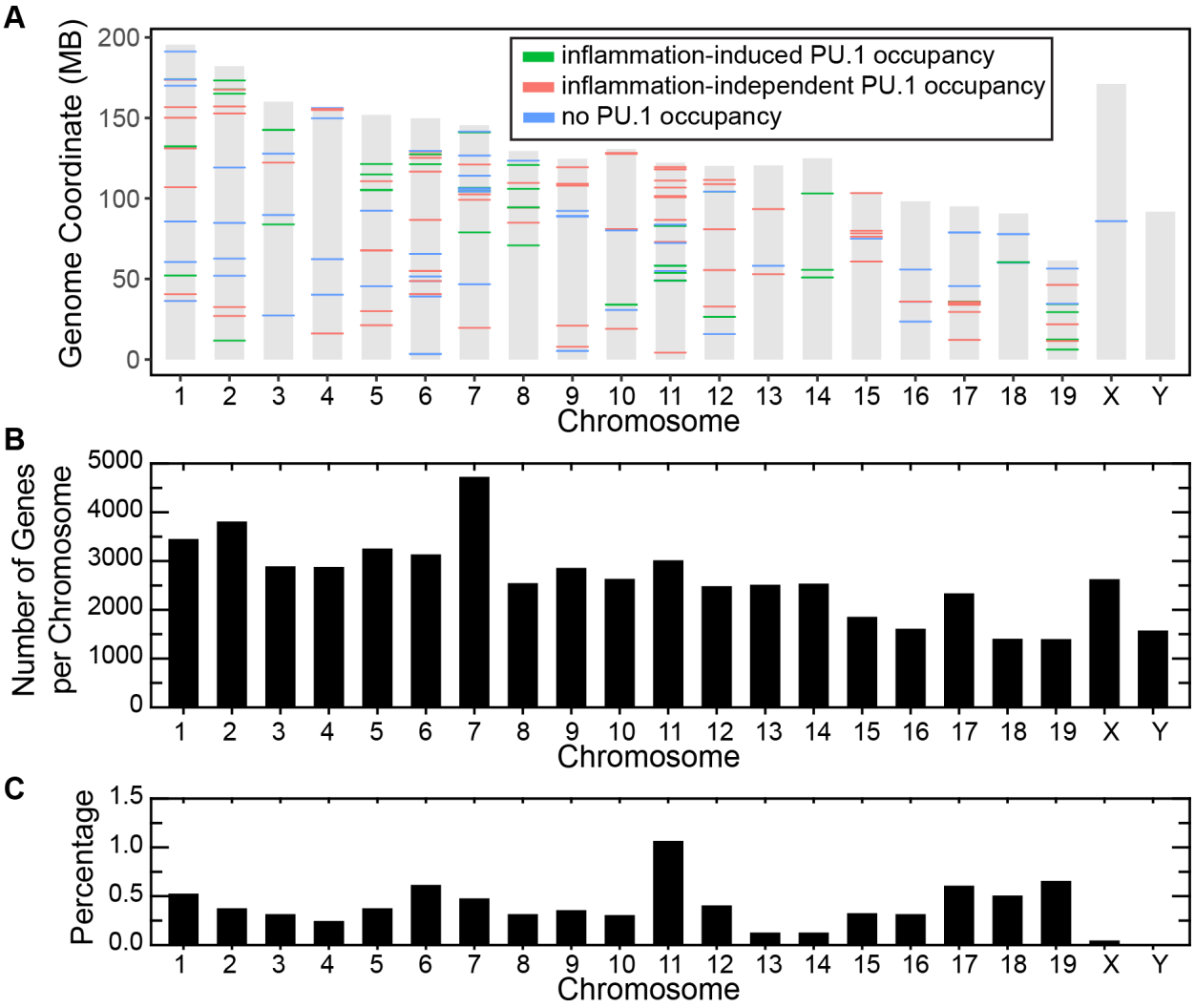


**Figure 4.12: Chromosomal distribution of the 217 inflammation-activated genes.** (**A**) Genomic locations of inflammation-activated genes are depicted for mouse chromosomes. Genes are colored by their regulatory modes. (**B**) The number of genes per chromosome. These genes were used to quantify RNA-seq data. (**C**) The number of inflammation-induced genes per chromosome expressed as a percentage.

> 1,000 nM) [268, 269]. GATA2$^{low}$ progenitors were treated with increasing concentrations of BMS-345541 for 1 h, followed by IFN$\gamma$ and $Pam_3CSK_4$ for 4 h. Wild-type cells, with or without IFN$\gamma$ and $Pam_3CSK_4$, served as negative controls. Genes exhibiting inflammation-induced PU.1 occupancy (*Cd40*, *Gbp5*, and *Iigp1*) were very sensitive to BMS-345541 at 1 and 5 $\mu$M, whereas PU.1-pre-bound genes (*Ccl3*, *Cd69*, and *Tnf*) were insensitive to BMS-345541 at these concentrations (Fig. 4.10, C and D). As another IKK$\beta$ inhibitor, IKK16 [270], also distinguished the inflammation-activated gene cohorts (Fig. 4.13), IKK$\beta$ activity is disproportionately important for the gene cohort requiring inflammation for PU.1 chromatin occupancy.

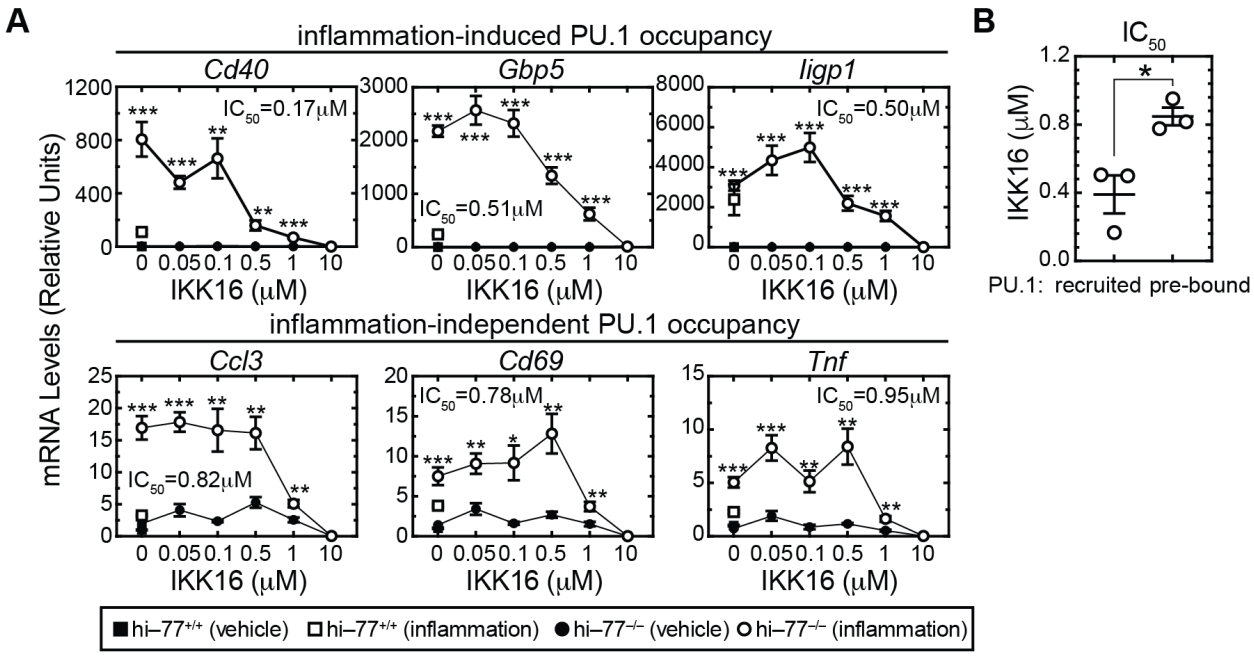


**Figure 4.13: Differential sensitivity to IKK$\beta$ inhibitor IKK16 of genes with inflammation-induced PU.1 occupancy versus PU.1-pre-bound genes.** (**A**) IKK16 dose-response curves of three representative genes from inflammation-induced PU.1 occupancy and inflammation-independent PU.1 occupancy. GATA2$^{low}$ progenitors were pretreated with increasing concentrations of IKK16 for 30 minutes and were treated with a combination of IFN$\gamma$ (1 ng/ml) and $Pam_3CSK_4$ (100 ng/ml) for 4 h (n = 3-12). Wild-type treated with or without IFN$\gamma$ and $Pam_3CSK_4$ served as negative controls. $IC_{50}$ for each gene was calculated using nonlinear regression. (**B**) The $IC_{50}$ of genes with inflammation-induced PU.1 occupancy and those with inflammation-independent PU.1 occupancy were compared. Data were presented as mean ± SEM. Multiple unpaired t-test in (A) and unpaired t-test in (B). * $P < 0.05$, ** $P < 0.01$, *** $P < 0.001$.

## 4.5 Inflammation reveals opposing functions of hematopoiesis regulatory proteins

Our comparison of transcriptomes from progenitors with normal and reduced GATA2 levels revealed genes activated by inflammation in GATA2$^{low}$ progenitors are enriched in motifs that bind signal-dependent transcription factors and RUNX motifs [52]. To determine if GATA2 antagonizes other transcription factors to regulate inflammation-induced transcription, we used Multiple Expectation Maximizations for Motif Elicitation (MEME) [271] to perform motif enrichment analysis at promoters and introns of inflammation-activated genes from our RNA-seq data (Fig. 4.14A). IFN$\gamma$ signaling utilizes members of the Signal Transducer and Activator of Transcription family and Interferon Regulatory Factor family, while TLR signaling utilizes NF-$\kappa$B to regulate transcription [17–21]. Motifs that bind these factors were enriched at inflammation-activated genes (Fig. 4.14B and Fig. 4.15, A and B). RUNX motifs were absent from promoters of genes activated in wild-type and enriched in GATA2$^{low}$ progenitors. RUNX motifs were not enriched at genes activated in GATA2$^{low}$PU.1$^{low}$ progenitors (Fig. 4.14B). Find Individual Motif Occurrences [272] analysis revealed that among 217 inflammation-activated DEGs in GATA2$^{low}$ cells, 70 genes harbored RUNX motifs in promoters. Motifs for the TAL-related factor NHLH1 (HEN1), DMRTB1, Hairy-related factor BHLHE40 (BHE40), ETS factor ELK1, and NF-$\kappa$B subunits were also enriched (Fig. 4.14B). RUNX1, RUNX2, and RUNX3 motifs were enriched in introns of wild-type, GATA2$^{low}$, and GATA2$^{low}$PU.1$^{low}$ cells in response to inflammation. ELK1 and HEN1 motifs were enriched in introns of GATA2$^{low}$, but not wild-type and GATA2$^{low}$PU.1$^{low}$ cells (Fig. 4.14B). The progenitors expressed *Runx1*, but not *Elk1*, *Hen1*, *Runx2*, and *Runx3*.

Since RUNX1 and GATA2 can co-localize on chromatin, it is assumed that they function collectively [83, 273, 274]. However, inflammation-activated genes harboring RUNX motifs were not induced in progenitors expressing normal GATA2 levels; the response

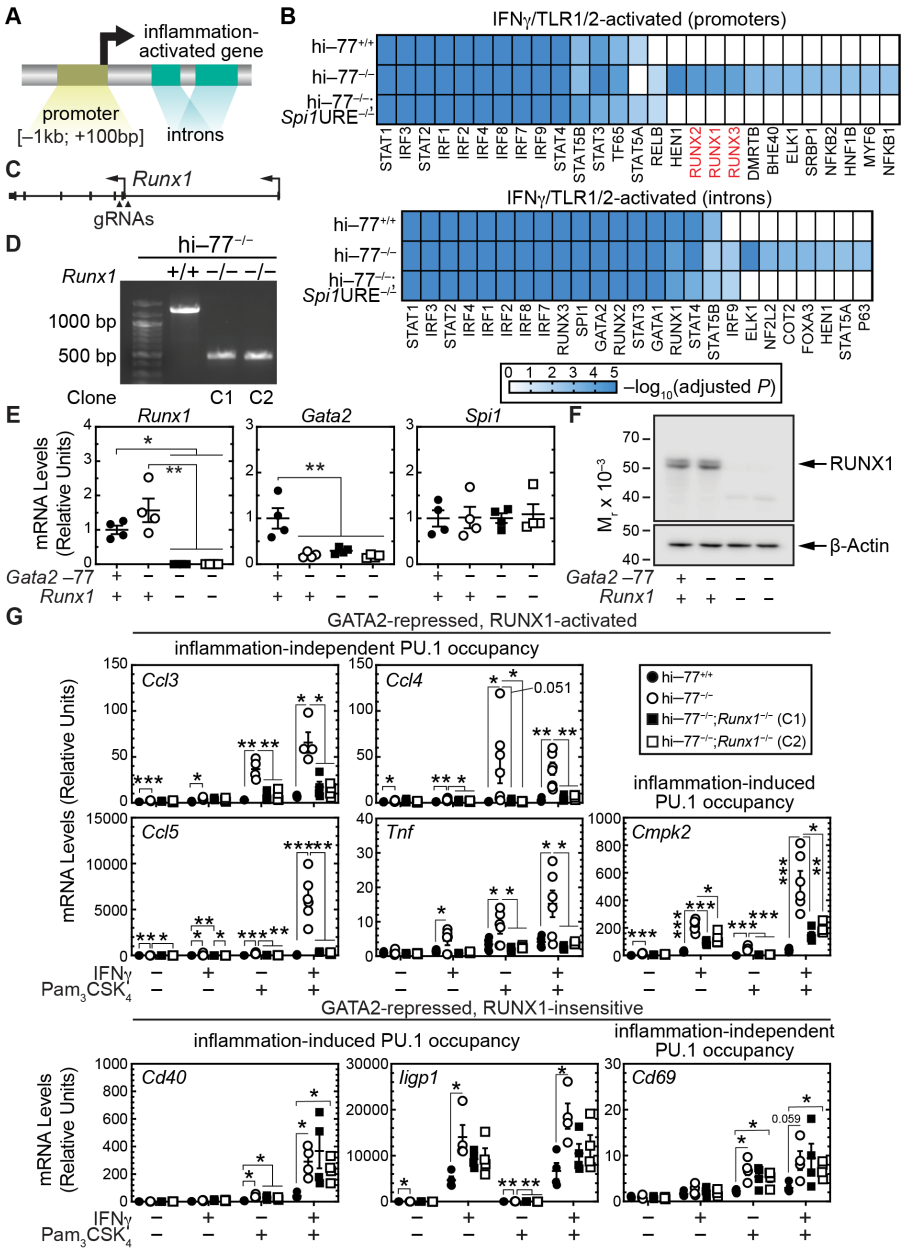


**Figure 4.14: Inflammation imparts opposing GATA2 and RUNX1 mechanisms.** (**A**) Schematic of promoters and introns used for motif enrichment analysis. (**B**) Heatmap showing motif enrichment at promoters (top) and introns (bottom) of inflammation-activated genes in wild-type, GATA2$^{low}$, and GATA2$^{low}$PU.1$^{low}$ cells. Motifs binding canonical inflammation-activated STAT, IRF, and NF-$\kappa$B are presented as positive controls. Motifs enriched in GATA2$^{low}$ but not wild-type or GATA2$^{low}$PU.1$^{low}$ progenitors were ranked based on $-\log_{10}(P$ value) and a $P$ cutoff of 0.005. Motifs with adjusted $P > 0.05$ were set to 1. (**C**) Schematic depicting positions of guide RNA for CRISPR/Cas9 tool to delete *Runx1* gene in GATA2$^{low}$ progenitors. (**D**) PCR-based genotyping assay for *Runx1*$^{-/-}$ allele in hi$-77^{-/-}$ progenitors. Two hi$-77^{-/-}$;*Runx1*$^{-/-}$ clonal lines are denoted as C1 and C2. (**E**) *Runx1*, *Gata2*, and *Spi1* expression (n = 4). (**F**) Representative Western blot analysis of RUNX1 with $\beta$-Actin as a control. (**G**) The responsiveness of genes to IFN$\gamma$ and $Pam_3CSK_4$ was quantified using RT-qPCR (n = 4-6). Statistics in (E) and (F): One-way ANOVA with Tukey's multiple comparisons test. * $P < 0.05$, ** $P < 0.01$, *** $P < 0.001$.

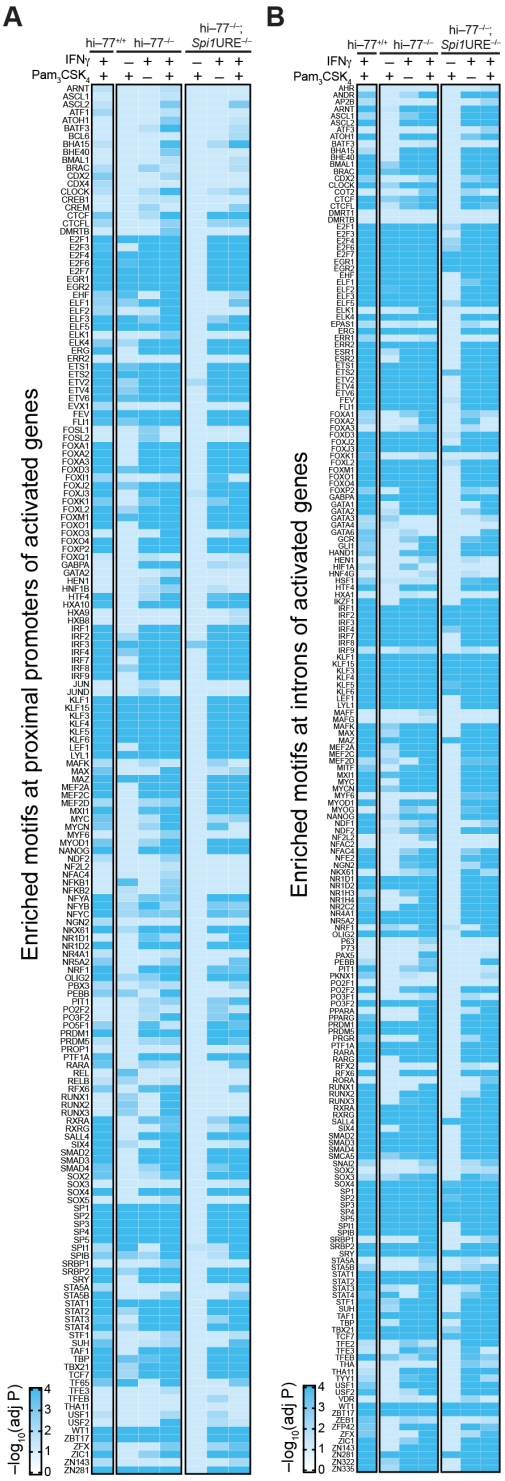


**Figure 4.15: Motif analysis of IFN$\gamma$ and TLR1/2-activated genes in wild-type, GATA2$^{low}$, and GATA2$^{low}$PU.1$^{low}$ progenitor cells.** The DEGs from IFN$\gamma$, Pam$_3$CSK$_4$, or IFN$\gamma$/Pam$_3$CSK$_4$-treated GATA2$^{low}$ and GATA2$^{low}$PU.1$^{low}$ progenitors were used to conduct motif enrichment analysis in proximal promoters (**A**) and introns (**B**). Motifs with adjusted $P >$ 0.05 were set to 0.05.

was considerably stronger in GATA2$^{low}$ progenitors, and RUNX motifs were not enriched when both GATA2 and PU.1 were reduced. We hypothesized that in GATA2$^{low}$ progenitors, RUNX1 functions in the inflammation-dependent activation mechanism. We tested if RUNX1 in GATA2$^{low}$ progenitors is required for IFN$\gamma$- and TLR-mediated transcription by using CRISPR/Cas9 to ablate the common exon 2 of three *Runx1* isoforms in hi$-77^{-/-}$ cells, which abrogated RUNX1 mRNA and protein (Fig. 4.14, C to F). RUNX1 loss did not affect *Gata2* or *Spi1* expression (Fig. 4.14E). We treated hi$-77^{+/+}$, hi$-77^{-/-}$, and hi$-77^{-/-}$;*Runx1*$^{-/-}$ (GATA2$^{low}$RUNX1$^{null}$) cells with IFN$\gamma$ and $Pam_3CSK_4$ for 4 h and quantified the responsiveness of inflammation-activated genes. The GATA2-repressed chemokine genes *Ccl3* and *Ccl4* and cytokine gene *Tnf* were pre-bound by PU.1 and highly elevated in GATA2$^{low}$ vs wild-type in response to signaling. RUNX1 loss attenuated activation of these genes to levels resembling wild-type cells (Fig. 4.14G). *Ccl5* resides in a cluster with *Ccl3* and *Ccl4*, and its inflammation-induced expression in GATA2$^{low}$RUNX1$^{null}$ cells was also reduced to a wild-type level. This behavior resembled reducing PU.1 in GATA2$^{low}$ progenitors (Fig. 4.16A). By contrast, the responsiveness of PU.1-pre-bound gene *Cd69* was not affected by RUNX1 loss (Fig. 4.14G). Inflammation-induced activation of *Cd40* and *Iigp1*, whose PU.1 occupancy was inflammation-inducible, in hi$-77^{-/-}$ cells was unaffected when RUNX1 was deleted (Fig. 4.14G). However, *Cmpk2*, which encodes Cytidine/Uridine Monophosphate Kinase 2, exhibits inflammation-induced PU.1 chromatin occupancy, and RUNX1 loss attenuated its induction (Fig. 4.14G). Based on RUNX1 chromatin occupancy from CUT&RUN data obtained with murine bone marrow GMPs [72], RUNX1 occupied the *Ccl3* promoter, *Ccl4* $-3.7$ kb, *Ccl5* $-19.9$ kb, *Tnf* $+1.3$ kb, and *Cmpk2* promoter and its $-9$ kb site (Fig. 4.16B). RUNX1 occupancy was undetectable at *Cd40* and *Iigp1*, while RUNX1 occupied the *Cd69* promoter, intron 1, and $-9.2$ kb site (Fig. 4.16C). Thus, loci exhibiting strong inflammation-induced transcription in GATA2$^{low}$ progenitors were either sensitive or insensitive to RUNX1 loss. Since the inflammation response is high in GATA2$^{low}$ cells and requires RUNX1, GATA2 and RUNX1 exert opposing functions at these loci, which

is not predictable from the co-localization, cooperativity paradigm.

## 4.6 Different molecular mechanisms governing progenitor genome sensing of qualitatively distinct inflammatory pathways

Prior studies revealed that RUNX1 loss in murine bone marrow GMP generated neutrophils with elevated TLR4 [71, 72]. Our results revealed that RUNX1 loss in GATA2$^{low}$ progenitors attenuated responses to IFN$\gamma$ and TLR1/2 signaling at certain loci, which raised the question of whether GATA2 and RUNX1 are required for genome sensing of the same or different TLR signals. We tested this using CRISPR/Cas9 to ablate *Runx1* exon 2 in wild-type cells to generate hi-*Runx1*$^{-/-}$ (RUNX1$^{null}$), which abrogated *Runx1* mRNA expression (Fig. 4.17, A and B). RUNX1 loss reduced *Gata2* expression by ∼50% in both clonal lines without impacting *Spi1* expression (Fig. 4.17B). hi−77$^{+/+}$, hi−77$^{-/-}$, and hi-*Runx1*$^{-/-}$ progenitors were treated with TLR1/2 agonist $Pam_3CSK_4$ or TLR4 agonist LPS for 4 h, and expression of inflammation-activated genes was quantified. GATA2 deficiency elevated *Ccl3* and *Ccl4* expression in the steady state vs. wild-type, while RUNX1 loss reduced their expression (Fig. 4.17C). Thus, opposing activities of GATA2 and RUNX1 establish the transcription state of these loci. In response to TLR1/2 and TLR4, the six genes were elevated in GATA2$^{low}$ cells. RUNX1$^{null}$ cells were non-responsive to the TLR1/2 agonist with all genes tested. However, RUNX1 loss increased expression of these genes in response to TLR4 agonist, with exceptions of *Ccl3* and *Ccl4* (Fig. 4.17C). GATA2 and RUNX1 are therefore differentially dedicated to controlling genome states that establish TLR1/2 vs. TLR4 signaling, respectively.

To elucidate mechanisms underlying the differential sensitivity to TLR agonists, we compared the consequences of GATA2 or RUNX1 loss for *Tlr1*, *Tlr2*, and *Tlr4* expression. GATA2 deficiency elevated *Tlr1* 21-fold ($P < 0.0001$) and *Tlr2* 2.7-fold ($P < 0.0001$) without affecting *Tlr4* expression relative to wild type (Fig. 4.17D). While RUNX1 loss did not

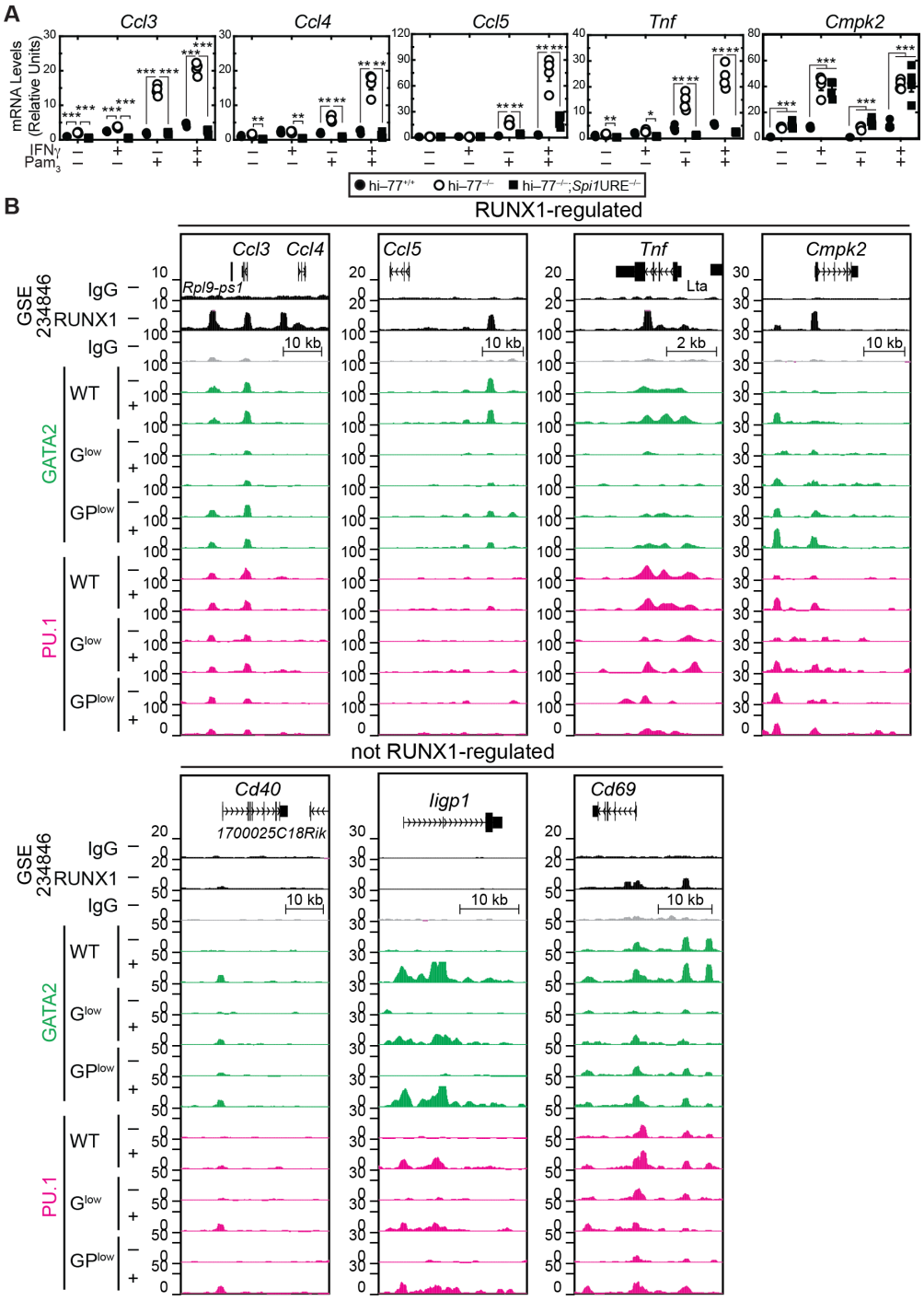


**Figure 4.16: RUNX1-dependent, inflammation-activated gene expression is associated with RUNX1 chromatin occupancy.** (**A**) *Ccl3*, *Ccl4*, *Ccl5*, *Tnf*, and *Cmpk2* responsiveness to IFN$\gamma$ and $Pam_3CSK_4$ in wild-type, GATA2$^{low}$, and GATA2$^{low}$PU.1$^{low}$ progenitors was quantified by RT-qPCR. Statistics: multiple unpaired t-tests. * $P < 0.05$, ** $P < 0.01$, *** $P < 0.001$. (**B**) RUNX1 CUT&RUN (GSE234846) with bone marrow Granulocyte Monocyte Progenitors (GMP) revealed occupancy at *Ccl3*, *Ccl4*, *Ccl5*, *Tnf*, and *Cmpk2* loci. RUNX1 occupied *Cd69*, but not *Cd40* and *Iigp1*, in un-treated bone marrow GMPs.

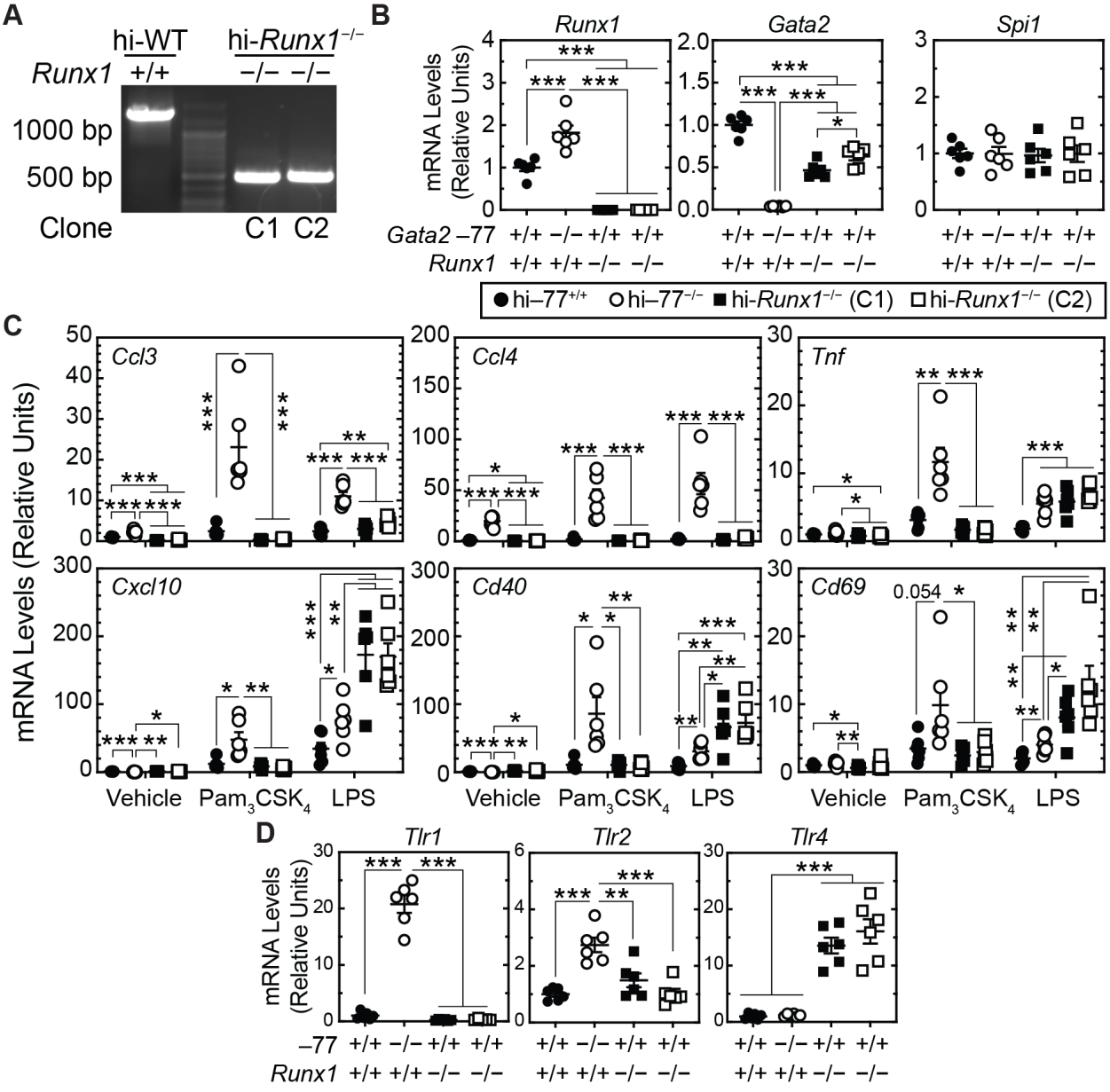


**Figure 4.17: Differential GATA2 and RUNX1 functions in genome sensing of qualitatively distinct inflammatory signals.** (**A**) PCR-based genotyping assay for *Runx1*$^{-/-}$ allele in hi$-77^{+/+}$ progenitors. (**B**) *Runx1*, *Gata2*, and *Spi1* expression was quantified using RT-qPCR. (**C**) The responsiveness of select genes to TLR1/2 agonist ($Pam_3CSK_4$) and TLR4 agonist (LPS) were quantitated using RT-qPCR. hi$-77^{+/+}$, hi$-77^{-/-}$, and hi-*Runx1*$^{-/-}$ progenitors were treated with vehicle, $Pam_3CSK_4$ (100 ng/ml) or LPS (100 ng/ml) for 4 h (n = 6). (**D**) *Tlr1*, *Tlr2*, and *Tlr4* expression in hi$-77^{+/+}$, hi$-77^{-/-}$, and hi-*Runx1*$^{-/-}$ progenitors was quantified using RT-qPCR. Statistics: One-way ANOVA with Tukey's multiple comparisons test. * $P < 0.05$, ** $P < 0.01$, *** $P < 0.001$.

affect *Tlr1* and *Tlr2* expression, it increased *Tlr4* expression 14- and 16-fold ($P < 0.0001$) in both clonal lines (Fig. 4.17D), consistent with the prior report of RUNX1 suppressing *Tlr4* expression in neutrophils [71]. The differential regulation of *Tlr* genes by GATA2 and RUNX1 may establish differential TLR1/2 vs. TLR4-induced transcriptional responses.

## 4.7 Discussion

Inflammation sensing by genomes reconfigures gene activity, enabling cells to adapt to microenvironment changes. For cells harboring a pathogenic genetic variant that amplifies the impact of inflammation on the genome, in principle, the exacerbated response may trigger pathogenesis. Although inflammatory mediators activate signal-dependent transcription factors *e.g.*, NF-$\kappa$B or AP1, that assemble complexes on enhancers and promoters, there are many unanswered questions on how qualitatively or quantitatively distinct permutations of inflammation impact genomes. Furthermore, the panoply of cytoplasmic and nuclear effectors that mediate inflammation-induced genome state changes is incompletely defined. Elucidating the mechanisms has high significance from fundamental and translational perspectives. We provide evidence for a genome-sensing paradigm involving antagonistic interactions between transcription factors not considered to be effectors of inflammation. This mechanism involved GATA2-PU.1 antagonism and GATA2-RUNX1 antagonism that occurred upon inflammation.

Our genomic analysis revealed inflammation-activated transcriptional mechanisms that differed at distinct genetic loci. Inflammation induced PU.1 occupancy at certain, but not all, inflammation-activated loci. Activation of loci with inflammation-induced PU.1 recruitment was exquisitely sensitive to pharmacological inhibitors of IKK$\beta$ kinase that phosphorylates I$\kappa$B, leading to its destruction. The disproportionate IKK$\beta$ requirement for inflammation-activated transcription of loci exhibiting PU.1 recruitment vs. loci with PU.1 occupancy preceding inflammation illustrates a critical locus-specific molecular step in inflammation sensing. IKK$\beta$ is required preferentially at inactive loci with closed chromatin

that require PU.1 recruitment. By contrast, loci with pre-bound PU.1 and open chromatin were considerably less sensitive to IKK$\beta$ inhibitors. These loci were transcriptionally active without inflammation, and inflammation further activated transcription. These results define a dual mechanism of inflammation sensing by the genome of GATA2$^{low}$ progenitors (Fig. 4.18), which was unpredictable from inflammation-induced transcriptional paradigms involving NF-$\kappa$B and AP1. In murine bone marrow–derived macrophages, TLR4 signaling induced NF-$\kappa$B chromatin occupancy and nucleosome remodeling at inflammation-activated loci with inaccessible chromatin in the basal state [103]. At loci accessible in the basal state, inflammation-activated genes harbored ETS motifs, although the specific ETS factor was not described. As our study analyzed regulatory complexes at and near promoters, it will be instructive to compare the results to analyses of broader genomic regions.

Through its HSPC-intrinsic activities, GATA2 is a vital determinant of hematopoiesis [34, 37]. Unlike transcription factors in which collaborating factors and coregulators are well established, factors and coregulators co-localize with GATA2 on chromatin, but the functional ramifications are unclear. An ensemble of transcription factors (GATA2, SCL/TAL1, RUNX1, FLI1, ERG, LYL1, and LMO2) termed the heptad complex co-localize and may function cooperatively [80, 83, 274]. Though GATA2-occupied sites with multi-factor occupancy are often enriched with motifs that bind heptad factors, previously, we demonstrated a reciprocal enrichment of WGATAR vs. ETS and RUNX motifs at GATA2-repressed loci [46]. Herein, we demonstrated that RUNX motifs were only enriched at promoters of inflammation-activated genes in GATA2$^{low}$ progenitors and not when PU.1 was reduced. Lowering RUNX1 in GATA2$^{low}$ progenitors revealed opposing activities of GATA2 and RUNX1 to confer inflammation-activated transcription in a locus-specific manner, which was unpredictable from existing paradigms.

It is instructive to consider the implications of opposing vs. cooperative molecular functions of GATA2 and RUNX1 and, more broadly, how inflammation creates or enables mechanisms not operational in a “normal” context. With a cooperativity model, perturbations

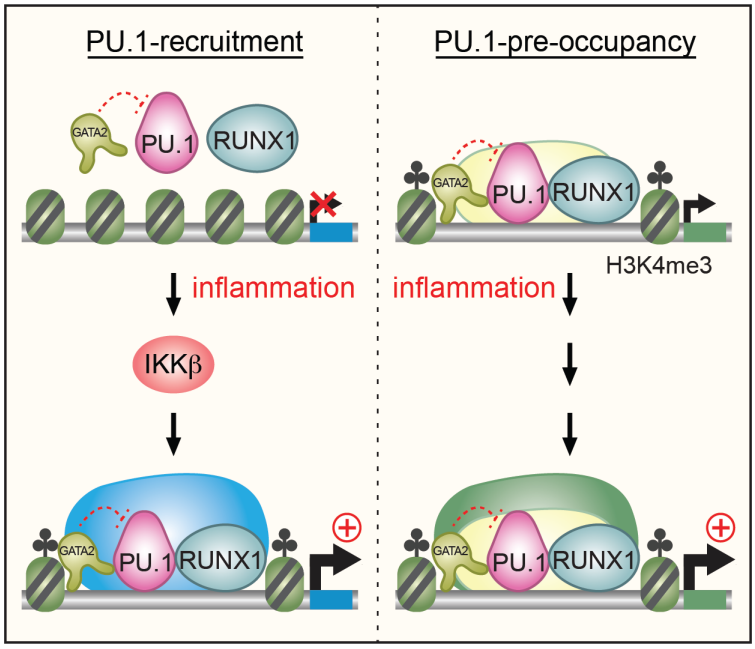


**Figure 4.18: Model for hematopoietic progenitor genome sensing of inflammation.** The hematopoietic progenitor genome utilizes a dual PU.1-dependent mechanism to sense and respond to inflammation. A gene cohort has inaccessible chromatin in the steady state, and inflammation increases chromatin accessibility and occupancy of the hematopoietic transcription factors GATA2 and PU.1 to activate transcription via an IKK$\beta$-dependent mechanism. At another inflammation-activated gene cohort, GATA2 and PU.1 occupancy precede inflammation, and this mechanism is not compromised by IKK$\beta$ inhibition. RUNX1 co-occupies chromatin with GATA2 and PU.1, yet GATA2 and RUNX1 differentially control inflammation-activated transcription, and transcriptional responses involving distinct TLR signaling pathways activated by unique pathogen-associated molecular patterns.

of factors in a complex would yield common consequences. Pathogenic GATA2 and RUNX1 variants share the consequence of creating bone marrow failure and leukemia predisposition, yet GATA2 and RUNX1 aberrations yield diseases with distinct clinical phenotypes. While GATA2 genetic variants cause GATA2 Deficiency Syndrome with monocyte, dendritic cell, B cell, and NK cell cytopenias [105, 193–195], RUNX1 variants cause RUNX1 Familial Platelet Disorder [67, 68, 275, 276]. As GATA2 regulates megakaryopoiesis [277], the differential phenotypes do not reflect the simple model that RUNX1, but not GATA2, has megakaryopoiesis-regulatory activity. Conceptually resembling GATA2$^{low}$ progenitors, in which inflammation hyperactivates cytokine/chemokine gene expression, RUNX1 loss elevates transcriptional responses to inflammation in neutrophils [71, 72]. Surprisingly, our study revealed that GATA2 and RUNX1 are vital for transcriptional responses to distinct inflammatory pathways: GATA2 for TLR1/2 and RUNX1 for TLR4.

Our study utilized GATA2$^{low}$ fetal progenitors, and GATA2 loss elevates inflammatory genes in primary and immortalized fetal progenitors [43, 52]. In an AML mouse model harboring a compound $Nras^{G12D/+};p53^{R172H/+}$ mutation, GATA2 was reduced in bone marrow HSPCs vs. wild type, which correlated with upregulated inflammatory genes *e.g.*, *Tlr1* and *Il6ra* [47]. These results complement our finding that GATA2$^{low}$ fetal progenitors elevate expression of inflammatory genes via PU.1-dependent and IKK$\beta$-dependent or -independent mechanisms, rendering progenitors hypersensitive to inflammatory mediators.

In summary, our study elucidated how the hematopoietic progenitor genome senses and responds to inflammation. GATA2 deficiency derepresses PU.1 activity, and inflammation induces PU.1 chromatin occupancy at a target gene cohort, while PU.1 constitutively occupies another cohort. Introducing IKK$\beta$ into GATA2 mechanisms and demonstrating that inflammation creates an antagonistic relationship between two hematopoiesis-promoting transcription factors, GATA2 and RUNX1, adds mechanistic depth to unravel how pathogen-instigated inflammation and inflammation of chronic disease alter HSPC functions. This mechanistic framework will enable studies to assess if remodeling genome function yields

adaptations that confer environmental protection and/or create vulnerabilities that trigger and/or accelerate progression of blood disease predisposition states.

# Chapter 5

# Conclusions and Future Directions

## 5.1 Linking GATA2 deficiency to inflammatory signaling

Among the constellation of clinical features in GATA2 Deficiency Syndrome, mycobacterial infection, immunodeficiency, and dysregulation of immune cell composition in the peripheral blood are variably penetrant, but the underlying mechanisms are not fully understood [105, 193–195]. Genetic murine models with disruption in the *Gata2* −77 kb and +9.5 kb enhancers provide innovative tools to study how GATA2 establishes and maintains a progenitor genome to sense and respond to inflammation. +9.5 enhancer harbors E-box-spacer-WGATAR and Ets motifs for multi-factor occupancy, including GATA2, TAL1, and ETS transcription factors [79, 80, 84, 119–121]. Mice lacking E-box-spacer-WGATAR on one allele and Ets motif on the other allele have normal *Gata2* levels with a minimal phenotype in steady state [123]. Still, the hematopoietic regeneration capacity of compound heterozygous animals becomes less responsive to the chemotherapy drug 5-Fluorouracil, Toll-Like Receptor (TLR) 4 signaling, and Granulocyte Colony Stimulating Factor (G-CSF) signaling [123, 127]. By contrast, −77 enhancer deletion downregulates *Gata2* expression by 75% in myeloerythroid progenitors and is embryonically lethal after embryonic day (E) 15.5 [38]. GATA2 deficiency resulting from the -77 enhancer ablation reduces the number of Granulocyte Progenitors (GPs) and increases the number of Monocyte Progenitors (MPs), causing an imbalance in the GP:MP ratio in E14.5 fetal liver [43, 44]. The aberrant hematopoiesis is associated with the elevated expression of genes encoding Interferon (IFN) signaling components, including Interferon Regulatory Factor 8 (IRF8), and TLRs [43, 52]. GATA2 deficiency creates a signaling crosstalk between IFN$\gamma$ and TLR1/2 to elevate cytokine/chemokine gene expression and protein production in primary and ER-HOXB8-immortalized (hi) $-77^{-/-}$ progenitors [52]. Blocking IFN$\gamma$ signaling via *Irf8* ablation increases the number of GPs and decreases the number of MPs to reverse the GP:MP ratio [44]. In contrast to IRF8 deletion, blocking TLR signaling by genetic ablation of TLR

adaptor Myeloid Differentiation 88 (MYD88) reduces the number of both GPs and MPs but does not reverse GP:MP imbalance [45]. These studies demonstrated the differential contribution of IFN$\gamma$ and TLR1/2 signaling to progenitor composition in GATA2-deficient fetal livers.

The elevated inflammatory signaling mechanistically involves the antagonistic activities of GATA2 with other hematopoietic transcription factors. Lowering the concentration of E26 Transformation Specific (ETS) transcription factor PU.1 by deleting the −14 kb enhancer of *Spi1*, encoding PU.1, impairs the transcriptional responses to inflammation in hi$-77^{-/-}$ (GATA2$^{low}$) progenitors [45]. Among GATA2-dependent inflammation-activated genes, PU.1 preoccupies a cohort of accessible loci in the steady state, and inflammatory signaling further elevates the transcription [45]. In another cohort of genes that are not accessible in the steady state, PU.1 is only recruited to the chromatin upon inflammation, and the transcription is uniquely sensitive to the pharmacological inhibitors of IKK$\beta$ activity [45]. The inflammatory responses further revealed the opposing activity of GATA2 and another hematopoietic transcription factor, RUNX-related Factor 1 (RUNX1). GATA2 and RUNX1 co-occupy chromatin with other heptad transcription factors, including TAL1, FLI1, ERG, LYL1, and LMO2, and they may function collectively to regulate hematopoiesis [79–83]. RUNX1$^{null}$ Granulocyte Monocyte Progenitors produce neutrophils with increased IFN$\gamma$ and TLR4 signaling capacity [71, 72]. However, RUNX1 deletion in GATA2$^{low}$ progenitors attenuates the responsiveness of select inflammation-activated genes to IFN$\gamma$-TLR1/2 signaling [45]. Since GATA2 deficiency elevates *Tlr1* and *Tlr2* and RUNX1 loss increases *Tlr4* expression, GATA2 and RUNX1 regulate qualitatively different inflammatory signaling pathways [45]. In aggregate, the interactions among the master regulators of hematopoiesis, GATA2, PU.1, and RUNX1, stringently control the progenitor genome to sense and respond to dynamically changing inflammatory milieu.

## 5.2 Interactions of GATA2 and PU.1 with canonical signal-dependent transcription factors at inflammation activated loci

The chromatin occupancy of GATA2 and PU.1 in response to inflammation parses inflammation-activated genes into two categories, PU.1-recruited and PU.1-prebound, with differential sensitivity to IKK$\beta$ inhibition [45], yet it is not fully understood how inflammation induces PU.1 occupancy at PU.1-recruited loci. Besides PU.1, the two groups of genes may require different protein complexes for transcriptional regulation, and the binding motifs present or absent at these loci may provide a mechanistic framework. To determine the differential enrichment of binding motifs harbored at PU.1-recruited vs. PU.1-prebound genes, we performed a comparative motif enrichment analysis using MEME. The analysis revealed the predominant enrichment of motifs for Signal Transducers and Activators of Transcription (STATs) and IRFs in PU.1-recruited genes and the dearth of binding motifs for signal-dependent transcription factors in PU.1-prebound genes (Figure 5.1). This raised the hypothesis that STATs and IRFs are uniquely required for the transcriptional responses of PU.1-recruited genes but not for PU.1-prebound genes. To test this hypothesis, we treated wild-type and GATA2$^{low}$ progenitors with increasing concentrations of JAK1/2 inhibitor Ruxolitinib for an hour, followed by IFN$\gamma$-TLR1/2 stimulation. Consistent with the IKK$\beta$ inhibition, JAK1/2 inhibition abrogated the responsiveness of PU.1-recruited genes (*Cd40*, *Gbp5*, and *Iigp1*) while not impacting PU.1-prebound gene induction (*Ccl3*, *Cd69*, and *Tnf*) (Figure 5.2).

How is PU.1 recruited to chromatin upon inflammation? The differential sensitivity to JAK1/2 inhibition between the two gene classes suggests a model in which inflammation-induced PU.1 occupancy requires the activation of transcription factors downstream of JAK signaling. Examining the published RNA-seq data (GSE279155) [45] revealed the eleva-

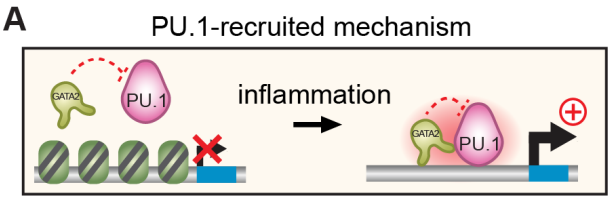


| motif sequence | name | *P* value |
|---|---|---|
| | FOXL2 | 6.3e-5 |
| | FOXM1 | 3.5e-4 |
| | GATA2 | 5.7e-4 |
| | STAT2 | 1.4e-3 |
| | PRDM1 | 2.4e-3 |
| | IRF1 | 2.8e-3 |
| | NFATC1 | 3.8e-3 |
| | IRF7 | 5.0e-3 |
| | STAT3 | 5.5e-3 |
| | FOXD3 | 7.0e-3 |
| | FOXJ3 | 8.2e-3 |
| | IRF9 | 8.4e-3 |
| | FOXJ2 | 9.7e-3 |
| | STAT1 | 1.3e-2 |
| | FOXO4 | 1.3e-2 |
| | GATA3 | 1.5e-2 |
| | GATA6 | 1.6e-2 |
| | DMRT1 | 1.7e-2 |
| | NR1I2 | 2.6e-2 |
| | NR4A1 | 2.7e-2 |

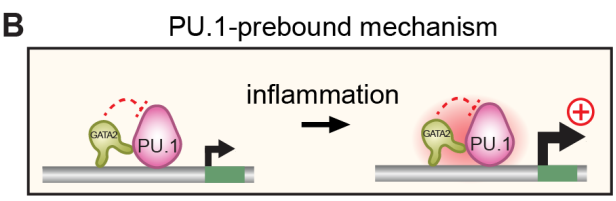


| motif sequence | name | *P* value |
|---|---|---|
| | MECP2 | 2.6e-3 |
| | ARNT | 4.7e-3 |
| | NR1H4 | 2.3e-2 |

**Figure 5.1: Differential motif enrichment at PU.1-recruited and PU.1-prebound loci.** (**A** and **B**) Top, models depicting PU.1-recruited (A) and PU.1-prebound (B) mechanisms. Bottom, binding motifs enriched at genes with corresponding mechanisms.

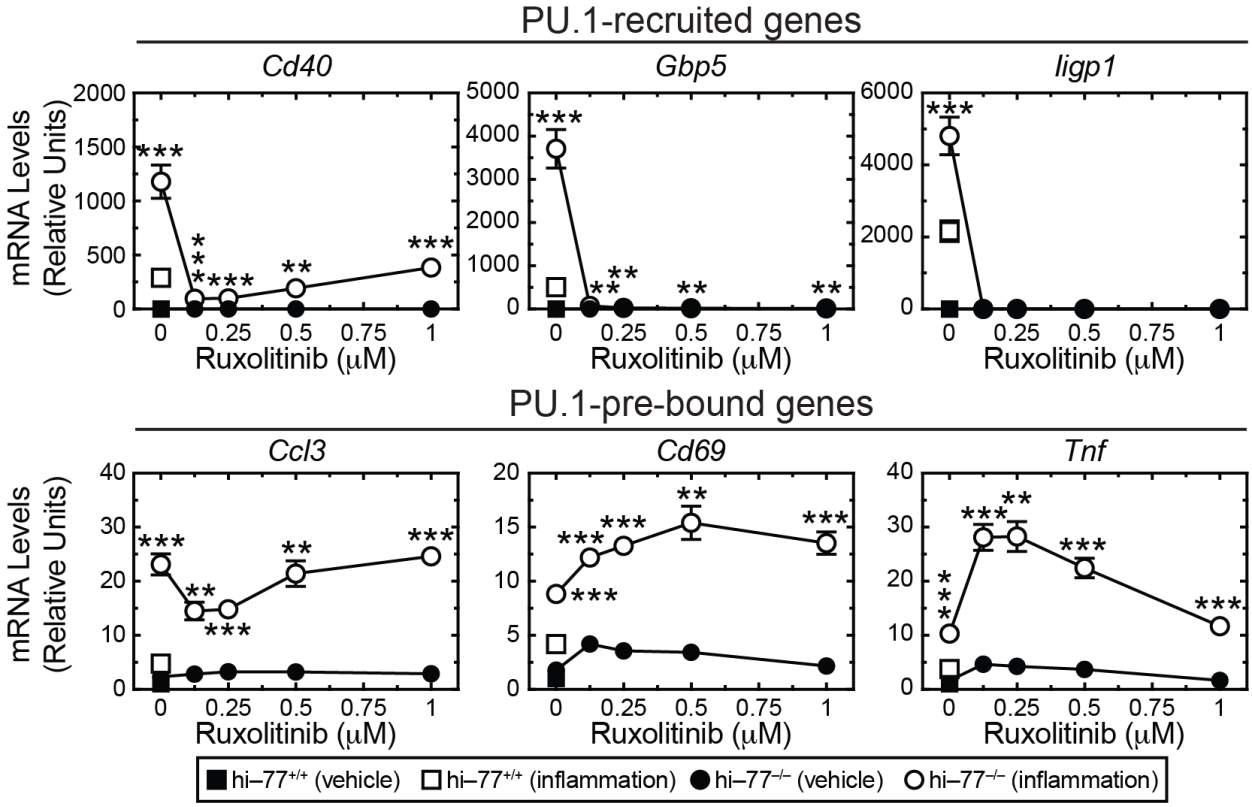


**Figure 5.2: Differential sensitivity of inflammation-activated genes to JAK1/2 inhibition.** Dose-response curve of three representative genes with PU.1-recruited and PU.1-prebound mechanisms to JAK1/2 inhibitor Ruxolitinib (n = 3-6, mean ± SEM). Statistics: multiple unpaired t-test. * $P < 0.05$, ** $P < 0.01$, *** $P < 0.001$.

tion of *Stat1*, *Stat3*, *Irf1*, and *Irf8* in response to inflammatory signaling in myeloerythroid progenitors (Figure 5.3). Since the STAT phosphorylation is an immediate step following JAK activation, it is attractive to ask if the absence of STAT1/3 impacts PU.1 chromatin occupancy. Multi-omic analyses will be performed to test the following models: 1) PU.1 occupancy requires STAT1/3 occupancy; 2) PU.1 occupancy precedes STAT1/3 occupancy; or 3) PU.1 occupancy is independent from STAT1/3 activity. Testing these models requires the generation of *Stat1* and *Stat3* deletion in hi$-77^{-/-}$ cells using CRISPR/Cas9 gene editing tool.

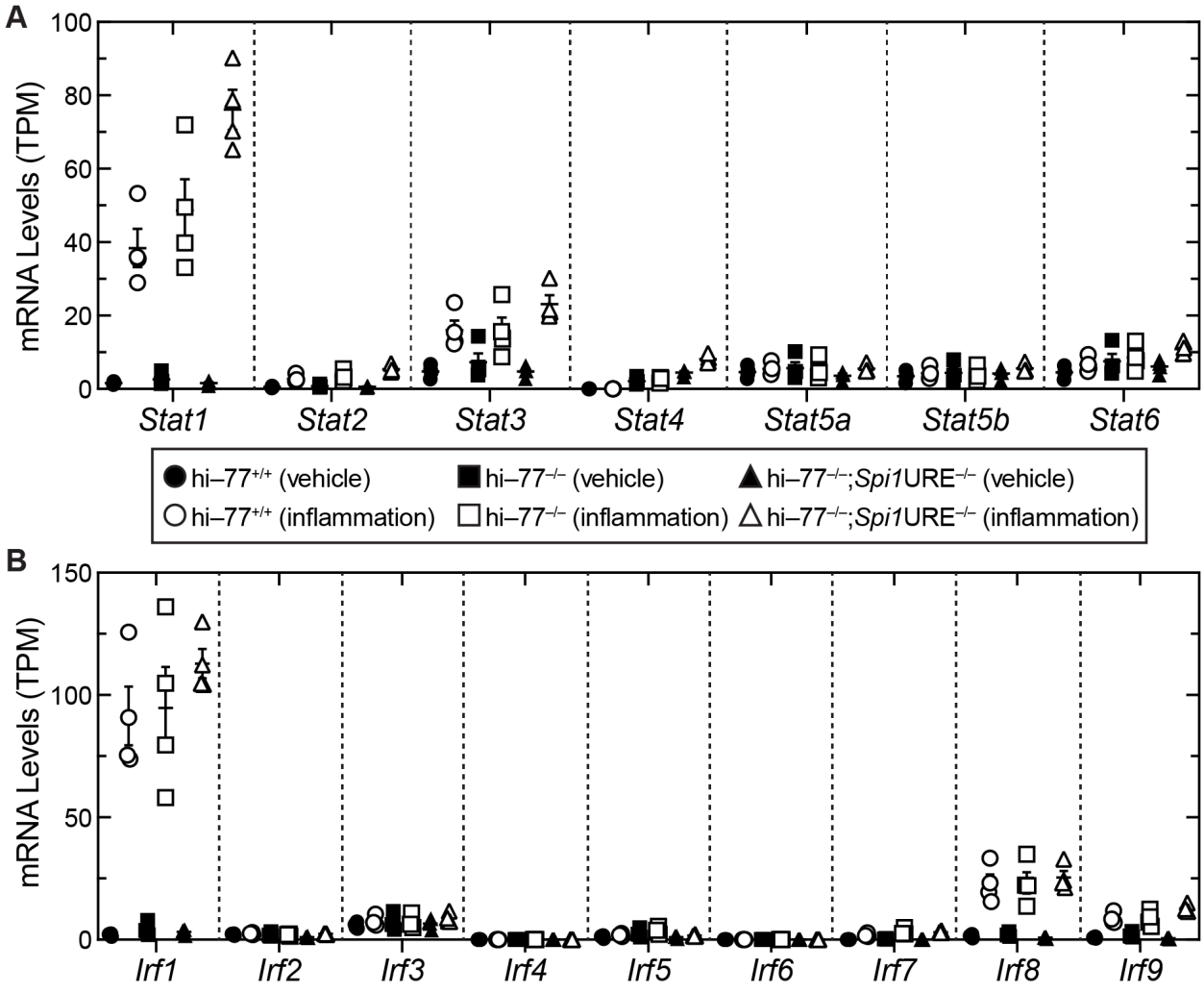


**Figure 5.3: Expression of STAT and IRF gene family in myeloerythroid progenitors.** (**A** and **B**) Expression profile of genes encoding Signal Transducers and Activators of Transcription STATs (A) and Interferon Regulatory Factors IRF (B) in hi$-77^{+/+}$, hi$-77^{-/-}$, and hi$-77^{-/-}$;*Spi1*URE$^{-/-}$ progenitors with or without inflammation from RNA-seq (GSE279155).

First, to determine if STAT1 or STAT3 or both factors are essential or contributory to the transcriptional responses, hi$-77^{-/-}$, hi$-77^{-/-}$;*Stat1*$^{-/-}$ (GATA2$^{low}$STAT1$^{null}$), hi$-77^{-/-}$; *Stat3*$^{-/-}$ (GATA2$^{low}$STAT3$^{null}$), and hi$-77^{-/-}$;*Stat1*$^{-/-}$;*Stat3*$^{-/-}$ (GATA2$^{low}$STAT1/3$^{null}$) will be treated with vehicle or inflammation amalgam for 4 hours, and the total RNAs are harvested for RNA-seq analysis. Multiple comparisons will reveal the GATA2-dependent inflammation-activated genes uniquely regulated by STAT1 or STAT3 and synergistically regulated by both factors. Integrating this RNA-seq with previously published RNA-seq data (GATA2$^{low}$ and GATA2$^{low}$PU.1$^{low}$ $-/+$ inflammation) will address whether STAT1 loss impacts PU.1-sensitive genes in response to inflammation to a lesser, greater, or equivalent extent relative to STAT3 loss. This comparison will allow one to prioritize STAT1 versus STAT3 for further investigation.

To determine if STAT1/3 is required for PU.1 recruitment to the chromatin upon inflammation, wild-type, GATA2$^{low}$, and GATA2$^{low}$STAT1/3$^{null}$ progenitors will be treated with vehicle or inflammation amalgam for 4 hours, and PU.1, GATA2, and STAT1 or STAT3 (based on RNA-seq analysis) occupancy will be mapped genome-wide using Cleavage Under Targets and Tagmentation (CUT&Tag). This analysis will determine whether STAT1/3 loss may abrogate PU.1 and GATA2 occupancy at all or a subset of PU.1-recruited loci. To determine if STAT1/3 is required for chromatin accessibility in response to inflammation, Assay for Transposase-Accessible Chromatin using Sequencing (ATAC-seq) will be performed using wild-type, GATA2$^{low}$, and GATA2$^{low}$STAT1/3$^{null}$ progenitors treated with vehicle or inflammation amalgam for 4 hours. ATAC-seq and PU.1/GATA2 CUT&Tag data will be integrated to determine if the PU.1-recruited loci remain less accessible as in steady state or become more accessible independently of STAT1/3 loss, and how the chromatin accessibility alteration correlates with PU.1 recruitment. These multi-omic data will advance the understanding of how inflammation influences the interaction between canonical signal-dependent transcription factors (STAT1/3) and hematopoietic regulators (PU.1 and GATA2) to establish genetic networks that regulate cellular processes.

## 5.3 Prospective interactions between GATA2 and Forkhead Box transcription factors to regulate inflammatory responses

Besides the presence of binding motifs for IFN$\gamma$-activated transcription factors STATs and IRFs, PU.1-recruited loci predominantly harbor motifs for Forkhead Box transcription factors compared to PU.1-prebound loci. Mining the published RNA-seq data (GSE279155 [45] and GSE199464 [46]) revealed that the majority of Forkhead Box family members are not expressed in myeloerythroid progenitors, save *Foxj3*, *Foxk2*, *Foxn2*, *Foxn3*, *Foxo3*, and *Foxp1* (Transcripts per Million $> 1$ in all replicates), with *Foxp1* at the highest expression levels in both datasets (Figure 5.4). Genetic mouse models demonstrated that FOXP1 constrains the hematopoietic stem cell and multipotent progenitor compartments [278], promotes early B cell development in fetal liver [279], regulates naive T cell quiescence [280], and suppresses myeloid differentiation [281]. Conditional deletion of FOXP1 in endothelial cells promotes inflammation via the activation of NLRP3 inflammasome [282]. FOXO3 occupies and suppresses *Irf7* transcription to limit type I IFN signaling in bone marrow macrophages [283]. By contrast, FOXO1 occupies cis-regulatory elements at *Tlr4* locus to promote TLR4 expression and signaling [284]. Deficiency of RICTOR, a component of the Mammalian Target of Rapamycin Complex 2 (mTORC2), causes the accumulation of FOXO1 in the nucleus, which elevates cytokine production in response to TLR4 signaling [285]. Forced expression of FOXO1 in Chimeric Antigen Receptor T cells induces chromatin accessibility at inflammatory genes, which harbor motifs for ETS and RUNX transcription factors [286]. These lines of evidence support a hypothesis in which Forkhead Box transcription factors function collectively with PU.1 and RUNX1 to regulate transcriptional responses to inflammation in GATA2$^{low}$ progenitors. It is compelling to ask if GATA2 antagonizes or cooperates with different Forkhead Box family members in inflammation contexts.

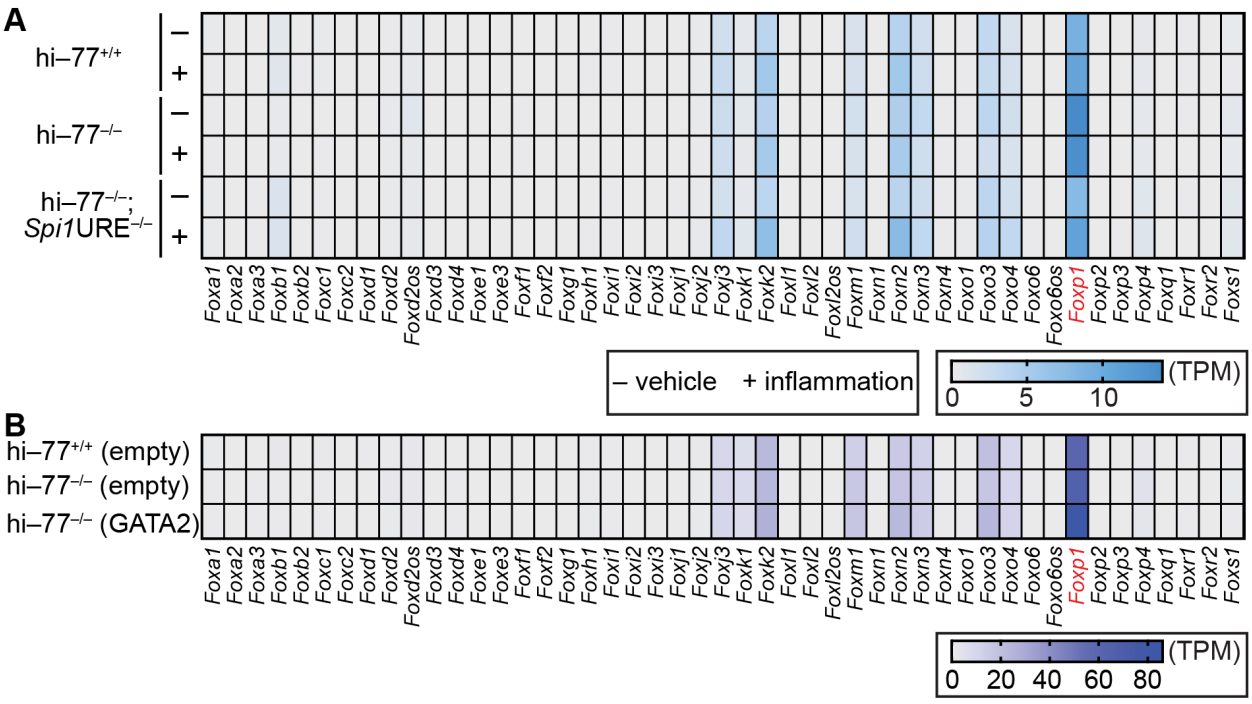


**Figure 5.4: Expression profiles of genes encoding Forkhead Box transcription factors in myeloerythroid progenitors.** (**A**) Forkhead Box gene expression hi$-77^{+/+}$, hi$-77^{-/-}$, and hi$-77^{-/-}$;*Spi1*URE$^{-/-}$ progenitors with or without inflammation from RNA-seq (GSE279155). (**B**) Forkhead Box gene expression in hi$-77^{+/+}$ infected with empty vector and hi$-77^{-/-}$ infected with empty vector or with GATA2 vector from RNA-seq (GSE19946).

## 5.4 Genetic interaction between GATA2 and RUNX1 to control inflammation sensing by the hematopoietic progenitor genome

The opposing activity of GATA2 and RUNX1 in regulating inflammatory signaling in fetal myeloerythroid progenitors is unexpected from the heptad transcription factor paradigm, and an *in vivo* model to test factor antagonism will reveal another layer of mechanism. *Gata2*$^{+/-}$;*Runx1*$^{+/-}$ murine compound heterozygosity was previously generated and yielded embryonic lethality before weaning [83]. A recent RUNX1 mouse strain (*Runx1*$^{R188Q/+}$) modeling the human RUNX1 genetic variant underlying Familial Platelet Disorder exhibits elevated cytokine production in bone marrow fluid, including CCL11, IL9, and IL6, relative to wild type [287]. Crossing *Gata2* $-77^{+/-}$ with *Runx1*$^{R188Q/+}$ to generate compound heterozygous $-77^{+/-}$;*Runx1*$^{R188Q/+}$ mice will provide an innovative tool to study GATA2 and RUNX1 germline variant interactions. To test whether the elevated inflammatory signaling in $-77^{-/-}$ progenitors are attenuated by RUNX1 R188Q mutant, the $-77^{+/-}$;*Runx1*$^{R188Q/+}$ mice will be used for timed matings to generate prioritized genotypes, including wild-type, $-77^{-/-}$, *Runx1*$^{R188Q/+}$, *Runx1*$^{R188Q/R188Q}$, $-77^{-/-}$;*Runx1*$^{R188Q/+}$, and $-77^{-/-}$;*Runx1*$^{R188Q/R188Q}$ embryos. The E14.5 fetal liver will be harvested for lineage-negative (Lin$^-$) progenitor isolation, and cells will be treated with vehicle or inflammation amalgam (IFN$\gamma$ and TLR1/2 agonist) for 4 hours. The responsiveness of select genes (*Tnf*, *Ccl3*, *Ccl4*, and *Ccl5*) [45] will be used as signaling readouts for Quantitative Real-Time Polymerase Chain Reaction (RT-qPCR). Based on this initial analysis, the RNA materials will be used to conduct an RNA-seq analysis to determine the scope of GATA2-RUNX1 interaction. In parallel, the fetal liver will be subjected to flow cytometry to determine if the RUNX1 R188Q mutant influences the progenitor composition (GP:MP ratio) of $-77^{-/-}$ fetal liver. Since *Runx1*$^{R188Q/R188Q}$ is embryonically lethal and the developmental stage at which viabil-

ity is terminated was not previously determined, it is possible that $-77^{-/-}$;*Runx1*$^{R188Q/R188Q}$ embryos may not survive until the fetal liver stage. Therefore, the $-77^{-/-}$;*Runx1*$^{R188Q/+}$ will be valuable for experimentation.

## 5.5 Building a dictionary of inflammation activators and repressors from the lineage-determining transcription factor repertoire

The differential contribution of the master regulators of hematopoiesis, GATA2, PU.1, and RUNX1, to inflammation sensing by the progenitor genome raises the question of whether other lineage-determining transcription factors also regulate inflammatory responses. To address this question, a high-throughput approach such as Perturb-seq will be valuable [288]. hi$-77^{+/+}$ progenitors will be infected with the lentiviral vector containing *Cas9* DNA to generate Cas9-expressing cells. Alternatively, Lin$^-$ progenitors can be isolated from the bone marrow of *Rosa26-Cas9* knock-in mice. Cells will be infected with a pool of single-guide (sg) RNAs targeting genes encoding lineage-determining transcription factors. sgRNAs targeting *Stat1* and *Rela* (*Nfkb3*) will be included as positive controls, as STAT1 and NF-$\kappa$B component p65 are known inflammation activators. A non-target vector serves as a negative control. After 7 days, cells will be treated with vehicle or inflammation amalgam containing IFN$\gamma$ and TLR1/2 agonist for 4 hours, and cells will be subjected to single-cell RNA-seq analysis. In the absence of lineage-determining transcription factors, the responsiveness of inflammation-activated genes may be induced to a greater or lesser extent or both in a locus-specific manner, hence, classifying the factors as inflammation repressors, activators, or dual regulators, respectively.

Based on the outcomes of the Perturb-seq experiment, top three lineage-determining transcription factors will be prioritized for chromatin occupancy analysis. hi$-77^{+/+}$ and hi$-77^{+/+}$ lacking gene encoding the prioritized transcription factor, *e.g.*, X, (hi-$X^{-/-}$) will

be treated with vehicle or inflammation amalgam for 4 h, and genome-wide chromatin occupancy of the transcription factor of interest will be mapped out using the CUT&Tag assay. This experiment will determine how inflammatory signaling influences the activity of lineage-determining transcription factors. It is attractive to ask if the dual modes of PU.1 regulation, *i.e.*, PU.1 recruitment and PU.1 pre-occupancy (Figure 4.18), are recapitulated with other lineage-determining transcription factors in inflammation contexts.

To determine if chromatin occupancy of the select transcription factor X is critical, contributory, or inconsequential to inflammation-activated genes in myeloerythroid progenitors, CRISPR/Cas9 gene editing tool will be used to delete prioritized sequences harboring the transcription factor CUT&Tag peaks at enhancers in hi-$X^{-/-}$ cells. Genes will be selected based on the following prioritization criteria, including the magnitude of the signal-dependent transcriptional response, transcription factor contribution to the response, evolutionary conservation of the predicted enhancer sequence, and whether publicly accessible ChIP-seq data reveals multi-factor occupancy. ChIP-qPCR will be used to determine if the deletion eliminates transcription factor X occupancy. hi-$X^{-/-}$ cells lacking X occupancy site will be stimulated with vehicle or inflammation amalgam for 4 h, and the responsiveness of candidate gene will be quantified using RT-qPCR. hi-$X^{-/-}$ cells treated with the same agonists served as a positive control. Two possible results from this experiment include: 1) the deletion eliminates transcription factor X occupancy and impairs signal-dependent transcription or 2) the deletion eliminates transcription factor X occupancy without affecting the response. If the deletion does not eliminate transcription factor X occupancy, but eliminates the X motif-containing sequence, this complicates the analysis, and such genes will not be analyzed further. Together, these analyses will demonstrate the functional importance of chromatin occupancy of lineage-determining transcription factors on inflammation-activated genes. Building such a dictionary of inflammation activators and repressors based on GATA2, PU.1, and RUNX1 examplars will establish a paradigm in which the lineage-determining transcription factors govern hematopoietic genome sensing of

inflammation in parallel with the canonical signal-dependent transcription factors.

## 5.6 Candidate model systems to study GATA2-dependent inflammation sensing mechanisms in adults

Although genetic studies using germline mutations and embryonic models often inform human pathologies, it is instructive to determine whether bone marrow hematopoietic stem and progenitor cells (HSPCs) utilize a similar mechanism in $-77^{-/-}$ fetal myeloerythroid progenitors to sense and respond to inflammation. There are several rigorous *in vitro* and *in vivo* model systems for mechanistic consideration. In a mouse strain harboring a compound heterozygous $Nras^{G12D/+};p53^{R172H/+}$ mutation to model Acute Myeloid Leukemia (AML), *Gata2* expression is downregulated, while genes encoding components of inflammatory signaling, including *Tlr1* and *Il6ra*, are upregulated in the bone marrow HSPCs relative to wild type [47]. It is informative to ask if the GATA2$^{low}$ AML HSPCs are hypersensitive to inflammatory signaling and whether the elevated innate immune machinery contributes to AML progression. Alternative strains include the R396Q [111, 112] and R398W [110] mice that model the GATA2 carboxy-terminal zinc finger mutations in human GATA2 Deficiency Syndrome. Although systemic inflammation using TLR4 ligand Lipopolysaccharide in $Gata2^{+/-}$ mice induces serum cytokine/chemokine production to a lesser extent compared to wild-type [58], many parameters need to be considered. GATA2 deficiency alters the granulocytic versus monocytic progenitor composition, leading to the skewed production of differentiating progeny [43, 44]. Systemic inflammation exerts a global impact on both non-hematopoietic and hematopoietic cells, including the defective hematopoietic progeny. Direct stimulation of isolated bone marrow HSPCs becomes important to test the influence of GATA2 mutants on the inflammation sensing of HSPC genome without being compromised by the defective hematopoietic system. In parallel to animal models, it is plausible to convert fibroblasts from patients with GATA2 Deficiency Syndrome into induced pluripotent stem cells, which are then directed to differentiate into HSPCs [289, 290]. This approach

provides an attractive path for mechanistic studies directly on human patient samples, but the complexity of the protocol and the prolonged culture may introduce unexpected mutations into the genome. An alternative approach is to induce HSPC mobilization from patient bone marrow into the peripheral blood using mobilizing agents, such as G-CSF or Plerixafor [123, 127], followed by cell sorting. The isolated HSPCs are then expanded *ex vivo* using the Polyvinyl Alcohol method established by Wilkinson and colleagues [291, 292]. In aggregate, these model systems will enable mechanistic studies to elucidate whether GATA2 mechanisms in inflammation contexts are conserved between embryos and adults, with potential clinical implications to advance the understanding of human pathologies.

# Bibliography


[1] C. A. Janeway. "Approaching the asymptote? Evolution and revolution in immunology". eng. In: *Cold Spring Harbor Symposia on Quantitative Biology* 54 Pt 1 (1989), pp. 1–13. ISSN: 0091-7451. DOI: 10.1101/sqb.1989.054.01.003.

[2] Ruslan Medzhitov. "The spectrum of inflammatory responses". eng. In: *Science (New York, N.Y.)* 374.6571 (Nov. 2021), pp. 1070–1075. ISSN: 1095-9203. DOI: 10.1126/science.abi5200.

[3] B. Lemaitre et al. "The dorsoventral regulatory gene cassette spätzle/Toll/cactus controls the potent antifungal response in Drosophila adults". eng. In: *Cell* 86.6 (Sept. 1996), pp. 973–983. ISSN: 0092-8674. DOI: 10.1016/s0092-8674(00)80172-5.

[4] R. Medzhitov, P. Preston-Hurlburt, and C. A. Janeway. "A human homologue of the Drosophila Toll protein signals activation of adaptive immunity". eng. In: *Nature* 388.6640 (July 1997), pp. 394–397. ISSN: 0028-0836. DOI: 10.1038/41131.

[5] A. Poltorak et al. "Defective LPS signaling in C3H/HeJ and C57BL/10ScCr mice: mutations in Tlr4 gene". eng. In: *Science (New York, N.Y.)* 282.5396 (Dec. 1998), pp. 2085–2088. ISSN: 0036-8075. DOI: 10.1126/science.282.5396.2085.

[6] S. T. Qureshi et al. "Endotoxin-tolerant mice have mutations in Toll-like receptor 4 (Tlr4)". eng. In: *The Journal of Experimental Medicine* 189.4 (Feb. 1999), pp. 615–625. ISSN: 0022-1007. DOI: 10.1084/jem.189.4.615.

[7] K. Hoshino et al. "Cutting edge: Toll-like receptor 4 (TLR4)-deficient mice are hyporesponsive to lipopolysaccharide: evidence for TLR4 as the Lps gene product". eng. In: *Journal of Immunology (Baltimore, Md.: 1950)* 162.7 (Apr. 1999), pp. 3749–3752. ISSN: 0022-1767.

[8] Su-Chang Lin, Yu-Chih Lo, and Hao Wu. "Helical assembly in the MyD88-IRAK4-IRAK2 complex in TLR/IL-1R signalling". eng. In: *Nature* 465.7300 (June 2010), pp. 885–890. ISSN: 1476-4687. DOI: 10.1038/nature09121.

[9] Vu N. Ngo et al. "Oncogenically active MYD88 mutations in human lymphoma". eng. In: *Nature* 470.7332 (Feb. 2011), pp. 115–119. ISSN: 1476-4687. DOI: 10.1038/nature09671.

[10] Chloé James et al. "A unique clonal JAK2 mutation leading to constitutive signalling causes polycythaemia vera". eng. In: *Nature* 434.7037 (Apr. 2005), pp. 1144–1148. ISSN: 1476-4687. DOI: 10.1038/nature03546.

[11] E. Joanna Baxter et al. "Acquired mutation of the tyrosine kinase JAK2 in human myeloproliferative disorders". eng. In: *Lancet (London, England)* 365.9464 (Mar. 2005), pp. 1054–1061. ISSN: 1474-547X. DOI: 10.1016/S0140-6736(05)71142-9.

[12] Robert Kralovics et al. "A gain-of-function mutation of JAK2 in myeloproliferative disorders". eng. In: *The New England Journal of Medicine* 352.17 (Apr. 2005), pp. 1779–1790. ISSN: 1533-4406. DOI: 10.1056/NEJMoa051113.

[13] Ross L. Levine et al. "Activating mutation in the tyrosine kinase JAK2 in polycythemia vera, essential thrombocythemia, and myeloid metaplasia with myelofibrosis". eng. In: *Cancer Cell* 7.4 (Apr. 2005), pp. 387–397. ISSN: 1535-6108. DOI: 10.1016/j.ccr.2005.03.023.

[14] Rajintha M. Bandaranayake et al. "Crystal structures of the JAK2 pseudokinase domain and the pathogenic mutant V617F". eng. In: *Nature Structural & Molecular Biology* 19.8 (Aug. 2012), pp. 754–759. ISSN: 1545-9985. DOI: 10.1038/nsmb.2348.

[15] R. Sen and D. Baltimore. "Multiple nuclear factors interact with the immunoglobulin enhancer sequences". eng. In: *Cell* 46.5 (Aug. 1986), pp. 705–716. ISSN: 0092-8674. DOI: 10.1016/0092-8674(86)90346-6.

[16] W. Lee et al. "Activation of transcription by two factors that bind promoter and enhancer sequences of the human metallothionein gene and SV40". eng. In: *Nature* 325.6102 (Jan. 1987), pp. 368–372. ISSN: 0028-0836. DOI: 10.1038/325368a0.

[17] C. Schindler et al. "Interferon-dependent tyrosine phosphorylation of a latent cytoplasmic transcription factor". eng. In: *Science (New York, N.Y.)* 257.5071 (Aug. 1992), pp. 809–813. ISSN: 0036-8075. DOI: 10.1126/science.1496401.

[18] K. Shuai et al. "Activation of transcription by IFN-gamma: tyrosine phosphorylation of a 91-kD DNA binding protein". eng. In: *Science (New York, N.Y.)* 258.5089 (Dec. 1992), pp. 1808–1812. ISSN: 0036-8075. DOI: 10.1126/science.1281555.

[19] X. Y. Fu et al. "The proteins of ISGF-3, the interferon alpha-induced transcriptional activator, define a gene family involved in signal transduction". eng. In: *Proceedings of the National Academy of Sciences of the United States of America* 89.16 (Aug. 1992), pp. 7840–7843. ISSN: 0027-8424. DOI: 10.1073/pnas.89.16.7840.

[20] O. Silvennoinen et al. "Interferon-induced nuclear signalling by Jak protein tyrosine kinases". eng. In: *Nature* 366.6455 (Dec. 1993), pp. 583–585. ISSN: 0028-0836. DOI: 10.1038/366583a0.

[21] Y. Kanno et al. "The genomic structure of the murine ICSBP gene reveals the presence of the gamma interferon-responsive element, to which an ISGF3 alpha subunit (or similar) molecule binds". eng. In: *Molecular and Cellular Biology* 13.7 (July 1993), pp. 3951–3963. ISSN: 0270-7306. DOI: 10.1128/mcb.13.7.3951-3963.1993.

[22] Yan Li et al. "Inflammatory signaling regulates embryonic hematopoietic stem and progenitor cell production". eng. In: *Genes & Development* 28.23 (Dec. 2014), pp. 2597–2612. ISSN: 1549-5477. DOI: 10.1101/gad.253302.114.

[23] Yanan Li et al. “Single-Cell Analysis of Neonatal HSC Ontogeny Reveals Gradual and Uncoordinated Transcriptional Reprogramming that Begins before Birth”. eng. In: *Cell Stem Cell* 27.5 (Nov. 2020), 732–747.e7. ISSN: 1875-9777. DOI: 10.1016/j.stem.2020.08.001.

[24] Yanan Li and Jeffrey A. Magee. “Transcriptional reprogramming in neonatal hematopoietic stem and progenitor cells”. eng. In: *Experimental Hematology* 101-102 (Sept. 2021), pp. 25–33. ISSN: 1873-2399. DOI: 10.1016/j.exphem.2021.07.004.

[25] Yanan Li et al. “Basal type I interferon signaling has only modest effects on neonatal and juvenile hematopoiesis”. eng. In: *Blood Advances* 7.11 (June 2023), pp. 2609–2621. ISSN: 2473-9537. DOI: 10.1182/bloodadvances.2022008595.

[26] Diego A. López et al. “Prenatal inflammation perturbs murine fetal hematopoietic development and causes persistent changes to postnatal immunity”. eng. In: *Cell Reports* 41.8 (Nov. 2022), p. 111677. ISSN: 2211-1247. DOI: 10.1016/j.celrep.2022.111677.

[27] Diego A. López et al. “Both maternal IFN exposure and acute prenatal infection with Toxoplasma gondii activate fetal hematopoietic stem cells”. eng. In: *The EMBO journal* 42.14 (July 2023), e112693. ISSN: 1460-2075. DOI: 10.15252/embj.2022112693.

[28] Diego A. López et al. “Prenatal inflammation remodels lung immunity and function by programming ILC2 hyperactivation”. eng. In: *Cell Reports* 43.7 (July 2024), p. 114365. ISSN: 2211-1247. DOI: 10.1016/j.celrep.2024.114365.

[29] Siddhartha Jaiswal et al. “Age-related clonal hematopoiesis associated with adverse outcomes”. eng. In: *The New England Journal of Medicine* 371.26 (Dec. 2014), pp. 2488–2498. ISSN: 1533-4406. DOI: 10.1056/NEJMoa1408617.

[30] Giulio Genovese et al. “Clonal hematopoiesis and blood-cancer risk inferred from blood DNA sequence”. eng. In: *The New England Journal of Medicine* 371.26 (Dec. 2014), pp. 2477–2487. ISSN: 1533-4406. DOI: 10.1056/NEJMoa1409405.

[31] David P. Steensma et al. “Clonal hematopoiesis of indeterminate potential and its distinction from myelodysplastic syndromes”. eng. In: *Blood* 126.1 (July 2015), pp. 9–16. ISSN: 1528-0020. DOI: 10.1182/blood-2015-03-631747.

[32] Anna Yeaton et al. “The Impact of Inflammation-Induced Tumor Plasticity during Myeloid Transformation”. eng. In: *Cancer Discovery* 12.10 (Oct. 2022), pp. 2392–2413. ISSN: 2159-8290. DOI: 10.1158/2159-8290.CD-21-1146.

[33] Alba Rodriguez-Meira et al. “Single-cell multi-omics identifies chronic inflammation as a driver of TP53-mutant leukemic evolution”. eng. In: *Nature Genetics* 55.9 (Sept. 2023), pp. 1531–1541. ISSN: 1546-1718. DOI: 10.1038/s41588-023-01480-1.

[34] F. Y. Tsai et al. “An early haematopoietic defect in mice lacking the transcription factor GATA-2”. eng. In: *Nature* 371.6494 (Sept. 1994), pp. 221–226. ISSN: 0028-0836. DOI: 10.1038/371221a0.

[35] Neil P. Rodrigues et al. “Haploinsufficiency of GATA-2 perturbs adult hematopoietic stem-cell homeostasis”. eng. In: *Blood* 106.2 (July 2005), pp. 477–484. ISSN: 0006-4971. DOI: 10.1182/blood-2004-08-2989.

[36] Kirby D. Johnson et al. “Cis-element mutated in GATA2-dependent immunodeficiency governs hematopoiesis and vascular integrity”. eng. In: *The Journal of Clinical Investigation* 122.10 (Oct. 2012), pp. 3692–3704. ISSN: 1558-8238. DOI: 10.1172/JCI61623.

[37] Xin Gao et al. “Gata2 cis-element is required for hematopoietic stem cell generation in the mammalian embryo”. eng. In: *The Journal of Experimental Medicine* 210.13 (Dec. 2013), pp. 2833–2842. ISSN: 1540-9538. DOI: 10.1084/jem.20130733.

[38] Kirby D. Johnson et al. “Cis-regulatory mechanisms governing stem and progenitor cell transitions”. eng. In: *Science Advances* 1.8 (Sept. 2015), e1500503. ISSN: 2375-2548. DOI: 10.1126/sciadv.1500503.

[39] Michael A. Spinner et al. “GATA2 deficiency: a protean disorder of hematopoiesis, lymphatics, and immunity”. eng. In: *Blood* 123.6 (Feb. 2014), pp. 809–821. ISSN: 1528-0020. DOI: 10.1182/blood-2013-07-515528.

[40] Rachel E. Dickinson et al. “The evolution of cellular deficiency in GATA2 mutation”. eng. In: *Blood* 123.6 (Feb. 2014), pp. 863–874. ISSN: 1528-0020. DOI: 10.1182/blood-2013-07-517151.

[41] Hiromi Yamazaki et al. “A remote GATA2 hematopoietic enhancer drives leukemogenesis in inv(3)(q21;q26) by activating EVI1 expression”. eng. In: *Cancer Cell* 25.4 (Apr. 2014), pp. 415–427. ISSN: 1878-3686. DOI: 10.1016/j.ccr.2014.02.008.

[42] Charu Mehta et al. “Integrating Enhancer Mechanisms to Establish a Hierarchical Blood Development Program”. eng. In: *Cell Reports* 20.12 (Sept. 2017), pp. 2966–2979. ISSN: 2211-1247. DOI: 10.1016/j.celrep.2017.08.090.

[43] Kirby D. Johnson et al. “Constructing and deconstructing GATA2-regulated cell fate programs to establish developmental trajectories”. eng. In: *The Journal of Experimental Medicine* 217.11 (Nov. 2020), e20191526. ISSN: 1540-9538. DOI: 10.1084/jem.20191526.

[44] Kirby D. Johnson, Alexandra A. Soukup, and Emery H. Bresnick. “GATA2 deficiency elevates interferon regulatory factor-8 to subvert a progenitor cell differentiation program”. eng. In: *Blood Advances* 6.5 (Mar. 2022), pp. 1464–1473. ISSN: 2473-9537. DOI: 10.1182/bloodadvances.2021006182.

[45] Vu L. Tran et al. “Dual mechanism of inflammation sensing by the hematopoietic progenitor genome”. eng. In: *Science Advances* 11.22 (May 2025), eadv3169. ISSN: 2375-2548. DOI: 10.1126/sciadv.adv3169.

[46] Mabel Minji Jung et al. “Pathogenic human variant that dislocates GATA2 zinc fingers disrupts hematopoietic gene expression and signaling networks”. eng. In: *The Journal of Clinical Investigation* 133.7 (Apr. 2023), e162685. ISSN: 1558-8238. DOI: 10.1172/JCI162685.

[47] Adhithi Rajagopalan et al. “A gain-of-function p53 mutant synergizes with oncogenic NRAS to promote acute myeloid leukemia in mice”. eng. In: *The Journal of Clinical Investigation* 133.24 (Dec. 2023), e173116. ISSN: 1558-8238. DOI: 10.1172/JCI173116.

[48] Alexander M. de Bruin et al. "IFN induces monopoiesis and inhibits neutrophil development during inflammation". eng. In: *Blood* 119.6 (Feb. 2012), pp. 1543–1554. ISSN: 1528-0020. DOI: 10.1182/blood-2011-07-367706.

[49] Katie A. Matatall et al. "Type II interferon promotes differentiation of myeloid-biased hematopoietic stem cells". eng. In: *Stem Cells (Dayton, Ohio)* 32.11 (Nov. 2014), pp. 3023–3030. ISSN: 1549-4918. DOI: 10.1002/stem.1799.

[50] K. De Luca et al. "The TLR1/2 agonist PAM(3)CSK(4) instructs commitment of human hematopoietic stem cells to a myeloid cell fate". eng. In: *Leukemia* 23.11 (Nov. 2009), pp. 2063–2074. ISSN: 1476-5551. DOI: 10.1038/leu.2009.155.

[51] Javier Megías et al. "Direct Toll-like receptor-mediated stimulation of hematopoietic stem and progenitor cells occurs in vivo and promotes differentiation toward macrophages". eng. In: *Stem Cells (Dayton, Ohio)* 30.7 (July 2012), pp. 1486–1495. ISSN: 1549-4918. DOI: 10.1002/stem.1110.

[52] Vu L. Tran et al. "Restricting genomic actions of innate immune mediators on fetal hematopoietic progenitor cells". English. In: *iScience* 26.4 (Apr. 2023). Publisher: Elsevier. ISSN: 2589-0042. DOI: 10.1016/j.isci.2023.106297. URL: https://www.cell.com/iscience/abstract/S2589-0042(23)00374-7 (visited on 06/27/2025).

[53] Amelia K. Linnemann et al. "Genetic framework for GATA factor function in vascular biology". eng. In: *Proceedings of the National Academy of Sciences of the United States of America* 108.33 (Aug. 2011), pp. 13641–13646. ISSN: 1091-6490. DOI: 10.1073/pnas.1108440108.

[54] G. Behre et al. "c-Jun is a JNK-independent coactivator of the PU.1 transcription factor". eng. In: *The Journal of Biological Chemistry* 274.8 (Feb. 1999), pp. 4939–4946. ISSN: 0021-9258. DOI: 10.1074/jbc.274.8.4939.

[55] Xinhui Zhao et al. "PU.1-c-Jun interaction is crucial for PU.1 function in myeloid development". eng. In: *Communications Biology* 5.1 (Sept. 2022), p. 961. ISSN: 2399-3642. DOI: 10.1038/s42003-022-03888-7.

[56] Shin'ya Ohmori et al. "The Il6 -39 kb enhancer containing clustered GATA2- and PU.1-binding sites is essential for Il6 expression in murine mast cells". eng. In: *iScience* 25.9 (Sept. 2022), p. 104942. ISSN: 2589-0042. DOI: 10.1016/j.isci.2022.104942.

[57] Jun Takai, Hinata Ueki, and Satoshi Uemura. "Induction of the zinc finger transcription factor GATA2 promotes kidney inflammation-related gene expression". eng. In: *The Journal of Biological Chemistry* (June 2025), p. 110372. ISSN: 1083-351X. DOI: 10.1016/j.jbc.2025.110372.

[58] Jun Takai et al. "Gata2 heterozygous mutant mice exhibit reduced inflammatory responses and impaired bacterial clearance". eng. In: *iScience* 24.8 (Aug. 2021), p. 102836. ISSN: 2589-0042. DOI: 10.1016/j.isci.2021.102836.

[59] Nils Schmerer et al. "A searchable atlas of pathogen-sensitive lncRNA networks in human macrophages". eng. In: *Nature Communications* 16.1 (May 2025), p. 4733. ISSN: 2041-1723. DOI: 10.1038/s41467-025-60084-x.

[60] J. A. Segre, C. Bauer, and E. Fuchs. "Klf4 is a transcription factor required for establishing the barrier function of the skin". eng. In: *Nature Genetics* 22.4 (Aug. 1999), pp. 356–360. ISSN: 1061-4036. DOI: 10.1038/11926.

[61] Jonathan K. Alder et al. "Kruppel-like factor 4 is essential for inflammatory monocyte differentiation in vivo". eng. In: *Journal of Immunology (Baltimore, Md.: 1950)* 180.8 (Apr. 2008), pp. 5645–5652. ISSN: 0022-1767. DOI: 10.4049/jimmunol.180.8.5645.

[62] Chun Shik Park et al. "KLF4 enhances transplantation-induced hematopoiesis by inhibiting TLRs and noncanonical NFB signaling at a steady state". eng. In: *Experimental Hematology* 144 (Apr. 2025), p. 104730. ISSN: 1873-2399. DOI: 10.1016/j.exphem.2025.104730.

[63] Q. Wang et al. "Disruption of the Cbfa2 gene causes necrosis and hemorrhaging in the central nervous system and blocks definitive hematopoiesis". eng. In: *Proceedings of the National Academy of Sciences of the United States of America* 93.8 (Apr. 1996), pp. 3444–3449. ISSN: 0027-8424. DOI: 10.1073/pnas.93.8.3444.

[64] T. Okuda et al. "AML1, the target of multiple chromosomal translocations in human leukemia, is essential for normal fetal liver hematopoiesis". eng. In: *Cell* 84.2 (Jan. 1996), pp. 321–330. ISSN: 0092-8674. DOI: 10.1016/s0092-8674(00)80986-1.

[65] Boyoung Shin et al. "Runx1 and Runx3 drive progenitor to T-lineage transcriptome conversion in mouse T cell commitment via dynamic genomic site switching". eng. In: *Proceedings of the National Academy of Sciences of the United States of America* 118.4 (Jan. 2021), e2019655118. ISSN: 1091-6490. DOI: 10.1073/pnas.2019655118.

[66] Boyoung Shin et al. "Runx factors launch T cell and innate lymphoid programs via direct and gene network-based mechanisms". eng. In: *Nature Immunology* 24.9 (Sept. 2023), pp. 1458–1472. ISSN: 1529-2916. DOI: 10.1038/s41590-023-01585-z.

[67] Jane E. Churpek and Emery H. Bresnick. "Transcription factor mutations as a cause of familial myeloid neoplasms". eng. In: *The Journal of Clinical Investigation* 129.2 (Feb. 2019), pp. 476–488. ISSN: 1558-8238. DOI: 10.1172/JCI120854.

[68] W. J. Song et al. "Haploinsufficiency of CBFA2 causes familial thrombocytopenia with propensity to develop acute myelogenous leukaemia". eng. In: *Nature Genetics* 23.2 (Oct. 1999), pp. 166–175. ISSN: 1061-4036. DOI: 10.1038/13793.

[69] Lea Cunningham et al. "Natural history study of patients with familial platelet disorder with associated myeloid malignancy". eng. In: *Blood* 142.25 (Dec. 2023), pp. 2146–2158. ISSN: 1528-0020. DOI: 10.1182/blood.2023019746.

[70] Amy C. Fan et al. "RUNX1 loss renders hematopoietic and leukemic cells dependent on IL-3 and sensitive to JAK inhibition". eng. In: *The Journal of Clinical Investigation* 133.19 (Oct. 2023), e167053. ISSN: 1558-8238. DOI: 10.1172/JCI167053.

[71] Dana C. Bellissimo et al. "Runx1 negatively regulates inflammatory cytokine production by neutrophils in response to Toll-like receptor signaling". eng. In: *Blood Advances* 4.6 (Mar. 2020), pp. 1145–1158. ISSN: 2473-9537. DOI: 10.1182/bloodadvances.2019000785.

[72] Alexandra U. Zezulin et al. "RUNX1 is required in granulocyte-monocyte progenitors to attenuate inflammatory cytokine production by neutrophils". eng. In: *Genes & Development* 37.13-14 (July 2023), pp. 605–620. ISSN: 1549-5477. DOI: 10.1101/gad.350418.123.

[73] T. Evans, M. Reitman, and G. Felsenfeld. "An erythrocyte-specific DNA-binding factor recognizes a regulatory sequence common to all chicken globin genes". eng. In: *Proceedings of the National Academy of Sciences of the United States of America* 85.16 (Aug. 1988), pp. 5976–5980. ISSN: 0027-8424. DOI: 10.1073/pnas.85.16.5976.

[74] L. Wall, E. deBoer, and F. Grosveld. "The human beta-globin gene 3' enhancer contains multiple binding sites for an erythroid-specific protein". eng. In: *Genes & Development* 2.9 (Sept. 1988), pp. 1089–1100. ISSN: 0890-9369. DOI: 10.1101/gad.2.9.1089.

[75] J. G. Omichinski et al. "NMR structure of a specific DNA complex of Zn-containing DNA binding domain of GATA-1". eng. In: *Science (New York, N.Y.)* 261.5120 (July 1993), pp. 438–446. ISSN: 0036-8075. DOI: 10.1126/science.8332909.

[76] E. A. Golemis, N. A. Speck, and N. Hopkins. "Alignment of U3 region sequences of mammalian type C viruses: identification of highly conserved motifs and implications for enhancer design". eng. In: *Journal of Virology* 64.2 (Feb. 1990), pp. 534–542. ISSN: 0022-538X. DOI: 10.1128/JVI.64.2.534-542.1990.

[77] I. N. Melnikova et al. "Sequence specificity of the core-binding factor". eng. In: *Journal of Virology* 67.4 (Apr. 1993), pp. 2408–2411. ISSN: 0022-538X. DOI: 10.1128/JVI.67.4.2408-2411.1993.

[78] J. Bravo et al. "The leukemia-associated AML1 (Runx1)–CBF beta complex functions as a DNA-induced molecular clamp". eng. In: *Nature Structural Biology* 8.4 (Apr. 2001), pp. 371–378. ISSN: 1072-8368. DOI: 10.1038/86264.

[79] I. A. Wadman et al. "The LIM-only protein Lmo2 is a bridging molecule assembling an erythroid, DNA-binding complex which includes the TAL1, E47, GATA-1 and Ldb1/NLI proteins". eng. In: *The EMBO journal* 16.11 (June 1997), pp. 3145–3157. ISSN: 0261-4189. DOI: 10.1093/emboj/16.11.3145.

[80] Ryan J. Wozniak et al. "Molecular hallmarks of endogenous chromatin complexes containing master regulators of hematopoiesis". eng. In: *Molecular and Cellular Biology* 28.21 (Nov. 2008), pp. 6681–6694. ISSN: 1098-5549. DOI: 10.1128/MCB.01061-08.

[81] Tohru Fujiwara et al. "Discovering hematopoietic mechanisms through genome-wide analysis of GATA factor chromatin occupancy". eng. In: *Molecular Cell* 36.4 (Nov. 2009), pp. 667–681. ISSN: 1097-4164. DOI: 10.1016/j.molcel.2009.11.001.

[82] Ming Yu et al. "Insights into GATA-1-mediated gene activation versus repression via genome-wide chromatin occupancy analysis". eng. In: *Molecular Cell* 36.4 (Nov. 2009), pp. 682–695. ISSN: 1097-4164. DOI: 10.1016/j.molcel.2009.11.002.

[83] Nicola K. Wilson et al. "Combinatorial transcriptional control in blood stem/progenitor cells: genome-wide analysis of ten major transcriptional regulators". eng. In: *Cell Stem Cell* 7.4 (Oct. 2010), pp. 532–544. ISSN: 1875-9777. DOI: 10.1016/j.stem.2010.07.016.

[84] Ryan J. Wozniak et al. "Context-dependent GATA factor function: combinatorial requirements for transcriptional control in hematopoietic and endothelial cells". eng. In: *The Journal of Biological Chemistry* 282.19 (May 2007), pp. 14665–14674. ISSN: 0021-9258. DOI: 10.1074/jbc.M700792200.

[85] Kyle J. Hewitt et al. "Hematopoietic Signaling Mechanism Revealed from a Stem/Progenitor Cell Cistrome". eng. In: *Molecular Cell* 59.1 (July 2015), pp. 62–74. ISSN: 1097-4164. DOI: 10.1016/j.molcel.2015.05.020.

[86] Kam-Wing Ling et al. "GATA-2 plays two functionally distinct roles during the ontogeny of hematopoietic stem cells". eng. In: *The Journal of Experimental Medicine* 200.7 (Oct. 2004), pp. 871–882. ISSN: 0022-1007. DOI: 10.1084/jem.20031556.

[87] Z. Cai et al. "Haploinsufficiency of AML1 affects the temporal and spatial generation of hematopoietic stem cells in the mouse embryo". eng. In: *Immunity* 13.4 (Oct. 2000), pp. 423–431. ISSN: 1074-7613. DOI: 10.1016/s1074-7613(00)00042-x.

[88] Weili Sun and James R. Downing. "Haploinsufficiency of AML1 results in a decrease in the number of LTR-HSCs while simultaneously inducing an increase in more mature progenitors". eng. In: *Blood* 104.12 (Dec. 2004), pp. 3565–3572. ISSN: 0006-4971. DOI: 10.1182/blood-2003-12-4349.

[89] Stephen J. Loughran et al. "The transcription factor Erg is essential for definitive hematopoiesis and the function of adult hematopoietic stem cells". eng. In: *Nature Immunology* 9.7 (July 2008), pp. 810–819. ISSN: 1529-2916. DOI: 10.1038/ni.1617.

[90] Samir Taoudi et al. "ERG dependence distinguishes developmental control of hematopoietic stem cell maintenance from hematopoietic specification". eng. In: *Genes & Development* 25.3 (Feb. 2011), pp. 251–262. ISSN: 1549-5477. DOI: 10.1101/gad.2009211.

[91] Liat Goldberg et al. "Genome-scale expression and transcription factor binding profiles reveal therapeutic targets in transgenic ERG myeloid leukemia". eng. In: *Blood* 122.15 (Oct. 2013), pp. 2694–2703. ISSN: 1528-0020. DOI: 10.1182/blood-2013-01-477133.

[92] Avigail Rein et al. "Cellular and metabolic characteristics of pre-leukemic hematopoietic progenitors with GATA2 haploinsufficiency". eng. In: *Haematologica* 108.9 (Sept. 2023), pp. 2316–2330. ISSN: 1592-8721. DOI: 10.3324/haematol.2022.279437.

[93] Stefan Gröschel et al. "A single oncogenic enhancer rearrangement causes concomitant EVI1 and GATA2 deregulation in leukemia". eng. In: *Cell* 157.2 (Apr. 2014), pp. 369–381. ISSN: 1097-4172. DOI: 10.1016/j.cell.2014.02.019.

[94] Leonie Smeenk et al. "Selective Requirement of MYB for Oncogenic Hyperactivation of a Translocated Enhancer in Leukemia". eng. In: *Cancer Discovery* 11.11 (Nov. 2021), pp. 2868–2883. ISSN: 2159-8290. DOI: 10.1158/2159-8290.CD-20-1793.

[95] Saori Katayama et al. “GATA2 haploinsufficiency accelerates EVI1-driven leukemogenesis”. eng. In: *Blood* 130.7 (Aug. 2017), pp. 908–919. ISSN: 1528-0020. DOI: 10.1182/blood-2016-12-756767.

[96] E. W. Scott et al. “Requirement of transcription factor PU.1 in the development of multiple hematopoietic lineages”. eng. In: *Science (New York, N.Y.)* 265.5178 (Sept. 1994), pp. 1573–1577. ISSN: 0036-8075. DOI: 10.1126/science.8079170.

[97] S. R. McKercher et al. “Targeted disruption of the PU.1 gene results in multiple hematopoietic abnormalities”. eng. In: *The EMBO journal* 15.20 (Oct. 1996), pp. 5647–5658. ISSN: 0261-4189.

[98] Frank Rosenbauer et al. “Acute myeloid leukemia induced by graded reduction of a lineage-specific transcription factor, PU.1”. eng. In: *Nature Genetics* 36.6 (June 2004), pp. 624–630. ISSN: 1061-4036. DOI: 10.1038/ng1361.

[99] Frank Rosenbauer et al. “Lymphoid cell growth and transformation are suppressed by a key regulatory element of the gene encoding PU.1”. eng. In: *Nature Genetics* 38.1 (Jan. 2006), pp. 27–37. ISSN: 1061-4036. DOI: 10.1038/ng1679.

[100] Justin C. Wheat et al. “Single-molecule imaging of transcription dynamics in somatic stem cells”. eng. In: *Nature* 583.7816 (July 2020), pp. 431–436. ISSN: 1476-4687. DOI: 10.1038/s41586-020-2432-4.

[101] Koichi R. Katsumura et al. “Molecular basis of crosstalk between oncogenic Ras and the master regulator of hematopoiesis GATA-2”. eng. In: *EMBO reports* 15.9 (Sept. 2014), pp. 938–947. ISSN: 1469-3178. DOI: 10.15252/embr.201438808.

[102] Koichi R. Katsumura et al. “GATA Factor-Dependent Positive-Feedback Circuit in Acute Myeloid Leukemia Cells”. eng. In: *Cell Reports* 16.9 (Aug. 2016), pp. 2428–2441. ISSN: 2211-1247. DOI: 10.1016/j.celrep.2016.07.058.

[103] An-Chieh Feng et al. “The transcription factor NF-B orchestrates nucleosome remodeling during the primary response to Toll-like receptor 4 signaling”. eng. In: *Immunity* 57.3 (Mar. 2024), 462–477.e9. ISSN: 1097-4180. DOI: 10.1016/j.immuni.2024.02.004.

[104] Carolina Chavez et al. “IRF1 cooperates with ISGF3 or GAF to form innate immune de novo enhancers in macrophages”. eng. In: *Science Signaling* 18.868 (Jan. 2025), eado8860. ISSN: 1937-9145. DOI: 10.1126/scisignal.ado8860.

[105] Amy P. Hsu et al. “Mutations in GATA2 are associated with the autosomal dominant and sporadic monocytopenia and mycobacterial infection (MonoMAC) syndrome”. eng. In: *Blood* 118.10 (Sept. 2011), pp. 2653–2655. ISSN: 1528-0020. DOI: 10.1182/blood-2011-05-356352.

[106] Koichi R. Katsumura et al. “Human leukemia mutations corrupt but do not abrogate GATA-2 function”. eng. In: *Proceedings of the National Academy of Sciences of the United States of America* 115.43 (Oct. 2018), E10109–E10118. ISSN: 1091-6490. DOI: 10.1073/pnas.1813015115.

[107] Koichi R. Katsumura et al. “Pathogenic GATA2 genetic variants utilize an obligate enhancer mechanism to distort a multilineage differentiation program”. eng. In: *Proceedings of the National Academy of Sciences of the United States of America* 121.10 (Mar. 2024), e2317147121. ISSN: 1091-6490. DOI: 10.1073/pnas.2317147121.

[108] Yatao Chen et al. “GATA3 differentially regulates the transcriptome via zinc finger 2-modulated phase separation”. eng. In: *Cell Reports* 44.5 (May 2025), p. 115702. ISSN: 2211-1247. DOI: 10.1016/j.celrep.2025.115702.

[109] Rodolfo Ghirlando and Cecelia D. Trainor. “Determinants of GATA-1 binding to DNA: the role of non-finger residues”. eng. In: *The Journal of Biological Chemistry* 278.46 (Nov. 2003), pp. 45620–45628. ISSN: 0021-9258. DOI: 10.1074/jbc.M306410200.

[110] Atsushi Hasegawa et al. “Heterozygous variants in GATA2 contribute to DCML deficiency in mice by disrupting tandem protein binding”. eng. In: *Communications Biology* 5.1 (Apr. 2022), p. 376. ISSN: 2399-3642. DOI: 10.1038/s42003-022-03316-w.

[111] Laetitia Largeaud et al. “GATA2 mutated allele specific expression is associated with a hyporesponsive state of HSC in GATA2 deficiency syndrome”. eng. In: *Blood Cancer Journal* 15.1 (Jan. 2025), p. 7. ISSN: 2044-5385. DOI: 10.1038/s41408-025-01213-z.

[112] Trent Hall et al. “Modeling GATA2 deficiency in mice: the R396Q mutation disrupts normal hematopoiesis”. eng. In: *Leukemia* 39.3 (Mar. 2025), pp. 734–747. ISSN: 1476-5551. DOI: 10.1038/s41375-024-02508-z.

[113] Enric Redondo Monte et al. “Specific effects of somatic GATA2 zinc finger mutations on erythroid differentiation”. eng. In: *Experimental Hematology* 108 (Apr. 2022), pp. 26–35. ISSN: 1873-2399. DOI: 10.1016/j.exphem.2022.02.002.

[114] Peggy Kirstetter et al. “Modeling of C/EBPalpha mutant acute myeloid leukemia reveals a common expression signature of committed myeloid leukemia-initiating cells”. eng. In: *Cancer Cell* 13.4 (Apr. 2008), pp. 299–310. ISSN: 1878-3686. DOI: 10.1016/j.ccr.2008.02.008.

[115] Oxana Bereshchenko et al. “Hematopoietic stem cell expansion precedes the generation of committed myeloid leukemia-initiating cells in C/EBPalpha mutant AML”. eng. In: *Cancer Cell* 16.5 (Nov. 2009), pp. 390–400. ISSN: 1878-3686. DOI: 10.1016/j.ccr.2009.09.036.

[116] Cristina Di Genua et al. “C/EBP and GATA-2 Mutations Induce Bilineage Acute Erythroid Leukemia through Transformation of a Neomorphic Neutrophil-Erythroid Progenitor”. eng. In: *Cancer Cell* 37.5 (May 2020), 690–704.e8. ISSN: 1878-3686. DOI: 10.1016/j.ccell.2020.03.022.

[117] Elizabeth Heyes et al. “TET2 lesions enhance the aggressiveness of CEBPA-mutant acute myeloid leukemia by rebalancing GATA2 expression”. eng. In: *Nature Communications* 14.1 (Oct. 2023), p. 6185. ISSN: 2041-1723. DOI: 10.1038/s41467-023-41927-x.

[118] Marcela Cavalcante de Andrade Silva et al. "Breaking the spatial constraint between neighboring zinc fingers: a new germline mutation in GATA2 deficiency syndrome". eng. In: *Leukemia* 35.1 (Jan. 2021), pp. 264–268. ISSN: 1476-5551. DOI: 10.1038/s41375-020-0820-2.

[119] Jeffrey A. Grass et al. "Distinct functions of dispersed GATA factor complexes at an endogenous gene locus". eng. In: *Molecular and Cellular Biology* 26.19 (Oct. 2006), pp. 7056–7067. ISSN: 0270-7306. DOI: 10.1128/MCB.01033-06.

[120] H. Liang et al. "Solution structure of the ets domain of Fli-1 when bound to DNA". eng. In: *Nature Structural Biology* 1.12 (Dec. 1994), pp. 871–875. ISSN: 1072-8368. DOI: 10.1038/nsb1294-871.

[121] Gong-Hong Wei et al. "Genome-wide analysis of ETS-family DNA-binding in vitro and in vivo". eng. In: *The EMBO journal* 29.13 (July 2010), pp. 2147–2160. ISSN: 1460-2075. DOI: 10.1038/emboj.2010.106.

[122] Alexandra A. Soukup et al. "Single-nucleotide human disease mutation inactivates a blood-regenerative GATA2 enhancer". eng. In: *The Journal of Clinical Investigation* 129.3 (Mar. 2019), pp. 1180–1192. ISSN: 1558-8238. DOI: 10.1172/JCI122694.

[123] Alexandra A. Soukup et al. "Conditionally pathogenic genetic variants of a hematopoietic disease-suppressing enhancer". eng. In: *Science Advances* 7.50 (Dec. 2021), eabk3521. ISSN: 2375-2548. DOI: 10.1126/sciadv.abk3521.

[124] Fabian Lim et al. "Affinity-optimizing enhancer variants disrupt development". eng. In: *Nature* 626.7997 (Feb. 2024), pp. 151–159. ISSN: 1476-4687. DOI: 10.1038/s41586-023-06922-8.

[125] Pedro M. G. Soares et al. "Inflammatory intestinal damage induced by 5-fluorouracil requires IL-4". eng. In: *Cytokine* 61.1 (Jan. 2013), pp. 46–49. ISSN: 1096-0023. DOI: 10.1016/j.cyto.2012.10.003.

[126] A. T. Sougiannis et al. "Impact of 5 fluorouracil chemotherapy on gut inflammation, functional parameters, and gut microbiota". eng. In: *Brain, Behavior, and Immunity* 80 (Aug. 2019), pp. 44–55. ISSN: 1090-2139. DOI: 10.1016/j.bbi.2019.02.020.

[127] Alexandra A. Soukup and Emery H. Bresnick. "Gata2 noncoding genetic variation as a determinant of hematopoietic stem/progenitor cell mobilization efficiency". eng. In: *Blood Advances* 7.24 (Dec. 2023), pp. 7564–7575. ISSN: 2473-9537. DOI: 10.1182/bloodadvances.2023011003.

[128] Leila Noetzli et al. "Germline mutations in ETV6 are associated with thrombocytopenia, red cell macrocytosis and predisposition to lymphoblastic leukemia". eng. In: *Nature Genetics* 47.5 (May 2015), pp. 535–538. ISSN: 1546-1718. DOI: 10.1038/ng.3253.

[129] Sabine Topka et al. "Germline ETV6 Mutations Confer Susceptibility to Acute Lymphoblastic Leukemia and Thrombocytopenia". eng. In: *PLoS genetics* 11.6 (June 2015), e1005262. ISSN: 1553-7404. DOI: 10.1371/journal.pgen.1005262.

[130] Michael Y. Zhang et al. "Germline ETV6 mutations in familial thrombocytopenia and hematologic malignancy". eng. In: *Nature Genetics* 47.2 (Feb. 2015), pp. 180–185. ISSN: 1546-1718. DOI: 10.1038/ng.3177.

[131] Mackenzie Bloom et al. "ETV6 represses inflammatory response genes and regulates HSPC function during stress hematopoiesis in mice". eng. In: *Blood Advances* 7.18 (Sept. 2023), pp. 5608–5623. ISSN: 2473-9537. DOI: 10.1182/bloodadvances.2022009313.

[132] Jing Fang et al. "Myeloid malignancies with chromosome 5q deletions acquire a dependency on an intrachromosomal NF-B gene network". eng. In: *Cell Reports* 8.5 (Sept. 2014), pp. 1328–1338. ISSN: 2211-1247. DOI: 10.1016/j.celrep.2014.07.062.

[133] Lucien P. Garo et al. "MicroRNA-146a limits tumorigenic inflammation in colorectal cancer". eng. In: *Nature Communications* 12.1 (Apr. 2021), p. 2419. ISSN: 2041-1723. DOI: 10.1038/s41467-021-22641-y.

[134] Laura Barreyro et al. "Dysregulated innate immune signaling cooperates with RUNX1 mutations to transform an MDS-like disease to AML". eng. In: *iScience* 27.6 (June 2024), p. 109809. ISSN: 2589-0042. DOI: 10.1016/j.isci.2024.109809.

[135] M. Okano, S. Xie, and E. Li. "Cloning and characterization of a family of novel mammalian DNA (cytosine-5) methyltransferases". eng. In: *Nature Genetics* 19.3 (July 1998), pp. 219–220. ISSN: 1061-4036. DOI: 10.1038/890.

[136] M. Okano et al. "DNA methyltransferases Dnmt3a and Dnmt3b are essential for de novo methylation and mammalian development". eng. In: *Cell* 99.3 (Oct. 1999), pp. 247–257. ISSN: 0092-8674. DOI: 10.1016/s0092-8674(00)81656-6.

[137] Shinsuke Ito et al. "Role of Tet proteins in 5mC to 5hmC conversion, ES-cell self-renewal and inner cell mass specification". eng. In: *Nature* 466.7310 (Aug. 2010), pp. 1129–1133. ISSN: 1476-4687. DOI: 10.1038/nature09303.

[138] Shinsuke Ito et al. "Tet proteins can convert 5-methylcytosine to 5-formylcytosine and 5-carboxylcytosine". eng. In: *Science (New York, N.Y.)* 333.6047 (Sept. 2011), pp. 1300–1303. ISSN: 1095-9203. DOI: 10.1126/science.1210597.

[139] Lu Wang et al. "TET2 coactivates gene expression through demethylation of enhancers". eng. In: *Science Advances* 4.11 (Nov. 2018), eaau6986. ISSN: 2375-2548. DOI: 10.1126/sciadv.aau6986.

[140] Chan-Wang J. Lio et al. "TET enzymes augment activation-induced deaminase (AID) expression via 5-hydroxymethylcytosine modifications at the Aicda superenhancer". eng. In: *Science Immunology* 4.34 (Apr. 2019), eaau7523. ISSN: 2470-9468. DOI: 10.1126/sciimmunol.aau7523.

[141] David A. Russler-Germain et al. "The R882H DNMT3A mutation associated with AML dominantly inhibits wild-type DNMT3A by blocking its ability to form active tetramers". eng. In: *Cancer Cell* 25.4 (Apr. 2014), pp. 442–454. ISSN: 1878-3686. DOI: 10.1016/j.ccr.2014.02.010.

[142] Jungeun An et al. "Acute loss of TET function results in aggressive myeloid cancer in mice". eng. In: *Nature Communications* 6 (Nov. 2015), p. 10071. ISSN: 2041-1723. DOI: 10.1038/ncomms10071.

[143] Isaac F. López-Moyado et al. "Paradoxical association of TET loss of function with genome-wide DNA hypomethylation". eng. In: *Proceedings of the National Academy of Sciences of the United States of America* 116.34 (Aug. 2019), pp. 16933–16942. ISSN: 1091-6490. DOI: 10.1073/pnas.1903059116.

[144] Grant A. Challen et al. "Dnmt3a is essential for hematopoietic stem cell differentiation". eng. In: *Nature Genetics* 44.1 (Dec. 2011), pp. 23–31. ISSN: 1546-1718. DOI: 10.1038/ng.1009.

[145] Allison Mayle et al. "Dnmt3a loss predisposes murine hematopoietic stem cells to malignant transformation". eng. In: *Blood* 125.4 (Jan. 2015), pp. 629–638. ISSN: 1528-0020. DOI: 10.1182/blood-2014-08-594648.

[146] Hamza Celik et al. "Enforced differentiation of Dnmt3a-null bone marrow leads to failure with c-Kit mutations driving leukemic transformation". eng. In: *Blood* 125.4 (Jan. 2015), pp. 619–628. ISSN: 1528-0020. DOI: 10.1182/blood-2014-08-594564.

[147] Myunggon Ko et al. "Ten-Eleven-Translocation 2 (TET2) negatively regulates homeostasis and differentiation of hematopoietic stem cells in mice". eng. In: *Proceedings of the National Academy of Sciences of the United States of America* 108.35 (Aug. 2011), pp. 14566–14571. ISSN: 1091-6490. DOI: 10.1073/pnas.1112317108.

[148] Kelly Moran-Crusio et al. "Tet2 loss leads to increased hematopoietic stem cell self-renewal and myeloid transformation". eng. In: *Cancer Cell* 20.1 (July 2011), pp. 11–24. ISSN: 1878-3686. DOI: 10.1016/j.ccr.2011.06.001.

[149] Zhe Li et al. "Deletion of Tet2 in mice leads to dysregulated hematopoietic stem cells and subsequent development of myeloid malignancies". eng. In: *Blood* 118.17 (Oct. 2011), pp. 4509–4518. ISSN: 1528-0020. DOI: 10.1182/blood-2010-12-325241.

[150] Cyril Quivoron et al. "TET2 inactivation results in pleiotropic hematopoietic abnormalities in mouse and is a recurrent event during human lymphomagenesis". eng. In: *Cancer Cell* 20.1 (July 2011), pp. 25–38. ISSN: 1878-3686. DOI: 10.1016/j.ccr.2011.06.003.

[151] L. Scourzic et al. "DNMT3A(R882H) mutant and Tet2 inactivation cooperate in the deregulation of DNA methylation control to induce lymphoid malignancies in mice". eng. In: *Leukemia* 30.6 (June 2016), pp. 1388–1398. ISSN: 1476-5551. DOI: 10.1038/leu.2016.29.

[152] Xiaotian Zhang et al. "DNMT3A and TET2 compete and cooperate to repress lineage-specific transcription factors in hematopoietic stem cells". eng. In: *Nature Genetics* 48.9 (Sept. 2016), pp. 1014–1023. ISSN: 1546-1718. DOI: 10.1038/ng.3610.

[153] Johanna C. Scheuermann et al. "Histone H2A deubiquitinase activity of the Polycomb repressive complex PR-DUB". eng. In: *Nature* 465.7295 (May 2010), pp. 243–247. ISSN: 1476-4687. DOI: 10.1038/nature08966.

[154] Zhen Dong et al. "A mutant ASXL1-BAP1-EHMT complex contributes to heterochromatin dysfunction in clonal hematopoiesis and chronic monomyelocytic leukemia". eng. In: *Proceedings of the National Academy of Sciences of the United States of America* 122.1 (Jan. 2025), e2413302121. ISSN: 1091-6490. DOI: 10.1073/pnas.2413302121.

[155] Ping Zhou et al. "Alpha-kinase 1 is a cytosolic innate immune receptor for bacterial ADP-heptose". eng. In: *Nature* 561.7721 (Sept. 2018), pp. 122–126. ISSN: 1476-4687. DOI: 10.1038/s41586-018-0433-3.

[156] Puneet Agarwal et al. "Microbial metabolite drives ageing-related clonal haematopoiesis via ALPK1". eng. In: *Nature* 642.8066 (June 2025), pp. 201–211. ISSN: 1476-4687. DOI: 10.1038/s41586-025-08938-8.

[157] N. Zioni et al. "Inflammatory signals from fatty bone marrow support DNMT3A driven clonal hematopoiesis". eng. In: *Nature Communications* 14.1 (Apr. 2023), p. 2070. ISSN: 2041-1723. DOI: 10.1038/s41467-023-36906-1.

[158] Jaime M. Reyes et al. "Hematologic DNMT3A reduction and high-fat diet synergize to promote weight gain and tissue inflammation". eng. In: *iScience* 27.3 (Mar. 2024), p. 109122. ISSN: 2589-0042. DOI: 10.1016/j.isci.2024.109122.

[159] Zhigang Cai et al. "Inhibition of Inflammatory Signaling in Tet2 Mutant Preleukemic Cells Mitigates Stress-Induced Abnormalities and Clonal Hematopoiesis". eng. In: *Cell Stem Cell* 23.6 (Dec. 2018), 833–849.e5. ISSN: 1875-9777. DOI: 10.1016/j.stem.2018.10.013.

[160] Zhigang Cai et al. "Hyperglycemia cooperates with Tet2 heterozygosity to induce leukemia driven by proinflammatory cytokine-induced lncRNA Morrbid". eng. In: *The Journal of Clinical Investigation* 131.1 (Jan. 2021), e140707, 140707. ISSN: 1558-8238. DOI: 10.1172/JCI140707.

[161] Qian Zhang et al. "Tet2 is required to resolve inflammation by recruiting Hdac2 to specifically repress IL-6". eng. In: *Nature* 525.7569 (Sept. 2015), pp. 389–393. ISSN: 1476-4687. DOI: 10.1038/nature15252.

[162] Skye C. McIver et al. "Dissecting Regulatory Mechanisms Using Mouse Fetal Liver-Derived Erythroid Cells". eng. In: *Methods in Molecular Biology (Clifton, N.J.)* 1698 (2018), pp. 67–89. ISSN: 1940-6029. DOI: 10.1007/978-1-4939-7428-3_4.

[163] Hogune Im et al. "Chromatin domain activation via GATA-1 utilization of a small subset of dispersed GATA motifs within a broad chromosomal region". eng. In: *Proceedings of the National Academy of Sciences of the United States of America* 102.47 (Nov. 2005), pp. 17065–17070. ISSN: 0027-8424. DOI: 10.1073/pnas.0506164102.

[164] Alexander Dobin et al. "STAR: ultrafast universal RNA-seq aligner". eng. In: *Bioinformatics (Oxford, England)* 29.1 (Jan. 2013), pp. 15–21. ISSN: 1367-4811. DOI: 10.1093/bioinformatics/bts635.

[165] Bo Li and Colin N. Dewey. "RSEM: accurate transcript quantification from RNA-Seq data with or without a reference genome". eng. In: *BMC bioinformatics* 12 (Aug. 2011), p. 323. ISSN: 1471-2105. DOI: 10.1186/1471-2105-12-323.

[166] Mark D. Robinson, Davis J. McCarthy, and Gordon K. Smyth. "edgeR: a Bioconductor package for differential expression analysis of digital gene expression data". eng. In: *Bioinformatics (Oxford, England)* 26.1 (Jan. 2010), pp. 139–140. ISSN: 1367-4811. DOI: 10.1093/bioinformatics/btp616.

[167] Matthew E. Ritchie et al. "limma powers differential expression analyses for RNA-sequencing and microarray studies". eng. In: *Nucleic Acids Research* 43.7 (Apr. 2015), e47. ISSN: 1362-4962. DOI: 10.1093/nar/gkv007.

[168] Timothy L. Bailey et al. "The MEME Suite". eng. In: *Nucleic Acids Research* 43.W1 (July 2015), W39–49. ISSN: 1362-4962. DOI: 10.1093/nar/gkv416.

[169] Hatice S. Kaya-Okur et al. "CUT&Tag for efficient epigenomic profiling of small samples and single cells". eng. In: *Nature Communications* 10.1 (Apr. 2019), p. 1930. ISSN: 2041-1723. DOI: 10.1038/s41467-019-09982-5.

[170] Yuefeng Li et al. "Chromatin and transcription factor profiling in rare stem cell populations using CUT&Tag". eng. In: *STAR protocols* 2.3 (Sept. 2021), p. 100751. ISSN: 2666-1667. DOI: 10.1016/j.xpro.2021.100751.

[171] Hatice S. Kaya-Okur et al. "Efficient low-cost chromatin profiling with CUT&Tag". eng. In: *Nature Protocols* 15.10 (Oct. 2020), pp. 3264–3283. ISSN: 1750-2799. DOI: 10.1038/s41596-020-0373-x.

[172] Marcel Martin. "Cutadapt removes adapter sequences from high-throughput sequencing reads". en. In: *EMBnet.journal* 17.1 (May 2011). Number: 1, pp. 10–12. ISSN: 2226-6089. DOI: 10.14806/ej.17.1.200. URL: https://journal.embnet.org/index.php/embnetjournal/article/view/200 (visited on 07/13/2025).

[173] Ben Langmead and Steven L. Salzberg. "Fast gapped-read alignment with Bowtie 2". en. In: *Nature Methods* 9.4 (Apr. 2012). Publisher: Nature Publishing Group, pp. 357–359. ISSN: 1548-7105. DOI: 10.1038/nmeth.1923. URL: https://www.nature.com/articles/nmeth.1923 (visited on 07/13/2025).

[174] T. C. Chou and P. Talalay. "Quantitative analysis of dose-effect relationships: the combined effects of multiple drugs or enzyme inhibitors". eng. In: *Advances in Enzyme Regulation* 22 (1984), pp. 27–55. ISSN: 0065-2571. DOI: 10.1016/0065-2571(84)90007-4.

[175] Taro Kawai and Shizuo Akira. "Toll-like receptors and their crosstalk with other innate receptors in infection and immunity". eng. In: *Immunity* 34.5 (May 2011), pp. 637–650. ISSN: 1097-4180. DOI: 10.1016/j.immuni.2011.05.006.

[176] Pamela C. Ronald and Bruce Beutler. "Plant and animal sensors of conserved microbial signatures". eng. In: *Science (New York, N.Y.)* 330.6007 (Nov. 2010), pp. 1061–1064. ISSN: 1095-9203. DOI: 10.1126/science.1189468.

[177] Yoshinori Nagai et al. "Toll-like receptors on hematopoietic progenitor cells stimulate innate immune system replenishment". eng. In: *Immunity* 24.6 (June 2006), pp. 801–812. ISSN: 1074-7613. DOI: 10.1016/j.immuni.2006.04.008.

[178] Triantafyllos Chavakis, Ioannis Mitroulis, and George Hajishengallis. "Hematopoietic progenitor cells as integrative hubs for adaptation to and fine-tuning of inflammation". eng. In: *Nature Immunology* 20.7 (July 2019), pp. 802–811. ISSN: 1529-2916. DOI: 10.1038/s41590-019-0402-5.

[179] Alberto Yáñez et al. "Detection of a TLR2 agonist by hematopoietic stem and progenitor cells impacts the function of the macrophages they produce". eng. In: *European Journal of Immunology* 43.8 (Aug. 2013), pp. 2114–2125. ISSN: 1521-4141. DOI: 10.1002/eji.201343403.

[180] L. G. Schuettpelz et al. "G-CSF regulates hematopoietic stem cell activity, in part, through activation of Toll-like receptor signaling". eng. In: *Leukemia* 28.9 (Sept. 2014), pp. 1851–1860. ISSN: 1476-5551. DOI: 10.1038/leu.2014.68.

[181] Aaron Burberry et al. "Infection mobilizes hematopoietic stem cells through cooperative NOD-like receptor and Toll-like receptor signaling". eng. In: *Cell Host & Microbe* 15.6 (June 2014), pp. 779–791. ISSN: 1934-6069. DOI: 10.1016/j.chom.2014.05.004.

[182] Jimmy L. Zhao et al. "Conversion of danger signals into cytokine signals by hematopoietic stem and progenitor cells for regulation of stress-induced hematopoiesis". eng. In: *Cell Stem Cell* 14.4 (Apr. 2014), pp. 445–459. ISSN: 1875-9777. DOI: 10.1016/j.stem.2014.01.007.

[183] Melinda E. Varney et al. "Loss of Tifab, a del(5q) MDS gene, alters hematopoiesis through derepression of Toll-like receptor-TRAF6 signaling". eng. In: *The Journal of Experimental Medicine* 212.11 (Oct. 2015), pp. 1967–1985. ISSN: 1540-9538. DOI: 10.1084/jem.20141898.

[184] Matthew B. Buechler, Holly M. Akilesh, and Jessica A. Hamerman. "Cutting Edge: Direct Sensing of TLR7 Ligands and Type I IFN by the Common Myeloid Progenitor Promotes mTOR/PI3K-Dependent Emergency Myelopoiesis". eng. In: *Journal of Immunology (Baltimore, Md.: 1950)* 197.7 (Oct. 2016), pp. 2577–2582. ISSN: 1550-6606. DOI: 10.4049/jimmunol.1600813.

[185] A. C. Herman et al. "Systemic TLR2 agonist exposure regulates hematopoietic stem cells via cell-autonomous and cell-non-autonomous mechanisms". eng. In: *Blood Cancer Journal* 6.6 (June 2016), e437. ISSN: 2044-5385. DOI: 10.1038/bcj.2016.45.

[186] Tomoya Muto et al. "Adaptive response to inflammation contributes to sustained myelopoiesis and confers a competitive advantage in myelodysplastic syndrome HSCs". eng. In: *Nature Immunology* 21.5 (May 2020), pp. 535–545. ISSN: 1529-2916. DOI: 10.1038/s41590-020-0663-z.

[187] Yumi Sasaki et al. "IL-6 Generated from Human Hematopoietic Stem and Progenitor Cells through TLR4 Signaling Promotes Emergency Granulopoiesis by Regulating Transcription Factor Expression". eng. In: *Journal of Immunology (Baltimore, Md.: 1950)* 207.4 (Aug. 2021), pp. 1078–1086. ISSN: 1550-6606. DOI: 10.4049/jimmunol.2100168.

[188] Steffen Boettcher et al. "Endothelial cells translate pathogen signals into G-CSF-driven emergency granulopoiesis". eng. In: *Blood* 124.9 (Aug. 2014), pp. 1393–1403. ISSN: 1528-0020. DOI: 10.1182/blood-2014-04-570762.

[189] Ailing Liu et al. "Cutting Edge: Hematopoietic Stem Cell Expansion and Common Lymphoid Progenitor Depletion Require Hematopoietic-Derived, Cell-Autonomous TLR4 in a Model of Chronic Endotoxin". eng. In: *Journal of Immunology (Baltimore, Md.: 1950)* 195.6 (Sept. 2015), pp. 2524–2528. ISSN: 1550-6606. DOI: 10.4049/jimmunol.1501231.

[190] Hitoshi Takizawa et al. "Pathogen-Induced TLR4-TRIF Innate Immune Signaling in Hematopoietic Stem Cells Promotes Proliferation but Reduces Competitive Fitness". eng. In: *Cell Stem Cell* 21.2 (Aug. 2017), 225–240.e5. ISSN: 1875-9777. DOI: 10.1016/j.stem.2017.06.013.

[191] Darlene A. Monlish et al. "Loss of Toll-like receptor 2 results in accelerated leukemogenesis in the NUP98-HOXD13 mouse model of MDS". eng. In: *Blood* 131.9 (Mar. 2018), pp. 1032–1035. ISSN: 1528-0020. DOI: 10.1182/blood-2017-08-801944.

[192] Darlene A. Monlish et al. "TLR2/6 signaling promotes the expansion of premalignant hematopoietic stem and progenitor cells in the NUP98-HOXD13 mouse model of MDS". eng. In: *Experimental Hematology* 88 (Aug. 2020), pp. 42–55. ISSN: 1873-2399. DOI: 10.1016/j.exphem.2020.07.001.

[193] Christopher N. Hahn et al. "Heritable GATA2 mutations associated with familial myelodysplastic syndrome and acute myeloid leukemia". eng. In: *Nature Genetics* 43.10 (Sept. 2011), pp. 1012–1017. ISSN: 1546-1718. DOI: 10.1038/ng.913.

[194] Pia Ostergaard et al. "Mutations in GATA2 cause primary lymphedema associated with a predisposition to acute myeloid leukemia (Emberger syndrome)". eng. In: *Nature Genetics* 43.10 (Sept. 2011), pp. 929–931. ISSN: 1546-1718. DOI: 10.1038/ng.923.

[195] Rachel Emma Dickinson et al. "Exome sequencing identifies GATA-2 mutation as the cause of dendritic cell, monocyte, B and NK lymphoid deficiency". eng. In: *Blood* 118.10 (Sept. 2011), pp. 2656–2658. ISSN: 1528-0020. DOI: 10.1182/blood-2011-06-360313.

[196] Jan Kazenwadel et al. "Loss-of-function germline GATA2 mutations in patients with MDS/AML or MonoMAC syndrome and primary lymphedema reveal a key role for GATA2 in the lymphatic vasculature". eng. In: *Blood* 119.5 (Feb. 2012), pp. 1283–1291. ISSN: 1528-0020. DOI: 10.1182/blood-2011-08-374363.

[197] Amy P. Hsu et al. "GATA2 haploinsufficiency caused by mutations in a conserved intronic element leads to MonoMAC syndrome". eng. In: *Blood* 121.19 (May 2013), 3830–3837, S1–7. ISSN: 1528-0020. DOI: 10.1182/blood-2012-08-452763.

[198] Juan Bautista Menendez-Gonzalez et al. "Gata2 as a Crucial Regulator of Stem Cells in Adult Hematopoiesis and Acute Myeloid Leukemia". eng. In: *Stem Cell Reports* 13.2 (Aug. 2019), pp. 291–306. ISSN: 2213-6711. DOI: 10.1016/j.stemcr.2019.07.005.

[199] Ali Abdelfattah et al. "Gata2 haploinsufficiency promotes proliferation and functional decline of hematopoietic stem cells with myeloid bias during aging". eng. In: *Blood Advances* 5.20 (Oct. 2021), pp. 4285–4290. ISSN: 2473-9537. DOI: 10.1182/bloodadvances.2021004726.

[200] Emery H. Bresnick and Kirby D. Johnson. "Blood disease-causing and -suppressing transcriptional enhancers: general principles and GATA2 mechanisms". eng. In: *Blood Advances* 3.13 (July 2019), pp. 2045–2056. ISSN: 2473-9537. DOI: 10.1182/bloodadvances.2019000378.

[201] Xiaona You et al. "Gata2 -77 enhancer regulates adult hematopoietic stem cell survival". eng. In: *Leukemia* 35.3 (Mar. 2021), pp. 901–905. ISSN: 1476-5551. DOI: 10.1038/s41375-020-0942-6.

[202] Katherine Y. King et al. "Irgm1 protects hematopoietic stem cells by negative regulation of IFN signaling". eng. In: *Blood* 118.6 (Aug. 2011), pp. 1525–1533. ISSN: 1528-0020. DOI: 10.1182/blood-2011-01-328682.

[203] Seth L. Masters et al. "NLRP1 inflammasome activation induces pyroptosis of hematopoietic progenitor cells". eng. In: *Immunity* 37.6 (Dec. 2012), pp. 1009–1023. ISSN: 1097-4180. DOI: 10.1016/j.immuni.2012.08.027.

[204] Eric M. Pietras et al. "Chronic interleukin-1 exposure drives haematopoietic stem cells towards precocious myeloid differentiation at the expense of self-renewal". eng. In: *Nature Cell Biology* 18.6 (June 2016), pp. 607–618. ISSN: 1476-4679. DOI: 10.1038/ncb3346.

[205] Katie A. Matatall et al. "Chronic Infection Depletes Hematopoietic Stem Cells through Stress-Induced Terminal Differentiation". eng. In: *Cell Reports* 17.10 (Dec. 2016), pp. 2584–2595. ISSN: 2211-1247. DOI: 10.1016/j.celrep.2016.11.031.

[206] Hiroki Kato et al. "Infection perturbs Bach2- and Bach1-dependent erythroid lineage 'choice' to cause anemia". eng. In: *Nature Immunology* 19.10 (Oct. 2018), pp. 1059–1070. ISSN: 1529-2916. DOI: 10.1038/s41590-018-0202-3.

[207] Francisco Caiado, Eric M. Pietras, and Markus G. Manz. "Inflammation as a regulator of hematopoietic stem cell function in disease, aging, and clonal selection". eng. In: *The Journal of Experimental Medicine* 218.7 (July 2021), e20201541. ISSN: 1540-9538. DOI: 10.1084/jem.20201541.

[208] Alexandra A. Soukup and Emery H. Bresnick. "GATA2 +9.5 enhancer: from principles of hematopoiesis to genetic diagnosis in precision medicine". eng. In: *Current Opinion in Hematology* 27.3 (May 2020), pp. 163–171. ISSN: 1531-7048. DOI: 10.1097/MOH.0000000000000576.

[209] P. Hoffmann et al. "Stimulation of human and murine adherent cells by bacterial lipoprotein and synthetic lipopeptide analogues". eng. In: *Immunobiology* 177.2 (May 1988), pp. 158–170. ISSN: 0171-2985. DOI: 10.1016/S0171-2985(88)80036-6.

[210] A. O. Aliprantis et al. "Cell activation and apoptosis by bacterial lipoproteins through toll-like receptor-2". eng. In: *Science (New York, N.Y.)* 285.5428 (July 1999), pp. 736–739. ISSN: 0036-8075. DOI: 10.1126/science.285.5428.736.

[211] Jin Young Kang et al. "Recognition of lipopeptide patterns by Toll-like receptor 2-Toll-like receptor 6 heterodimer". eng. In: *Immunity* 31.6 (Dec. 2009), pp. 873–884. ISSN: 1097-4180. DOI: 10.1016/j.immuni.2009.09.018.

[212] Ching-Aeng Lim et al. “Genome-wide mapping of RELA(p65) binding identifies E2F1 as a transcriptional activator recruited by NF-kappaB upon TLR4 activation”. eng. In: *Molecular Cell* 27.4 (Aug. 2007), pp. 622–635. ISSN: 1097-2765. DOI: 10.1016/j.molcel.2007.06.038.

[213] Osamu Takeuchi et al. “Cutting edge: role of Toll-like receptor 1 in mediating immune response to microbial lipoproteins”. eng. In: *Journal of Immunology (Baltimore, Md.: 1950)* 169.1 (July 2002), pp. 10–14. ISSN: 0022-1767. DOI: 10.4049/jimmunol.169.1.10.

[214] Mi Sun Jin et al. “Crystal structure of the TLR1-TLR2 heterodimer induced by binding of a tri-acylated lipopeptide”. eng. In: *Cell* 130.6 (Sept. 2007), pp. 1071–1082. ISSN: 0092-8674. DOI: 10.1016/j.cell.2007.09.008.

[215] O. Takeuchi et al. “Discrimination of bacterial lipoproteins by Toll-like receptor 6”. eng. In: *International Immunology* 13.7 (July 2001), pp. 933–940. ISSN: 0953-8178. DOI: 10.1093/intimm/13.7.933.

[216] G. R. Guy et al. “Interleukin 1 and tumor necrosis factor activate common multiple protein kinases in human fibroblasts”. English. In: *Journal of Biological Chemistry* 266.22 (Aug. 1991). Publisher: Elsevier, pp. 14343–14352. ISSN: 0021-9258, 1083-351X. DOI: 10.1016/S0021-9258(18)98690-4. URL: https://www.jbc.org/article/S0021-9258(18)98690-4/abstract (visited on 07/14/2025).

[217] T. A. Bird et al. “Interleukin-1 represents a new modality for the activation of extracellular signal-regulated kinases/microtubule-associated protein-2 kinases.” English. In: *Journal of Biological Chemistry* 266.33 (Nov. 1991). Publisher: Elsevier, pp. 22661–22670. ISSN: 0021-9258, 1083-351X. DOI: 10.1016/S0021-9258(18)54621-4. URL: https://www.jbc.org/article/S0021-9258(18)54621-4/abstract (visited on 07/14/2025).

[218] J. Saklatvala et al. “Interleukin 1 and tumour necrosis factor activate the mitogen-activated protein (MAP) kinase kinase in cultured cells”. eng. In: *FEBS letters* 334.2 (Nov. 1993), pp. 189–192. ISSN: 0014-5793. DOI: 10.1016/0014-5793(93)81709-9.

[219] M. Muzio et al. “The human toll signaling pathway: divergence of nuclear factor kappaB and JNK/SAPK activation upstream of tumor necrosis factor receptor-associated factor 6 (TRAF6)”. eng. In: *The Journal of Experimental Medicine* 187.12 (June 1998), pp. 2097–2101. ISSN: 0022-1007. DOI: 10.1084/jem.187.12.2097.

[220] N. W. Schröder et al. “Activation of mitogen-activated protein kinases p42/44, p38, and stress-activated protein kinases in myelo-monocytic cells by Treponema lipoteichoic acid”. eng. In: *The Journal of Biological Chemistry* 276.13 (Mar. 2001), pp. 9713–9719. ISSN: 0021-9258. DOI: 10.1074/jbc.M008954200.

[221] C. Y. Kuan et al. “The Jnk1 and Jnk2 protein kinases are required for regional specific apoptosis during early brain development”. eng. In: *Neuron* 22.4 (Apr. 1999), pp. 667–676. ISSN: 0896-6273. DOI: 10.1016/s0896-6273(00)80727-8.

[222] Myoung Sook Han et al. “JNK expression by macrophages promotes obesity-induced insulin resistance and inflammation”. eng. In: *Science (New York, N.Y.)* 339.6116 (Jan. 2013), pp. 218–222. ISSN: 1095-9203. DOI: 10.1126/science.1227568.

[223] Young Jun Kang et al. “Macrophage deletion of p38alpha partially impairs lipopolysaccharide-induced cellular activation”. eng. In: *Journal of Immunology (Baltimore, Md.: 1950)* 180.7 (Apr. 2008), pp. 5075–5082. ISSN: 0022-1767. DOI: 10.4049/jimmunol.180.7.5075.

[224] Kyle Tretina et al. “Interferon-induced guanylate-binding proteins: Guardians of host defense in health and disease”. eng. In: *The Journal of Experimental Medicine* 216.3 (Mar. 2019), pp. 482–500. ISSN: 1540-9538. DOI: 10.1084/jem.20182031.

[225] Alexandra Kresse et al. “Analyses of murine GBP homology clusters based on in silico, in vitro and in vivo studies”. eng. In: *BMC genomics* 9 (Apr. 2008), p. 158. ISSN: 1471-2164. DOI: 10.1186/1471-2164-9-158.

[226] Bae-Hoon Kim et al. “A family of IFN--inducible 65-kD GTPases protects against bacterial infection”. eng. In: *Science (New York, N.Y.)* 332.6030 (May 2011), pp. 717–721. ISSN: 1095-9203. DOI: 10.1126/science.1201711.

[227] Masahiro Yamamoto et al. “A cluster of interferon--inducible p65 GTPases plays a critical role in host defense against Toxoplasma gondii”. eng. In: *Immunity* 37.2 (Aug. 2012), pp. 302–313. ISSN: 1097-4180. DOI: 10.1016/j.immuni.2012.06.009.

[228] Avinash R. Shenoy et al. “GBP5 promotes NLRP3 inflammasome assembly and immunity in mammals”. eng. In: *Science (New York, N.Y.)* 336.6080 (Apr. 2012), pp. 481–485. ISSN: 1095-9203. DOI: 10.1126/science.1217141.

[229] Stéphane Deschamps et al. “The mouse Ifi200 gene cluster: genomic sequence, analysis, and comparison with the human HIN-200 gene cluster”. eng. In: *Genomics* 82.1 (July 2003), pp. 34–46. ISSN: 0888-7543. DOI: 10.1016/s0888-7543(03)00092-2.

[230] Spyridon Stavrou et al. “Nucleic acid recognition orchestrates the anti-viral response to retroviruses”. eng. In: *Cell Host & Microbe* 17.4 (Apr. 2015), pp. 478–488. ISSN: 1934-6069. DOI: 10.1016/j.chom.2015.02.021.

[231] Kelly M. Storek et al. “cGAS and Ifi204 cooperate to produce type I IFNs in response to Francisella infection”. eng. In: *Journal of Immunology (Baltimore, Md.: 1950)* 194.7 (Apr. 2015), pp. 3236–3245. ISSN: 1550-6606. DOI: 10.4049/jimmunol.1402764.

[232] Hideya Kawaji et al. “Exploration of novel motifs derived from mouse cDNA sequences”. eng. In: *Genome Research* 12.3 (Mar. 2002), pp. 367–378. ISSN: 1088-9051. DOI: 10.1101/gr.193702.

[233] Yunjian Xu, Magnus Johansson, and Anna Karlsson. “Human UMP-CMP kinase 2, a novel nucleoside monophosphate kinase localized in mitochondria”. eng. In: *The Journal of Biological Chemistry* 283.3 (Jan. 2008), pp. 1563–1571. ISSN: 0021-9258. DOI: 10.1074/jbc.M707997200.

[234] Alessandro Michelucci et al. “Immune-responsive gene 1 protein links metabolism to immunity by catalyzing itaconic acid production”. eng. In: *Proceedings of the National Academy of Sciences of the United States of America* 110.19 (May 2013), pp. 7820–7825. ISSN: 1091-6490. DOI: 10.1073/pnas.1218599110.

[235] Luke A. J. O'Neill and Maxim N. Artyomov. "Itaconate: the poster child of metabolic reprogramming in macrophage function". eng. In: *Nature Reviews. Immunology* 19.5 (May 2019), pp. 273–281. ISSN: 1474-1741. DOI: 10.1038/s41577-019-0128-5.

[236] Marah C. Runtsch et al. "Itaconate and itaconate derivatives target JAK1 to suppress alternative activation of macrophages". eng. In: *Cell Metabolism* 34.3 (Mar. 2022), 487–501.e8. ISSN: 1932-7420. DOI: 10.1016/j.cmet.2022.02.002.

[237] Shotaro Maedera et al. "GLUT6 is a lysosomal transporter that is regulated by inflammatory stimuli and modulates glycolysis in macrophages". eng. In: *FEBS letters* 593.2 (Jan. 2019), pp. 195–208. ISSN: 1873-3468. DOI: 10.1002/1873-3468.13298.

[238] K. Sakata et al. "Cloning of a lymphatic peptide/histidine transporter". eng. In: *The Biochemical Journal* 356.Pt 1 (May 2001), pp. 53–60. ISSN: 0264-6021. DOI: 10.1042/0264-6021:3560053.

[239] Steffen Boettcher et al. "Cutting edge: LPS-induced emergency myelopoiesis depends on TLR4-expressing nonhematopoietic cells". eng. In: *Journal of Immunology (Baltimore, Md.: 1950)* 188.12 (June 2012), pp. 5824–5828. ISSN: 1550-6606. DOI: 10.4049/jimmunol.1103253.

[240] Veerendra Munugalavadla et al. "Repression of c-kit and its downstream substrates by GATA-1 inhibits cell proliferation during erythroid maturation". eng. In: *Molecular and Cellular Biology* 25.15 (Aug. 2005), pp. 6747–6759. ISSN: 0270-7306. DOI: 10.1128/MCB.25.15.6747-6759.2005.

[241] Huie Jing et al. "Exchange of GATA factors mediates transitions in looped chromatin organization at a developmentally regulated gene locus". eng. In: *Molecular Cell* 29.2 (Feb. 2008), pp. 232–242. ISSN: 1097-2765. DOI: 10.1016/j.molcel.2007.11.020.

[242] Kyle J. Hewitt et al. "GATA Factor-Regulated Samd14 Enhancer Confers Red Blood Cell Regeneration and Survival in Severe Anemia". eng. In: *Developmental Cell* 42.3 (Aug. 2017), 213–225.e4. ISSN: 1878-1551. DOI: 10.1016/j.devcel.2017.07.009.

[243] Koichi R. Katsumura, Emery H. Bresnick, and GATA Factor Mechanisms Group. "The GATA factor revolution in hematology". eng. In: *Blood* 129.15 (Apr. 2017), pp. 2092–2102. ISSN: 1528-0020. DOI: 10.1182/blood-2016-09-687871.

[244] Y. Wei et al. "Toll-like receptor alterations in myelodysplastic syndrome". eng. In: *Leukemia* 27.9 (Sept. 2013), pp. 1832–1840. ISSN: 1476-5551. DOI: 10.1038/leu.2013.180.

[245] A. Ozinsky et al. "The repertoire for pattern recognition of pathogens by the innate immune system is defined by cooperation between toll-like receptors". eng. In: *Proceedings of the National Academy of Sciences of the United States of America* 97.25 (Dec. 2000), pp. 13766–13771. ISSN: 0027-8424. DOI: 10.1073/pnas.250476497.

[246] Nicholas J. Gay et al. "Assembly and localization of Toll-like receptor signalling complexes". eng. In: *Nature Reviews. Immunology* 14.8 (Aug. 2014), pp. 546–558. ISSN: 1474-1741. DOI: 10.1038/nri3713.

[247] Luana Chiquetto Paracatu et al. "Toll-like receptor and cytokine expression throughout the bone marrow differs between patients with low- and high-risk myelodysplastic syndromes". eng. In: *Experimental Hematology* 110 (June 2022), pp. 47–59. ISSN: 1873-2399. DOI: 10.1016/j.exphem.2022.03.011.

[248] Maria Kleppe et al. "JAK-STAT pathway activation in malignant and nonmalignant cells contributes to MPN pathogenesis and therapeutic response". eng. In: *Cancer Discovery* 5.3 (Mar. 2015), pp. 316–331. ISSN: 2159-8290. DOI: 10.1158/2159-8290.CD-14-0736.

[249] Tian Yi Zhang et al. "IL-6 blockade reverses bone marrow failure induced by human acute myeloid leukemia". eng. In: *Science Translational Medicine* 12.538 (Apr. 2020), eaax5104. ISSN: 1946-6242. DOI: 10.1126/scitranslmed.aax5104.

[250] Jennifer J. Trowbridge and Daniel T. Starczynowski. "Innate immune pathways and inflammation in hematopoietic aging, clonal hematopoiesis, and MDS". eng. In: *The Journal of Experimental Medicine* 218.7 (July 2021), e20201544. ISSN: 1540-9538. DOI: 10.1084/jem.20201544.

[251] Yang Mei et al. "Bone marrow-confined IL-6 signaling mediates the progression of myelodysplastic syndromes to acute myeloid leukemia". eng. In: *The Journal of Clinical Investigation* 132.17 (Sept. 2022), e152673. ISSN: 1558-8238. DOI: 10.1172/JCI152673.

[252] Jonathan C. Walsh et al. "Cooperative and antagonistic interplay between PU.1 and GATA-2 in the specification of myeloid cell fates". eng. In: *Immunity* 17.5 (Nov. 2002), pp. 665–676. ISSN: 1074-7613. DOI: 10.1016/s1074-7613(02)00452-1.

[253] T. Tamura et al. "ICSBP directs bipotential myeloid progenitor cells to differentiate into mature macrophages". eng. In: *Immunity* 13.2 (Aug. 2000), pp. 155–165. ISSN: 1074-7613. DOI: 10.1016/s1074-7613(00)00016-9.

[254] Alberto Yáñez et al. "IRF8 acts in lineage-committed rather than oligopotent progenitors to control neutrophil vs monocyte production". eng. In: *Blood* 125.9 (Feb. 2015), pp. 1452–1459. ISSN: 1528-0020. DOI: 10.1182/blood-2014-09-600833.

[255] H. Wesche et al. "MyD88: an adapter that recruits IRAK to the IL-1 receptor complex". eng. In: *Immunity* 7.6 (Dec. 1997), pp. 837–847. ISSN: 1074-7613. DOI: 10.1016/s1074-7613(00)80402-1.

[256] M. Muzio et al. "IRAK (Pelle) family member IRAK-2 and MyD88 as proximal mediators of IL-1 signaling". eng. In: *Science (New York, N.Y.)* 278.5343 (Nov. 1997), pp. 1612–1615. ISSN: 0036-8075. DOI: 10.1126/science.278.5343.1612.

[257] Sven Heinz et al. "Simple combinations of lineage-determining transcription factors prime cis-regulatory elements required for macrophage and B cell identities". eng. In: *Molecular Cell* 38.4 (May 2010), pp. 576–589. ISSN: 1097-4164. DOI: 10.1016/j.molcel.2010.05.004.

[258] Renato Ostuni et al. "Latent enhancers activated by stimulation in differentiated cells". eng. In: *Cell* 152.1-2 (Jan. 2013), pp. 157–171. ISSN: 1097-4172. DOI: 10.1016/j.cell.2012.12.018.

[259] Alessandra Mancino et al. "A dual cis-regulatory code links IRF8 to constitutive and inducible gene expression in macrophages". eng. In: *Genes & Development* 29.4 (Feb. 2015), pp. 394–408. ISSN: 1549-5477. DOI: 10.1101/gad.257592.114.

[260] Y. Li et al. "Regulation of the PU.1 gene by distal elements". eng. In: *Blood* 98.10 (Nov. 2001), pp. 2958–2965. ISSN: 0006-4971. DOI: 10.1182/blood.v98.10.2958.

[261] Bradley E. Bernstein et al. "Genomic maps and comparative analysis of histone modifications in human and mouse". eng. In: *Cell* 120.2 (Jan. 2005), pp. 169–181. ISSN: 0092-8674. DOI: 10.1016/j.cell.2005.01.001.

[262] Nathaniel D. Heintzman et al. "Distinct and predictive chromatin signatures of transcriptional promoters and enhancers in the human genome". eng. In: *Nature Genetics* 39.3 (Mar. 2007), pp. 311–318. ISSN: 1061-4036. DOI: 10.1038/ng1966.

[263] Benjamin J. Frisch et al. "Functional inhibition of osteoblastic cells in an in vivo mouse model of myeloid leukemia". eng. In: *Blood* 119.2 (Jan. 2012), pp. 540–550. ISSN: 1528-0020. DOI: 10.1182/blood-2011-04-348151.

[264] Bin Zhang et al. "Altered microenvironmental regulation of leukemic and normal stem cells in chronic myelogenous leukemia". eng. In: *Cancer Cell* 21.4 (Apr. 2012), pp. 577–592. ISSN: 1878-3686. DOI: 10.1016/j.ccr.2012.02.018.

[265] S. F. Ziegler et al. "Molecular characterization of the early activation antigen CD69: a type II membrane glycoprotein related to a family of natural killer cell activation antigens". eng. In: *European Journal of Immunology* 23.7 (July 1993), pp. 1643–1648. ISSN: 0014-2980. DOI: 10.1002/eji.1830230737.

[266] M. López-Cabrera et al. "Molecular cloning, expression, and chromosomal localization of the human earliest lymphocyte activation antigen AIM/CD69, a new member of the C-type animal lectin superfamily of signal-transmitting receptors". eng. In: *The Journal of Experimental Medicine* 178.2 (Aug. 1993), pp. 537–547. ISSN: 0022-1007. DOI: 10.1084/jem.178.2.537.

[267] Leonhard X. Heinz et al. "TASL is the SLC15A4-associated adaptor for IRF5 activation by TLR7-9". eng. In: *Nature* 581.7808 (May 2020), pp. 316–322. ISSN: 1476-4687. DOI: 10.1038/s41586-020-2282-0.

[268] James R. Burke et al. "BMS-345541 is a highly selective inhibitor of I kappa B kinase that binds at an allosteric site of the enzyme and blocks NF-kappa B-dependent transcription in mice". eng. In: *The Journal of Biological Chemistry* 278.3 (Jan. 2003), pp. 1450–1456. ISSN: 0021-9258. DOI: 10.1074/jbc.M209677200.

[269] Mindy I. Davis et al. "Comprehensive analysis of kinase inhibitor selectivity". eng. In: *Nature Biotechnology* 29.11 (Oct. 2011), pp. 1046–1051. ISSN: 1546-1696. DOI: 10.1038/nbt.1990.

[270] Rudolf Waelchli et al. "Design and preparation of 2-benzamido-pyrimidines as inhibitors of IKK". eng. In: *Bioorganic & Medicinal Chemistry Letters* 16.1 (Jan. 2006), pp. 108–112. ISSN: 0960-894X. DOI: 10.1016/j.bmcl.2005.09.035.

[271] T. L. Bailey and C. Elkan. "Fitting a mixture model by expectation maximization to discover motifs in biopolymers". eng. In: *Proceedings. International Conference on Intelligent Systems for Molecular Biology* 2 (1994), pp. 28–36. ISSN: 1553-0833.

[272] Charles E. Grant, Timothy L. Bailey, and William Stafford Noble. "FIMO: scanning for occurrences of a given motif". eng. In: *Bioinformatics (Oxford, England)* 27.7 (Apr. 2011), pp. 1017–1018. ISSN: 1367-4811. DOI: 10.1093/bioinformatics/btr064.

[273] Marloes R. Tijssen et al. "Genome-wide analysis of simultaneous GATA1/2, RUNX1, FLI1, and SCL binding in megakaryocytes identifies hematopoietic regulators". eng. In: *Developmental Cell* 20.5 (May 2011), pp. 597–609. ISSN: 1878-1551. DOI: 10.1016/j.devcel.2011.04.008.

[274] Shruthi Subramanian et al. "Genome-wide transcription factor-binding maps reveal cell-specific changes in the regulatory architecture of human HSPCs". eng. In: *Blood* 142.17 (Oct. 2023), pp. 1448–1462. ISSN: 1528-0020. DOI: 10.1182/blood.2023021120.

[275] Dana C. Bellissimo and Nancy A. Speck. "RUNX1 Mutations in Inherited and Sporadic Leukemia". eng. In: *Frontiers in Cell and Developmental Biology* 5 (2017), p. 111. ISSN: 2296-634X. DOI: 10.3389/fcell.2017.00111.

[276] Claire C. Homan et al. "The RUNX1 database (RUNX1db): establishment of an expert curated RUNX1 registry and genomics database as a public resource for familial platelet disorder with myeloid malignancy". eng. In: *Haematologica* 106.11 (Nov. 2021), pp. 3004–3007. ISSN: 1592-8721. DOI: 10.3324/haematol.2021.278762.

[277] Hui Huang et al. "Differentiation-dependent interactions between RUNX-1 and FLI-1 during megakaryocyte development". eng. In: *Molecular and Cellular Biology* 29.15 (Aug. 2009), pp. 4103–4115. ISSN: 1098-5549. DOI: 10.1128/MCB.00090-09.

[278] Françoise Levavasseur et al. "FOXP1 contributes to murine hematopoietic stem cell functionality". eng. In: *Experimental Hematology* 149 (May 2025), p. 104815. ISSN: 1873-2399. DOI: 10.1016/j.exphem.2025.104815.

[279] Hui Hu et al. "Foxp1 is an essential transcriptional regulator of B cell development". eng. In: *Nature Immunology* 7.8 (Aug. 2006), pp. 819–826. ISSN: 1529-2908. DOI: 10.1038/ni1358.

[280] Xiaoming Feng et al. "Transcription factor Foxp1 exerts essential cell-intrinsic regulation of the quiescence of naive T cells". eng. In: *Nature Immunology* 12.6 (June 2011), pp. 544–550. ISSN: 1529-2916. DOI: 10.1038/ni.2034.

[281] Can Shi et al. "Down-regulation of the forkhead transcription factor Foxp1 is required for monocyte differentiation and macrophage function". eng. In: *Blood* 112.12 (Dec. 2008), pp. 4699–4711. ISSN: 1528-0020. DOI: 10.1182/blood-2008-01-137018.

[282] Tao Zhuang et al. "Endothelial Foxp1 Suppresses Atherosclerosis via Modulation of Nlrp3 Inflammasome Activation". eng. In: *Circulation Research* 125.6 (Aug. 2019), pp. 590–605. ISSN: 1524-4571. DOI: 10.1161/CIRCRESAHA.118.314402.

[283] Vladimir Litvak et al. "A FOXO3-IRF7 gene regulatory circuit limits inflammatory sequelae of antiviral responses". eng. In: *Nature* 490.7420 (Oct. 2012), pp. 421–425. ISSN: 1476-4687. DOI: 10.1038/nature11428.

[284] Wuqiang Fan et al. "FoxO1 regulates Tlr4 inflammatory pathway signalling in macrophages". eng. In: *The EMBO journal* 29.24 (Dec. 2010), pp. 4223–4236. ISSN: 1460-2075. DOI: 10.1038/emboj.2010.268.

[285] Jonathan Brown et al. "Mammalian target of rapamycin complex 2 (mTORC2) negatively regulates Toll-like receptor 4-mediated inflammatory response via FoxO1". eng. In: *The Journal of Biological Chemistry* 286.52 (Dec. 2011), pp. 44295–44305. ISSN: 1083-351X. DOI: 10.1074/jbc.M111.258053.

[286] Jack D. Chan et al. "FOXO1 enhances CAR T cell stemness, metabolic fitness and efficacy". eng. In: *Nature* 629.8010 (May 2024), pp. 201–210. ISSN: 1476-4687. DOI: 10.1038/s41586-024-07242-1.

[287] Mohd Hafiz Ahmad et al. "Runx1-R188Q germ line mutation induces inflammation and predisposition to hematologic malignancies in mice". eng. In: *Blood Advances* 7.23 (Dec. 2023), pp. 7304–7318. ISSN: 2473-9537. DOI: 10.1182/bloodadvances.2023010398.

[288] Atray Dixit et al. "Perturb-Seq: Dissecting Molecular Circuits with Scalable Single-Cell RNA Profiling of Pooled Genetic Screens". eng. In: *Cell* 167.7 (Dec. 2016), 1853–1866.e17. ISSN: 1097-4172. DOI: 10.1016/j.cell.2016.11.038.

[289] Moonjung Jung et al. "GATA2 deficiency and human hematopoietic development modeled using induced pluripotent stem cells". eng. In: *Blood Advances* 2.23 (Dec. 2018), pp. 3553–3565. ISSN: 2473-9537. DOI: 10.1182/bloodadvances.2018017137.

[290] Elizabeth S. Ng et al. "Long-term engrafting multilineage hematopoietic cells differentiated from human induced pluripotent stem cells". eng. In: *Nature Biotechnology* (Sept. 2024). ISSN: 1546-1696. DOI: 10.1038/s41587-024-02360-7.

[291] Adam C. Wilkinson et al. "Long-term ex vivo haematopoietic-stem-cell expansion allows nonconditioned transplantation". eng. In: *Nature* 571.7763 (July 2019), pp. 117–121. ISSN: 1476-4687. DOI: 10.1038/s41586-019-1244-x.

[292] Adam C. Wilkinson et al. "Long-term ex vivo expansion of mouse hematopoietic stem cells". eng. In: *Nature Protocols* 15.2 (Feb. 2020), pp. 628–648. ISSN: 1750-2799. DOI: 10.1038/s41596-019-0263-2.